Treatment of
Model Uncertainties
In Structural Dynamics

Thesis by
Lambros S. Katafygiotis

In Partial Fulfillment of the Requirements
for the Degree of
Doctor of Philosophy

California Institute of Technology
Pasadena, California

1991

(Submitted May 1, 1991)

Acknowledgements

I would like to express my sincere gratitude and appreciation to my advisor, Professor J.L. Beck, for his enthusiastic guidance and his continuous support and encouragement throughout the course of my research. His continuous availability, along with the many useful discussions, are greatly appreciated.

I am grateful to the California Institute of Technology for the generous financial support it provided me during my stay here.

I would also like to thank all my professors for the excellent education they offered me during my graduate studies. I also want to thank the people in Thomas for the happy and friendly environment they created.

My deepest thanks goes to Kostas Papadimitriou for his warm friendship and the many memorable experiences we shared. The help of Suzette Martinez with the typing of this thesis is greatly appreciated. I also want to thank Cecilia Lin for her expert help with the illustrations.

Finally, I am deeply grateful to my parents, Solon and Irmela, to whom this thesis is dedicated, for their love and their continuous support in the pursuit of my educational goals.

Abstract

The uncertainties related to the modeling of the dynamic behavior of a structure are analyzed using a probabilistic approach.

First, the case of preliminary design is addressed, where the structure has not yet been built. A new efficient and accurate numerical method is proposed to investigate the resulting uncertainties in the structural response due to uncertainties in the modeling process, where engineering judgement is used to quantify the latter uncertainties.

Second, the case where records of measured structural response are available to reduce the uncertainties in the structural models is addressed. The posterior probability distribution of the uncertain parameters is found to be very peaked at the values of some optimal parameters. These optimal parameters can be obtained by minimizing a positive-definite measure-of-fit function. A new efficient minimization algorithm is proposed to resolve difficulties in convergence of existing methods. The identifiability of the optimal parameters is also addressed. The problem of finding the whole set of the optimal models that have the same output at the observed degrees of freedom is resolved for the first time, by presenting an algorithm which methodically and efficiently searches the parameter space.

Table of Contents

List of Figures

List of Tables

Chapter 1

Introduction

1.1 Motivation and Objectives

Uncertainties are inherent when investigating any engineering or physical problem. The principle of uncertainty of quantum mechanics, formulated by Heisenberg, states that the accurate measurement of either of two related quantities, such as position and momentum or energy and time, produces uncertainties in the measurement of the other. Uncertainty in this context is the inaccuracy of measurements, and accounts for possible differences between the measured value and the unknown true value of a quantity. Uncertainty is not only associated with a measured quantity, but also with quantities whose values are predicted using empirical or mathematical models. In this case, uncertainty reflects the inaccuracy involved in predicting the value of a quantity, and accounts for possible differences between a predicted value based on existing relevant information, and the unknown true value of this quantity. Because the uncertainty can take on various values over a range, it is treated as a random variable, that is, a variable whose possible values have an associated probability distribution describing how plausible each value is for the uncertain quantity, on the basis of the given information.

In structural dynamics, the uncertainties involved can be divided into two major categories:

1. Uncertainties in the specification of the applied external loads. Many of

the structural excitations encountered in practice are uncertain before their occurence. Some examples are: seismic excitations, blast loadings on structures, water wave excitations, wind excitations, aerodynamic turbulences, etc. The terminology "random vibration" analysis is often used to designate the particular category of problems dealing with the response of deterministic systems to uncertain loads. There exists an extensive body of work in this area, which is well reviewed by Benaroya and Rehak [1988]. Random vibration analysis is not the principal subject of this work.

2. Uncertainties related to modeling the structure itself. Figure 1.1 helps to visualize the uncertainties introduced during such a modeling. It is assumed that a class of models is specified by choosing the general mathematical form which is expected to describe the essential features of the input-output relation of the system. There are two types of uncertainty introduced when modeling the structural behavior with a model of the specified class. The first type of uncertainty is concerned with which model in the class is the most appropriate to model the system. This type of uncertainty will be referred to as "parameter uncertainty," since certain parameters must be assigned unique values in order to specify a particular model within the given class; therefore, uncertainty in the specification of the most appropriate model within the class can be viewed as uncertainty in the specification of its parameter values. For example, there is uncertainty when choosing the stiffness or damping parameters of a finite element model, caused by variations in material properties, manufacturing and assembly techniques, uncertainties in measurements due to testing errors, variation of the physical properties with the passage of time as a result of wear and tear, etc. The second type of uncertainty is concerned with how well the class of models approximates the behavior of the system, and is due to the inaccuracies and assumptions introduced in the mathematical modeling of the structure, such as lack of understanding of the materials' constitutive behavior, inexact

modeling of boundary conditions and simplifications introduced in order to make the model computationally feasible. This second type of uncertainty, which stems from the fact that no mathematical model is good enough to exactly represent the behavior of a real system, is the cause of what will be referred to as "model error."

If we introduce probability to describe the parameter uncertainties, they may be mathematically modeled as random variables, as stochastic processes in space, or as stochastic processes in time. Systems with uncertain parameters fluctuating in time, constitute the field of "parameter random vibrations," and are well reviewed by Ibrahim [1983], but this subject is not of direct interest in this work. In some instances, such as shrinkage and creep, the system evolves as a time-dependent stochastic process [Bazant and Wang, 1984; Bazant 1986]. Time-dependent, uncertain parameters will not be considered in this work. The terms "stochastic field" or "random field" are often used to denote stochastic processes in space. Simulation and perturbation techniques are often used [Shinozuka 1987; Shinozuka and Deodatis, 1988; Vanmarcke et al., 1986] to obtain the statistical properties of the response of systems with probabilistically-modeled spatial distribution of material properties. This work will focus on discrete, time-invariant systems, and, therefore, the uncertain parameters will be modeled as random variables. To describe the model error probabilistically, an appropriate probability model will be adopted. Here, this probabilistic formulation will be based on an output-error approach.

The uncertainty of structural characteristics has a direct relationship to the reliability of many engineering structures. The degree of sensitivity of structural response to a possible variation of a structural parameter is of great importance during a reliability analysis, especially if a small perturbation can result in significant changes of the free or forced response amplitudes. For example, this sensitivity analysis is of great concern to those who are involved in the control of large flexible space structures [Meirovitch et al., 1983], since when a control

system is designed for natural frequencies whose values are assumed to be exact, the model errors and structural parameter uncertainties may deteriorate the performance of the control loop, and may even make the controlled system unstable. The property of robustness is therefore desirable, that is, the control system's performance is desired to be relatively insensitive to model errors and structural parameter uncertainties.

1.2 Outline of This Work

It is the objective of this dissertation to analyze the uncertainties of a structural model, and to present techniques to account for them when calculating the structural response to a given excitation. Although the motivation stems from an interest in the analysis of the response of structural systems, such as buildings, bridges, and dams, to earthquake excitations, most of the discussion and results presented are general and can easily be extended to other applications of structural dynamics. It will be assumed that the structural model lies within a class of parametric models, and that the statistical uncertainties of the model are described by the uncertainties of its parameters and the model error for the class. The model parameters will be assumed to be time-invariant but uncertain, and, therefore, a time-independent joint probability density function will be assigned to them. Probability will be used in the Bayesian context, that is, probability is treated as a multi-valued logic for plausible reasoning, and not as a relative frequency of events in the "long run."

Two different approaches are used in modeling the dynamics of a structure and analyzing the uncertainties associated with the chosen model, depending on whether test data is available or not. In Chapter 2, the problem addressed is updating of the description of model uncertainties when no records of measured response of the structure are available. This is particularly the case during design, when the structure has not yet been built. In this case, the structural

model can either be based on empirical code-type formulas, or it can be synthesized from the structural drawings using finite element techniques, supplemented by empirical methods in order to estimate parameters, such as those describing structural damping, which are difficult to determine by synthesis. The uncertainties of the model parameters, as well as the uncertainty due to model error, are quantified using any available information and the engineer's judgement and experience. The joint probability density function assigned to the uncertain parameters corresponds to an *a priori* probability density function within the context of Bayesian probability.

An extensive number of publications demonstrating various methods of estimating the statistics of the uncertain model response given the statistics of the parameter uncertainties are available. Some publications used simulation methods to investigate the effects of uncertainties in structural properties [Shinozuka 1972; Shinozuka and Jan, 1972], while others used perturbation methods to compute first and second moment statistics of response quantities [Chen and Saroka, 1973, 1974; Contreras 1980; Hisada and Nakagiri, 1981, 1982; Vanmarcke and Grigoriou, 1983; Branstetter and Paez, 1986; Liu et al., 1988b; Liu et al., 1987]. Simulation techniques are quite powerful but, in general, are very costly and time consuming, since they require a large number of numerical solutions. This disadvantage becomes evident when one deals with large or even medium-sized systems, where numerical simulation becomes unrealistic on conventional digital computers. In addition, simulations provide limited insight into the behavior and sensitivity of the system under different parameter uncertainties. Perturbation techniques, on the other hand, are easily integrated into existing computer codes of deterministic structural dynamics, but they suffer from inaccuracy and questions of convergence when dynamic, particularly transient, and wave propagation problems are considered. Liu et al. [1988a] came across these problems when using the second moment approach method, based on a truncated Taylor series expansion of the model response with respect to the uncertain model parameters.

Beck and Katafygiotis [1989] showed that much better results are obtained using a truncated Fourier series expansion of the model response with respect to the uncertain model parameters. Jensen [1989] extended this idea to more general orthogonal series expansions. In Chapter 2 a new, efficient approximate method is presented to investigate the uncertainties in the structural response due to uncertainties in the modeling process.

In Chapter 3, the problem addressed is updating of the description of model uncertainties when records of structural response are available. In this case, structural information contained in the available records is extracted, and is used to update the initial estimates of parameter uncertainty, and the uncertainty of the model error. The probability density function modeling the uncertainties of the parameters and the model error, after the updating, is also referred to as the posterior probability density function. The posterior probability density function is usually very peaked at the values of some "optimal" parameters. These parameters optimize, within the framework of an "output-error" approach, the match between the recorded and the corresponding model responses. It is asymptotically correct for large sample sizes to use only the models corresponding to these optimal parameters, when the model response and its associated uncertainty is calculated for structural response predictions [Beck 1990].

It is shown that conventional minimization algorithms used during the optimization are inefficient and time consuming. At the same time, they suffer from severe convergence difficulties, which prevent them from reaching the global optimal parameters. A new algorithm is presented to overcome these difficulties.

Furthermore, in Chapter 3, the issue of identifiability of the optimal parameters is explored. The optimal parameters are said to be identifiable if they can be determined uniquely from the given input and output of the system. Exploring identifiability in the case of real data is a very difficult task, because of the presence of model error and measurement noise. Even for the case of simulated

data with zero model error, the issue of identifiability has not been completely resolved. Uniqueness of the optimal parameters reached by means of an optimization algorithm is often assumed. In other instances, although theoretical analysis shows that uniqueness is rather unlikely [Udwadia et al., 1978a; Udwadia et al., 1978b], no tool is given to assist in a systematic search for finding all sets of optimal parameters. A new methodology is presented to search the parameter space for "output equivalent" sets of parameters, that is, for sets of parameters corresponding to models having exactly the same response at the observed degrees of freedom when subjected to the same input. In the case of noise-free data and no model error, this methodology resolves the identifiability issue. In the case of real data, there is no guarantee that all optimal solutions are "output equivalent" to each other. Therefore, in the case of real data, the task of finding all optimal solutions becomes extremely difficult, especially because there may no longer be a finite number. Although it is still not within reach to guarantee that all possible sets of optimal parameters have been found, the set of all "output equivalent" optimal parameters is at least a first step toward accounting for the identifiability of the optimal parameters in the predictive response.

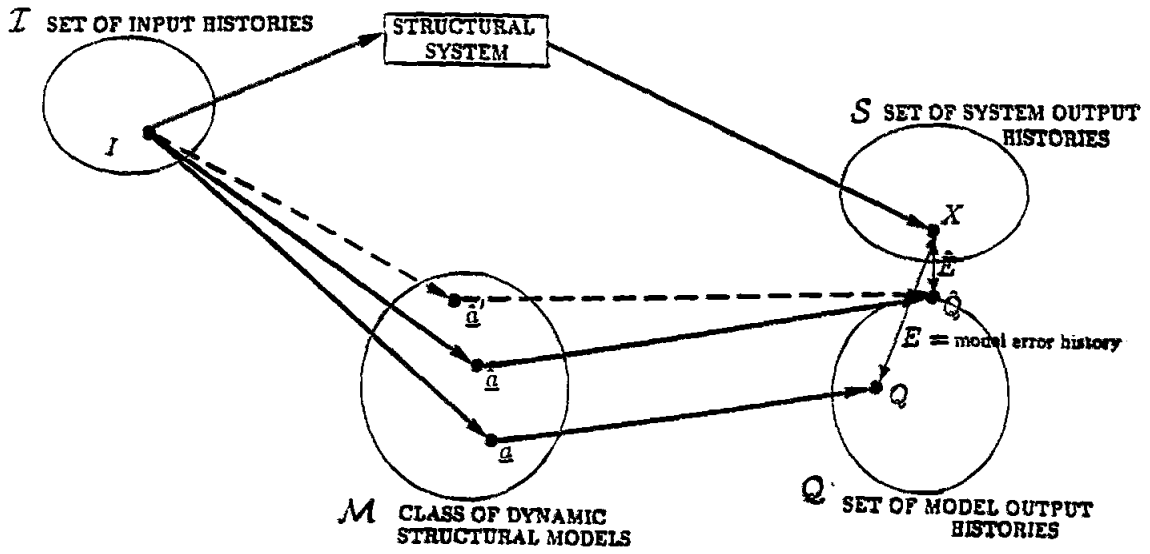

Figure 1.1 Uncertainties in the modeling of the dynamic behavior of a structural system. The input I is assumed known. Each parameter $\underline{a}$ specifies a particular model in the class $\mathcal{M}$ with corresponding model output history Q. X denotes the system output history, and E denotes the model error history. The sets $\mathcal{S}$ and $\mathcal{Q}$ do not overlap because of the existence of model error. For some optimal model(s) corresponding to some optimal parameter(s) $\hat{\underline{a}}$, the model error reaches its minimum. The parameter uncertainty is concerned with estimating the optimal parameters, and the uncertainty due to model error is concerned with quantifying its "magnitude."

Chapter 2

Structural Uncertainties in Preliminary Design

2.1 Introduction

This chapter deals with uncertainties in the mathematical modeling of a structure when no records of measured response of the structure are available. It is assumed that a parametric model has been chosen to represent the input-output relationship of the structure. The uncertainties associated with the choice of the mathematical model, and the techniques used to account for these uncertainties when calculating the structural response, will be the focus of this chapter. The goal is to provide the engineer doing dynamic design with a tool to go beyond checking the nominal dynamic response to specified excitations for a preliminary design; the engineer will be able to examine the associated uncertainty in the response, due to the fact that the completed structure will not have precisely the model parameter values that were assumed, and also due to the fact that no model gives an exact description of a structure's dynamics. A brief discussion of the mathematical modeling of a structure follows, based on Beck [1978].

2.2 Modeling of a Structure

A structural model is defined here to be a mathematical representation which approximates the relation between the input and output of a structural system. The terms input and output are used here in the technical sense; in the case of existing data, they refer to the observed portions of the excitation and the response, while in the case where no data exists, they refer to the assumed

excitation and the response quantities which are to be predicted.

The models that can be employed are classified into two principal categories, parametric and non-parametric. At the preliminary design stage, only parametric models are available, since non-parametric models must be identified from records of structural response; they cannot be derived directly by theory. A parametric model consists of a particular mathematical form chosen to describe the essential features of the input-output relation of the system under study, but certain parameters must be assigned values before the model is completely specified. When referring to the general mathematical form describing the internal structure of a system, the term "theoretical model" will be used. A useful interpretation of a theoretical model is that it is a generic form defining a whole class of models $\mathcal{M}$. Let $\underline{a}$ denote the parameters which are needed to completely specify a parametric model, then a particular model is specified by the pair $(\mathcal{M}, \underline{a})$. To illustrate this, consider a one-story building subjected to base excitation represented by the single-degree of freedom (SDOF) linear model of Figure 2.2. This model is mathematically expressed in the time domain by the differential equation:

$$m\ddot{q} + c\dot{q} + kq = -m\ddot{z}(t) \; ; \; q(0) = q_0, \dot{q}(0) = \dot{q}_0 \tag{2.2.1}$$

where $q(t)$ is the relative displacement of the model and $\ddot{z}(t)$ is the base acceleration; the mass m, the viscous damping c, and the stiffness k, are the physical parameters, which, along with the initial displacement q_0 and the initial velocity $\dot{q}_0$, constitute the set of parameters to be specified. Therefore, $\underline{a} = [m, c, k, q_0, \dot{q}_0]^T$.

Equation (2.2.1) can be rewritten using alternative parameters:

$$\ddot{q} + 2\zeta\omega\dot{q} + \omega^2 q = -\ddot{z}(t) \; ; \; q(0) = q_0, \dot{q}(0) = \dot{q}_0 \tag{2.2.2}$$

where ω, the fundamental frequency of oscillation, and ζ, the damping ratio, are now the model parameters, which, along with the initial conditions q_0 and $\dot{q}_0$, constitute the set of parameters to be specified. Therefore, $\underline{a} = [\omega, \zeta, q_0, \dot{q}_0]^T$.

The parameters $\underline{a}$ can be chosen from empirical code-type formulas, using the engineer's judgement and experience, or can be constructed by synthesis, using structural drawings. For example, the mass or stiffness elements can be derived from the properties of the structural subcomponents and their interactions, using a finite element discretization, while the damping ratios cannot be constructed by synthesis; their values must be assigned empirically from experience obtained from existing similar structures.

It is obvious that when parameters are to be chosen from empirical code-type formulas, there is an uncertainty as to which value corresponds to the model which will more realistically represent the real structure's behavior. Yet even for the parameters which are evaluated by structural synthesis, there is a great deal of uncertainty when estimating them, due to uncertainties associated with the properties of structural and nonstructural components and their interconnections, and due to the simplifications and assumptions necessary to ensure that the model is computationally feasible. If deterministic values are assigned to the model parameters $\underline{a}$, these uncertainties are not accounted for, and the computed structural response will represent only one result in a spectrum of possibilities. To treat the parameter uncertainties when evaluating the structural response, a probabilistic approach can be followed. A probabilistic approach can also be followed to account for model error, that is, the errors caused by the inability of any model within the particular class to represent the real structural behavior. The probabilistic modeling of the structural model uncertainties will be addressed, but first, the concepts of Bayesian probability are defined in the following section.

2.3 Probability Logic

We employ probability to quantify the uncertainties involved, but we use a "Bayesian" interpretation, that is, we treat probability as a multi-valued logic for

plausible reasoning subject to certain axioms [Beck 1990; Jaynes 1968, Jeffreys 1961]. Specifically, the probability of a given b, $P(a|b)$ denotes a measure of the plausibility of the proposition a given the information stated in proposition b. The propositions may refer to observations or measurements, or they may refer to hypotheses about probability models, for example. Note that for most of the applications of interest in this study, the common interpretation of probability as a relative frequency of occurences in the long run does not make sense.

The calculus of probability logic is defined by the axioms of mathematical (Boolean) logic together with three additional axioms:

$$1)\ 0 \leq P(a|b) \leq 1 \quad \text{and} \quad P(a|a) = 1, \quad 2)\ P(a|b) + P(\text{not } a|b) = 1$$

$$\text{and} \quad 3)\ P(a,b|c) = P(a|b,c)P(b|c)$$

where "," represents the propositional conjunction "and." It has been shown [Cox 1961], that the content of axioms 2) and 3) is a necessary consequence of the requirement of consistency with mathematical logic, although the form of all three axioms is conventional. The axioms lead to esssentially the same calculus as the Kolmogorov axioms of "mathematical" probability, except that all probabilities are "conditional" in the sense of Kolmogorov, because the plausibility of a proposition clearly depends on the information available.

At this point, Bayes' theorem is stated:

$$P(a|b,c) = \frac{P(b|a,c)P(a|c)}{P(b|c)} \tag{2.3.1}$$

Bayes' theorem is a consequence of the above stated axioms of probability logic and can be applied to data to extract information about the values of a parameter set of a model [Beck 1990; Box and Tiao, 1973; Peterka 1981]. This will become evident in Chapter 3, where it is assumed that structural response data are available.

2.4 Probabilistic Modeling of Structural Model Uncertainties

Often the uncertainties associated with some of the model parameters are considered negligible compared with the uncertainties of the other parameters, and, therefore, these parameters are treated as deterministic. For example, the initial conditions are often treated as deterministic because the system is assumed to start from rest, or the masses associated with the different degrees of freedom (dof) of a structure are often assumed known accurately enough from the structural drawings, so that they can be considered fixed. These parameters will be treated as an inseparable part of the theoretical model so that the parameters $\underline{a}$ needed to specify a particular model within the class refer to the uncertain parameters only. Figure 2.1 helps to visualize the procedure leading to the probabilistic modeling of the structural response.

Consider a theoretical model $\mathcal{M}$ with uncertain parameters $\underline{a} \in R^{N_a}$. To account for the initial parameter uncertainties, $\mathcal{M}$ is assumed to specify a joint probability distribution $\pi_{\underline{a}}(\underline{a})$ so that $p(\underline{a}|\mathcal{M}) = \pi_{\underline{a}}(\underline{a})$. This joint probability density function (pdf) $\pi_{\underline{a}}(\underline{a})$, assigned without using test data from the structure, is often called the "prior" distribution, and it is chosen subjectively based on past experience dealing with similar structures. Usually, a convenient mathematical form is chosen which is roughly consistent with the engineer's judgement regarding the relative plausibilites of different values of $\underline{a}$. Often, knowing one parameter a_j does not influence judgement of the plausibilities of values of the other parameters, so the parameters are mutually irrelevant to one another and their pdf's can be specified independently. In the case of correlated uncertain parameters, the fact that the associated covariance matrix can be diagonalized can be utilized to obtain a new transformed set of uncorrelated parameters [Liu et al., 1986; Dias et al., 1986]. Therefore, without loss of generality, it will be

assumed that the joint pdf can be expressed as the product of the separate pdf's:

$$\pi_{\underline{a}}(\underline{a}) = \prod_{j=1}^{N_a} \pi_{a_j}(a_j) \tag{2.4.1}$$

Let $\underline{q}(t;\underline{a},I,\mathcal{M}) \in R^{N_R}$ be the deterministic response at time t of a particular model $M = M(\mathcal{M},\underline{a})$ to an input I. Let $\underline{x}(t;I)$ denote the response that would be observed if the real structure was subjected to the same input. In the following, for the sake of brevity, the symbols t and I will often be assumed without being explicitly written. For example, $\underline{x} \equiv \underline{x}(t) \equiv \underline{x}(t;I)$. If discrete times are being used, then $\underline{x}_n \equiv \underline{x}(t_n) \equiv \underline{x}(t_n;I)$. Also, often when the parameters $\underline{a}$ of a theoretical model $\mathcal{M}$ are referenced, the symbol $\mathcal{M}$ is assumed. For example, $\underline{q}(t;\underline{a},I,\mathcal{M}) \equiv \underline{q}(t;\underline{a},I) \equiv \underline{q}(t;\underline{a}) \equiv \underline{q}(\underline{a})$.

As mentioned earlier, because of the simplifications and assumptions used in choosing the particular class of models $\mathcal{M}$, there is an uncertainty concerning how accurately the response of any of its members M can predict the real response. To account for this model error, a class of probability models $\mathcal{M}_P$ parameterized by $[\underline{a}^T,\underline{\sigma}^T]^T \in R^{N_a+N_\sigma}$ is introduced, that is, $\mathcal{M}_P$ prescribes a function f giving the probability of the system output:

$$p(\underline{x}|\underline{a},\underline{\sigma},\mathcal{M}_P) = f(\underline{x};\underline{a},\underline{\sigma}) \tag{2.4.2}$$

The dependence on the input I has been suppressed in the notation at both sides of (2.4.2), and will remain suppressed throughout this chapter. $\mathcal{M}_P$ is also specifying the prior pdf $\pi_{\underline{a},\underline{\sigma}}(\underline{a},\underline{\sigma})$, so that $p(\underline{a},\underline{\sigma}|\mathcal{M}_P) = \pi_{\underline{a},\underline{\sigma}}(\underline{a},\underline{\sigma})$. Assuming $\underline{a}$ and $\underline{\sigma}$ to be independent leads to $\pi_{\underline{a},\underline{\sigma}}(\underline{a},\underline{\sigma}) = \pi_{\underline{a}}(\underline{a})\pi_{\underline{\sigma}}(\underline{\sigma})$. The pdf $\pi_{\underline{\sigma}}(\underline{\sigma})$ is chosen subjectively, as was done for $\pi_{\underline{a}}(\underline{a})$. It will be assumed that $f(\underline{x};\underline{a},\underline{\sigma})$ is a joint Gaussian distribution with mean $\underline{q}(\underline{a})$ and covariance matrix $\Sigma(\underline{\sigma})$ so that:

$$\begin{aligned} f(\underline{x};\underline{a},\underline{\sigma}) &= G(\underline{x};\underline{q}(\underline{a}),\Sigma(\underline{\sigma})) \\ &\equiv \frac{1}{(2\pi)^{\frac{N_R}{2}}|\Sigma(\underline{\sigma})|^{\frac{1}{2}}} \exp\left(-\frac{1}{2}[\underline{x}-\underline{q}(\underline{a})]^T\Sigma^{-1}(\underline{\sigma})[\underline{x}-\underline{q}(\underline{a})]\right) \end{aligned} \tag{2.4.3}$$

If the uncertainties for each of the elements x_j of $\underline{x}$ are assumed independent of each other, then the covariance matrix is diagonal with elements σ_j^2. In this case:

$$f(\underline{x};\underline{a},\underline{\sigma}) = \prod_{j=1}^{N_R} G(x_j; q_j(\underline{a}), \sigma_j^2) \tag{2.4.4}$$

where

$$G(x_j; q_j(\underline{a}), \sigma_j^2) = \frac{1}{\sqrt{2\pi}\sigma_j} \exp\left(-\frac{(x_j - q_j(\underline{a}))^2}{2\sigma_j^2}\right) \tag{2.4.5}$$

Under the additional assumption that all σ_j's are equal to σ, (2.4.4) becomes:

$$f(\underline{x};\underline{a},\sigma) = \frac{1}{(\sqrt{2\pi}\sigma)^{N_R}} \exp\left(-\frac{1}{2\sigma^2}\sum_{j=1}^{N_R}(x_j - q_j(\underline{a}))^2\right) \tag{2.4.6}$$

Denote by $S(\underline{a}) \subseteq R^{N_a}$ and $S(\underline{\sigma}) \subseteq R^{N_\sigma}$ the set of allowable values of $\underline{a}$ and $\underline{\sigma}$. The pdf $p(\underline{x}|\mathcal{M}_P)$ of the response $\underline{x}(t)$, based on the axioms of probability logic and assuming that $\underline{a}$ and $\underline{\sigma}$ are independently distributed, can be expressed as:

$$\begin{aligned} p(\underline{x}|\mathcal{M}_P) &= \int_{S(\underline{a})}\int_{S(\underline{\sigma})} p(\underline{x}|\underline{a},\underline{\sigma},\mathcal{M}_P)p(\underline{a}|\mathcal{M}_P)p(\underline{\sigma}|\mathcal{M}_P)d\underline{a}d\underline{\sigma} \\ &= \int_{S(\underline{a})}\int_{S(\underline{\sigma})} f(\underline{x};\underline{a},\underline{\sigma})\pi_{\underline{a}}(\underline{a})\pi_{\underline{\sigma}}(\underline{\sigma})d\underline{a}d\underline{\sigma} \end{aligned} \tag{2.4.7}$$

The first two moments of the above distribution, assuming $f(\underline{x};\underline{a},\underline{\sigma})$ is given by (2.4.3), are proved in Appendix A to be:

$$\bar{\underline{x}} \equiv E[\underline{x}|\mathcal{M}_P] = \int_{S(\underline{a})} \underline{q}(\underline{a})\pi_{\underline{a}}(\underline{a})d\underline{a} \tag{2.4.8}$$

$$\mathrm{Cov}(\underline{x}) = \int_{S(\underline{a})} \underline{q}(\underline{a})\underline{q}(\underline{a})^T\pi_{\underline{a}}(\underline{a})d\underline{a} - \bar{\underline{x}}\bar{\underline{x}}^T + \int_{S(\underline{\sigma})} \Sigma(\underline{\sigma})\pi_{\underline{\sigma}}(\underline{\sigma})d\underline{\sigma} \tag{2.4.9}$$

Under the additional assumption of uncorrelated uncertainties of the elements x_j of $\underline{x}$, which is the assumption that led to expression (2.4.4), the expressions for the first two moments of x_j become:

$$\bar{x}_j \equiv E[x_j|\mathcal{M}_P] = \int_{S(\underline{a})} q_j(\underline{a})\pi_{\underline{a}}(\underline{a})d\underline{a} \tag{2.4.10}$$

$$\mathrm{Var}(x_j) = \int_{S(\underline{a})} q_j^2(\underline{a})\pi_{\underline{a}}(\underline{a})d\underline{a} - \bar{x}_j^2 + E[\sigma_j^2] \tag{2.4.11a}$$

or, if the additional assumption of equal variances $\sigma_j = \sigma$ is employed:

$$\mathrm{Var}(x_j) = \int_{S(\underline{a})} q_j^2(\underline{a})\pi_{\underline{a}}(\underline{a})d\underline{a} - \bar{x}_j^2 + E[\sigma^2] \tag{2.4.11b}$$

By noting that:

$$\begin{aligned} \bar{q}_j \equiv E[q_j|M] &= \int_{S(\underline{a})} q_j(\underline{a})p(\underline{a}|M)d\underline{a} \\ &= \int_{S(\underline{a})} q_j(\underline{a})\pi_{\underline{a}}(\underline{a})d\underline{a} \end{aligned} \tag{2.4.12}$$

equation (2.4.10) implies that:

$$\bar{x}_j = \bar{q}_j \tag{2.4.13}$$

that is, the expected structural response is the mean model response. Also by noting that:

$$\begin{aligned} \mathrm{Var}(q_j) = \mathrm{Var}(q_j|M) = &= \int_{S(\underline{a})} (q_j(\underline{a}) - \bar{q}_j)^2 p(\underline{a}|M)d\underline{a} \\ &= \int_{S(\underline{a})} q_j^2(\underline{a})\pi_{\underline{a}}(\underline{a})d\underline{a} - \bar{q}_j^2 \end{aligned} \tag{2.4.14}$$

equations (2.4.11a) and (2.4.11b) imply that:

$$\mathrm{Var}(x_j) = \mathrm{Var}(q_j) + E[\sigma_j^2] \tag{2.4.15a}$$

or

$$\mathrm{Var}(x_j) = \mathrm{Var}(q_j) + E[\sigma^2] \tag{2.4.15b}$$

Hence, the variance of the structural response is equal to the variance of the model response due to the uncertain parameters, plus the mean variance of the model error.

The rest of this chapter focuses on the evaluation of the first two moments of the q_j's given by (2.4.12) and (2.4.14) and is an extension of the work presented in Beck and Katafygiotis [1989]. The first two moments of the x_j's are then given by (2.4.13) and (2.4.15a) or (2.4.15b). In the following section, some of the techniques most used to evaluate the first two moments of the q_j's are reviewed and evaluated.

2.5 Evaluation of Existing Techniques

It can be seen from expressions (2.4.12) and (2.4.14) that the evaluation of the first two moments of the q_j's requires integration over an N_a-dimensional space. This, and the fact that the model response $\underline{q}(\underline{a})$ does not depend linearly on $\underline{a}$, make this problem difficult. Analytical evaluation of these high-dimensional integrals is generally not possible, except for very specific cases where particular choices of $\underline{a}$ and $\pi_{\underline{a}}(\underline{a})$ are assumed. The particular case of a SDOF oscillator, where its frequency and damping ratio are uncertain and probabilistically modeled by independent Gamma distributions, is a specific example that can be treated analytically and will be addressed later in Section 2.9. Therefore, numerical techniques have been developed to evaluate approximations of the above integrals. These methods can be broadly classified into two major categories: (1) methods using a statistical approach and (2) methods using a non-statistical approach. The first category consists of simulation techniques, among which the Monte Carlo method is the most prevalent one. Simulations can become computationally prohibitive, since their accuracy depends on the sample size, in accordance with the "Weak Law of Large Numbers"[Larson 1979]. Numerical integration methods and perturbation methods belong to the second category. Numerical integration methods suffer from the same disadvantage as simulation methods, in that they, too, can become prohibitively expensive, since the number of response solutions to be evaluated increases exponentially with the dimension N_a of the integrals to be approximated. In addition, both simulation and numer-

ical integration methods provide limited insight into the behavior and sensitivity of the system under different parameter uncertainties. Perturbation techniques, on the other hand, have been very attractive because of their computational efficiency, and also because they are easily integrated into existing computer codes of deterministic structural dynamics. The most severe drawback of perturbation methods is that they can become very inaccurate when the assumed parameter uncertainties are not sufficiently "small" [Liu et al., 1988a]. This disadvantage becomes particularly significant when problems of dynamic nature are analyzed, as will be shown in the next section, where the most commonly employed perturbation method, known as the second moment approach, is presented.

2.5.1 Second Moment Approach

The second moment approach (SMA) is an approximate perturbation method often used to evaluate the first two moments of a function of uncertain variables. It is based on a truncated Taylor series expansion of the function about the expected value of its uncertain variables; only terms up to second order are retained [Ditlevsen 1981]. This function approximation is used later to derive its first two moments. To clarify ideas, consider the particular case where the first two moments of q_j are desired. Expanding $q_j(\underline{a})$ in a Taylor series about the expected value $\underline{\bar{a}}$ of its uncertain parameter vector $\underline{a}$, and retaining the first three terms only, we obtain:

$$q_j(\underline{a}) \cong q_j(\underline{\bar{a}}) + \sum_{k=1}^{N_a} \left(\left. \frac{\partial q_j(\underline{a})}{\partial a_k} \right|_{\underline{a}=\underline{\bar{a}}} (a_k - \bar{a}_k) \right) + \frac{1}{2} \sum_{k=1}^{N_a} \sum_{l=1}^{N_a} \left(\left. \frac{\partial^2 q_j(\underline{a})}{\partial a_k \partial a_l} \right|_{\underline{a}=\underline{\bar{a}}} (a_k - \bar{a}_k)(a_l - \bar{a}_l) \right) \tag{2.5.1}$$

By replacing $q_j(\underline{a})$ in (2.4.12) and (2.4.14) with the above approximation, the SMA approximate expressions for the expected value and the variance of q_j are

obtained:

$$\bar{q}_j \cong q_j(\underline{\bar{a}}) + \frac{1}{2}\sum_{k=1}^{N_a}\sum_{l=1}^{N_a}\left(\left.\frac{\partial^2 q_j(\underline{a})}{\partial a_k \partial a_l}\right|_{\underline{a}=\underline{\bar{a}}} \mathrm{Cov}(a_k, a_l)\right) \tag{2.5.2}$$

$$\mathrm{Var}(q_j) \cong \sum_{k=1}^{N_a}\sum_{l=1}^{N_a}\left(\left.\frac{\partial q_j(\underline{a})}{\partial a_k}\right|_{\underline{a}=\underline{\bar{a}}} \left.\frac{\partial q_j(\underline{a})}{\partial a_l}\right|_{\underline{a}=\underline{\bar{a}}} \mathrm{Cov}(a_k, a_l)\right) \tag{2.5.3}$$

Under the assumptions of (2.4.1):

$$\mathrm{Cov}(a_k, a_l) = \delta_{kl} \tag{2.5.4}$$

where δ_{kl} is the Kronecker delta function. Therefore, Equations (2.5.2) and (2.5.3) can be simplified:

$$\bar{q}_j \cong q_j(\underline{\bar{a}}) + \frac{1}{2}\sum_{k=1}^{N_a}\left.\frac{\partial^2 q_j(\underline{a})}{(\partial a_k)^2}\right|_{\underline{a}=\underline{\bar{a}}} \mathrm{Var}(a_k) \tag{2.5.5}$$

$$\mathrm{Var}(q_j) \cong \sum_{k=1}^{N_a}\left(\left.\frac{\partial q_j(\underline{a})}{\partial a_k}\right|_{\underline{a}=\underline{\bar{a}}}\right)^2 \mathrm{Var}(a_k) \tag{2.5.6}$$

It is important to note that all that is required by the SMA method for calculation of the first two moments of a function of uncertain variables is the mean value and the covariance matrix of the uncertain parameters. In contrast, both simulation and numerical integration methods require knowledge of the joint probability density function $\pi_{\underline{a}}(\underline{a})$. The accuracy of the SMA method is controlled by the variance of its uncertain parameters; the smaller these variances, the better the accuracy, since the approximation of $q_j(\underline{a})$ by the truncated Taylor series expansion of (2.5.1) becomes more accurate as $|\underline{a} - \underline{\bar{a}}|$ becomes smaller. The important question of how "small" the parameter variances have to be in order to obtain acceptable accuracy using SMA has not yet been fully resolved.

In the next section, an application using SMA is illustrated. It will be shown that even for the case of "reasonable" parameter uncertainty, viewed from a preliminary design standpoint, SMA can lead to very inaccurate results when applied to problems of structural dynamics.

2.5.2 An Application Using SMA

Consider a one-story building subjected to base excitation and represented by the viscously damped SDOF linear model of Figure 2.2. Assuming zero initial conditions, this model can be expressed mathematically by the differential equation:

$$\ddot{q} + 2\zeta\omega\dot{q} + \omega^2 q = -\ddot{z}(t) \; ; \; q(0) = 0, \; \dot{q}(0) = 0 \tag{2.5.7}$$

where $\omega = \sqrt{\frac{k}{m}}$ is the natural frequency of oscillation and $\zeta = \frac{c}{2m\omega}$ is the damping ratio. Assume, for illustrative purposes, that the damping ratio ζ is deterministically known, while the frequency ω is uncertain, with a mean value $E[\omega] = \bar{\omega}$ and a variance $\mathrm{Var}(\omega) = \sigma_\omega^2$. This is a case of a single uncertain parameter, $\underline{a} = [\omega]$. The truncated Taylor expansion of (2.5.1) becomes:

$$q(t,\omega) \cong q_0(t) + q_1(t)(\omega - \bar{\omega}) + \frac{1}{2}q_2(t)(\omega - \bar{\omega})^2 \tag{2.5.8}$$

where

$$q_0(t) \equiv q(t;\bar{\omega}), \; q_1(t) \equiv \left.\frac{\partial q(t;\omega)}{\partial \omega}\right|_{\omega=\bar{\omega}} \text{ and } q_2(t) \equiv \left.\frac{\partial^2 q(t;\omega)}{\partial \omega^2}\right|_{\omega=\bar{\omega}} \tag{2.5.9}$$

The differential equations for $q_0(t), q_1(t)$ and $q_2(t)$ are given by:

$$\ddot{q}_0 + 2\zeta\bar{\omega}\dot{q}_0 + \bar{\omega}^2 q_0 = -\ddot{z}(t) \; ; q_0(0) = 0 \; , \; \dot{q}_0(0) = 0 \tag{2.5.10}$$

$$\ddot{q}_1 + 2\zeta\bar{\omega}\dot{q}_1 + \bar{\omega}^2 q_1 = -2\zeta\dot{q}_0 - 2\bar{\omega}q_0 \; ; \; q_1(0) = 0 \; , \; \dot{q}_1(0) = 0 \tag{2.5.11}$$

$$\ddot{q}_2 + 2\zeta\bar{\omega}\dot{q}_2 + \bar{\omega}^2 q_2 = -4\zeta\dot{q}_1 - 4\bar{\omega}q_1 - 2q_0 \; ; \; q_2(0) = 0 \; , \; \dot{q}_2(0) = 0 \tag{2.5.12}$$

Equations (2.5.11) and (2.5.12) are obtained through two consecutive differentiations of (2.5.7), with respect to ω, followed by the replacement of ω with $\bar{\omega}$. Note that the differential equations (2.5.10), (2.5.11), and (2.5.12) governing the terms of the Taylor series are identical, except for the nonhomogenous terms.

The first two moments of $q(t)$ are given according to (2.5.5) and (2.5.6) by:

$$\bar{q}(t) \simeq q_0(t) + \frac{1}{2}q_2(t)\mathrm{Var}(\omega) \tag{2.5.13}$$

and

$$\mathrm{Var}(q(t)) \simeq q_1^2(t)\mathrm{Var}(\omega) \tag{2.5.14}$$

To evaluate the accuracy of the SMA method, a specific numerical example is examined in the next section.

2.5.3 Numerical Example and Evaluation of SMA

Let $\zeta = 0.05$ be the fixed value of the damping ratio, and let the uncertain natural frequency ω be uniformly distributed over the interval $\Omega = [1.7\pi, 2.3\pi]\frac{rad}{sec}$. The resulting expected frequency is $\bar{\omega} = 2\pi\frac{rad}{sec} = 1.0\ Hz$, and the standard deviation is $\sigma_\omega = 0.1732\pi\frac{rad}{sec} = 0.0866\ Hz$. To quantify the uncertainty of a parameter, its coefficient of variation is often used; in this case $\alpha_\omega = \frac{\sigma_\omega}{\bar{\omega}} = 8.66\%$. The base acceleration is taken to be the 1940 El Centro earthquake record, NS component, shown in Figure 2.3. The mean model response $\bar{q}(t)$ and its coefficient of variation $\sigma_q(t) = \mathrm{Var}(q(t))^{\frac{1}{2}}$ are calculated by using both the SMA method and the numerical integration method, and are presented in Figure 2.4 and Figure 2.5. The results of the numerical integration method are assumed to be accurate, since convergence was monitored and achieved. It becomes obvious by viewing these last two figures that the SMA method performs very poorly, although the given coefficient of variation α_ω corresponds to reasonable levels of expected uncertainty for the preliminary design stage.

In Figure 2.6, the cause of the previous poor approximations is depicted. The model response at $t = 5\ sec$ is plotted against the model's natural frequency ω, over part of the frequency range Ω; the solid curve corresponds to the exact case representing the left hand side of (2.5.8), while the dashed-dotted parabola corresponds to the approximation assumed by the truncated Taylor series expansion given by the right hand side of (2.5.8). It can be seen that the truncated Taylor series cannot follow the oscillatory character of $q(t;\omega)$. To overcome this weakness of the SMA method, a new method under the name Fourier Series Ap-

proach has been developed [Beck and Katafygiotis, 1989]. This method is based on the expansion of the model response in a truncated Fourier series rather than a truncated Taylor series, as done in the SMA method.

Figure 2.7 examines the dependence of the expected model response and its coefficient of variation on the particular probability distribution assumed for the uncertain frequency ω. The solid curves correspond to the earlier assumed uniform distribution for ω, while the dashed-dotted curves correspond to ω being Gamma distributed with the same first two moments as in the uniform case. Both sets of curves are obtained using the numerical integration method. By comparing these two sets of curves, it can be concluded that knowledge of the first two moments of the uncertain parameter are adequate to approximate the first two moments of the uncertain response.

It can be concluded from the results obtained for the numerical example studied in this section that the SMA method, when applied to problems of dynamic response can be quite inaccurate, even for medium or small parameter uncertainties; nevertheless, this should not diminish the value of the SMA method when applied to problems of non-oscillatory character. The need for the development of a new approximate method to calculate the statistics of the dynamic response of a structural system with uncertain parameters is evident. The desired method should be accurate and efficient, and able to account for multi-degree of freedom systems. Such a method has been developed and is presented in the rest of this chapter for the class of linear, classically damped, multi-degree of freedom models with uncertain parameters; in the next section, this class of models is defined and some of its primary features are reviewed.

2.6 A Class of Linear Structural Models

Consider the class $\mathcal{M}_{N_d}$ of N_d-degree of freedom linear structural models, defined by the following equation of motion:

$$M\ddot{\underline{q}} + C\dot{\underline{q}} + K\underline{q} = -M\underline{b}\ddot{z}(t) \quad ; \quad \underline{q}(0) = \underline{q}_0, \dot{\underline{q}}(0) = \dot{\underline{q}}_0 \tag{2.6.1}$$

This mathematical model can be viewed as an idealization of a structural system which consists of a distribution of lumped masses linked by linear, massless springs and dashpots, sitting on a rigid base which is moving in only one direction, with an acceleration $\ddot{z}(t)$. The $N_d \times N_d$ matrices M, C, and K are the mass, the damping and the stiffness matrix, respectively. The vector $\underline{q} = [q_1, q_2, \ldots, q_{N_d}]^T$ consists of the generalized displacements relative to the base of each degree of freedom. while
$\underline{q} + \underline{b}z$ represent the corresponding total or absolute generalized displacements. The components of the vector $\underline{b} = [b_1, b_2, \ldots, b_{N_d}]^T$ are called pseudo-static influence coefficients, and they are known from the prescribed geometry of the structural model.

The theoretical model given by Equation (2.6.1) is often used as a planar model for buildings. In this case, all degrees of freedom represent horizontal displacements parallel to a fixed vertical plane at points in the structure, and $\ddot{z}$ is taken to be the horizontal component of the base acceleration parallel to this fixed plane; in this case all the components of $\underline{b}$ are unity:

$$\underline{b} = [1, 1, \ldots, 1]^T \tag{2.6.2}$$

The parameters of the theoretical model given by Equation (2.6.1) are the elements of M, C, and K, and the components of the initial conditions $\underline{q}_0$ and $\dot{\underline{q}}_0$. The following section reviews certain restrictions and the uncertainties regarding the choice of the values of these parameters.

2.6.1 Uncertainty and Allowable Values of the Model Parameters

There are certain physical properties that must be reflected by the theoretical model of (2.6.1) which impose restrictions on the allowable values of its parameters. In the case of uncertain parameters, these restrictions also affect the choice of the corresponding probability density function; for example, the pdf $\pi_{a_j}(a_j)$ of an uncertain parameter a_j, which is restricted to remain positive has to satisfy:

$$\pi_{a_j}(a_j) = 0 \quad \text{for } a_j \leq 0 \tag{2.6.3}$$

Also, there are different degrees of uncertainty associated with the different parameters for the class $\mathcal{M}_{N_d}$, so that the uncertainties associated with some of the parameters can be neglected, and the corresponding parameters are treated as being deterministic.

1) Mass Matrix The mass matrix M is assumed to be diagonal and positive definite:

$$M = \begin{bmatrix} m_1 & 0 & \cdots & 0 \\ 0 & m_2 & \cdots & 0 \\ \vdots & \vdots & \ddots & \vdots \\ 0 & 0 & \cdots & m_{N_d} \end{bmatrix} \; ; \; m_i > 0 \tag{2.6.4}$$

There is much less uncertainty when estimating the values of the lumped masses m_i, using the structural drawings, than when estimating the values of the elements of the damping or the stiffness matrix. Therefore, the elements m_i of M are usually assumed to be deterministic.

2)Damping Matrix The damping matrix $C = [c_{ij}]$ is required to be symmetric and positive semi-definite:

$$C = C^T \tag{2.6.5}$$

and

$$\underline{\dot{x}}^T C \underline{\dot{x}} \geq 0 \qquad \forall \; \underline{\dot{x}} \in R^{N_d} \tag{2.6.6}$$

It is assumed that classically damped modes exist, which means that the mode-shapes are assumed to be the same in the damped and undamped case. Con-

sequently, the modeshapes must be generalized eigenvectors of both K and C with respect to M, which is equivalent to requiring $M^{-1}K$ and $M^{-1}C$ to be commutative (Caughey and O'Kelly, 1965):

$$CM^{-1}K = KM^{-1}C \tag{2.6.7}$$

The values of the damping elements c_{ij} cannot be constructed by synthesis from the structural drawings; instead, their values can be recovered from the empirically estimated values of the modal damping ratios. Therefore, uncertainties concerning the damping of a structural model will be accounted for by regarding uncertainties of the more "physically meaningful" modal damping ratios ζ_i, rather than uncertainties of the elements c_{ij}.

3) Stiffness Matrix The stiffness matrix $K = [k_{ij}]$ is required to be symmetric and positive definite:

$$K = K^T \tag{2.6.8}$$

and

$$x^T K x > 0 \quad \forall\, \underline{x} \in R^{N_d} \tag{2.6.9}$$

There are uncertainties associated with estimating the values of each of the k_{ij}'s. Instead of modeling the possibly large number of uncertain parameters k_{ij}, which are possibly correlated to each other, the stiffness matrix will be parameterized by introducing the parameters $\theta_i, i = 1, \ldots, N_\theta$, so that:

$$K = K_0 + \sum_{i=1}^{N_\theta} \theta_i K_i \tag{2.6.10}$$

The new uncertain dimensionless parameter θ_i scales the stiffness contribution K_i of a certain substructure to the total stiffness matrix; K_0 accounts for the stiffness contributions of the substructures with deterministic stiffnesses. It is assumed that the $K_i, i = 0, 1, \ldots, N_\theta$ are all symmetric positive semi-definite $N_d \times N_d$ matrices. Each $\theta_i, i = 1, 2, \ldots, N_\theta$ is assumed to take nonnegative values, and

therefore its corresponding pdf must satisfy:

$$\pi_{\theta_i}(\theta_i) = 0 \quad \text{for} \quad \theta_i < 0 \; ; \; i = 1, 2, \ldots, N_\theta \tag{2.6.11}$$

The expected value of the scaling parameters is usually taken to be unity:

$$\bar{\theta}_i \equiv E[\theta_i] = 1 \quad ; \quad i = 1, 2, \ldots, N_\theta \tag{2.6.12}$$

which assumes that each of the K_i's is the expected contribution of a given substructure to the total stiffness matrix. The K_i's might be based on a finite-element model of the structure, for example.

4) Initial Conditions The initial conditions $\underline{q}_0$ and $\dot{\underline{q}}_0$ will be treated as being deterministically known. Usually, it will be assumed that the system starts from rest; in this case, $\underline{q}_0 = \dot{\underline{q}}_0 = \underline{0}$.

It is convenient to rewrite Equation (2.6.1) using a modal formulation, since the equations of motion obtained are uncoupled.

2.6.2 Modal Analysis

Let $\Phi = [\underline{\phi}^{(1)}, \underline{\phi}^{(2)}, \ldots, \underline{\phi}^{(N_d)}]^T$ denote the modeshape matrix, whose columns are the generalized eigenvectors of K, so that:

$$K\underline{\phi}^{(r)} = \omega_r^2 M \underline{\phi}^{(r)} \quad ; \quad r = 1, \ldots, N_d \tag{2.6.13a}$$

or

$$K\Phi = M\Phi\Omega^2 \tag{2.6.13b}$$

where

$$\Omega^2 \equiv \begin{bmatrix} \omega_1^2 & 0 & \cdots & 0 \\ 0 & \omega_2^2 & \cdots & 0 \\ \vdots & \vdots & \ddots & \vdots \\ 0 & 0 & \cdots & \omega_{N_d}^2 \end{bmatrix}$$

and $\omega_r > 0$, $r = 1, 2, \ldots, N_d$ are the modal frequencies in an ascending order; that is: $\omega_r \leq \omega_s$ for $r < s$. If $\omega_r \neq \omega_s$, it is easy to show that:

$$\underline{\phi}^{(r)^T} M \underline{\phi}^{(s)} = 0 \tag{2.6.14}$$

In the case of repeated modal frequencies, when $\omega_r = \omega_s$, the $\underline{\phi}^{(r)}$ and $\underline{\phi}^{(s)}$ can still be chosen so that (2.6.14) holds. Therefore, the modeshape matrix Φ can be assumed to be orthogonal with respect to the mass matrix M:

$$\bar{M} \equiv \Phi^T M \Phi = \begin{bmatrix} \bar{m}_1 & 0 & \cdots & 0 \\ 0 & \bar{m}_2 & \cdots & 0 \\ \vdots & \vdots & \ddots & \vdots \\ 0 & 0 & \cdots & \bar{m}_{N_d} \end{bmatrix} \tag{2.6.15}$$

The diagonal matrix $\bar{M}$ is the so-called generalized mass matrix. Furthermore, the modeshapes can be normalized so that they constitute an orthonormal basis for R^{N_d} with respect to M:

$$\bar{M} \equiv \Phi^T M \Phi = I \tag{2.6.16a}$$

or

$$\sum_{i=1}^{N_d} m_i \phi_i^{(r)} \phi_i^{(s)} = \delta_{rs} \tag{2.6.16b}$$

where I is the identity matrix of order N_d. Because of the assumption that classically damped modes exist, it can be shown that the columns of Φ are also generalized eigenvectors of C, so:

$$C\underline{\phi}^{(r)} = d_r M \underline{\phi}^{(r)} \quad ; \quad r = 1, 2, \ldots, N_d \tag{2.6.17a}$$

or

$$C\Phi = M\Phi D \tag{2.6.17b}$$

where

$$D \equiv \begin{bmatrix} d_1 & 0 & \cdots & 0 \\ 0 & d_2 & \cdots & 0 \\ \vdots & \vdots & \ddots & \vdots \\ 0 & 0 & \cdots & d_{N_d} \end{bmatrix}$$

The modal damping ratios are defined by:

$$\zeta_r = \frac{d_r}{2\omega_r} \quad ; \quad r = 1, 2, \ldots, N_d \tag{2.6.18}$$

Since C is positive semi-definite, $d_r \geq 0$ and hence, $\zeta_r \geq 0$, $r = 1,2,\ldots,N_d$. Premultiplying Equations (2.6.13b) and (2.6.17b) by Φ^T, and using Equation (2.6.15), we obtain:

$$\Phi^T K \Phi = \bar{M}\Omega^2 \tag{2.6.19}$$

and

$$\Phi^T C \Phi = \bar{M} D \tag{2.6.20}$$

Since the eigenvectors $\underline{\phi}^{(r)}$ form a basis for the N_d-dimensional space R^{N_d}, the generalized displacement vector function $\underline{q}(t)$ in Equation (2.6.1) can be written as:

$$\underline{q}(t) = \Phi \underline{\xi}(t) = \sum_{r=1}^{N_d} \xi_r(t) \underline{\phi}^{(r)} \tag{2.6.21}$$

where $\underline{\xi}(t)$ is the vector of coordinates of $\underline{q}(t)$ with respect to the basis formed by the eigenvectors $\underline{\phi}^{(r)}$, $r = 1,2,\ldots N_d$. Substituting (2.6.21) into (2.6.1) we obtain:

$$M\Phi\ddot{\underline{\xi}} + C\Phi\dot{\underline{\xi}} + K\Phi\underline{\xi} = -M\underline{b}\ddot{z}(t) \tag{2.6.22}$$

Premultiplying (2.6.22) by Φ^T, and using Equations (2.6.15), (2.6.19), and (2.6.20), we obtain:

$$\ddot{\underline{\xi}} + D\dot{\underline{\xi}} + \Omega^2\underline{\xi} = -\underline{\alpha}\ddot{z}(t) \tag{2.6.23}$$

where $\underline{\alpha}$ is the vector of modal participation factors given by:

$$\underline{\alpha} \equiv \bar{M}^{-1}\Phi^T M\underline{b} = \Phi^{-1}\underline{b} \tag{2.6.24}$$

The initial conditions for Equation (2.6.23) are given by:

$$\underline{\xi}(0) = \Phi^{-1}\underline{q}(0) \quad , \quad \dot{\underline{\xi}}(0) = \Phi^{-1}\dot{\underline{q}}(0) \tag{2.6.25}$$

In component form (2.6.23) becomes:

$$\ddot{\xi}_r + 2\zeta_r\omega_r\dot{\xi}_r + \omega_r^2\xi_r = -\alpha_r\ddot{z}(t) \quad ; \quad r = 1,2,\ldots,N_d \tag{2.6.26}$$

Define $q_i^{(r)}(t)$, the contribution to q_i from the r^{th} mode, by:

$$q_i^{(r)}(t) = \xi_r(t)\phi_i^{(r)} \tag{2.6.27}$$

so that (2.6.21) may be rewritten:

$$q_i(t) = \sum_{r=1}^{N_d} q_i^{(r)}(t) \quad ; \quad i = 1, 2, \ldots, N_d \tag{2.6.28}$$

Equation (2.6.26) leads to:

$$\ddot{q}_i^{(r)}(t) + 2\zeta_r\omega_r\dot{q}_i^{(r)} + \omega_r^2 q_i^{(r)} = -\beta_i^{(r)}\ddot{z}(t) \tag{2.6.29}$$

where

$$\beta_i^{(r)} = \phi_i^{(r)}\alpha_r \tag{2.6.30}$$

The parameter $\beta_i^{(r)}$ is called the "effective participation factor" for the r^{th} mode at the i^{th} degree-of-freedom, and it is independent of the normalization chosen for $\underline{\phi}^{(r)}$, such as that given by Equation (2.6.16b) [Beck 1978]. Let B denote the matrix of effective participation factors, that is, $[B]_{ij} = \beta_i^{(j)}$. Since the r^{th} column of B corresonds to the r^{th} modeshape appropriately scaled, B can be viewed as a particular choice of the modeshape matrix Φ. Notice that the effective participation factors satisfy the following constraints, which follow from (2.6.24) and (2.6.30):

$$\sum_{r=1}^{N_d} \beta_i^{(r)} = \sum_{r=1}^{N_d} \phi_i^{(r)}\alpha_r = (\Phi\underline{\alpha})_i = b_i \tag{2.6.31}$$

Assuming a model in $\mathcal{M}_{N_d}$ with known mass, damping and stiffness matrix leads, by solving the corresponding eigenvalue problem, to a unique set of modal parameters $\{\omega_r, \zeta_r, \beta_i^{(r)}; i, r = 1, \ldots, N_d\}$. Conversely, it can be shown that knowing the above set of modal parameters, and for a given mass matrix M, a unique stiffness and damping matrix can be determined, given by:

$$K = MB\Omega^2 B^{-1} = MB\Omega^2(B^T MB)^{-1}B^T M \tag{2.6.32a}$$

and

$$C = MBDB^{-1} = MBD(B^TMB)^{-1}B^TM \tag{2.6.32b}$$

In component form, these equations become:

$$k_{ij} = m_i m_j \sum_{r=1}^{N_d} \frac{\omega_r^2 \beta_i^{(r)} \beta_j^{(r)}}{\sum_{k=1}^{N_d} m_k (\beta_k^{(r)})^2} \tag{2.6.33a}$$

and

$$c_{ij} = 2m_i m_j \sum_{r=1}^{N_d} \frac{\zeta_r \omega_r \beta_i^{(r)} \beta_j^{(r)}}{\sum_{k=1}^{N_d} m_k (\beta_k^{(r)})^2} \tag{2.6.33b}$$

The initial conditions for (2.6.29) are given by:

$$q_i^{(r)}(0) = \xi_r(0)\phi_i^{(r)} \quad , \quad \dot{q}_i^{(r)}(0) = \dot{\xi}_r(0)\phi_i^{(r)} \tag{2.6.34}$$

where $\xi_r(0)$ and $\dot{\xi}_r(0)$ are given by (2.6.25).

Often, when the dynamic response of models with large numbers of degrees of freedom is examined, the contribution of the higher modes is negligible. Therefore, assuming that only the contribution of the first $N_m \leq N_d$ modes is considered, the sum in Equation (2.6.28) is approximated by:

$$q_i(t) \cong \sum_{r=1}^{N_m} q_i^{(r)}(t) \tag{2.6.35}$$

Equation (2.6.35), along with Equations (2.6.29) and (2.6.30), constitute the main steps of a modal analysis to solve for the dynamic response $\underline{q}(t)$ of the theoretical model of (2.6.1). The parameters involved in solving for the response $q_i(t)$ at the i^{th} degree of freedom, using this modal formulation, are: $\{\omega_r, \zeta_r, \beta_i^{(r)}, q_i^{(r)}(0), \dot{q}_i^{(r)}(0) : \ r = 1, 2, \ldots, N_m\}$. Of these parameters, the initial conditions $q_i^{(r)}(0), \dot{q}_i^{(r)}(0)$ will be considered deterministically known, according to the discussion in Section 2.6.1. According to the same discussion, the uncertainty in the damping forces is introduced as uncertainty in the values of the modal damping ratios ζ_r, rather than as uncertainty in the elements of the

damping matrix. Finally, the modal frequencies ω_r and the effective participation factors $\beta_i^{(r)}$ are functions of the uncertain parameters $\underline{\theta}$ involved in estimating the stiffness matrix K [see Equation (2.6.10)]; therefore, their uncertainties will be estimated from the uncertainties of the θ_i's.

From the above, it can be concluded that the vector of the original uncertain parameters $\underline{a}$ involved in the analysis of the N_d-degree of freedom structural model of (2.6.1) consists of the vector of the uncertain stiffness parameters $\underline{\theta} = [\theta_1, \theta_2, \ldots, \theta_{N_\theta}]^T$ and the vector of the uncertain modal damping ratios $\underline{\zeta} = [\zeta_1, \zeta_2, \ldots, \zeta_{N_m}]^T$. The domain of each of the ζ_i's and θ_i's must be a subset of the non-negative real axis: $\underline{\zeta} \in S(\underline{\zeta}) \subseteq [0, \infty)^{N_m}$ and $\underline{\theta} \in S(\underline{\theta}) \subseteq [0, \infty)^{N_\theta}$, where $S(\underline{\zeta}), S(\underline{\theta})$ are the domains of $\underline{\zeta}$ and $\underline{\theta}$, respectively.

Often, the additional constraint of the existence of "oscillatory modes" is assumed, which means that each mode is less than critically damped; in this case, $\underline{\zeta} \in S(\underline{\zeta}) \subseteq [0, 1)^{N_m}$. In the following section, the probabilistic modeling of the original uncertain parameters $\underline{a}$ is addressed. This will be followed by a discussion on the evaluation of the uncertainties of parameters dependent on $\underline{\theta}$, such as the modal frequencies $\omega_r = \omega_r(\underline{\theta})$, and the effective participation factors $\beta_i^{(r)} = \beta_i^{(r)}(\underline{\theta})$.

2.7 Probabilistic Modeling of Original Uncertain Parameters

As discussed in the previous section, it is assumed that the original uncertain parameters are: $\underline{a} = [\theta_1, \theta_2, \ldots, \theta_{N_\theta}, \zeta_1, \zeta_2, \ldots, \zeta_{N_m}]^T$. The uncertainties of the other modal parameters controlling the dynamic response will be evaluated in terms of the uncertainties of these $N_a = N_m + N_\theta$ parameters. It is assumed that knowing one parameter a_j does not influence judgement of the plausibilities of the values of the remaining parameters, so the parameters are mutually irrelevant to one another, and their pdf's can be specified independently. Therefore, the joint pdf $\pi_{\underline{a}}(\underline{a})$ can be expressed according to Equation (2.4.1) as a product of

the separate pdf's $\pi_{a_j}(a_j)$, $j = 1,2,\ldots,N_a$. Since each of the a_j's is defined only for nonnegative values, the choice of π_{a_j} must satisfy (2.6.3). Such a probability density function is given by the Gamma distribution $g(a_j;\mu_{a_j},\nu_{a_j})$ defined by:

$$\begin{aligned}\pi_{a_j}(a_j) = g(a_j;\mu_{a_j},\nu_{a_j}) &= \frac{\mu_{a_j}^{\nu_{a_j}}}{\Gamma(\nu_{a_j})} a_j^{\nu_{a_j}-1} e^{-\mu_{a_j} a_j} \quad ; \quad a_j \geq 0 \\ &= 0 \quad ; \quad a_j < 0\end{aligned} \tag{2.7.1}$$

where $\nu_{a_j} > 0$, $\mu_{a_j} > 0$ and $\Gamma(\nu_{a_j})$ is the Gamma function defined by:

$$\Gamma(\nu_{a_j}) = \int_0^\infty e^{-t} t^{\nu_{a_j}-1} dt \quad ; \quad \nu_{a_j} > -1 \tag{2.7.2}$$

The closed form solutions of the following broad class of integrals will prove important throughout the rest of this chapter:

$$\begin{aligned}&\int_0^\infty a_j^\beta e^{-\gamma a_j} \sin(\delta a_j) g(a_j;\mu_{a_j},\nu_{a_j}) da_j \\ &= \frac{\Gamma(\nu_{a_j}+\beta)}{\Gamma(\nu_{a_j})} \frac{\mu_{a_j}^{\nu_{a_j}}}{\left[(\gamma+\mu_{a_j})^2+\delta^2\right]^{\frac{\nu_{a_j}+\beta}{2}}} \sin\left[(\nu_{a_j}+\beta)\arctan\frac{\delta}{(\gamma+\mu_{a_j})}\right]\end{aligned} \tag{2.7.3a}$$

$$\begin{aligned}&\int_0^\infty a_j^\beta e^{-\gamma a_j} \cos(\delta a_j) g(a_j;\mu_{a_j},\nu_{a_j}) da_j \\ &= \frac{\Gamma(\nu_{a_j}+\beta)}{\Gamma(\nu_{a_j})} \frac{\mu_{a_j}^{\nu_{a_j}}}{\left[(\gamma+\mu_{a_j})^2+\delta^2\right]^{\frac{\nu_{a_j}+\beta}{2}}} \cos\left[(\nu_{a_j}+\beta)\arctan\frac{\delta}{(\gamma+\mu_{a_j})}\right]\end{aligned} \tag{2.7.3b}$$

where $\beta > -(\nu_{a_j}+1)$ and $\gamma > -\mu_{a_j}$.

The expected value and the variance of a_j are given by:

$$\begin{aligned}\bar{a}_j \equiv E[a_j] &= \int_0^\infty a_j g(a_j;\mu_{a_j},\nu_{a_j}) da_j \\ &= \frac{\nu_{a_j}}{\mu_{a_j}}\end{aligned} \tag{2.7.4}$$

$$\sigma_{a_j}^2 \equiv \mathrm{Var}(a_j) \equiv E\left[(a_j - \bar{a}_j)^2\right] = \int_0^\infty (a_j - \bar{a}_j)^2 g(a_j; \mu_{a_j}, \nu_{a_j}) da_j = \frac{\nu_{a_j}}{\mu_{a_j}^2} \tag{2.7.5}$$

Given the expected value $\bar{a}_j$ and the standard deviation σ_{a_j}, the parameters μ_{a_j}, ν_{a_j} defining the corresponding Gamma distribution are given according to (2.7.4) and (2.7.5) by:

$$\mu_{a_j} = \frac{\bar{a}_j}{\sigma_{a_j}^2} = \frac{1}{\bar{a}_j \alpha_{a_j}^2}, \quad \nu_{a_j} = \frac{\bar{a}_j^2}{\sigma_{a_j}^2} = \frac{1}{\alpha_{a_j}^2} \tag{2.7.6}$$

where $\alpha_{a_j} \equiv \frac{\sigma_{a_j}}{\bar{a}_j}$, is the coefficient of variation of a_j.

In Figure 2.8a, the Gamma distribution of an uncertain variable a_j corresponding to one of the θ_i's is plotted, assuming $\bar{a}_j = 1$ and $\alpha_{a_j} = .10$; the corresponding values of the distribution parameters are $(\mu_{a_j}, \nu_{a_j}) = (100., 100.)$. In Figure 2.8b, the Gamma distribution is plotted for some typical values, assuming a_j corresponds to an uncertain damping ratio ζ_i; in this case, the assumed values are $\bar{a}_j = .05$ and $\alpha_{a_j} = .20$, with corresponding parameters $(\mu_{a_j}, \nu_{a_j}) = (500., 25.)$. In the following, Gamma distributions are chosen to represent each of the independent pdf's $\pi_{a_j}(a_j)$. For the a_j's which correspond to the uncertain damping ratios ζ_i's, an additional condition is required to ensure existence of oscillatory modes:

$$\pi_{a_j}(a_j) = 0 \quad \text{for} \quad a_j \geq 1 \quad ; \quad 1 \leq j \leq N_m \tag{2.7.7}$$

This last condition is practically satisfied for typical values of $\bar{\zeta}$ and α_ζ, as can be seen in Figure 2.8b.

2.8 Probabilistic Modeling of Uncertain Modal Parameters

Equation (2.6.28) and (2.6.29) play an important role in the analysis of the dynamic response of multi-degree of freedom linear structures. It can be

seen, by looking at Equation (2.6.29), that the uncertain parameters involved in calculating the response $\underline{q}$ are: the damping ratios $\underline{\zeta} = [\zeta_1, \zeta_2, \ldots, \zeta_{N_m}]^T$, the natural frequencies $\underline{\omega} = [\omega_1, \omega_2, \ldots \omega_{N_m}]^T$, and the effective participation factors $\beta = [\beta_1^{(1)}, \ldots, \beta_1^{(N_m)}, \beta_2^{(1)}, \ldots, \beta_2^{(N_m)}, \ldots, \beta_{N_d}^{(N_m)}]^T$. As mentioned earlier, $\underline{\omega}$ and $\underline{\beta}$ are functions of the uncertain parameters $\underline{\theta}$. Although the uncertainties in the θ_i's are assumed uncorrelated, this is not true for the elements of $\underline{\omega}$ and $\underline{\beta}$; therefore, the joint pdf $\pi_{\underline{\omega},\underline{\beta}}(\underline{\omega}, \underline{\beta})$ cannot be written as a product of independent pdf's of the elements of $\underline{\omega}$ and $\underline{\beta}$. On the other hand, since $\underline{\zeta}$ and $\underline{\theta}$ were assumed uncorrelated, so are $\underline{\zeta}$ and $[\underline{\omega}^T, \underline{\beta}^T]^T$. Several publications [Scheidt and Purkert, 1983; Collins and Thomson, 1969; Schiff and Bogdanoff, 1972a,b] investigated the uncertainties in the eigenvalues and eigenvectors due to uncertainties in the elements of the mass and stiffness matrices, using perturbation methods. Perturbation techniques perform well when analyzing eigenvalue problems with uncertain mass or stiffness parameters, since the eigenvalues and the eigenvector components are smooth functions of these parameters. To illustrate this, consider a linear three-story planar shear building, as shown in Figure 2.9 for the general N_d-story case, with uniform mass $m_i = m_0$, $i = 1, 2, 3$, and interstory stiffnesses $k_i = k_0\theta_i$, $i = 1, 2, 3$, where $k_0 = 2000 m_0 sec^{-2}$; in this particular case $N_\theta = N_d$. It is assumed here that $E[\theta_i] = 1$, $i = 1, 2, 3$, so that the expected stiffness distribution is a uniform one. Figure 2.10 shows the variation of the modal frequencies when each one of the θ_i's is, in turn, varied up to 50% from its expected value of unity, while all other θ_j's, $j \neq i$ are kept equal to unity. Similarly, Figure 2.11 shows the variation of the effective participation factors at each story for the different modes. As can be seen from these plots, all the corresponding curves are smooth, and can be approximated well by symmetric quadratic polynomials of the θ_i's:

$$\omega_r(\underline{\theta}) \cong c_{0,\omega_r} + \sum_{i=1}^{N_\theta} c_{i,\omega_r}\theta_i + \sum_{i=1}^{N_\theta}\sum_{j=1}^{N_\theta} c_{ij,\omega_r}\theta_i\theta_j \quad ; \quad r = 1, 2, \ldots, N_m \qquad (2.8.1a)$$

where

$$c_{ij,\omega_r} = c_{ji,\omega_r} \tag{2.8.1b}$$

and

$$\beta_k^{(r)}(\underline{\theta}) \simeq c_{0,\beta_k^{(r)}} + \sum_{i=1}^{N_\theta} c_{i,\beta_k^{(r)}}\theta_i + \sum_{i=1}^{N_\theta}\sum_{j=1}^{N_\theta} c_{ij,\beta_k^{(r)}}\theta_i\theta_j \quad ; \quad r = 1,2,\ldots,N_m \ , \ k = 1,2,\ldots,N_d \tag{2.8.2a}$$

where

$$c_{ij,\beta_k^{(r)}} = c_{ji,\beta_k^{(r)}} \tag{2.8.2b}$$

In order to approximate a function $f(\underline{\theta})$ with a quadratic polynomial of the above form, the following vector of coefficients has to be evaluated:

$$\underline{c}_f = [c_{0,f}, c_{1,f}, \ldots, c_{N_\theta,f}, c_{11,f}, c_{12,f}, \ldots, c_{1N_\theta,f}, c_{22,f}, c_{23,f}, \ldots, c_{N_\theta N_\theta,f}]^T \tag{2.8.3}$$

The length of this vector is $N_l = 1 + N_\theta + \frac{N_\theta(N_\theta+1)}{2} = \frac{N_\theta^2+3N_\theta+2}{2}$. If $f(\underline{\theta})$ is expanded in a Taylor series about $\bar{\theta}$, it is easy to evaluate each of the elements of $\underline{c}_f$ in terms of the coefficients of this Taylor expansion, that is, in terms of $f(\bar{\theta})$, $\frac{\partial f}{\partial \theta_i}|_{\theta=\bar{\theta}}$, $\frac{\partial^2 f}{\partial \theta_i \partial \theta_j}|_{\theta=\bar{\theta}}$. There exist analytical expressions for evaluating the first and second order partial derivatives of the frequencies ω_r, and the modeshape components $\varphi_i^{(r)}$, with respect to the components of $\underline{\theta}$. The analytical expression for $\frac{\partial \omega_r}{\partial \theta_i}$ is derived in Appendix B, and it will be used widely in Chapter 3. It is desirable, however, that the sought quadratic polynomial approximates $f(\underline{\theta})$ well over the whole domain of interest of $\underline{\theta}$'s, rather than only locally, in the neighborhood of the expected value $\underline{\bar{\theta}}$. The domain of interest for the $\underline{\theta}$'s extends about the expected value $\underline{\bar{\theta}}$, and a few standard deviations σ_{θ_i} away in each θ_i direction. Therefore, the coefficients $\underline{c}_f$ are obtained by requiring the quadratic approximation to pass through N_l points $\left(\underline{\theta}^{(i)}, f(\underline{\theta}^{(i)})\right); i = 1,\ldots,N_l$. This requirement can be expressed as:

$$A\underline{c}_f = \underline{\tilde{f}} \tag{2.8.4}$$

where $\underline{c}_f$ is given by (2.8.3), $\underline{\tilde{f}}$ is a vector of length N_l:

$$\underline{\tilde{f}} = \left[f(\underline{\theta}^{(1)}), \ldots, f(\underline{\theta}^{(N_l)})\right]^T \tag{2.8.5}$$

and A is a $N_l \times N_l$ matrix given by:

$$A = \begin{bmatrix} \underline{\tilde{\theta}}^{(1)^T} \\ \underline{\tilde{\theta}}^{(2)^T} \\ \vdots \\ \underline{\tilde{\theta}}^{(N_l)^T} \end{bmatrix} \tag{2.8.6}$$

where $\underline{\tilde{\theta}}^{(i)}$ is a vector of length N_l:

$$\underline{\tilde{\theta}}^{(i)} = \left[1, \theta_1^{(i)}, \theta_2^{(i)}, \ldots, \theta_{N_\theta}^{(i)}, \theta_1^{(i)^2}, \theta_1^{(i)}\theta_2^{(i)}, \ldots, \theta_1^{(i)}\theta_{N_\theta}^{(i)}, \theta_2^{(i)^2}, \theta_2^{(i)}\theta_3^{(i)}, \ldots, \theta_{N_\theta}^{(i)^2}\right]^T \tag{2.8.7}$$

The remaining point of discussion for implementing the quadratic approximation for $f(\underline{\theta})$ is regarding the choice of the points $\underline{\theta}^{(i)}, i = 1, 2, \ldots, N_l$. One point is chosen to be the expected value $\underline{\bar{\theta}}$. Next, for each direction θ_i, two points are chosen at distance $\pm\gamma\sigma_{\theta_i}$ about $\underline{\bar{\theta}}$; that is: $\underline{\theta} = [\bar{\theta}_1, \ldots, \bar{\theta}_i \pm \gamma\sigma_{\theta_i}, \ldots, \bar{\theta}_{N_\theta}]^T$. The remaining $\frac{N_\theta(N_\theta-1)}{2}$ points are chosen to be about $\underline{\bar{\theta}}$, at distances $+\gamma\sigma_{\theta_i}$ and $+\gamma\sigma_{\theta_j}$ along the directions θ_i and θ_j, respectively, and for each possible combination of i and j; that is: $\underline{\theta} = [\bar{\theta}_1, \ldots, \bar{\theta}_i + \gamma\sigma_{\theta_i}, \ldots, \bar{\theta}_j + \gamma\sigma_{\theta_j}, \ldots, \bar{\theta}_{N_\theta}]^T$. Such a choice of points $\underline{\theta}^{(i)}, i = 1, 2, \ldots, N_l$, is schematically shown in Figure 2.12, for the case where $N_\theta = 3$. A good value for the parameter γ as shown in Appendix C is $\gamma = \sqrt{3}$.

Let $\underline{\tilde{\theta}} = \underline{\tilde{\theta}}(\underline{\theta})$ denote the following vector function:

$$\underline{\tilde{\theta}}(\underline{\theta}) = [1, \theta_1, \theta_2, \ldots, \theta_{N_\theta}, \theta_1^2, \theta_1\theta_2, \ldots, \theta_1\theta_{N_\theta}, \theta_2^2, \theta_2\theta_3, \ldots, \theta_{N_\theta}^2]^T \tag{2.8.8}$$

The quadratic approximation of $f(\underline{\theta})$ can then be expressed as:

$$f(\underline{\theta}) \simeq \underline{c}_f^T \underline{\tilde{\theta}}(\underline{\theta}) \tag{2.8.9}$$

The expected value of $f(\underline{\theta})$ is approximated by:

$$\bar{f}(\underline{\theta}) \equiv E[f(\underline{\theta})] \simeq \underline{c}_f^T \bar{\underline{\tilde{\theta}}} \tag{2.8.10}$$

where

$$\begin{aligned} \bar{\underline{\tilde{\theta}}} &\equiv E[\underline{\tilde{\theta}}(\underline{\theta})] \\ &= [1, \bar{\theta}_1, \bar{\theta}_2, \ldots, \bar{\theta}_{N_\theta}, \bar{\theta_1^2}, \bar{\theta}_1\bar{\theta}_2, \ldots, \bar{\theta}_1\bar{\theta}_{N_\theta}, \bar{\theta_2^2}, \bar{\theta}_2\bar{\theta}_3, \ldots, \bar{\theta_{N_\theta}^2}]^T \end{aligned} \tag{2.8.11}$$

where

$$\begin{aligned} \bar{\theta_i^2} &= E[\theta_i^2] = E[\theta_i]^2 + \sigma_{\theta_i}^2 \quad ; \quad i = 1, \ldots, N_\theta \\ \text{and for } i \neq j \qquad E[\theta_i\theta_j] &= E[\theta_i]E[\theta_j] = \bar{\theta}_i\bar{\theta}_j \end{aligned} \tag{2.8.12}$$

since the θ_i's are assumed to be independent distributed.

Similarly, $f(\theta)^2$ is approximated utilizing a quadratic polynomial:

$$f(\theta)^2 \simeq \underline{c}_{f^2}^T \tilde{\theta}(\underline{\theta}) \tag{2.8.13}$$

where the coefficients $\underline{c}_{f^2}$ are given by Equations (2.8.4) and (2.8.5), modified as follows:

$$A\underline{c}_{f^2} = \underline{\tilde{f}}^2 \tag{2.8.14}$$

where

$$\underline{\tilde{f}}^2 = \left[f(\underline{\theta}^{(1)})^2, \ldots, f(\underline{\theta}^{(N_l)})^2\right]^T \tag{2.8.15}$$

The approximation for the expected value of $f(\underline{\theta})^2$ is given, according to (2.8.10), by:

$$E[f(\underline{\theta})^2] \simeq \underline{c}_{f^2}^T \bar{\underline{\tilde{\theta}}} \tag{2.8.16}$$

Finally, the variance of $f(\underline{\theta})$ is approximated by combining (2.8.10) and (2.8.16):

$$\begin{aligned} \sigma_f^2 \equiv \mathrm{Var}\,(f(\underline{\theta})) &\equiv E\left[(f(\underline{\theta}) - \bar{f}(\underline{\theta}))^2\right] \\ &= E\left[f(\underline{\theta})^2\right] - \bar{f}(\underline{\theta})^2 \\ &= \underline{c}_{f^2}^T \bar{\underline{\tilde{\theta}}} - \left(\underline{c}_f^T \bar{\underline{\tilde{\theta}}}\right)^2 \end{aligned} \tag{2.8.17}$$

By applying the above steps to each modal frequency $\omega_r = \omega_r(\underline{\theta})$, approximations for its expected value $\bar{\omega}_r$ and its standard deviation σ_{ω_r} can be obtained. Furthermore, it is assumed that the marginal pdf of ω_r can be approximated well by the Gamma distribution $g(\omega_r; \mu_{\omega_r}, \nu_{\omega_r})$, where the parameters $\mu_{\omega_r}, \nu_{\omega_r}$ are chosen to correspond to $\bar{\omega}_r, \sigma_{\omega_r}$, according to (2.7.6). Figure 2.13 compares the marginal pdf for each modal frequency using the above discussed gamma distribution approximation, with the marginal pdf obtained through simulations, for the three-story shear model mentioned earlier in this section. Each θ_i in this example is assumed to be gamma distributed with $(\bar{\theta}_i, \alpha_{\theta_i}) = (1.0, 0.1)$; $i = 1, 2, 3$. It can be seen that the two curves compare very well.

When there are two closely spaced modes, it may occur that for different values of $\underline{\theta}$ the modal frequencies corresponding to two different modes of vibration switch order. This should be accounted for when the coefficients of the quadratic polynomials in (2.8.1a) and (2.8.2a) are sought, using (2.8.4) and (2.8.5). Specifically, the elements of the vector $\underline{\tilde{f}}$ in (2.8.5), as well as the elements of the row vectors of A given by (2.8.7), where f might represent ω_r or $\beta_k^{(r)}$, must correspond to the same physical mode of vibration, rather than to modes corresponding to frequencies with the same position in a sequence of ascending order.

It should be noted that the computational effort required to obtain a quadratic approximation of all the needed modal quantities amounts to solving for and storing the eigenvalues and eigenvectors corresponding to the first N_m modes of N_l eigenvalue problems, and to factorizing the matrix A given by (2.8.6). These calculations can be done rather efficiently.

The expected value and the variance of the effective participation factors $\beta_k^{(r)}$ can be evaluated similarly. The quadratic approximation (2.8.2a) for $\beta_k^{(r)}(\underline{\theta})$ performs well unless the curvature of $\beta_k^{(r)}(\underline{\theta})$ changes sharply. This may occur in the case of "almost" periodic structures where the "mode localization" phe-

nomenon occurs [Hodges 1982; Bendiksen 1986]. However, the required statistical information regarding the effective participation factors will be addressed in later sections.

2.9 SDOF Oscillator with Uncertain Frequency and Damping Ratio

Consider the differential equation (2.5.7) of a SDOF classically damped structural model with zero initial conditions. The solution of (2.5.7) is given by:

$$q(t;\omega,\zeta) = -\int_0^t h(\tau;\omega,\zeta)\ddot{z}(t-\tau)d\tau \tag{2.9.1}$$

where $h(\tau;\omega,\zeta)$ is the impulse response function:

$$h(\tau;\omega,\zeta) = \frac{1}{\omega_d}e^{-\zeta\omega\tau}\sin(\omega_d\tau) \tag{2.9.2}$$

and ω_d is the damped frequency:

$$\omega_d = \omega\sqrt{1-\zeta^2} \tag{2.9.3}$$

The expected value of $q(t)$ is given according to (2.4.12) by:

$$\begin{aligned}\bar{q}(t) \equiv E[q(t)] &= -\int_0^\infty\int_0^\infty\left[\int_0^t h(\tau;\omega,\zeta)\ddot{z}(t-\tau)d\tau\right]\pi_{\omega,\zeta}(\omega,\zeta)d\omega d\zeta \\ &= -\int_0^t \bar{h}(\tau)\ddot{z}(t-\tau)d\tau\end{aligned} \tag{2.9.4}$$

where $\bar{h}(\tau)$ is the expected impulse response function:

$$\bar{h}(\tau) = \int_0^\infty\int_0^\infty h(\tau;\omega,\zeta)\pi_{\omega,\zeta}(\omega,\zeta)d\omega d\zeta \tag{2.9.5}$$

Evaluating the two-dimensional integral (2.9.5) analytically, assuming that ω and ζ are uncorrelated, is generally not possible. If ζ is assumed fixed, then (2.9.5)

becomes a one-dimensional integral which can be evaluated analytically for particular choices of $\pi_\omega(\omega)$; such choices for $\pi_\omega(\omega)$, for example, are a truncated uniform or a Gamma distribution. In accordance with the previous two sections, it is assumed that the uncertain parameters ω and ζ, with known expected values and coefficients of variations, are probabilistically modeled by independent Gamma distributions, according to (2.7.1) and (2.7.6), so:

$$\pi_{\omega,\zeta}(\omega,\zeta) = \pi_\omega(\omega)\pi_\zeta(\zeta) = g(\omega;\mu_\omega,\nu_\omega)g(\zeta;\mu_\zeta,\nu_\zeta) \tag{2.9.6}$$

Equation (2.9.5) cannot be evaluated analytically for this choice of $\pi(\omega,\zeta)$, since it does not fall within the category prescribed by (2.7.3a or b).

The first step toward reaching a form which is amenable to analytical solution is dealing with the term $\sqrt{1-\zeta^2}$ appearing in ω_d. Approximating $\sqrt{1-\zeta^2}$ with the first two contributing terms of its Taylor expansion leads to:

$$\sqrt{1-\zeta^2} \simeq 1 - \frac{\zeta^2}{2} \tag{2.9.7}$$

It can be seen that approximations for its expected value and variance are:

$$E[\sqrt{1-\zeta^2}] \simeq 1 - \frac{E[\zeta^2]}{2} = 1 - \frac{\nu_\zeta(\nu_\zeta+1)}{2\mu_\zeta^2} \tag{2.9.8}$$

and

$$\mathrm{Var}\left(\sqrt{1-\zeta^2}\right) \simeq \frac{1}{4}\left(E[\zeta^4] - E^2[\zeta^2]\right) = \frac{\nu_\zeta(\nu_\zeta+1)(2\nu_\zeta+3)}{2\mu_\zeta^4} \tag{2.9.9}$$

Substituting into the above equation some typical values of uncertainty for ζ, it can be seen that the coefficient of variation of $\sqrt{1-\zeta^2}$ is much smaller than the coefficient of variation of ζ; for example, the values of Figure 2.8b ($\bar{\zeta} = 0.05, a_\zeta = 0.20$), with corresponding parameters $(\mu_\zeta,\nu_\zeta) = (500.,25.)$, result in $E[\sqrt{1-\zeta^2}] \simeq 0.9987$ and $\alpha_{\sqrt{1-\zeta^2}} \simeq 0.000526$. Therefore, $\sqrt{1-\zeta^2}$ can be considered as deterministic with value $\sqrt{1-E[\zeta^2]}$. As a result of this observation,

it can be concluded that the parameters $a_1 \equiv \omega_d = \omega\sqrt{1-\zeta^2}$ and $a_2 \equiv \frac{\zeta}{\sqrt{1-\zeta^2}}$ can also be treated as independent with the following statistics:

$$(\bar{a}_1, \alpha_{a_1}) = \left(\bar{\omega}\sqrt{1 - E[\zeta^2]}, \alpha_\omega\right) \tag{2.9.10}$$

$$(\bar{a}_2, \alpha_{a_2}) = \left(\bar{\zeta}/\sqrt{1 - E[\zeta^2]}, \alpha_\zeta\right) \tag{2.9.11}$$

Furthermore, it can be shown that the pdf's corresponding to the transformed parameters a_1, a_2 are still Gamma distributions (see Appendix D). Substituting (2.9.2) into (2.9.5) and using the transformed parameters a_1, a_2 we obtain:

$$\bar{h}(\tau) = \int_0^\infty \int_0^\infty \frac{1}{a_1} e^{-a_1 a_2 \tau} \sin(a_1\tau) g(a_1; \mu_{a_1}, \nu_{a_1}) g(a_2; \mu_{a_2}, \nu_{a_2}) da_1 da_2 \tag{2.9.12}$$

The coupling term $e^{-a_1 a_2 \tau}$ appearing in the above integral prohibits expressing (2.9.12) as a product of two one-dimensional integrals involving a_1 and a_2, respectively. By expanding $e^{-a_1 a_2 \tau}$ in a Taylor series about $(\bar{a}_1, \bar{a}_2)$, and by keeping only terms up to second order, we obtain:

$$\begin{aligned} e^{-a_1 a_2 \tau} &\simeq e^{-\bar{a}_1 \bar{a}_2 \tau} \left[1 - \bar{a}_2\tau(a_1 - \bar{a}_1) - \bar{a}_1\tau(a_2 - \bar{a}_2) + 0.5\left(\bar{a}_2^2\tau^2(a_1 - \bar{a}_1)^2\right.\right. \\ &\qquad \left.\left. + \bar{a}_1^2\tau^2(a_2 - \bar{a}_2)^2 + (\bar{a}_1\bar{a}_2\tau^2 - \tau)(a_1 - \bar{a}_1)(a_2 - \bar{a}_2)\right)\right] \\ &= c_{00} + c_{10}a_1 + c_{01}a_2 + c_{20}a_1^2 + c_{11}a_1a_2 + c_{02}a_2^2 \\ &= \sum_{i=0}^{2} \sum_{j=0}^{2-i} c_{ij} a_1^i a_2^j \end{aligned} \tag{2.9.13}$$

Substituting this approximation for $e^{-a_1 a_2 \tau}$ into (2.9.12) leads to:

$$\bar{h}(\tau) \simeq \sum_{i=0}^{2} \sum_{j=0}^{2-i} c_{ij} \bar{h}_{1,i}(\tau)\ \bar{h}_{2,j}(\tau) \tag{2.9.14}$$

where

$$\bar{h}_{1,i}(\tau) = \int_0^\infty a_1^{i-1} \sin(a_1\tau) g(a_1; \mu_{a_1}, \nu_{a_1}) da_1 \tag{2.9.15}$$

and

$$\bar{h}_{2,j}(\tau) = \int_0^\infty a_2^j g(a_2; \mu_{a_2}, \nu_{a_2}) da_2 \tag{2.9.16}$$

Notice that $\bar{h}_{1,i}(\tau)$ and $\bar{h}_{2,j}(\tau)$ can be evaluated analytically according to (2.7.3a or b).

An alternative approximate evaluation of $\bar{h}(\tau)$, requiring less computational effort than that required by employing the approximation (2.9.14), is described next. A new parameter $a_3 = a_1 a_2 = \omega\zeta$ is introduced, and, as an approximation, it is assumed that it is Gamma distributed with the following first two moments:

$$\bar{a}_3 = \bar{\omega}\bar{\zeta} \qquad \mathrm{Var}(a_3) = (\bar{\omega}\sigma_\zeta)^2 + (\bar{\zeta}\sigma_\omega)^2 + \sigma_\omega^2\sigma_\zeta^2 \tag{2.9.17}$$

Furthermore, as an additional approximation, it will be assumed that the transformed parameters a_1 and a_3 are uncorrelated. Equation (2.9.12) can be approximated using these parameters:

$$\bar{h}(\tau) \simeq \bar{h}_{1,0}(\tau)\bar{h}_3(\tau) \tag{2.9.18}$$

where $\bar{h}_{1,0}(\tau)$ is given by (2.9.15) and $\bar{h}_3(\tau)$ is given by:

$$\bar{h}_3(\tau) = \int_0^\infty e^{-a_3\tau} g(a_3; \mu_{a_3}, \nu_{a_3}) da_3 \tag{2.9.19}$$

Both $\bar{h}_{1,0}(\tau)$ and $\bar{h}_3(\tau)$ can be expressed analytically using (2.7.3a or b).

Figure 2.14 compares $\bar{q}(t)$ calculated from (2.9.4), using the approximation for $\bar{h}(\tau)$ given by (2.9.18), and $\bar{q}(t)$ calculated using numerical integration of (2.9.4) and (2.9.5), for a SDOF oscillator with independent Gamma distributions for ω and ζ, with $(\bar{\omega}, a_\omega) = (1Hz, 10\%)$, and $(\bar{\zeta}, a_\zeta) = (0.05, 20\%)$. The curves corresponding to the approximate and exact solutions are almost indistinguishable.

The expected value of $q^2(t)$ is given by:

$$E[q^2(t)] = \int_0^\infty \int_0^\infty \left[\int_0^t \int_0^t h(\tau_1;\omega,\zeta)h(\tau_2;\omega,\zeta)\ddot{z}(t-\tau_1)\ddot{z}(t-\tau_2)d\tau_1 d\tau_2 \right] \times \pi_{\omega,\zeta}(\omega,\zeta)d\omega d\zeta \tag{2.9.20}$$

$$= \int_0^t \int_0^t \tilde{h}(\tau_1,\tau_2)\ddot{z}(t-\tau_1)\ddot{z}(t-\tau_2)d\tau_1 d\tau_2$$

where

$$\tilde{h}(\tau_1,\tau_2) = \int_0^\infty \int_0^\infty h(\tau_1;\omega,\zeta)h(\tau_2;\omega,\zeta)\pi_{\omega,\zeta}(\omega,\zeta)d\omega d\zeta \tag{2.9.21}$$

In order to obtain an analytical expression of (2.9.21), a transformation of the variables (ω,ζ) to (a_1,a_2) or (a_1,a_3) is utilized as before. The computational effort required to approximate $\tilde{h}(\tau_1,\tau_2)$ is less if the set of variables (a_1,a_3) is used:

$$\tilde{h}(\tau_1,\tau_2) \simeq \tilde{h}_{1,0}(\tau_1,\tau_2)\tilde{h}_3(\tau_1,\tau_2) \tag{2.9.22}$$

where

$$\tilde{h}_{1,i}(\tau_1,\tau_2) = \frac{1}{2}\int_0^\infty a_1^{i-2}\cos\left(a_1(\tau_1-\tau_2)\right) g(a_1;\mu_{a_1},\nu_{a_1})da_1 - \frac{1}{2}\int_0^\infty a_1^{i-2}\cos\left(a_1(\tau_1+\tau_2)\right) g(a_1;\mu_{a_1},\nu_{a_1})da_1 \tag{2.9.23}$$

and

$$\tilde{h}_3(\tau_1,\tau_2) = \int_0^\infty e^{-a_3(\tau_1+\tau_2)} g(a_3;\mu_{a_3},\nu_{a_3})da_3 \tag{2.9.24}$$

Although only the evaluation of $\tilde{h}_{1,0}$ is required in (2.9.22), a general formula is given which will prove useful later. Notice that $\tilde{h}_{1,i}(\tau_1,\tau_2)$ and $\tilde{h}_3(\tau_1,\tau_2)$ can be expressed analytically using (2.7.3a or b).

Equation (2.9.20) can be evaluated using the Fourier Transform (FT) and the Convolution Theorem. The FT of a function of two variables $f(t_1,t_2)$ is given

by:

$$F(\xi_1,\xi_2) = \int_{-\infty}^{\infty}\int_{-\infty}^{\infty} f(t_1,t_2)e^{-i(\xi_1 t_1+\xi_2 t_2)}dt_1 dt_2 \tag{2.9.25}$$

while the Inverse Fourier Transform (IFT) is given by:

$$f(t_1,t_2) = \frac{1}{4\pi^2}\int_{-\infty}^{\infty}\int_{-\infty}^{\infty} F(\xi_1,\xi_2)e^{i(\xi_1 t_1+\xi_2 t_2)}d\xi_1 d\xi_2 \tag{2.9.26}$$

The Convolution Theorem for a function of two variables is expressed as follows:

$$\begin{aligned} &\text{If} \quad g(t_1,t_2) = \int_{-\infty}^{\infty}\int_{-\infty}^{\infty} f_1(\tau_1,\tau_2)f_2(t_1-\tau_1,t_2-\tau_2)d\tau_1 d\tau_2 \\ &\text{then} \quad G(\xi_1,\xi_2) = F_1(\xi_1,\xi_2)F_2(\xi_1,\xi_2) \end{aligned} \tag{2.9.27}$$

In order to use the Convolution Theorem (2.9.27), Equation (2.9.20) is rewritten:

$$\begin{aligned} E[q(t_1)q(t_2)] &= \int_0^{t_1}\int_0^{t_2} \tilde{h}(\tau_1,\tau_2)\ddot{z}(t_1-\tau_1)\ddot{z}(t_2-\tau_2)d\tau_1 d\tau_2 \\ &= \int_{-\infty}^{\infty}\int_{-\infty}^{\infty} \tilde{h}(\tau_1,\tau_2)\tilde{z}\left((t_1-\tau_1),(t_2-\tau_2)\right)d\tau_1 d\tau_2 \end{aligned} \tag{2.9.28}$$

where

$$\tilde{z}(\tau_1,\tau_2) = \ddot{z}(\tau_1)\ddot{z}(\tau_2) \tag{2.9.29}$$

and it is assumed that:

$$\tilde{z}(\tau_1,\tau_2) = \tilde{h}(\tau_1,\tau_2) = 0 \quad \text{if} \quad \tau_1 < 0 \text{ or } \tau_2 < 0 \tag{2.9.30}$$

Applying the Convolution Theorem of (2.9.27) and using the IFT of (2.9.26), Equation (2.9.28) leads to:

$$E[q(t_1)q(t_2)] = \frac{1}{4\pi^2}\int_{-\infty}^{\infty}\int_{-\infty}^{\infty} \tilde{H}(\xi_1,\xi_2)\tilde{Z}(\xi_1,\xi_2)e^{i(\xi_1 t_1+\xi_2 t_2)}d\xi_1 d\xi_2 \tag{2.9.31}$$

where $\tilde{H}(\xi_1,\xi_2)$ is the FT of $\tilde{h}(t_1,t_2)$, and $\tilde{Z}(\xi_1,\xi_2)$ is the FT of $\tilde{z}(t_1,t_2) = \ddot{z}(t_1)\ddot{z}(t_2)$

It is important to notice that:

$$\tilde{Z}(\xi_1,\xi_2) = \ddot{Z}(\xi_1)\ddot{Z}(\xi_2) \tag{2.9.32}$$

where $\ddot{Z}$ is the one-dimensional (1-D) FT of $\ddot{z}(t)$. Also, since only $E[q^2(t)]$ is of interest here, Equation (2.9.31) may be rewritten as follows:

$$\begin{aligned} E[q^2(t)] &= \frac{1}{4\pi^2}\int_{-\infty}^{\infty}\int_{-\infty}^{\infty}\tilde{H}(\xi_1,\xi_2)\tilde{Z}(\xi_1,\xi_2)e^{i(\xi_1+\xi_2)t}d\xi_1 d\xi_2 \\ &= \frac{1}{4\pi^2}\int_{-\infty}^{\infty}\left[\int_{-\infty}^{\infty}\tilde{H}(\xi_1,\eta-\xi_1)\tilde{Z}(\xi_1,\eta-\xi_1)d\xi_1\right]e^{i\eta t}d\eta \\ &= \frac{1}{2\pi}\int_{-\infty}^{\infty}\tilde{Q}(\eta)e^{i\eta t}d\eta \end{aligned} \tag{2.9.33}$$

where

$$\tilde{Q}(\eta) = \frac{1}{2\pi}\int_{-\infty}^{\infty}\tilde{H}(\xi_1,\eta-\xi_1)\tilde{Z}(\xi_1,\eta-\xi_1)d\xi_1 \tag{2.9.34}$$

Equation (2.9.33) states that $\tilde{Q}(\eta)$ is the 1-D FT of $E[q^2(t)]$. The last two observations lead to the conclusion that in order to obtain $E[q^2(t)]$ using FT, only one 2-D FT is needed and that is to obtain $\tilde{H}(\xi_1,\xi_2)$.

In practice, the Fourier Transform is evaluated by numerical integration using a finite number of its sampled points. Suppose that an even number N of consecutive sampled values of a function of one variable $f(t)$ is given:

$$f_n = f(t_n)\ ,\ t_n = n\Delta t\ ;\ n = 0,1,\ldots,N-1 \tag{2.9.35}$$

The Fourier Transform $F(\xi)$ is estimated at the following N discrete frequencies:

$$\xi_n = \frac{2\pi n}{N\Delta t} \quad ; \quad n = 0,1,2,\ldots,N-1 \tag{2.9.36}$$

The one-dimensional Fourier Transform $F(\xi)$ can then be approximated at these discrete frequencies by the discrete sum:

$$F_n = F(\xi_n) \simeq \Delta t\sum_{k=0}^{N-1} f_k e^{-i\xi_n t_k} = \Delta t\sum_{k=0}^{N-1} f_k e^{-\frac{2\pi i n k}{N}} \tag{2.9.37}$$

The Inverse Fourier Transform is then approximated by:

$$f_n = f(t_n) \simeq \frac{1}{2\pi N \Delta t} \sum_{k=0}^{N-1} F_k e^{i\xi_k t_n} = \frac{1}{2\pi N \Delta t} \sum_{k=0}^{N-1} F_k e^{\frac{2\pi i n k}{N}} \tag{2.9.38}$$

Using the values of a function of two variables $f(t_1, t_2)$ over a two-dimensional grid:

$$f_{n_1,n_2} = f(n_1 \Delta t, n_2 \Delta t) \quad ; \quad n_1, n_2 = 0, 1, \ldots, N-1 \tag{2.9.39}$$

the two-dimensional Fourier Transform $F(\xi_1, \xi_2)$ is approximated at the discrete values of a two-dimensional grid of frequencies by the sum:

$$F_{n_1,n_2} = F\left(\frac{2\pi n_1}{N\Delta t}, \frac{2\pi n_2}{N\Delta t}\right) \simeq \Delta t^2 \sum_{k_1=0}^{N-1} \sum_{k_2=0}^{N-1} f_{k_1,k_2} e^{-\frac{2\pi i (n_1 k_1 + n_2 k_2)}{N}} \tag{2.9.40}$$
$$; \quad n_1, n_2 = 0, 1, 2, \ldots, N-1$$

The inverse 2-D Fourier Transform is approximated by:

$$f_{n_1,n_2} = f(n_1 \Delta t, n_2 \Delta t) \simeq \frac{1}{4\pi^2 N^2 \Delta t^2} \sum_{k_1=0}^{N-1} \sum_{k_2=0}^{N-1} F_{k_1,k_2} e^{\frac{2\pi i (n_1 k_1 + n_2 k_2)}{N}} \tag{2.9.41}$$

The above sums can be evaluated using the Fast Fourier Transform (FFT).

The computational effort required for a 1-D FFT is of order $N \log_2 N$, while the one required for a 2-D FFT, assuming a grid of N^2 sampled points, is of order $(N \log_2 N)^2$. Aside from this increased computational effort, 2-D FFT's also require much larger memory space. Assume that a convolution-type integral of the form $f(t) = \int_0^t f_1(\tau)\, f_2(t-\tau) d\tau$, $t \in [0, T]$ has to be evaluated at discrete points spaced by Δt. Then the 1-D FFT's of $f_1(t)$ and $f_2(t)$ are calculated using discrete points $f_1(t_n)$ and $f_2(t_n)$, $t_n = n\Delta t$, $n = 0, 1, 2, \ldots, N_1 - 1$; N_1 is chosen to have the form $N_1 = k2^\lambda$ and to satisfy $T_1 = N_1 \Delta t \geq 2T$, while $f_1(t_n)$ and $f_2(t_n)$ are assigned zero values for $t_n \geq T$. Adding these zeros is necessary to avoid wraparound problems; the possible values for k are $k = 2$ or $k = 3$, depending on the particular version of 1-D FFT program used [Hall 1982]. Similarly, if 2-D FFT's are used to evaluate integrals of the form $g(t_1, t_2) =$

$\int_0^{t_1}\int_0^{t_2} g_1(\tau_1,\tau_2)g_2(t_1-\tau_1,t_2-\tau_2)d\tau_1 d\tau_2$, $(t_1,t_2) \in [0,T]\times[0,T]$, at a grid of discrete points spaced by Δt, then the 2-D FFT's of $g_1(t_1,t_2)$ and $g_2(t_1,t_2)$ are calculated using discrete points $g_1(t_n,t_m)$ and $g_2(t_n,t_m)$, with $t_n = n\Delta t$, $t_m = m\Delta t$; $n,m = 0,1,2,\ldots,N_1-1$. N_1 is chosen as before in the 1-D case, and $f_1(t_n,t_m) = f_2(t_n,t_m) = 0$ if $t_n \geq T$ or $t_m \geq T$. So a 2-D FFT requires the storing of a $N_1 \times N_1$ complex-valued matrix, while a 1-D FFT requires only the storing of a complex-valued array of length N_1.

From the above, it becomes obvious that 2-D FFT's should be avoided if possible. As discussed earlier in this section, in order to obtain $E[q^2(t)]$ using FT, only one 2-D FT is needed, and that is to obtain $\tilde{H}(\xi_1,\xi_2)$. This is accomplished by using (2.9.32) to evaluate $\tilde{Z}(\xi_1,\xi_2)$, and by evaluating $\tilde{Q}(\eta)$, the 1-D FT of $E[q^2(t)]$, by means of (2.9.34). The form of the above equations, where discrete data are employed, is discussed next.

Let $\underline{\ddot{Z}} = [\ddot{Z}_0,\ddot{Z}_1,\ldots,\ddot{Z}_{N_1-1}]^T$, where $\ddot{Z}_n = \ddot{Z}(\xi_n)$, be the discrete FT of $\ddot{z}(t)$, when N_1 discrete sampled points $\ddot{z}(t_n)$, $n = 0,1,\ldots,N_1-1$ are used; $\underline{\ddot{Z}}$ is then a complex-valued array of length N_1. The $N_1 \times N_1$ complex-valued matrix $\tilde{Z} = [\tilde{Z}_{nm}]$ corresponding to the discrete FT of $\tilde{z}(\tau_1,\tau_2) = \ddot{z}(\tau_1)\ddot{z}(\tau_2)$ when the discrete values $\tilde{z}(\tau_n,\tau_m)$; $n,m = 0,1,\ldots,N_1-1$ are employed, is given by:

$$\tilde{Z} = \underline{\ddot{Z}}\underline{\ddot{Z}}^T \tag{2.9.42}$$

Equation (2.9.42) is the discrete form of (2.9.32). Let $H = [H_{nm}]$ be the $N_1 \times N_1$ complex-valued matrix, obtained through a 2-D FFT of the discrete values $\tilde{h}(t_n,t_m)$; $n,m = 0,1,\ldots,N_1-1$. Let $\underline{\tilde{Q}} = [\tilde{Q}_0,\tilde{Q}_1,\ldots,\tilde{Q}_{N_1-1}]^T$, where $\tilde{Q}_n = \tilde{Q}(\xi_n)$, be the 1-D discrete FT of $E[q^2(t)]$. $\tilde{Q}_n$ can be obtained from:

$$\tilde{Q}_n = \frac{1}{2\pi N_1 \Delta t}\sum_{i=0}^{N_1-1}\sum_{j=0}^{N_1-1}\tilde{H}_{ij}\tilde{Z}_{ij}f(j;i,n) \; ; \; n = 0,1,\ldots,N_1-1 \tag{2.9.43}$$

where

$$\begin{aligned} f(j;i,n) &= 1 \quad \text{if} \quad i+j=n \quad \text{or} \quad i+j=n+N_1 \\ &= 0 \quad \text{otherwise} \end{aligned} \tag{2.9.44}$$

Equation (2.9.43) is the discrete form of (2.9.34).

The variance of $q(t)$ is given by:

$$\text{Var}\,(q(t)) \equiv \sigma_q(t)^2 = E[q(t)^2] - \bar{q}(t)^2 \tag{2.9.45}$$

Throughout this chapter $\bar{q}(t)$ is calculated from (2.9.4), using the approximation of (2.9.18), and $E[q(t)^2]$ is calculated from (2.9.20), utilizing FFT's as discussed in this section and the approximation (2.9.22). Figure 2.15 compares $\sigma_q(t)$, calculated as above, and $\sigma_q(t)$ obtained using numerical integrations in (2.9.20) and (2.9.21); the same data is used as in Figure 2.14. It can be seen that the discrepancies between the curves for the approximate and exact solutions are very small.

2.10 MDOF Structural Model With Uncertain Parameters

The response $q_i(t)$ of the i^{th} degree of freedom (dof) of an N_d dof structural model is given by (2.6.35), when only the contribution of the first $N_m \leq N_d$ modes is considered. The contribution of each mode $q_i^{(r)}$ is given by (2.6.29) along with (2.6.34). The uncertainties assumed initially are associated with the parameters $\underline{a} = [\underline{\theta}^T, \underline{\zeta}^T]^T = [\theta_1, \theta_2, \ldots, \theta_{N_\theta}, \zeta_1, \zeta_2, \ldots, \zeta_{N_m}]^T$ and their modeling was discussed in Section 2.7. The resulting uncertainties of the modal parameters $\omega^{(r)}, \beta_i^{(r)}$; $r = 1, 2, \ldots, N_m$, were discussed in Section 2.8. In Section 2.9, the statistics of the uncertain response of a SDOF oscillator were calculated. In the next section the issue of calculating the statistics of a single modal contribution $q_i^{(r)}(t)$ is addressed.

2.10.1 Statistics of $q_i^{(r)}(t)$

By comparing Equations (2.6.29) and (2.5.7), it can be seen that the equation for $q_i^{(r)}(t; \underline{\theta}, \zeta_r)$ is given by the equation of a SDOF oscillator with frequency $\omega_r(\underline{\theta})$ and damping ratio ζ_r, and with forcing function $-\beta_i^{(r)}(\underline{\theta})\ddot{z}(t)$

instead of just $-\ddot{z}(t)$. The solution of (2.6.29) is therefore given by (2.9.1), modified as follows:

$$q_i^{(r)}(t;\underline{\theta},\zeta_r) = -\int_0^t g_i^{(r)}(\tau;\omega_r(\underline{\theta}),\zeta_r)\ddot{z}(t-\tau)d\tau \tag{2.10.1}$$

where

$$g_i^{(r)}(\tau;\omega_r(\underline{\theta}),\zeta_r) = h(\tau;\omega_r(\underline{\theta}),\zeta_r)\beta_i^{(r)}(\underline{\theta}) \tag{2.10.2}$$

and $h(\tau;\omega_r(\underline{\theta}),\zeta_r)$ is given by (2.9.2). The expected value of $q_i^{(r)}(t)$ is given by:

$$\bar{q}_i^{(r)}(t) = -\int_0^t \bar{g}_i^{(r)}(\tau)\ddot{z}(t-\tau)d\tau \tag{2.10.3}$$

where

$$\begin{aligned}\bar{g}_i^{(r)}(\tau) &= \int_{S(\underline{\theta})}\int_0^\infty g_i^{(r)}(\tau;\omega_r(\underline{\theta}),\zeta_r)\pi_{\underline{\theta}}(\underline{\theta})\pi_{\zeta_r}(\zeta_r)d\underline{\theta}d\zeta_r \\ &= \int_{S(\underline{\theta})}\int_0^\infty h(\tau;\omega_r(\underline{\theta}),\zeta_r)\beta_i^{(r)}(\underline{\theta})\pi_{\underline{\theta}}(\underline{\theta})\pi_{\zeta_r}(\zeta_r)d\underline{\theta}d\zeta_r\end{aligned} \tag{2.10.4}$$

Note that while a 2-D integration is needed to evaluate $\bar{h}(\tau)$ in the SDOF case, integration over a $(N_\theta+1)$-dimensional space is required to evaluate $\bar{g}_i^{(r)}(t)$ in the MDOF case. If numerical integration is used to calculate (2.10.4), the computational effort will grow exponentially with $(N_\theta+1)$. It is obvious that this amount of calculation may become prohibitive for a large, or even for a medium, number N_θ of uncertain parameters. To overcome this difficulty, a transformation of the variables $\underline{\theta}$ is introduced. Assume a new set of variables $\underline{\tilde{\eta}}^{(r)} = [\omega_r, (\underline{\eta}^{(r)})^T]^T$, where $\underline{\eta}^{(r)}$ is a vector of length $N_\theta - 1$, such that each $\underline{\theta}$ is uniquely mapped into a vector of transformed variables $\underline{\tilde{\eta}}^{(r)}$. Assume also that this mapping between $\underline{\theta}$'s and $\underline{\tilde{\eta}}^{(r)}$'s is one-to-one, that is, each $\underline{\tilde{\eta}}^{(r)}$ is also uniquely mapped into a $\underline{\theta}$ in the space $S(\underline{\theta})$. The functional relationship $\underline{\tilde{\eta}}^{(r)} = \underline{\tilde{\eta}}^{(r)}(\underline{\theta})$ is specified only for the first element of $\underline{\tilde{\eta}}^{(r)}$, that is, $\tilde{\eta}_1^{(r)} = \omega_r(\underline{\theta})$; the functional relationship

for the remaining elements of $\underline{\tilde{\eta}}^{(r)}$, that is, $\underline{\eta}^{(r)} = \underline{\eta}^{(r)}(\underline{\theta})$ is not specified here, but is assumed to be such that the overall mapping $\underline{\tilde{\eta}}^{(r)} = \underline{\tilde{\eta}}^{(r)}(\underline{\theta})$ is one-to-one. Although the pdf $\pi_{\underline{\theta}}(\underline{\theta})$ can be written as a product of the independent pdf's $\pi_{\theta_j}(\theta_j) = g(\theta_j; \mu_{\theta_j}, \nu_{\theta_j})$, this is not any more true for $\pi_{\underline{\tilde{\eta}}^{(r)}}(\underline{\tilde{\eta}}^{(r)})$. The marginal distribution of the first element of $\underline{\tilde{\eta}}^{(r)}$, given by the $(N_\theta - 1)$-dimensional integral:

$$\pi_{\omega_r}(\omega_r) = \int_{S(\underline{\eta}^{(r)})} \pi_{\underline{\tilde{\eta}}^{(r)}}(\underline{\tilde{\eta}}^{(r)}) d\underline{\eta}^{(r)} = \int_{S(\underline{\eta}^{(r)})} \pi_{\underline{\tilde{\eta}}^{(r)}}(\omega_r, \underline{\eta}^{(r)}) d\underline{\eta}^{(r)} \tag{2.10.5}$$

can be approximated according to Section 2.8, with a Gamma distribution:

$$\pi_{\omega_r}(\omega_r) \simeq g(\omega_r; \mu_{\omega_r}, \nu_{\omega_r}) \tag{2.10.6}$$

Notice also the following relation stemming from the third axiom of Section 2.3:

$$\pi_{\underline{\tilde{\eta}}^{(r)}}(\underline{\tilde{\eta}}^{(r)}) = \pi_{\underline{\tilde{\eta}}^{(r)}}(\omega_r, \underline{\eta}^{(r)}) = \pi_{\omega_r}(\omega_r) \pi_{\underline{\eta}^{(r)}|\omega_r}(\underline{\eta}^{(r)}|\omega_r) \tag{2.10.7}$$

Equation (2.10.4) can be rewritten using the new set of variables as:

$$\bar{g}_i^{(r)}(\tau) = \int_{S(\underline{\tilde{\eta}}^{(r)})} \int_0^\infty h(\tau; \omega_r, \zeta_r) \beta_i^{(r)}(\underline{\tilde{\eta}}^{(r)}) \pi_{\underline{\tilde{\eta}}^{(r)}}(\underline{\tilde{\eta}}^{(r)}) \pi_{\zeta_r}(\zeta_r) d\underline{\tilde{\eta}}^{(r)} d\zeta_r \tag{2.10.8}$$

Substitute (2.10.7) into (2.10.8):

$$\begin{aligned} \bar{g}_i^{(r)}(\tau) = & \int_{S(\underline{\eta}^{(r)})} \int_0^\infty \int_0^\infty h(\tau; \omega_r, \zeta_r) \beta_i^{(r)}(\underline{\tilde{\eta}}^{(r)}) \pi_{\underline{\eta}^{(r)}|\omega_r}(\underline{\eta}^{(r)}|\omega_r) \\ & \pi_{\omega_r}(\omega_r) \pi_{\zeta_r}(\zeta_r) d\underline{\eta}^{(r)} d\omega_r d\zeta_r \\ = & \int_0^\infty \int_0^\infty h(\tau; \omega_r, \zeta_r) \bar{\beta}_i^{(r)}(\omega_r) \pi_{\omega_r}(\omega_r) \pi_{\zeta_r}(\zeta_r) d\omega_r d\zeta_r \end{aligned} \tag{2.10.9}$$

where $\bar{\beta}_i^{(r)}(\omega_r)$ is the conditional expected value of $\beta_i^{(r)}$, when ω_r is kept fixed:

$$\begin{aligned} \bar{\beta}_i^{(r)}(\omega_r) \equiv E[\beta_i^{(r)}|\omega_r] = & \int_{S(\underline{\eta}^{(r)})} \beta_i^{(r)}(\underline{\tilde{\eta}}^{(r)}) \pi_{\underline{\eta}^{(r)}|\omega_r}(\underline{\eta}^{(r)}|\omega_r) d\underline{\eta}^{(r)} \\ = & \int_{S(\underline{\eta}^{(r)})} \beta_i^{(r)}(\omega_r, \underline{\eta}^{(r)}) \pi_{\underline{\eta}^{(r)}|\omega_r}(\underline{\eta}^{(r)}|\omega_r) d\underline{\eta}^{(r)} \end{aligned} \tag{2.10.10}$$

Assuming $\bar{\beta}_i^{(r)}(\omega_r)$ is calculated, Equation (2.10.9) implies that only a 2-D integration is required to obtain $\bar{g}_i^{(r)}(\tau)$. Instead of evaluating $\bar{\beta}_i^{(r)}(\omega_r)$ by calculating the $(N_\theta - 1)$-dimensional integral of (2.10.10), an approximate polynomial expression for $\bar{\beta}_i^{(r)}(\omega_r)$ is assumed. Retaining only terms up to first order we obtain:

$$\bar{\beta}_i^{(r)}(\omega_r) \simeq c_{i,0}^{(r)} + c_{i,1}^{(r)}\omega_r \tag{2.10.11}$$

The coefficients $c_{i,0}^{(r)}$ and $c_{i,1}^{(r)}$ can be evaluated as follows. Utilizing Equations (2.10.10) and (2.10.7) we obtain:

$$\begin{aligned}\int_0^\infty \bar{\beta}_i^{(r)}(\omega_r)\pi_{\omega_r}(\omega_r)d\omega_r &= \int_{S(\underline{\eta}^{(r)})} \int_0^\infty \beta_i^{(r)}(\omega_r, \underline{\eta}^{(r)})\pi_{\underline{\eta}^{(r)}|\omega_r}(\underline{\eta}^{(r)}|\omega_r)\pi_{\omega_r}(\omega_r)d\underline{\eta}^{(r)}d\omega_r \\ &= \int_{S(\underline{\tilde{\eta}}^{(r)})} \beta_i^{(r)}(\underline{\tilde{\eta}}^{(r)})\pi_{\underline{\tilde{\eta}}^{(r)}}(\underline{\tilde{\eta}}^{(r)})d\underline{\tilde{\eta}}^{(r)} \\ &= E[\beta_i^{(r)}]\end{aligned} \tag{2.10.12}$$

Multiplying both sides of (2.10.11) with $\pi_{\omega_r}(\omega_r)$, integrating with respect to ω_r, and utilizing (2.10.12) we obtain:

$$E[\beta_i^{(r)}] \simeq c_{i,0}^{(r)} + c_{i,1}^{(r)}\bar{\omega}_r \tag{2.10.13}$$

The value of $E[\beta_i^{(r)}]$ can be approximated according to the discussion of Section 2.8, by:

$$E[\beta_i^{(r)}] \simeq \underline{c}_{\beta_i^{(r)}}^T \bar{\bar{\underline{\theta}}} \tag{2.10.14}$$

Similarly, multiplying both sides of (2.10.11) with $\omega_r\pi_{\omega_r}(\omega_r)$ and integrating with respect to ω_r we obtain:

$$E[\omega_r\beta_i^{(r)}] \simeq c_{i,0}^{(r)}\bar{\omega}_r + c_{i,1}^{(r)}\bar{\omega}_r^2 \tag{2.10.15}$$

where $\bar{\omega}_r^2 = E[\omega_r^2]$ and $E[\omega_r\beta_i^{(r)}]$ can be approximated by:

$$E[\omega_r\beta_i^{(r)}] \simeq \underline{c}_{\omega_r\beta_i^{(r)}}^T \bar{\bar{\underline{\theta}}} \tag{2.10.16}$$

The elements of $\underline{c}_{\omega_r \beta_i^{(r)}}$ are the coefficients of a quadratic approximation of $\omega_r(\underline{\theta})\beta_i^{(r)}(\underline{\theta})$, according to the discussion of Section 2.8. Equations (2.10.13) and (2.10.15) can be solved to obtain $c_{i,0}^{(r)}$ and $c_{i,1}^{(r)}$:

$$\begin{bmatrix} c_{i,0}^{(r)} \\ c_{i,1}^{(r)} \end{bmatrix} = \begin{bmatrix} 1 & \bar{\omega}_r \\ \bar{\omega}_r & \bar{\omega_r^2} \end{bmatrix}^{-1} \begin{bmatrix} E[\beta_i^{(r)}] \\ E[\omega_r \beta_i^{(r)}] \end{bmatrix} \tag{2.10.17}$$

Figure 2.16 compares the conditional expected values of the effective participation factors of the first mode of a three-story shear building structure when the corresponding modal frequency ω_1 is kept fixed, that is, $\bar{\beta}_i^{(1)}(\omega_1) = E[\beta_i^{(1)}|\omega_1], i = 1, 2, 3$, using two different approaches. The first approach uses simulations while the second uses the linear approximation (2.10.11), with the coefficients $c_{i,0}^{(1)}, c_{i,1}^{(1)}$ evaluated through (2.10.17), as discussed above. In this particular example, a uniform mass distribution $m_i = m_0, i = 1, 2, 3$ and an interstory stiffness distribution $k_i = k_0\theta_i, i = 1, 2, 3$, where $k_0 = 2000 m_o \text{sec}^{-2}$, are assumed. Each θ_i is assumed to be Gamma distributed with $(\bar{\theta}_i, \alpha_{\theta_i}) = (1., .10)$. It can be seen from Figure 2.16 that the linear approximation is very good over the frequency range for which $\pi_{\omega_1}(\omega_1)$ would produce a significant contribution to an integral like (2.10.9).

Substituting $\bar{\beta}_i^{(r)}(\omega_r)$ with its linear approximation (2.10.11) into Equation (2.10.9) leads to:

$$\bar{g}_i^{(r)}(\tau) = c_{i,0}^{(r)} \tilde{g}_0^{(r)}(\tau) + c_{i,1}^{(r)} \tilde{g}_1^{(r)}(\tau) \tag{2.10.18}$$

where

$$\tilde{g}_l^{(r)}(\tau) = \int_0^\infty \int_0^\infty h(\tau; \omega_r, \zeta_r) \omega_r^l \pi_{\omega_r}(\omega_r) \pi_{\zeta_r}(\zeta_r) d\omega_r d\zeta_r \ ; \ l = 0, 1 \tag{2.10.19}$$

As in Section 2.9, the above 2-D integrals may be approximated by integrals accepting a closed form solution if the transformed variables $(a_1^{(r)}, a_3^{(r)}) = (\omega_r \sqrt{1 - E[\zeta_r^2]}\ , \omega_r \zeta_r)$ are employed:

$$\tilde{g}_l^{(r)}(\tau) \simeq \frac{1}{(\sqrt{1 - E[\zeta_r^2]})^l} \bar{h}_{1,l}^{(r)}(\tau) \bar{h}_3^{(r)}(\tau) \quad ; \quad l = 0, 1 \tag{2.10.20}$$

where $\bar{h}_{1,l}^{(r)}(\tau)$ and $\bar{h}_3^{(r)}(\tau)$ are given by (2.9.15) and (2.9.19), respectively. The superscript (r) implies that the variables a_1, a_3 are replaced by $a_1^{(r)}, a_3^{(r)}$ in these equations.

The expected value of $q_i^{(r)}(t)^2$ is given by:

$$E[q_i^{(r)}(t)^2] = \int_0^t \int_0^t \bar{g}_i^{(r,r)}(\tau_1, \tau_2)\ddot{z}(t-\tau_1)\ddot{z}(t-\tau_2)d\tau_1 d\tau_2 \tag{2.10.21}$$

where

$$\bar{g}_i^{(r,r)}(\tau_1, \tau_2) = \int_{S(\underline{\theta})} \int_0^\infty h(\tau_1; \omega_r(\underline{\theta}), \zeta_r)h(\tau_2; \omega_r(\underline{\theta}), \zeta_r)\beta_i^{(r)}(\underline{\theta})^2 \pi_{\underline{\theta}}(\underline{\theta})\pi_{\zeta_r}(\zeta_r)d\underline{\theta}d\zeta_r \tag{2.10.22}$$

Following the same steps as earlier for $\bar{g}_i^{(r)}(t)$, Equation (2.10.22) can be rewritten as:

$$\bar{g}_i^{(r,r)}(\tau_1, \tau_2) = \int_0^\infty \int_0^\infty h(\tau_1; \omega_r, \zeta_r)h(\tau_2; \omega_r, \zeta_r)E[(\beta_i^{(r)})^2|\omega_r]\pi_{\omega_r}(\omega_r)\pi_{\zeta_r}(\zeta_r)d\omega_r d\zeta_r \tag{2.10.23}$$

where

$$E\left[(\beta_i^{(r)})^2|\omega_r\right] = \int_{S(\underline{\eta}^{(r)})} \beta_i^{(r)}(\omega_r, \underline{\eta}^{(r)})^2 \pi_{\underline{\eta}^{(r)}|\omega_r}(\underline{\eta}^{(r)}|\omega_r)d\underline{\eta}^{(r)} \tag{2.10.24}$$

As earlier, $E[(\beta_i^{(r)})^2|\omega_r]$ is linearly approximated:

$$E[(\beta_i^{(r)})^2|\omega_r] \simeq c_{i,0}^{(r,r)} + c_{i,1}^{(r,r)}\omega_r \tag{2.10.25}$$

where the coefficients $c_{i,0}^{(r,r)}$ and $c_{i,1}^{(r,r)}$ may be recovered, in a similar way as before, from:

$$\begin{bmatrix} c_{i,0}^{(r,r)} \\ c_{i,1}^{(r,r)} \end{bmatrix} = \begin{bmatrix} 1 & \bar{\omega}_r \\ \bar{\omega}_r & \bar{\omega_r^2} \end{bmatrix}^{-1} \begin{bmatrix} E[(\beta_i^{(r)})^2] \\ E[\omega_r(\beta_i^{(r)})^2] \end{bmatrix} \tag{2.10.26}$$

where $E[(\beta_i^{(r)})^2]$ and $E[\omega_r(\beta_i^{(r)})^2]$ can be evaluated as before, utilizing quadratic approximations for $\beta_i^{(r)}(\underline{\theta})^2$ and $\omega_r(\underline{\theta})\beta_i^{(r)}(\underline{\theta})^2$, according to the discussion of Section 2.8. Substituting (2.10.25) into (2.10.23) leads to:

$$\bar{g}_i^{(r,r)}(\tau_1, \tau_2) = c_{i,0}^{(r,r)}\tilde{g}_0^{(r,r)}(\tau_1, \tau_2) + c_{i,1}^{(r,r)}\tilde{g}_1^{(r,r)}(\tau_1, \tau_2) \tag{2.10.27}$$

where

$$\tilde{g}_l^{(r,r)}(\tau_1,\tau_2) = \int_0^\infty \int_0^\infty h(\tau_1;\omega_r,\zeta_r)h(\tau_2;\omega_r,\zeta_r)\omega_r^l \pi_{\omega_r}(\omega_r)\pi_{\zeta_r}(\zeta_r)d\omega_r d\zeta_r \ ; \ l=0,1 \tag{2.10.28}$$

Using the transformed variables $(a_1^{(r)}, a_3^{(r)})$, the following approximations are derived:

$$\tilde{g}_l^{(r,r)}(\tau_1,\tau_2) \simeq \frac{1}{(\sqrt{1-E[\zeta_r^2]})^l}\tilde{h}_{1,l}^{(r)}(\tau_1,\tau_2)\tilde{h}_3^{(r)}(\tau_1,\tau_2) \tag{2.10.29}$$

where $\tilde{h}_{1,l}^{(r)}(\tau_1,\tau_2)$ and $\tilde{h}_3^{(r)}(\tau_1,\tau_2)$ are given by (2.9.23) and (2.9.24), respectively. The superscript (r) implies that the variables a_1, a_3 are replaced by $a_1^{(r)}, a_3^{(r)}$ in these equations.

Figure 2.17 compares the expected value of the contribution of the first mode to the response of the third floor of a three-story shear building structure for two different approaches: numerical integration (solid curve) and the methodology discussed in this section (dashed-dotted curve). In this particular example, it is assumed that there is a uniform mass distribution $m_i = m_0$, $i = 1,2,3$, and an interstory stiffness distribution $k_i = k_0\theta_i$, $i = 1,2,3$ where $k_0 = 2000 m_0 \text{sec}^{-2}$; each θ_i is Gamma distributed with $(\bar{\theta}_i, \alpha_{\theta_i}) = (1, .10)$ and the damping ratios are also independently Gamma distributed with $(\bar{\zeta}_r, \alpha_{\zeta_r}) = (0.05, .20)$, $r = 1,2,3$. It can be seen that the two curves representing the approximate and exact solutions are almost indistinguishable. Figure 2.18 makes the same comparison for the corresponding standard deviation. It can be seen that the two curves compare well.

2.10.2 Statistics of $q_i(t)$

The response $q_i(t)$ of the i^{th} dof of an N_d-dof structural model, when only the contribution of the first N_m modes is considered, is given by (2.6.35).

The expected value of $q_i(t)$ is therefore given by:

$$\bar{q}_i(t) \equiv E[q_i(t)] \simeq \sum_{r=1}^{N_m} \bar{q}_i^{(r)}(t) \tag{2.10.30}$$

where the evaluation of the $\bar{q}_i^{(r)}(t)$'s was discussed in Section 2.10.1. The expected value of $q_i(t)^2$ is given by:

$$E[q_i(t)^2] \simeq \sum_{r=1}^{N_m} \sum_{s=1}^{N_m} E\left[q_i^{(r)}(t) q_i^{(s)}(t)\right] \tag{2.10.31}$$

In Section 2.10.1, the evaluation of $E[q_i^{(r)}(t)^2]$ was discussed. Therefore, the remaining issue for discussion is the evaluation of the terms $E\left[q_i^{(r)}(t) q_i^{(s)}(t)\right]$ when $r \neq s$. It can be seen that:

$$E\left[q_i^{(r)}(t) q_i^{(s)}(t)\right] = \int_0^t \int_0^t \bar{g}_i^{(r,s)}(\tau_1, \tau_2) \ddot{z}(t-\tau_1) \ddot{z}(t-\tau_2) d\tau_1 d\tau_2 \tag{2.10.32}$$

where

$$\begin{aligned} \bar{g}_i^{(r,s)}(\tau_1, \tau_2) = \int_{S(\underline{\theta})} \int_0^\infty \int_0^\infty & h(\tau_1; \omega_r(\underline{\theta}), \zeta_r) h(\tau_2; \omega_s(\underline{\theta}), \zeta_s) \beta_i^{(r)}(\underline{\theta}) \beta_i^{(s)}(\underline{\theta}) \\ & \times \pi_{\underline{\theta}}(\underline{\theta}) \pi_{\zeta_r}(\zeta_r) \pi_{\zeta_s}(\zeta_s) d\underline{\theta} d\zeta_r d\zeta_s \end{aligned} \tag{2.10.33}$$

The task is to evaluate this $(N_\theta + 2)$-dimensional integral. Assume a transformed set of variables $\tilde{\underline{\eta}}^{(r,s)} = [\omega_r, \omega_s, \underline{\eta}^{(r,s)}]^T$, where $\underline{\eta}^{(r,s)}$ is a vector of length $N_\theta - 2$, such that there is a one-to-one mapping between $\underline{\theta}$'s and $\tilde{\underline{\eta}}^{(r,s)}$'s.

The joint marginal distribution $\pi_{\omega_r,\omega_s}(\omega_r, \omega_s)$ is defined as:

$$\pi_{\omega_r,\omega_s}(\omega_r, \omega_s) = \int_{S(\underline{\eta}^{(r,s)})} \pi_{\tilde{\underline{\eta}}^{(r,s)}}(\tilde{\underline{\eta}}^{(r,s)}) d\underline{\eta}^{(r,s)} = \int_{S(\underline{\eta}^{(r,s)})} \pi_{\tilde{\underline{\eta}}^{(r,s)}}(\omega_r, \omega_s, \underline{\eta}^{(r,s)}) d\underline{\eta}^{(r,s)} \tag{2.10.34}$$

Notice that $\pi_{\omega_r,\omega_s}(\omega_r, \omega_s)$ is not the product of the marginal distributions $\pi_{\omega_r}(\omega_r)$ and $\pi_{\omega_s}(\omega_s)$, each of which, as discussed previously, may be adequately described by a Gamma distribution. However, the following relation holds:

$$\pi_{\omega_r,\omega_s}(\omega_r, \omega_s) = \pi_{\omega_r}(\omega_r) \pi_{\omega_s|\omega_r}(\omega_s|\omega_r) \tag{2.10.35}$$

The following relation follows from the third axiom of Section 2.3:

$$\pi_{\underline{\tilde{\eta}}^{(r,s)}}(\underline{\tilde{\eta}}^{(r,s)}) = \pi_{\underline{\tilde{\eta}}^{(r,s)}}(\omega_r, \omega_s, \underline{\eta}^{(r,s)}) = \pi_{\omega_r,\omega_s}(\omega_r, \omega_s)\pi_{\underline{\eta}^{(r,s)}|\omega_r,\omega_s}(\underline{\eta}^{(r,s)}|\omega_r, \omega_s) \tag{2.10.36}$$

The conditional expected value of $\beta_i^{(r)}\beta_i^{(s)}$ when ω_r and ω_s are kept fixed is:

$$E\left[\beta_i^{(r)}\beta_i^{(s)}|\omega_r, \omega_s\right] = \int\limits_{S(\underline{\eta}^{(r,s)})} \beta_i^{(r)}(\underline{\tilde{\eta}}^{(r,s)})\beta_i^{(s)}(\underline{\tilde{\eta}}^{(r,s)})\pi_{\underline{\eta}^{(r,s)}|\omega_r,\omega_s}(\underline{\eta}^{(r,s)}|\omega_r, \omega_s)d\underline{\eta}^{(r,s)} \tag{2.10.37}$$

Equation (2.10.33) can be rewritten using these transformed variables:

$$\bar{g}_i^{(r,s)}(\tau_1, \tau_2) = \int\limits_{S(\underline{\tilde{\eta}}^{(r,s)})} \int\limits_0^\infty \int\limits_0^\infty h(\tau_1; \omega_r, \zeta_r)h(\tau_2; \omega_s, \zeta_s)\beta_i^{(r)}(\underline{\tilde{\eta}}^{(r,s)})\beta_i^{(s)}(\underline{\tilde{\eta}}^{(r,s)}) \times \pi_{\underline{\tilde{\eta}}^{(r,s)}}(\underline{\tilde{\eta}}^{(r,s)})\pi_{\zeta_r}(\zeta_r)\pi_{\zeta_s}(\zeta_s)d\underline{\tilde{\eta}}^{(r,s)}d\zeta_r d\zeta_s \tag{2.10.38}$$

Integrating out the variables $\underline{\eta}^{(r,s)}$ by utilizing Equations (2.10.36) and (2.10.37) leads to:

$$\bar{g}_i^{(r,s)}(\tau_1, \tau_2) = \int_0^\infty \int_0^\infty \int_0^\infty \int_0^\infty h(\tau_1; \omega_r, \zeta_r)h(\tau_2; \omega_s, \zeta_s)E\left[\beta_i^{(r)}\beta_i^{(s)}|\omega_r, \omega_s\right] \times \pi_{\omega_r,\omega_s}(\omega_r, \omega_s)\pi_{\zeta_r}(\zeta_r)\pi_{\zeta_s}(\zeta_s)d\omega_r d\omega_s d\zeta_r d\zeta_s \tag{2.10.39}$$

As before, instead of calculating the $(N_\theta - 2)$-dimensional integral of (2.10.37), a polynomial approximation of two variables ω_r, ω_s is assumed. It is sufficient, as will be seen later with an example, if only the zeroth order term is retained:

$$E\left[\beta_i^{(r)}\beta_i^{(s)}|\omega_r, \omega_s\right] = c_{i,0}^{(r,s)} \tag{2.10.40}$$

The value of $c_{i,0}^{(r,s)}$ is chosen so that:

$$c_{i,0}^{(r,s)} = E\left[\beta_i^{(r)}\beta_i^{(s)}\right] \tag{2.10.41}$$

The value of $E\left[\beta_i^{(r)}\beta_i^{(s)}\right]$ is evaluated utilizing quadratic approximations for $\beta_i^{(r)}(\underline{\theta})\beta_i^{(s)}(\underline{\theta})$, according to the discusion of Section 2.8. The conditional marginal distribution $\pi_{\omega_s|\omega_r}(\omega_s|\omega_r)$ is assumed to be Gamma distributed:

$$\pi_{\omega_s|\omega_r}(\omega_s|\omega_r) = g\left(\omega_s; \mu'_{\omega_s}(\omega_r), \nu'_{\omega_s}(\omega_r)\right) \tag{2.10.42}$$

where $\mu'_{\omega_s}(\omega_r), \nu'_{\omega_s}(\omega_r)$ are specified according to (2.7.6) from the expected value $E[\omega_s|\omega_r]$ and the variance $\mathrm{Var}[\omega_s|\omega_r]$; the values of these quantities are evaluated using the following polynomial approximations:

$$E[\omega_s|\omega_r] = c_0^{(r,s)} + c_1^{(r,s)}\omega_r \tag{2.10.43}$$

and

$$E[\omega_s^2|\omega_r] = \tilde{c}_0^{(r,s)} + \tilde{c}_1^{(r,s)}\omega_r \tag{2.10.44}$$

The expressions for the coefficients $[c_0^{(r,s)}, c_1^{(r,s)}]^T$ and $[\tilde{c}_0^{(r,s)}, \tilde{c}_1^{(r,s)}]^T$ are similar to these of Equations (2.10.17) and (2.10.26):

$$\begin{bmatrix} c_0^{(r,s)} \\ c_1^{(r,s)} \end{bmatrix} = \begin{bmatrix} 1 & \bar{\omega}_r \\ \bar{\omega}_r & \bar{\omega_r^2} \end{bmatrix}^{-1} \begin{bmatrix} E[\omega_s] \\ E[\omega_r\omega_s] \end{bmatrix} \tag{2.10.45}$$

and

$$\begin{bmatrix} \tilde{c}_0^{(r,s)} \\ \tilde{c}_1^{(r,s)} \end{bmatrix} = \begin{bmatrix} 1 & \bar{\omega}_r \\ \bar{\omega}_r & \bar{\omega_r^2} \end{bmatrix}^{-1} \begin{bmatrix} E[\omega_s^2] \\ E[\omega_r\omega_s^2] \end{bmatrix} \tag{2.10.46}$$

In order to further simplify the calculation of the 4-dimensional integral of (2.10.39), the transformed variables $a_1^{(r)} = \omega_r\sqrt{1-E(\zeta_r^2)}, a_3^{(r)} = \omega_r\zeta_r$, $a_1^{(s)} = \omega_s\sqrt{1-E(\zeta_r^2)}$ and $a_3^{(s)} = \omega_s\zeta_s$ are introduced. As before, the additional approximation is adopted, namely, that all the pairs of the above variables, except for the pair $(a_1^{(r)}, a_1^{(s)})$ are independently distributed. As far as the joint pdf $\pi_{a_1^{(r)},a_1^{(s)}}(a_1^{(r)}, a_1^{(s)})$ is concerned, it follows from (2.10.35) and (2.10.42) that:

$$\begin{aligned} \pi_{a_1^{(r)},a_1^{(s)}}(a_1^{(r)}, a_1^{(s)}) &= \pi_{a_1^{(r)}}(a_1^{(r)})\pi_{a_1^{(s)}|a_1^{(r)}}(a_1^{(s)}|a_1^{(r)}) \\ &= g(a_1^{(r)}; \mu_{a_1^{(r)}}, \nu_{a_1^{(r)}})g(a_1^{(s)}; \mu'_{a_1^{(s)}}(a_1^{(r)}), \nu'_{a_1^{(s)}}(a_1^{(r)})) \end{aligned} \tag{2.10.47}$$

Equation (2.10.39) can be rewritten using (2.10.40) and the above transformed variables as:

$$\bar{g}_i^{(r,s)}(\tau_1, \tau_2) \simeq c_{i,0}^{(r,s)}\tilde{g}_i^{(r,s)}(\tau_1, \tau_2) \tag{2.10.48}$$

where

$$\tilde{g}_i^{(r,s)}(\tau_1,\tau_2) = \int_0^\infty \int_0^\infty \int_0^\infty \int_0^\infty h(\tau_1;a_1^{(r)},a_3^{(r)})h(\tau_2;a_1^{(s)},a_3^{(s)}) \times \pi_{a_1^{(r)},a_1^{(s)}}(a_1^{(r)},a_1^{(s)})\pi_{a_3^{(r)}}(a_3^{(r)})\pi_{a_3^{(s)}}(a_3^{(s)})da_1^{(r)}da_1^{(s)}da_3^{(r)}da_3^{(s)}$$
$$= c_{i,0}^{(r,s)}\bar{h}_3^{(r)}(\tau_1)\bar{h}_3^{(s)}(\tau_2) \times \int_0^\infty a_1^{(r)^{-1}}\sin(a_1^{(r)}\tau_1)\bar{h}_{1,0}^{(s)}(\tau_2;a_1^{(r)})g(a_1^{(r)};\mu_{a_1^{(r)}},\nu_{a_1^{(r)}})da_1^{(r)} \quad (2.10.49)$$

where $\bar{h}_3^{(r)}(\tau_1)$ and $\bar{h}_3^{(s)}(\tau_2)$ are given by (2.9.19), with the superscript (r) or (s) appropriately carried over to a_3, and $\bar{h}_{1,0}^{(s)}(\tau_2;a_1^{(r)})$ is given by:

$$\bar{h}_{1,0}^{(s)}(\tau_2;a_1^{(r)}) = \int_0^\infty a_1^{(s)^{-1}}\sin(a_1^{(s)}\tau_2)g\left(a_1^{(s)};\mu'_{a_1^{(s)}}(a_1^{(r)}),\nu'_{a_1^{(s)}}(a_1^{(r)})\right)da_1^{(s)} \quad (2.10.50)$$

Equations (2.10.48) and (2.10.49) imply that in order to evaluate $\bar{g}_i^{(r,s)}(\tau_1,\tau_2)$ for given τ_1 and τ_2, only a one-dimensional integral needs to be calculated using numerical integration, since $\bar{h}_3^{(r)}(\tau_1),\bar{h}_3^{(s)}(\tau_2)$ and $\bar{h}_{1,0}^{(s)}(\tau_2;a_1^{(r)})$ can be expressed analytically using (2.7.3a or b). Finally, $E[q_i^{(r)}(t)q_i^{(s)}(t)]$ is evaluated from (2.10.32), using FFT's according to the discussion of Section 2.9.

Figure 2.19 compares the expected value of the response, due to all three modes of vibration, at the third floor of a three-story shear building structure for two different approaches: numerical integration and the methodology discussed in this section. The same data is used as in Figures 2.17 and 2.18 of the example of the previous section. It can be seen that the curves representing the approximate and exact solutions are almost indistinguishable. Figure 2.20 makes the same comparison for the corresponding standard deviation. It can be seen that the two curves compare well.

2.11 Summary and Conclusions

The primary steps of the procedure presented in this chapter, to approximate the statistics of the dynamic response of an uncertain N_d-dof model of a structure, are reviewed here. Also, for the steps involving a substantial amount of computations, the order of computations involved is given.

1) A number of $N_l = (N_\theta^2 + 3N_\theta + 2)/2$ eigenvalue problems are solved. The amount of computation involved is $O(N_l \times N_d^3)$.

2) The $N_l \times N_l$ matrix A of (2.8.6) is formed and factorized. The computational effort is $O(N_l^3)$.

3) By solving (2.8.4), the coefficients of the quadratic approximation (2.8.9) are obtained for the following functions of $\underline{\theta}$: $\omega_r(\underline{\theta}), \omega_r^2(\underline{\theta}), \omega_r(\underline{\theta})\omega_s(\underline{\theta})$, $\omega_r(\underline{\theta})\omega_s^2(\underline{\theta})$, $\beta_i^{(r)}(\underline{\theta})$, $\beta_i^{(r)}(\underline{\theta})^2$, $\omega_r(\underline{\theta})\beta_i^{(r)}(\underline{\theta})$, $\omega_r(\underline{\theta})\beta_i^{(r)}(\underline{\theta})^2$, $\beta_i^{(r)}(\underline{\theta})\beta_i^{(s)}(\underline{\theta})$, where $r = 1, \ldots, N_m$, $s = 1, \ldots, r-1$ and $i =$ the dof's where the response statistics are to be computed. The expected values of the above quantities are computed through (2.8.10).

4) The coefficients $c_{i,l}^{(r)}$ and $c_{i,l}^{(r,r)}$, $l = 0, 1$ are computed through (2.10.17) and (2.10.26), respectively, and $c_{i,0}^{(r,s)}$ is computed from (2.10.41). The values of r, s and i are the same as in Step 3.

5) Let $T_f = N_T \Delta t$ be the length of the time interval over which the statistics of the response are to be calculated. The functions $\tilde{g}_l^{(r)}(\tau), l = 0, 1$ are evaluated through (2.10.20) at the discrete points $\tau_n = n\Delta t, n = 0, 1 \ldots, N_T$. Similarly, the functions $\tilde{g}_l^{(r,r)}(\tau_1, \tau_2), l = 0, 1$ and $\tilde{g}^{(r,s)}(\tau_1, \tau_2)$ are evaluated through (2.10.29) and (2.10.49), respectively, at the discrete points $(\tau_n, \tau_m) = (n\Delta t, m\Delta t)$, $n, m = 0, \ldots, N_T - 1$. The values of r, s are the same as in Step 3. The computational effort of this step is $O(N_m^2 N_T)$.

6) The final expression for $E[q_i(t)]$ is given by:

$$E[q_i(t)] = \sum_{r=1}^{N_m} \sum_{l=1}^{2} c_{i,l}^{(r)} \tilde{q}_l^{(r)}(t) \tag{2.11.1}$$

where $$\tilde{q}_l^{(r)}(t) = -\int_0^t \tilde{g}_l^{(r)}(\tau)\ddot{z}(t-\tau)d\tau \tag{2.11.2}$$

The final expression for $E[q_i^2(t)]$ is given by:

$$E[q_i(t)] = \sum_{r=1}^{N_m} \sum_{l=1}^{2} c_{i,l}^{(r,r)} \tilde{q}_l^{(r,r)}(t) + 2\sum_{r=2}^{N_m} \sum_{s=1}^{r-1} c_{i,0}^{(r,s)} \tilde{q}^{(r,s)}(t) \tag{2.11.3}$$

where

$$\tilde{q}_l^{(r,r)}(t) = -\int_0^t \int_0^t \tilde{g}_l^{(r,r)}(\tau_1,\tau_2)\ddot{z}(t-\tau_1)\ddot{z}(t-\tau_2)d\tau_1 d\tau_2 \tag{2.11.4}$$

$$\tilde{q}^{(r,s)}(t) = -\int_0^t \int_0^t \tilde{g}^{(r,s)}(\tau_1,\tau_2)\ddot{z}(t-\tau_1)\ddot{z}(t-\tau_2)d\tau_1 d\tau_2 \tag{2.11.5}$$

The integrals in (2.11.2), (2.11.4) and (2.11.5) are evaluated using FFT's. Most of the computational effort required is used to evaluate the discrete 2-D FT's of $\tilde{g}_l^{(r,r)}(\tau_1,\tau_2)$ and $\tilde{g}^{(r,s)}(\tau_1,\tau_2)$. If $N_1 = 2^{\mathrm{INT}(\log_2 N_T)+2}$, then the leading term of the amount of calculations involved in this step is $O(N_1^2 N_m^2)$. This amount of calculations is generally larger than that involved in any of the previous steps. Finally, the expressions for $E[x_i(t)]$ and $\mathrm{Var}(x_i(t))$ are given by (2.4.13) and (2.4.15a).

The following conclusions can be drawn from the results presented in this chapter:

1) The leading term of the amount of calculations required by the approximate method presented in this chapter is $O(N_1^2 N_m^2)$.

2) This leading term does not involve the parameter count N_θ.

3) The extra computational effort required to evaluate the statistics of the response at a different dof is minimal, since only the coefficients $c_{i,l}^{(r)}, c_{i,l}^{(r,r)}$, $c_{i,0}^{(r,s)}$ have to be evaluated for each additional dof, while the time functions $\tilde{q}_l^r(t), \tilde{q}_l^{(r,r)}(t), \tilde{q}^{(r,s)}(t)$ remain the same.

4) Steps very similar to the ones described in this chapter can be followed if, instead of displacements, other output response quantities are of interest, e.g., accelerations or internal forces. For a structural system with uncertain parameters, knowledge of the first moments of the quantities describing the state of the system is not sufficient to calculate the first moments of all possible output quantities. For example, the uncertain internal forces of a structural element are a function of the uncertain stiffness of the element and of the resulting uncertain generalized displacements of the element; since the uncertainties in the stiffness and the uncertainties in the generalized displacements are not independent, knowledge of their first two moments alone is not enough to calculate the first two moments of the uncertain internal forces.

The value of the proposed approximate method is established by comparing the amount of calculations it requires, which is $O(N_1^2 N_m^2)$, to the amount of calculations required by the numerical integration method, which is $O(N_T d^{(N_\theta + N_m)})$, where d is the number of discrete points chosen along the direction of each uncertain parameter: the latter number of calculations may become prohibitive for modeling structural systems. Furthermore, the results obtained using the proposed approximate method are very close to the ones obtained by simulations or by numerical integration, as was shown with a specific example in Figures 2.19 and 2.20. It is concluded from the above that the proposed method is an efficient and accurate method to calculate the uncertainties of the dynamic response of a structural system with uncertain parameters. The method provides a tool for the engineer during design of a structure to investigate the resulting uncertainties in the structural response due to uncertainties in the modeling process.

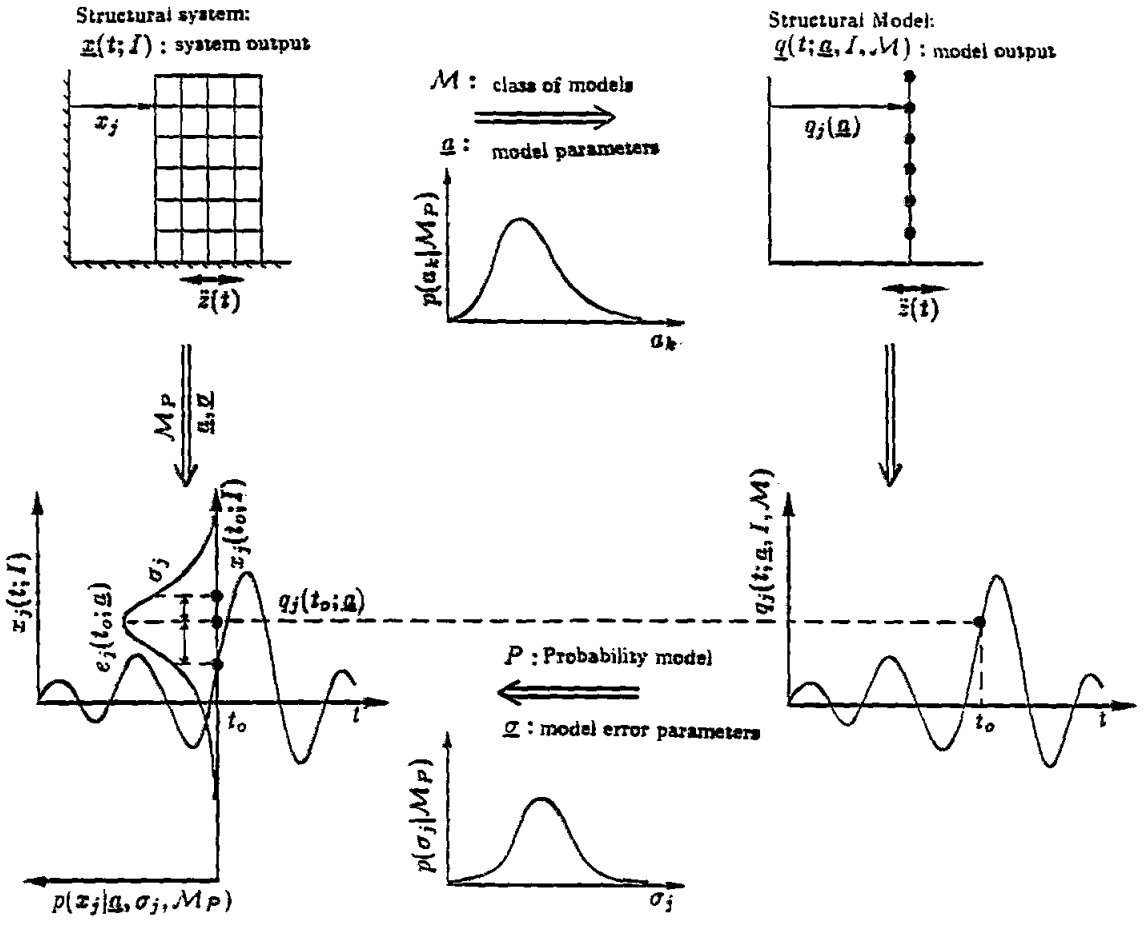

Figure 2.1 Schematic representation of the steps leading to the probabilistic modeling of a structural response.

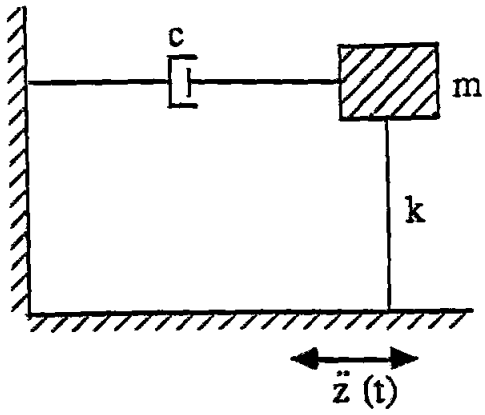

Figure 2.2 SDOF linear model of one-story building structure excited by ground acceleration.

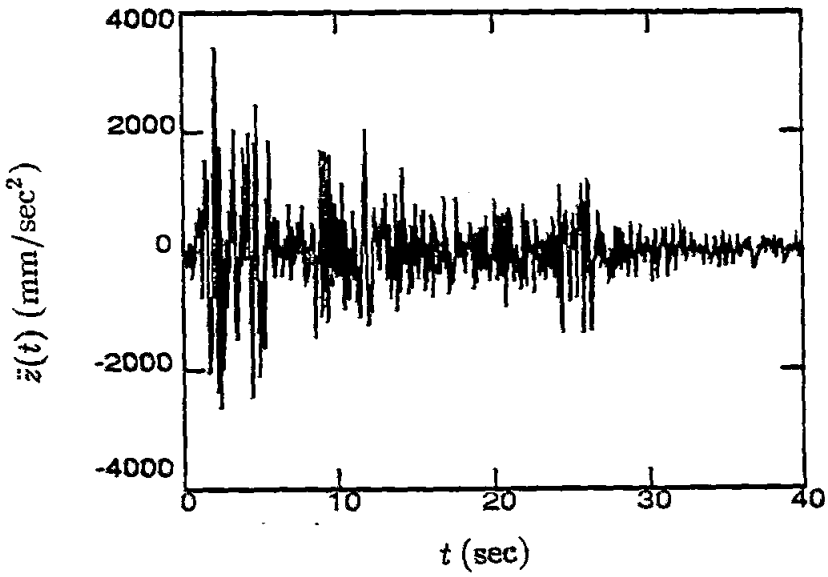

Figure 2.3 El Centro S00E acceleration record of the Imperial Valley Earthquake, May 18, 1940. This "El Centro record" is the applied base excitation in all numerical applications of this thesis.

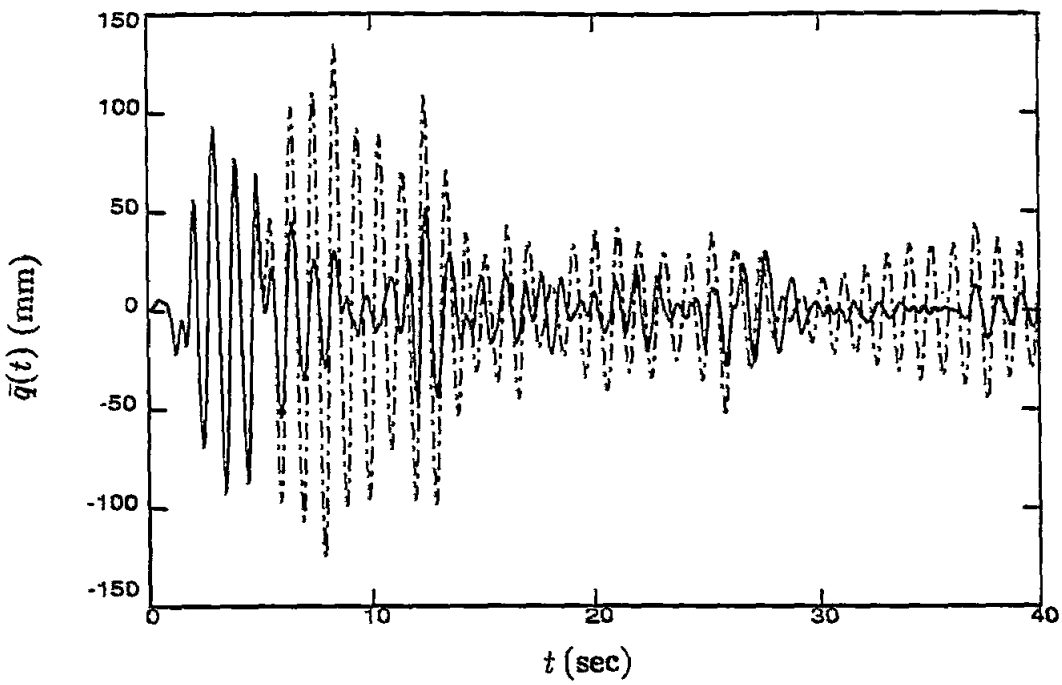

Figure 2.4 Expected response $\bar{q}(t)$, of a SDOF oscillator with fixed damping ratio $\zeta = 0.05$, and uncertain natural frequency ω, uniformly distributed over the interval $\Omega = [1.7\pi, 2.3\pi]\frac{\text{rad}}{\text{sec}}$ (El Centro record). Two methods are used to obtain $\bar{q}(t)$: (1) numerical integration (solid curve) and (2) SMA (dashed-dotted curve).

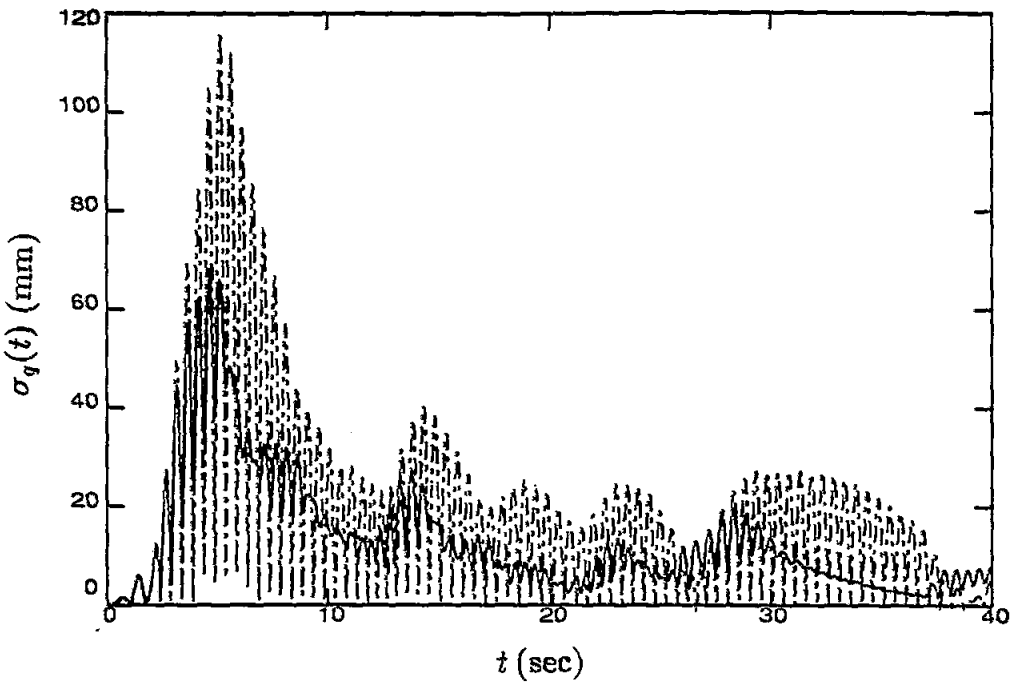

Figure 2.5 Standard deviation of the response $\sigma_q(t)$ for the SDOF oscillator of Figure 2.4. The solid curve is obtained using numerical integration, while the dashed-dotted curve is obtained using SMA.

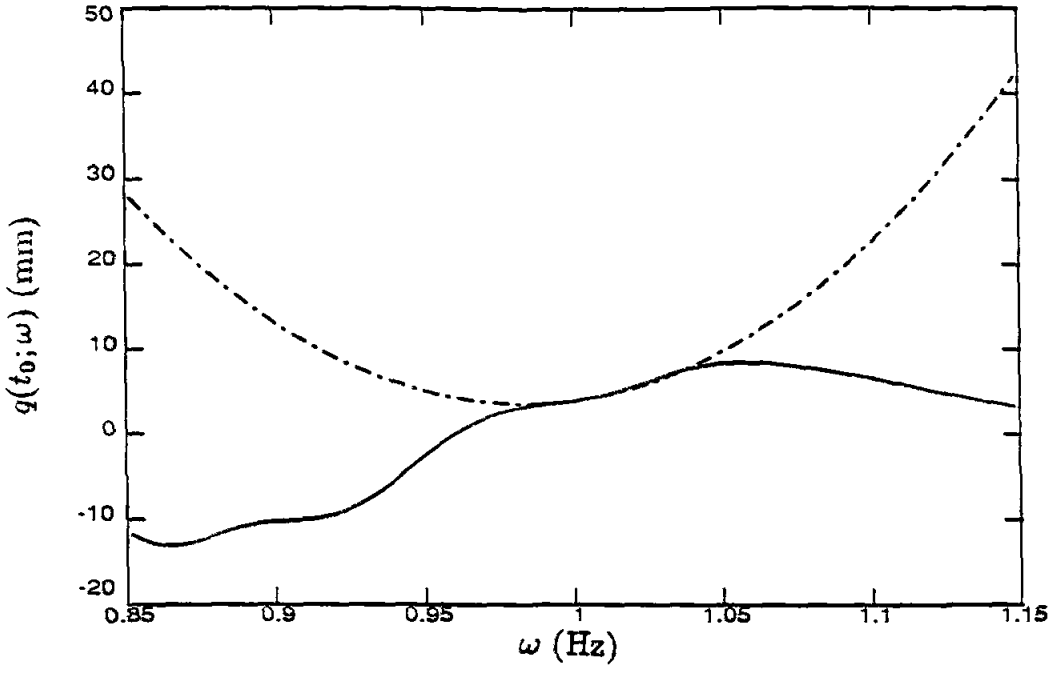

Figure 2.6 Response $q(t;\omega)$ at fixed time $t = t_0 = 5$ sec, against the natural frequency ω in Hz for the SDOF oscillator of Figure 2.4. The solid curve is exact, while the dashed-dotted parabola corresponds to the truncated Taylor series expansion given by the right hand side of (2.5.8).

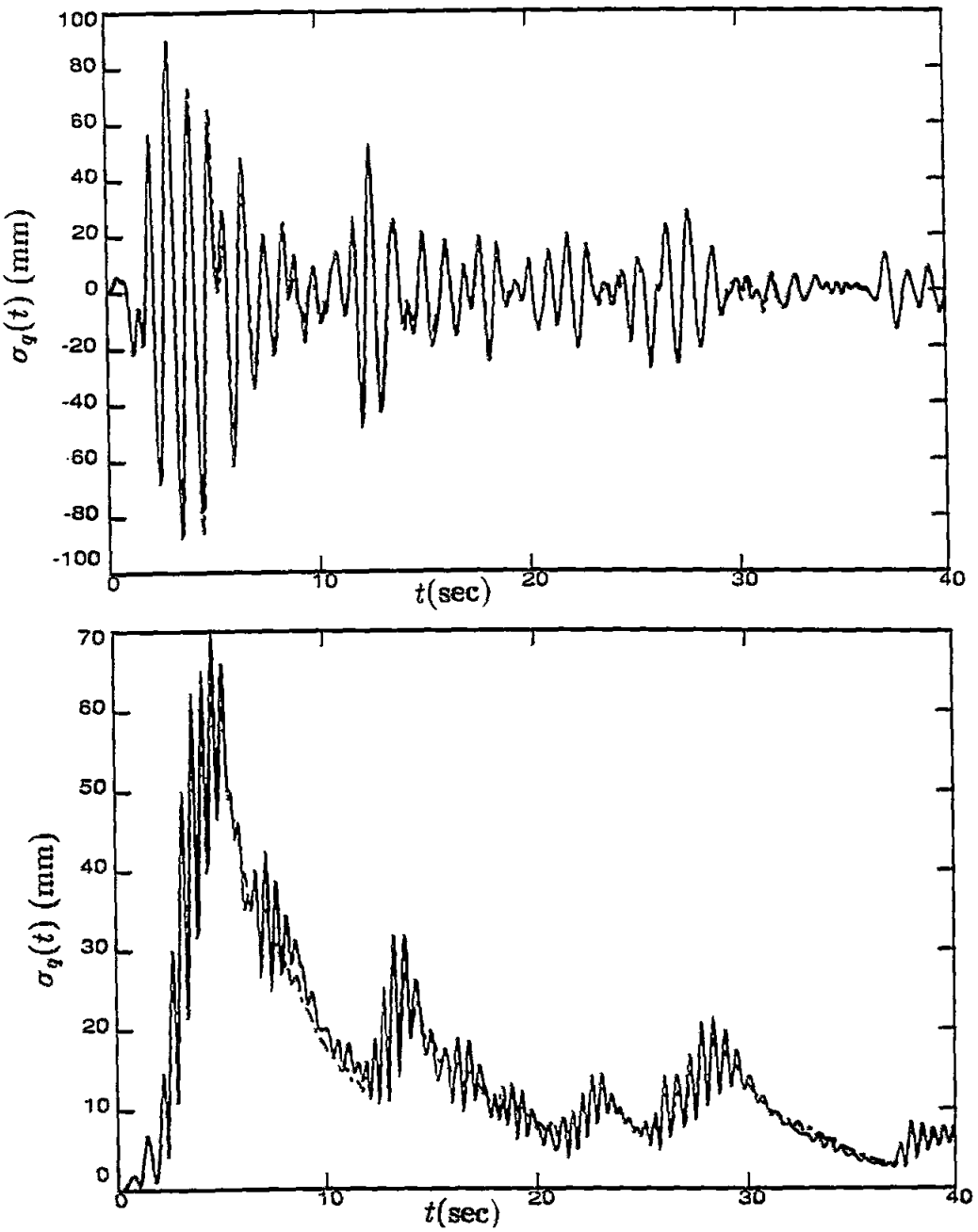

Figure 2.7 Expected response $\bar{q}(t)$ and its corresponding standard deviation $\sigma_q(t)$, for a SDOF oscillator with fixed damping ratio $\zeta = 0.05$ and uncertain natural frequency (El Centro record). The solid curve corresponds to ω being uniformly distributed over the interval $[0.85, 1.15]$Hz, resulting in $(\bar{\omega}, \alpha_\omega) = (1\text{Hz}, 8.66\%)$, while the dashed-dotted curve corresponds to ω being Gamma distributed with the same two first moments as in the previous case.

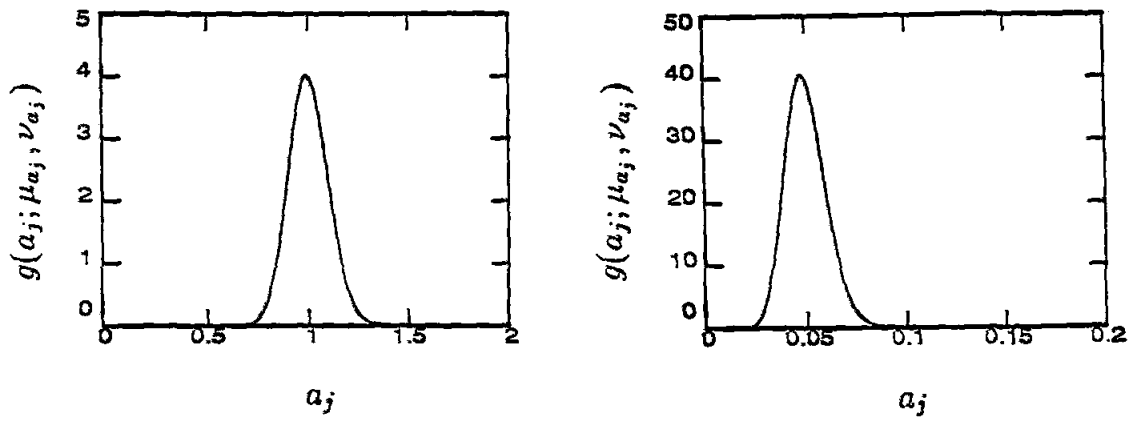

Figure 2.8 (a) Gamma distribution of an uncertain parameter a_j with $\bar{a}_j = 1$ and $\alpha_{a_j} = 0.10$ ($\mu_{a_j} = 100, \nu_{a_j} = 100$).

(b) Gamma distribution of an uncertain parameter a_j with $\bar{a}_j = 0.05$ and $\alpha_{a_j} = 0.20$ ($\mu_{a_j} = 500, \nu_{a_j} = 25$).

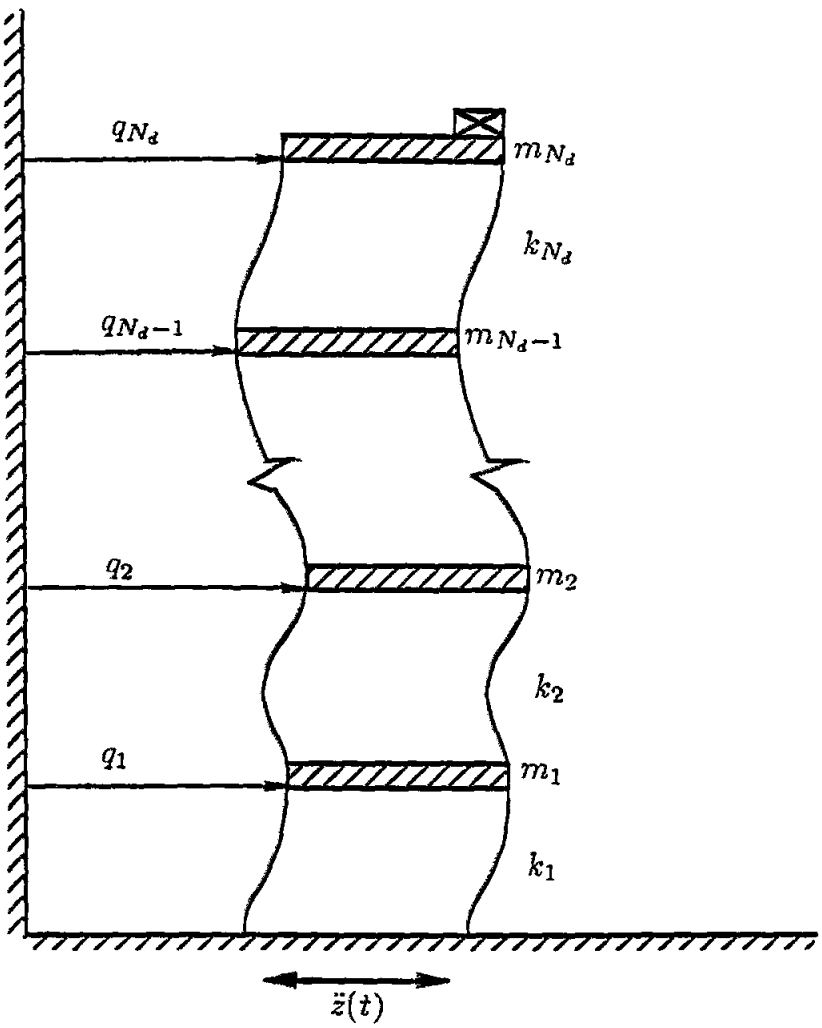

Figure 2.9 Multi-story planar shear building structure excited by a ground acceleration.

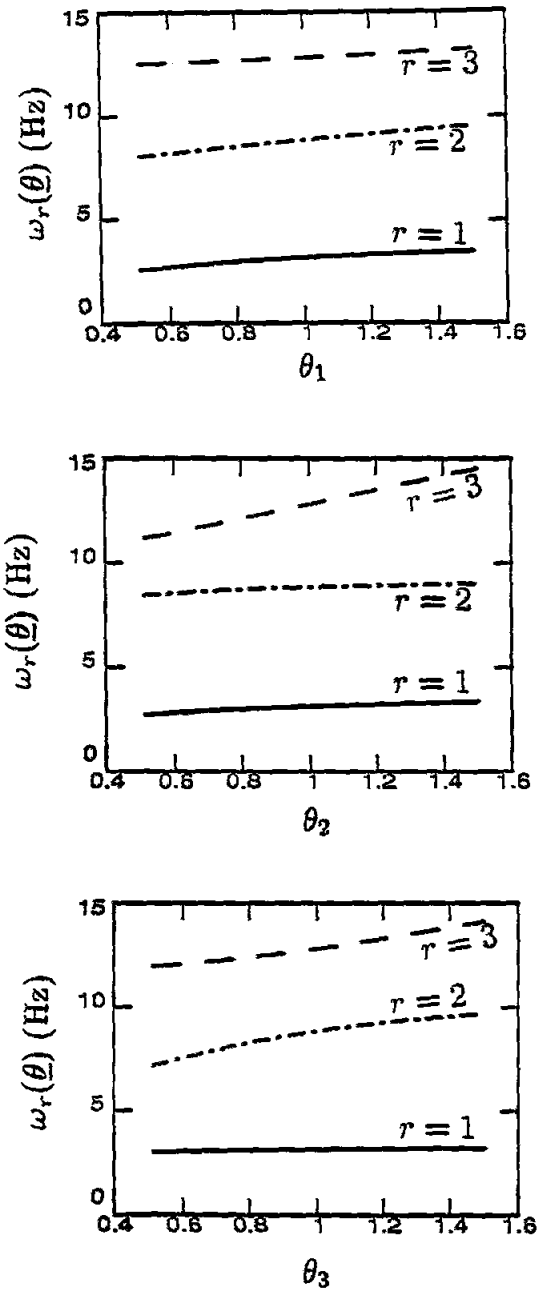

Figure 2.10 Modal frequencies $\omega_r(\underline{\theta}), r = 1,2,3$ against $\theta_i, i = 1,2,3$ for a three-story planar shear building with uniform mass $m_i = m_0$ and inter-story stiffness $k_i = k_0\theta_i, i = 1,2,3$ $(k_0 = 2000 m_0 sec^{-2})$; while each θ_i is varied, the remaining $\theta_j \neq \theta_i$ are kept constant, equal to unity.

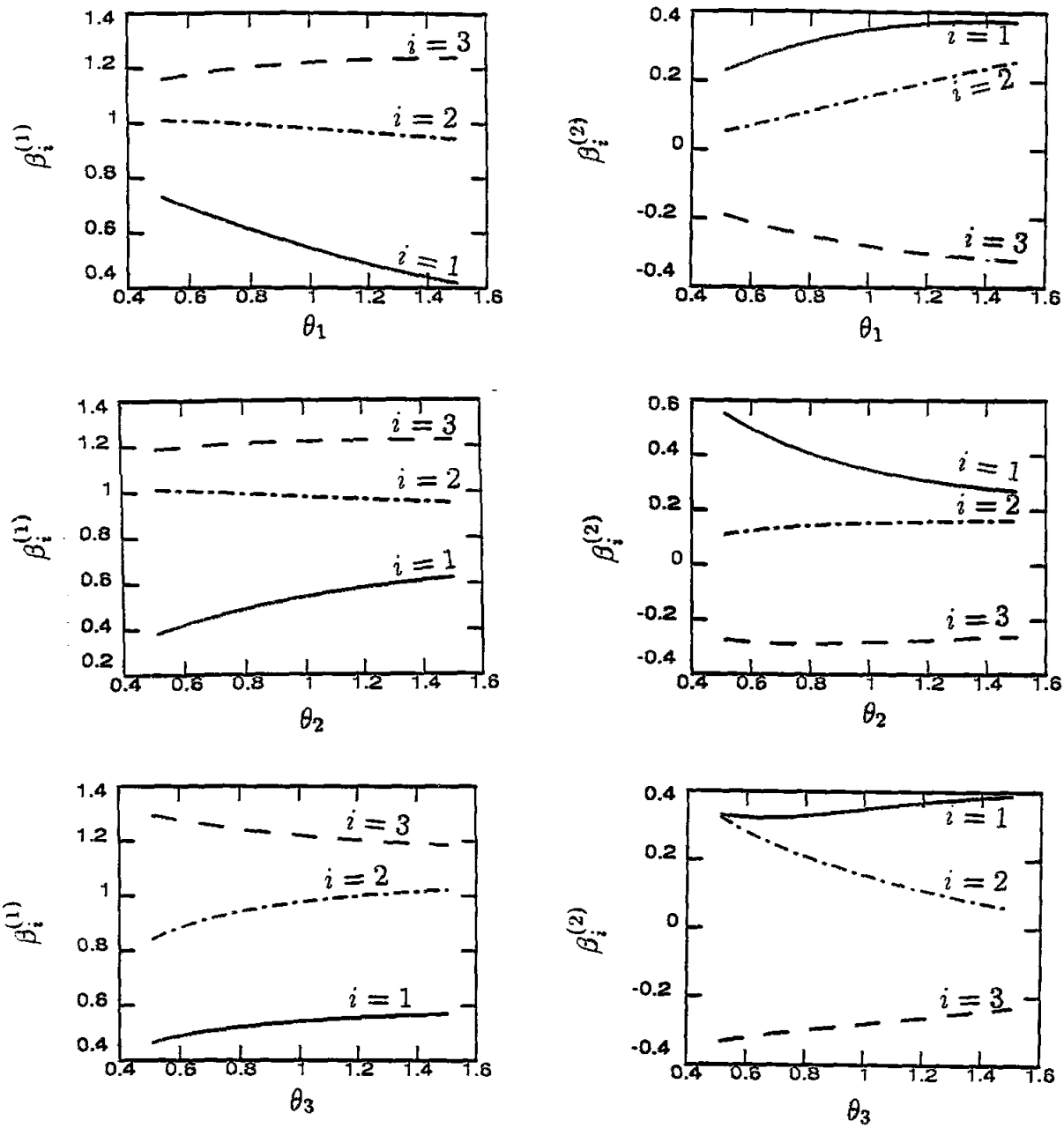

Figure 2.11 Effective participation factors at the different floors $\beta_k^{(r)}(\underline{\theta}), k = 1,2,3$, against $\theta_i, i = 1,2,3$, for the different modes $r = 1,2,3$, of the three-story planar shear building of Figure 2.10; while each θ_i is varied, the remaining $\theta_j \neq \theta_i$ are kept constant, equal to unity.

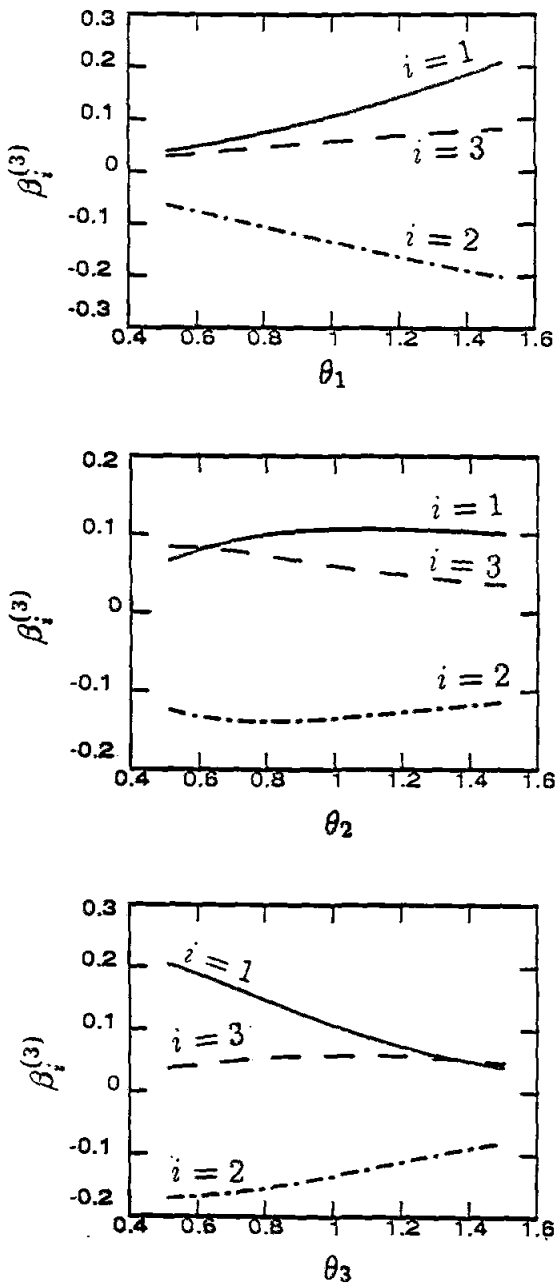

Figure 2.11 Continued.

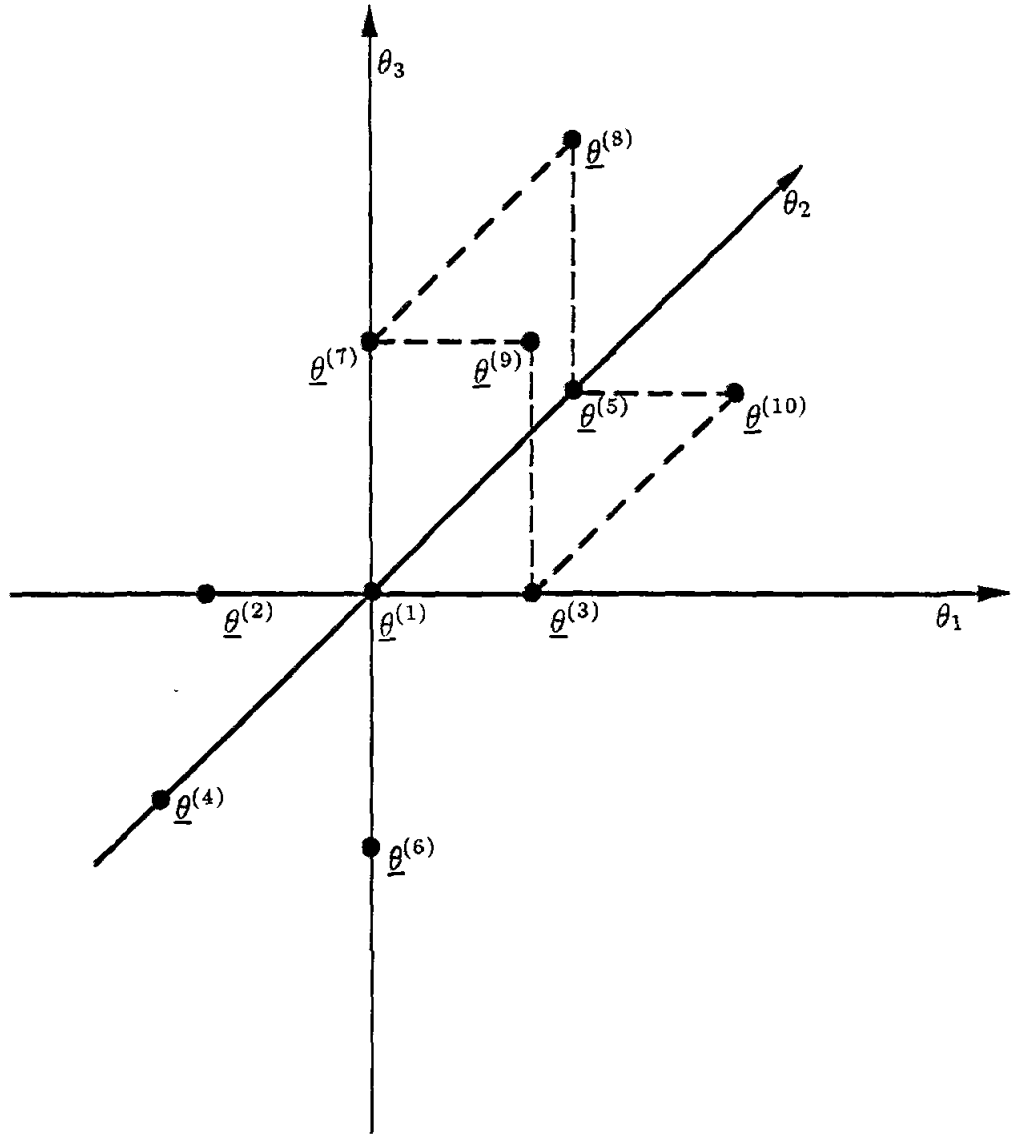

Figure 2.12 Points $\underline{\theta}^{(i)}$ chosen to interpolate quadratic approximations in $\underline{\theta}$ to various modal quantities, which are functions of $\underline{\theta}$, as discussed in Section 2.8. In this case, $N_\theta = 3$, resulting in $N_l = 10$ required points $\underline{\theta}^{(i)}$.

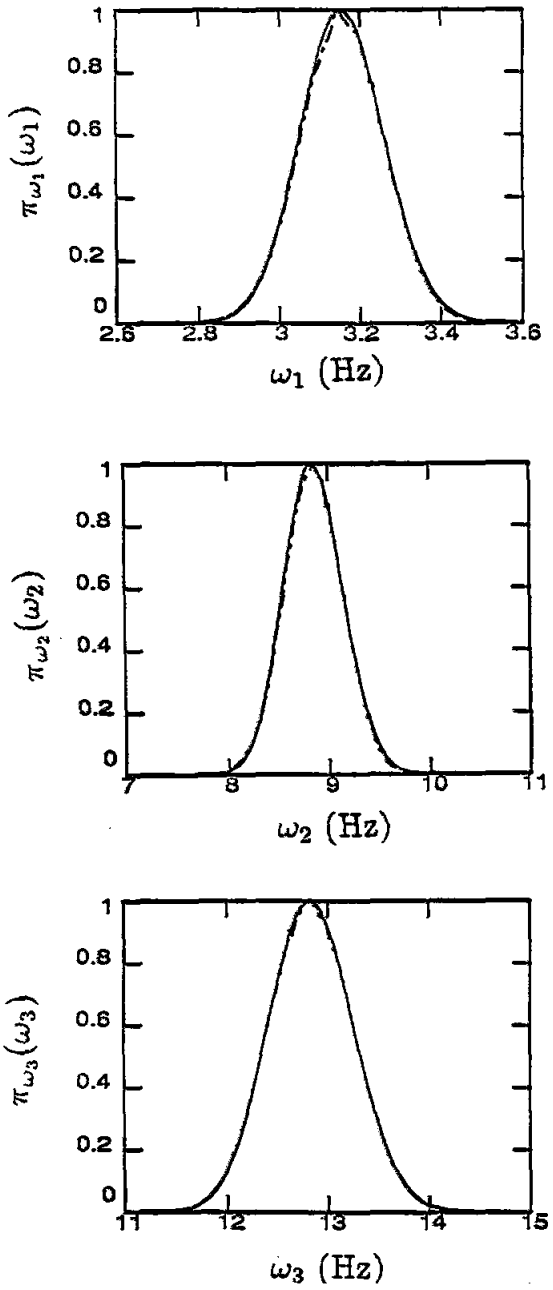

Figure 2.13 Normalized pdfs of the modal frequencies $\omega_r, r = 1,2,3$, for the three-story planar shear building of Figure 2.10. Each $\theta_i = 1,2,3$ is assumed to be independently Gamma distributed with $(\bar{\theta}_i, \alpha_{\theta_i}) =$ (1., .10). The solid curve is obtained using the approximations in Section 2.8, while the dashed-dotted curve is obtained using simulations.

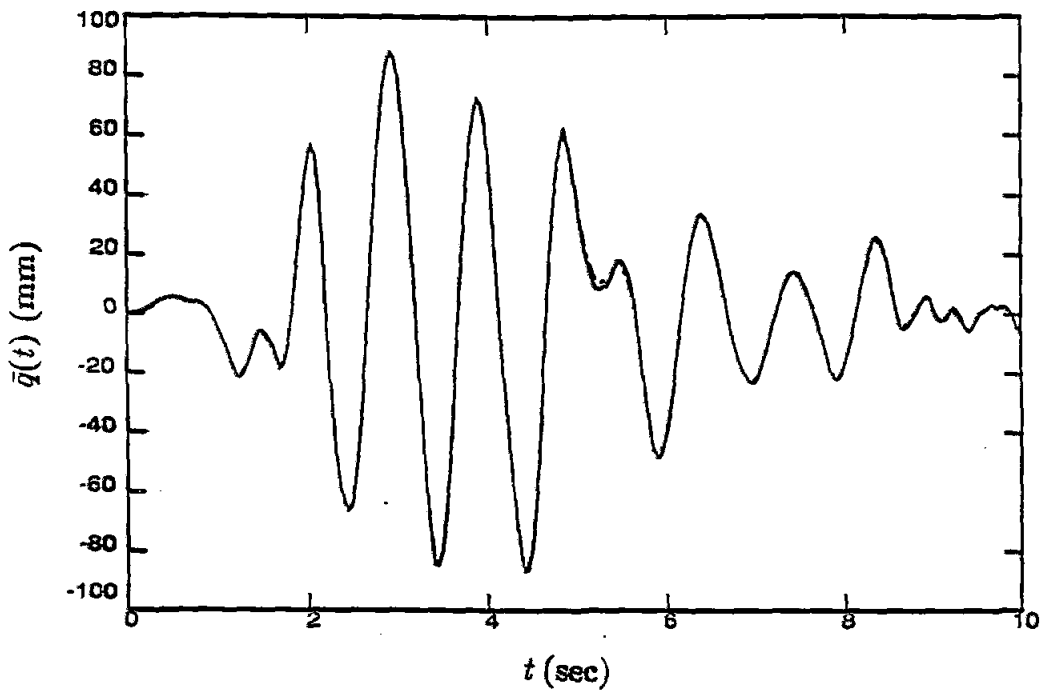

Figure 2.14 Expected response $\bar{q}(t)$ of a SDOF oscillator with independently Gamma distributed damping ratio ζ and frequency ω; $\bar{\omega} = 1$Hz, $\alpha_\omega = 0.10, \bar{\zeta} = 0.05, \alpha_\zeta = 0.20$ (El Centro record). The solid curve is obtained using numerical integration, while the dashed-dotted curve is obtained using the approximations of Section 2.9.

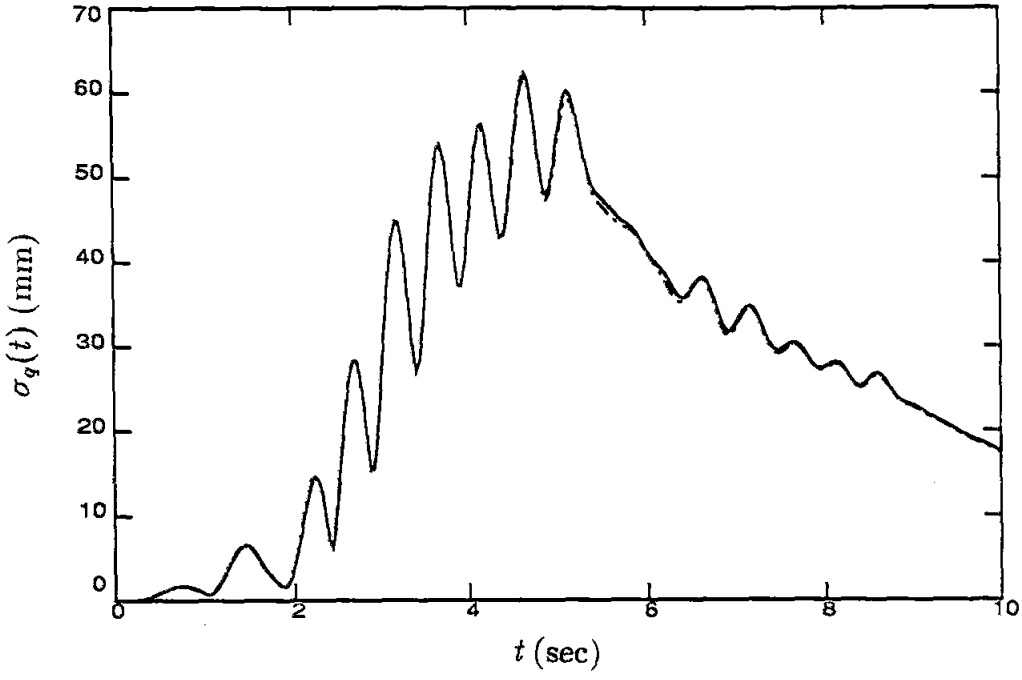

Figure 2.15 Standard deviation $\sigma_q(t)$ for the SDOF oscillator of Figure 2.14. The solid curve is obtained using numerical integration, while the dashed-dotted curve is obtained using the approximations of Section 2.9.

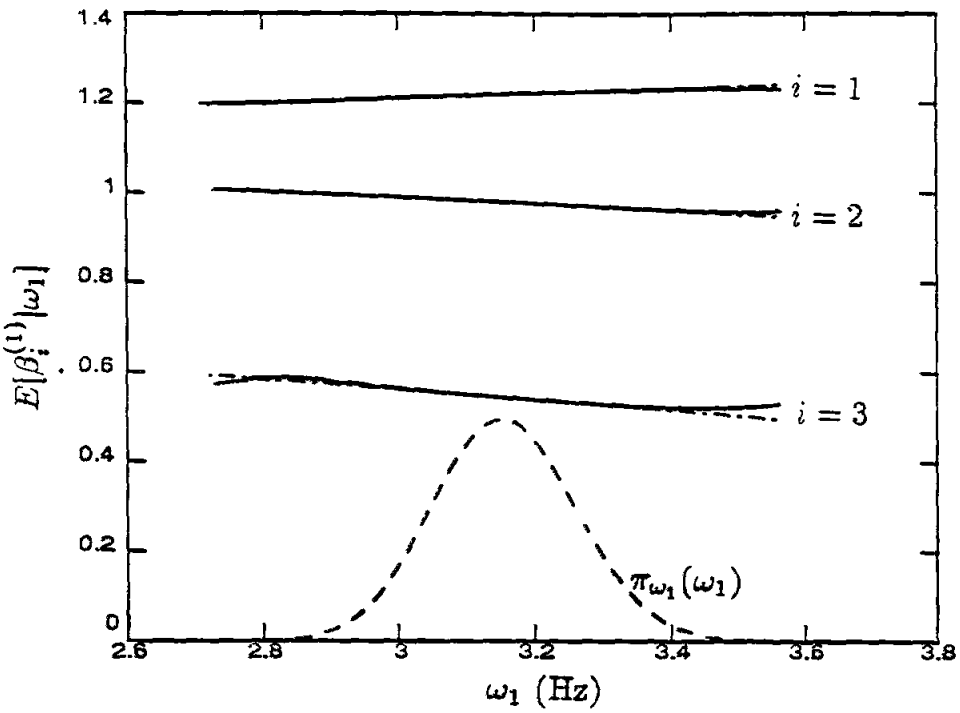

Figure 2.16 $E[\beta_i^{(1)}|\omega_1]$ for a three-story shear building with uniform mass $m_i = m_0$ and interstory stiffness $k_i = k_0\theta_i$, $i = 1,2,3$ ($k_0 = 2000 m_0 sec^{-2}$). Each θ_i, $i = 1,2,3$ is assumed independently Gamma distributed with $(\bar{\theta}_i, \alpha_{\theta_i}) = (1.,.10)$. The solid curve is obtained using simulations, while the dashed-dotted curve is obtained using the linear approximation (2.10.11). The dashed curve corresponds to the marginal pdf of ω_1, appropriately scaled.

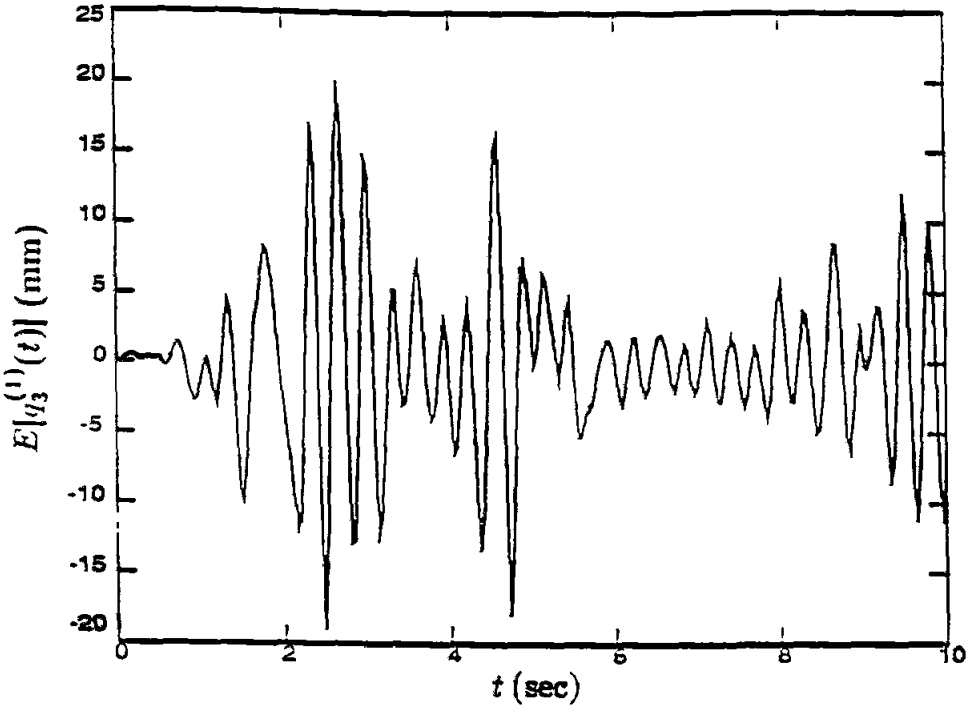

Figure 2.17 $E[q_3^{(1)}(t)]$ for a three-story shear building with uniform mass $m_i = m_0$ and interstory stiffness $k_i = k_0\theta_i$, $i = 1, 2, 3$ ($k_0 = 2000 m_0 sec^{-2}$). Each θ_i, $i = 1, 2, 3$ and each damping ratio ζ_r, $r = 1, 2, 3$ are assumed independently Gamma distributed with $(\bar{\theta}_i, \alpha_{\theta_i}) = (1..10)$ and $(\bar{\zeta}_r, \alpha_{\zeta_r}) = (0.05, .20)$ (El Centro record). The solid curve is obtained using numerical integration. while the dashed-dotted curve is obtained using the methodology of Section 2.10.1.

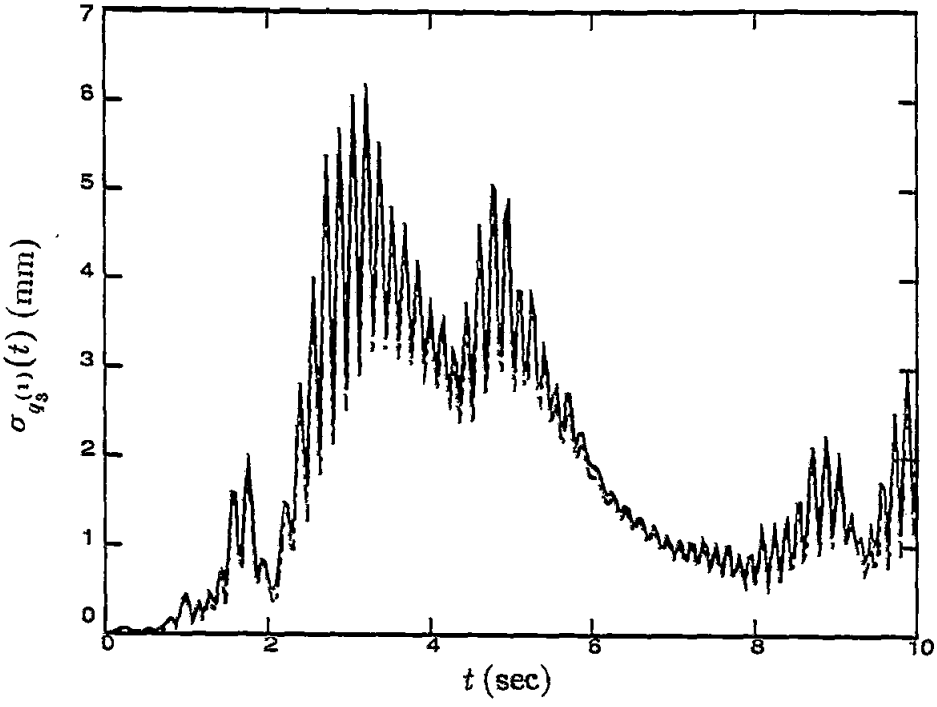

Figure 2.18 $\sigma_{q_3^{(1)}}(t)$ for the same three-story shear building as in Figure 2.17. The solid curve is obtained using numerical integration, while the dashed-dotted curve is obtained using the methodology of Section 2.10.1.

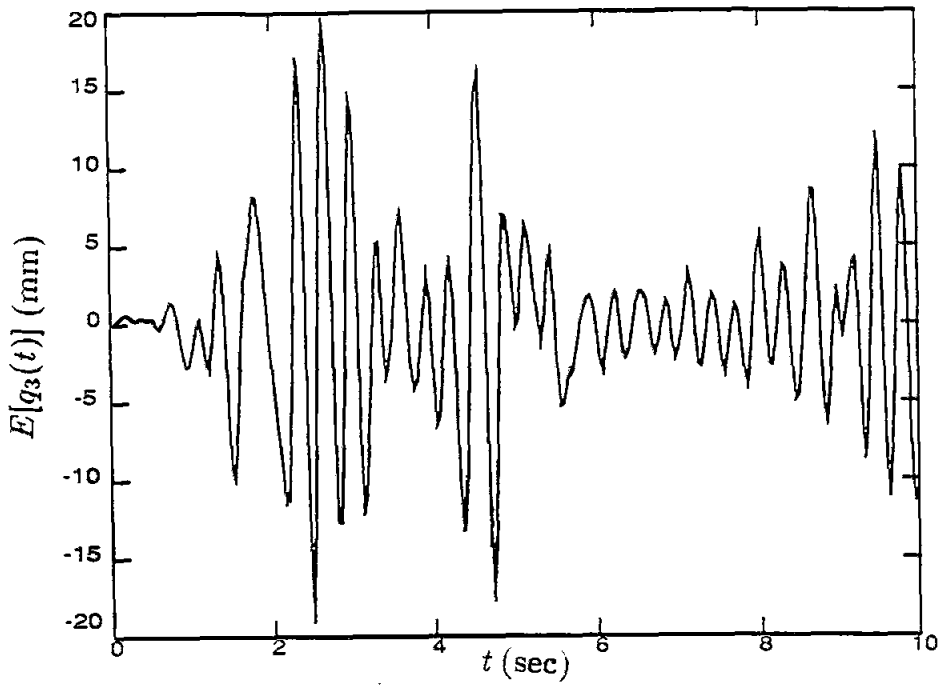

Figure 2.19 $E[q_3(t)]$ for the three-story shear building of Figure 2.17. The solid curve is obtained using numerical integration, while the dashed-dotted curve is obtained using the methodology of Section 2.10.

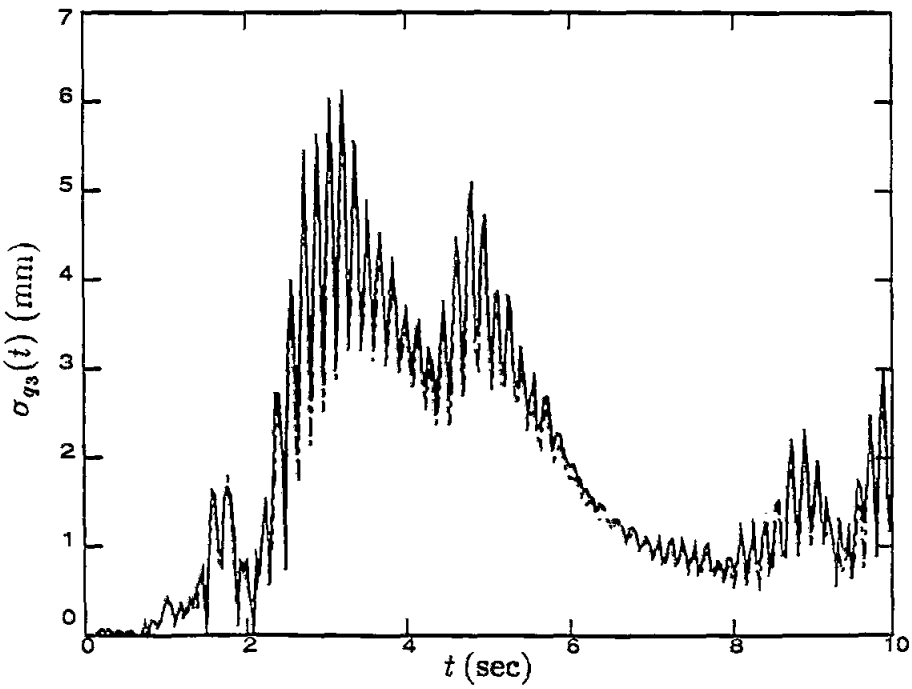

Figure 2.20 $\sigma_{q_3}(t)$ for the three-story shear building of Figure 2.17. The solid curve is obtained using numerical integration, while the dashed-dotted curve is obtained using the methodology of Section 2.10.

Chapter 3

Improving Response Predictions Utilizing Dynamic Testing

3.1 Introduction

This chapter is concerned with the updating of a mathematical model of a structure by using existing records of structural response. The initial uncertainties of the model parameters, as well as the initial uncertainty of the model error, are updated by extracting the structural information contained in the available records. The probability density function modeling the uncertainties of the parameters and the model error, after the updating, is also referred to as the posterior probability density function. The degrees of freedom where instrumentation allowed for output measurements will be referred to as observed or measured dof. Usually, the recorded output consists of the acceleration histories at these dof; in this case, the updated posterior pdf is evaluated by utilizing these recorded acceleration records directly rather than utilizing velocity or displacement histories obtained through integration of the acceleration histories, since such an integration process accentuates long-period errors in the digitized data. The goals of this chapter are the following:

1) To evaluate the posterior pdf's of the uncertain parameters and the model error by utilizing the recorded output histories at the measured degrees of freedom of the structure for a given excitation.

2) To utilize this updated posterior pdf to predict: (a) the statistics of the uncertain unobserved output quantities of interest for the above given exci-

tation or (b) the statistics of all the uncertain output quantities of interest, at both observed and unobserved dof, for a different excitation.

The problem of evaluating the posterior pdf of the uncertain parameters and the model error is essentially the problem of Bayesian statistical system identification [Beck 1990]. Aside from predictions, the posterior pdf of the uncertain parameters may be used for the purpose of monitoring the structure's health or for applying effective control strategies for the structure. In the next section, some definitions and notation are introduced to mathematically formulate the whole problem of interest.

3.2 Some Definitions and Notation

Let $\hat{Z}_{1,N} = \{\underline{\hat{z}}(n) \in R^{N_I} : n = 1, 2, \ldots, N\}$ and $\hat{X}_{1,N} = \{\underline{\hat{x}}^o(n) \in R^{N_o} : n = 1, 2, \ldots, N\}$ be the sampled observed input and output histories for a structural system with a sampling interval of Δt. Assume that an N_d-degree of freedom theoretical model $\mathcal{M}$ has been chosen to describe the input-output behavior of the system and let $\underline{a}$ be the vector of the model's uncertain parameters with an associated joint prior pdf $\pi_{\underline{a}}(\underline{a})$. $\mathcal{M}$ provides a functional relationship between the model output vector of quantities of interest $\underline{q}(n;\underline{a}) \in R^{N_R}$ at time $t_n = n\Delta t$ and the system input $Z_{1,n}$:

$$\underline{q}(n;\underline{a}) = \underline{q}(n;\underline{a}, Z_{1,n}, \mathcal{M}) \tag{3.2.1}$$

Throughout this chapter, the dependence of $\underline{q}(n;\underline{a})$ on the input $Z_{1,n}$ and the theoretical model $\mathcal{M}$ will be suppressed in the notation. Also, define the vector $\underline{x}(n) \in R^{N_R}$ consisting of all system output quantities of interest at time $t_n = n\Delta t$ corresponding to $\underline{q}(n)$, including the N_o observed output quantities. Without loss of generality, the elements of $\underline{x}(n)$ and $\underline{q}(n)$ are assumed arranged so that the first N_o of them correspond to the observed, and the remaining $N_u = N_R - N_o$ to the unobserved, output quantities of interest. For example, $\underline{x}(n) = [\underline{x}^o(n)^T, \underline{x}^u(n)^T]^T$, where $\underline{x}^o(n) \in R^{N_o}$ and $\underline{x}^u(n) \in R^{N_u}$. Assuming that

for modern instrumentation the measurement noise is negligible compared with the model error, it follows that $\underline{x}^o(n) = \hat{\underline{x}}^o(n)$ and $\underline{z}(n) = \hat{\underline{z}}(n)$ for $n \leq N$.

To account for model error, the class of models $\mathcal{M}$ is extended to a class of probability models $\mathcal{M}_P$, parameterized by $\tilde{\underline{a}} = [\underline{a}^T, \underline{\sigma}^T]^T \in R^{N_a+N_s}$. $\mathcal{M}_P$ prescribes a function g_M, or equivalently g'_M, describing the joint pdf of the system's output history given the input history as follows:

$$\begin{aligned} p(X_{1,M}|\tilde{\underline{a}}, Z_{1,M}, \mathcal{M}_P) &= g_M(X_{1,M}; \tilde{\underline{a}}, Z_{1,M}) \\ &= g'_M(X^o_{1,M}, X^u_{1,M}; \tilde{\underline{a}}, Z_{1,M}) \end{aligned} \tag{3.2.2}$$

where $X^o_{1,M} = \{\underline{x}^o(n) \in R^{N_o}; n = 1, 2, \ldots, M\}$ and $X^u_{1,M} = \{\underline{x}^u(n) \in R^{N_u}; n = 1, 2, \ldots, M\}$. $\mathcal{M}_P$ is also specifying the prior pdf, so that:

$$p(\tilde{\underline{a}}|\mathcal{M}_P) \equiv \pi_{\tilde{\underline{a}}}(\tilde{\underline{a}}) \tag{3.2.3}$$

Let $S(X^u_{1,M})$ and $S(X^o_{1,M})$ denote the space formed by the range of $X^u_{1,M}$ and $X^o_{1,M}$, respectively:

$$\begin{aligned} p(X^o_{1,M}|\tilde{\underline{a}}, Z_{1,M}, \mathcal{M}_P) &= \int_{S(X^u_{1,M})} p(X_{1,M}|\tilde{\underline{a}}, Z_{1,M}, \mathcal{M}_P) d\underline{x}^u(1) \ldots d\underline{x}^u(M) \\ &= \int_{S(X^u_{1,M})} g'_M(X^o_{1,M}, X^u_{1,M}; \tilde{\underline{a}}, Z_{1,M}) d\underline{x}^u(1) \ldots d\underline{x}^u(M) \\ &\equiv f^o_M(X^o_{1,M}; \tilde{\underline{a}}, Z_{1,M}) \end{aligned} \tag{3.2.4}$$

and

$$\begin{aligned} p(X^u_{1,M}|\tilde{\underline{a}}, Z_{1,M}, \mathcal{M}_P) &= \int_{S(X^o_{1,M})} p(X_{1,M}|\tilde{\underline{a}}, Z_{1,M}, \mathcal{M}_P) d\underline{x}^o(1) \ldots d\underline{x}^o(M) \\ &= \int_{S(X^o_{1,M})} g'_M(X^o_{1,M}, X^u_{1,M}; \tilde{\underline{a}}, Z_{1,M}) d\underline{x}^o(1) \ldots d\underline{x}^o(M) \\ &\equiv f^u_M(X^u_{1,M}; \tilde{\underline{a}}, Z_{1,M}) \end{aligned} \tag{3.2.5}$$

Different choices in modeling the model error, such as the equation-error or the output-error approach, lead to different probability models $\mathcal{M}_P$. While the

equation-error approach is appropriate to account for model error due to measurement errors in the input data, it does not account properly for model error introduced due to more important factors, such as nonlinearities in the real system not accounted for by the theoretical model. An output-error approach, on the other hand, is appropriate to account for both model error and measurement noise. The probabilistic formulation in this chapter is based on an output error approach as presented in the next section, and follows closely Beck [1990]. Here, this approach is extended to treat predictions of unobserved output quantities of interest by including the parameters $\underline{a}^u$ and $\underline{\sigma}^u$, which are not locally identifiable. Also, computationally feasible numerical algorithms are developed to evaluate the optimal observed parameters in both the globally and locally identifiable cases.

3.3 Output-Error Approach

The output error $\underline{e}(n)$ is defined to be the difference between the system output and the model output, so:

$$\underline{x}(n) = \underline{q}(n;\underline{a}) + \underline{e}(n) \tag{3.3.1}$$

where as mentioned earlier, the dependence of $\underline{q}$ on the input and the theoretical model, as stated in (3.2.1), has been suppressed in the notation. Also, the dependence of $\underline{x}(n)$ on the input $Z_{1,n}$ has been suppressed in the notation. A class of probability models P is selected, parameterized by $\underline{\sigma} \in R^{N_\sigma}$, prescribing a function h_M to describe the joint pdf of the output error, so:

$$p(\underline{e}(1),\ldots,\underline{e}(M)|\underline{\sigma},P) = h_M(\underline{e}(1),\ldots,\underline{e}(M);\underline{\sigma}) \tag{3.3.2}$$

By specifying the classes $\mathcal{M}$ and P, the class $\mathcal{M}_P$ is specified. The function g_M in (3.2.2) is specified as:

$$g_M(X_{1,M};\tilde{\underline{a}},Z_{1,M}) = h_M\left((\underline{x}(1)-\underline{q}(1;\underline{a})),\ldots,(\underline{x}(M)-\underline{q}(M;\underline{a}));\underline{\sigma}\right) \tag{3.3.3}$$

where $\tilde{\underline{a}} = [\underline{a}^T, \underline{\sigma}^T]^T$. Defining $E_{1,M} = \{\underline{e}(1), \ldots, \underline{e}(M)\}$, notice that:

$$\begin{aligned} p(E_{1,M}|\underline{\sigma}, P) &= p(\underline{e}(M)|E_{1,M-1}, \underline{\sigma}, P)p(E_{1,M-1})|\underline{\sigma}, P) \\ &= p(\underline{e}(M)|E_{1,M-1}, \underline{\sigma}, P)p(\underline{e}(M-1)|E_{1,M-2}, \underline{\sigma}, P)p(E_{1,M-2}|\underline{\sigma}, P) \\ &\ldots \\ &= \prod_{n=1}^{M} p(\underline{e}(n)|E_{1,n-1}, \underline{\sigma}, P) \end{aligned} \tag{3.3.4}$$

where $E_{1,0}$ is the null statement. Equation (3.3.4) implies that the function h_M can be prescribed equivalently by specifying the function h'_n:

$$h'_n(\underline{e}(n); E_{1,n-1}, \underline{\sigma}) = p(\underline{e}(n)|\underline{e}(1), \ldots, \underline{e}(n-1), \underline{\sigma}, P) \tag{3.3.5}$$

since then:

$$h_M = \prod_{n=1}^{M} h'_n \tag{3.3.6}$$

If the sequence $\{\underline{e}(n)\}$ is modeled by an ARMA model of order k, then $h'_n(\underline{e}(n); E_{1,n-1}, \underline{\sigma}) = h'_n(\underline{e}(n); E_{n-k,n-1}, \underline{\sigma})$. The higher k, the more complicated the analysis becomes, without significant improvement in the amount of structural information extracted from the available records. Assuming that the sequence $\{\underline{e}(n)\}$ is a zero-mean stationary Gaussian white-noise sequence leads to the standard output-error approach. The white-noise assumption implies temporal statistical independence, that is, the error $\underline{e}(n)$ is statistically independent of the errors $\underline{e}(1), \ldots, \underline{e}(n-1)$, so:

$$h'_n(\underline{e}(n); E_{1,n-1}, \underline{\sigma}) = h'(\underline{e}(n); \underline{\sigma}) = G(\underline{0}, \Sigma(\underline{\sigma})) \tag{3.3.7}$$

where $G(\underline{0}, \Sigma(\underline{\sigma}))$ is a joint Gaussian distribution with zero mean and a time independent $N_R \times N_R$ covariance matrix $\Sigma(\underline{\sigma})$. Substituting (3.3.7) into (3.3.6) leads to:

$$h_M(E_{1,M}; \underline{\sigma}) = \frac{1}{(2\pi)^{\frac{MN_R}{2}} |\Sigma(\underline{\sigma})|^{\frac{M}{2}}} \exp\left(-\frac{1}{2} \sum_{n=1}^{M} \underline{e}^T(n) \Sigma^{-1}(\underline{\sigma}) \underline{e}(n) \right) \tag{3.3.8}$$

From (3.3.8) and (3.3.3):

$$g_M(X_{1,M};\tilde{\underline{a}},Z_{1,M}) = \frac{1}{(2\pi)^{\frac{MN_R}{2}}|\Sigma(\underline{\sigma})|^{\frac{M}{2}}} \exp\left(-\frac{1}{2}\sum_{n=1}^{M}(\underline{x}(n)-\underline{q}(n;\underline{a}))^T\Sigma^{-1}(\underline{\sigma})(\underline{x}(n)-\underline{q}(n;\underline{a}))\right) \tag{3.3.9}$$

Additionally, spatial statistical independence is assumed between all elements of $\underline{e}(n)$, that is, each model error $e_i(n)$ is assumed independently Gaussian distributed with zero mean and variance depending only on the corresponding physical quantity. For example, all model errors corresponding to accelerations at different dof are assumed independently Gaussian distributed with zero mean and variance σ_a^2, while, for example, all errors corresponding to displacements at different dof are also assumed independently Gaussian distributed with zero mean, but with variance σ_d^2. This assumption leads to a diagonal $\Sigma(\underline{\sigma})$. Since all observed quantities generally represent the same physical quantity, usually accelerations at different dof, it will be assumed that:

$$\Sigma(\underline{\sigma}) = \begin{bmatrix} \Sigma^o(\sigma^o) & 0 \\ 0 & \Sigma^u(\underline{\sigma}) \end{bmatrix} \tag{3.3.10}$$

where $\Sigma^o(\sigma^o)$ is a $N_o \times N_o$ diagonal matrix with identical diagonal elements $(\sigma^o)^2$, that is, $[\Sigma^o(\sigma^o)]_{ij} = (\sigma^o)^2\delta_{ij}$, and the covariance matrix for the unobserved output $\Sigma^u(\underline{\sigma})$ is a $N_u \times N_u$ diagonal matrix, with its diagonal terms being squares of elements of $\underline{\sigma}$. Let $\underline{\sigma} = [\sigma^o, \underline{\sigma}^{u^T}]^T$, and $\underline{a} = [\underline{a}^{o^T}, \underline{a}^{u^T}]^T$, where $\underline{a}^o$ is such that $q_i(n;\underline{a}) = q_i(n;\underline{a}^o), i = 1,2,\ldots,N_o$, that is, $\underline{a}^o$ contains the parameters controlling the model output at the observed dof. The vector $\underline{a}^u$ is defined as consisting of the remaining elements of $\underline{a}$; notice however, that the model output at the unobserved degrees of freedom may depend on all parameters in $\underline{a}$, not just $\underline{a}^u$, so in general $q_i(n;\underline{a}) \neq q_i(n;\underline{a}^u), i = N_o+1,\ldots,N_o+N_u$. The parameter vectors $\underline{a}^o, \underline{a}^u$ are defined by the theoretical model $\mathcal{M}$ and the choice of the observed output quantities, along with the choice of the unobserved output quantities of interest. For example, consider a theoretical model based on a modal

approach and assume that the output quantities of interest are the accelerations at all dof, while the observed output consists only of accelerations at specific dof; in this case, the modal participation factors at the unobserved dof are not needed in specifying the model response at the observed dof and therefore do not belong in the vector $\underline{a}^o$, while they are needed to specify the model response at the unobserved dof and, therefore, belong in the vector $\underline{a}^u$. If, instead, a theoretical model based on a finite element approach is employed in the above example, as discussed in Section 2.6, then the complete vector $\underline{a}$, consisting of the stiffness parameter vector $\underline{\theta}$ and the damping ratio vector $\underline{\zeta}$, is needed to specify the model response at the observed dof. Therefore $\underline{a}^o = \underline{a}$.

For the sake of brevity in the notations, the following vectors are introduced: $\tilde{\underline{a}}^o \equiv [\underline{a}^{o^T}, \sigma^o]^T$, $\tilde{\underline{a}}^u \equiv [\underline{a}^{u^T}, \underline{\sigma}^{u^T}]^T$, $\underline{e}^o(n;\underline{a}^o) \equiv \underline{x}^o(n) - \underline{q}^o(n;\underline{a}^o) \in R^{N_o}$, $\underline{e}^u(n;\underline{a}) \equiv \underline{x}^u(n) - \underline{q}^u(n;\underline{a}) \in R^{N_u}$, $\hat{\underline{e}}^o(n;\underline{a}^o) \equiv \hat{\underline{x}}^o(n) - \underline{q}^o(n;\underline{a}^o) \in R^{N_o}$.

If $\Sigma(\underline{\sigma})$ is given by (3.3.10), Equation (3.3.9) becomes:

$$\begin{aligned} g_M(X_{1,M};\tilde{\underline{a}},Z_{1,M}) &= g'_M(X^o_{1,M},X^u_{1,M};\tilde{\underline{a}},Z_{1,M}) \\ &= \frac{1}{(2\pi(\sigma^o)^2)^{\frac{MN_o}{2}}}\exp\left(-\frac{1}{2(\sigma^o)^2}\sum_{n=1}^{M}\sum_{i=1}^{N_o}e_i^o(n;\underline{a}^o)^2\right) \\ &\times \quad \frac{1}{(2\pi)^{\frac{MN_u}{2}}|\Sigma_u(\underline{\sigma})|^{\frac{M}{2}}}\exp\left(-\frac{1}{2}\sum_{n=1}^{M}\sum_{i=1}^{N_u}\frac{e_i^u(n;\underline{a})^2}{[\Sigma^u(\underline{\sigma})]_{ii}}\right) \end{aligned} \tag{3.3.11}$$

Substituting (3.3.11) into (3.2.4) leads to:

$$\begin{aligned} p(X^o_{1,M}|\underline{a},\underline{\sigma},Z_{1,M},\mathcal{M}_P) &= \frac{1}{(2\pi(\sigma^o)^2)^{\frac{MN_o}{2}}}\exp\left(-\frac{1}{2(\sigma^o)^2}\sum_{n=1}^{M}\sum_{i=1}^{N_o}e_i^o(n;\underline{a}^o)^2\right) \\ &\equiv f^o_M(X^o_{1,M};\tilde{\underline{a}}^o,Z_{1,M}) \end{aligned} \tag{3.3.12}$$

which implies that:

$$p(X^o_{1,M}|\tilde{\underline{a}},Z_{1,M},\mathcal{M}_P) = p(X^o_{1,M}|\tilde{\underline{a}}^o,Z_{1,M},\mathcal{M}_P) \tag{3.3.13}$$

Similarly, substituting (3.3.11) into (3.2.5) leads to:

$$p(X^u_{1,M}|\tilde{\underline{a}}, Z_{1,M}, \mathcal{M}_P) = \frac{1}{(2\pi)^{\frac{MN_u}{2}}|\Sigma^u(\underline{\sigma})|^{\frac{M}{2}}}\exp\left(-\frac{1}{2}\sum_{n=1}^{M}\sum_{i=1}^{N_u}\frac{e^u_i(n;\underline{a})^2}{[\Sigma^u(\underline{\sigma})]_{ii}}\right)$$
$$\equiv f^u_M(X^u_{1,M};\tilde{\underline{a}}, Z_{1,M}) \tag{3.3.14}$$

Notice that $f^u_M(X^u_{1,M};\tilde{\underline{a}}, Z_{1,M}) \neq f^u_M(X^u_{1,M};\tilde{\underline{a}}^u, Z_{1,M})$. Also, notice that:

$$\begin{aligned} p(X_{1,M}|\tilde{\underline{a}}, Z_{1,M}, \mathcal{M}_P) &\equiv g_M(X_{1,M};\tilde{\underline{a}}, Z_{1,M}) \\ &= f^o_M(X^o_{1,M}|\tilde{\underline{a}}^o, Z_{1,M}) f^u_M(X^u_{1,M}|\tilde{\underline{a}}, Z_{1,M}) \\ &\equiv p(X^o_{1,M}|\tilde{\underline{a}}^o, Z_{1,M}, \mathcal{M}_P) p(X^u_{1,M}|\tilde{\underline{a}}, Z_{1,M}, \mathcal{M}_P) \end{aligned} \tag{3.3.15}$$

that is, $X^o_{1,M}$ and $X^u_{1,M}$ are independently distributed when the parameters $\tilde{\underline{a}}$ are given.

3.4 Posterior pdf of Uncertain Parameters

Let $\mathcal{D}_N$ denote the set of observed data, consisting of the observed input history $\hat{Z}_{1,N}$ and output history $\hat{X}_{1,N}$. As in Section 3.2, it is assumed that for modern instrumentation the measurement noise is negligible compared with the model error. Therefore, the observed input and output histories are assumed to be identical with the corresponding system input and output histories, respectively. The updated, or "posterior," joint pdf of $\{\tilde{\underline{a}}\}$ is given by Bayes' Theorem (2.3.1):

$$\begin{aligned} p(\tilde{\underline{a}}|\mathcal{D}_N, \mathcal{M}_P) &= \frac{p(\hat{X}_{1,N}|\tilde{\underline{a}}, \hat{Z}_{1,N}, \mathcal{M}_P) p(\tilde{\underline{a}}|\mathcal{M}_P)}{p(\hat{X}_{1,N}|\hat{Z}_{1,N}, \mathcal{M}_P)} \\ &= k p(\hat{X}_{1,N}|\tilde{\underline{a}}, \hat{Z}_{1,N}, \mathcal{M}_P) p(\tilde{\underline{a}}|\mathcal{M}_P) \\ &= k f^o_N(\hat{X}_{1,N};\tilde{\underline{a}}^o)\pi_{\tilde{\underline{a}}}(\tilde{\underline{a}}) \end{aligned} \tag{3.4.1}$$

where

$$k^{-1} = p(\hat{X}_{1,N}|\hat{Z}_{1,N}, \mathcal{M}_P) = \int_{S(\tilde{\underline{a}})} p(\hat{X}_{1,N}|\tilde{\underline{a}}, \hat{Z}_{1,N}, \mathcal{M}_P) p(\tilde{\underline{a}}|\mathcal{M}_P) d\tilde{\underline{a}} \tag{3.4.2}$$

$S(\cdot)$ is defined to be the domain of the quantity in the parenthesis. The prior joint pdf $p(\underline{\tilde{a}}|\mathcal{M}_P)$ can be rewritten:

$$p(\underline{\tilde{a}}|\mathcal{M}_P) = p(\underline{\tilde{a}}^u|\underline{\tilde{a}}^o, \mathcal{M}_P)p(\underline{\tilde{a}}^o|\mathcal{M}_P) \tag{3.4.3}$$

where

$$p(\underline{\tilde{a}}^o|\mathcal{M}_P) = \int_{S(\underline{\tilde{a}}^u)} p(\underline{\tilde{a}}|\mathcal{M}_P)d\underline{\tilde{a}}^u \equiv \pi_{\underline{\tilde{a}}^o}(\underline{\tilde{a}}^o) \tag{3.4.4}$$

Substituting (3.4.3) into (3.4.1) and integrating out $\underline{\tilde{a}}^u$ leads to:

$$\begin{aligned} p(\underline{\tilde{a}}^o|\mathcal{D}_N, \mathcal{M}_P) &= kp(\hat{X}_{1,N}|\underline{\tilde{a}}^o, \hat{Z}_{1,N}, \mathcal{M}_P)p(\underline{\tilde{a}}^o|\mathcal{M}_P) \\ &= kf_N^o(\hat{X}_{1,N}; \underline{\tilde{a}}^o, \hat{Z}_{1,N})\pi_{\underline{\tilde{a}}^o}(\underline{\tilde{a}}^o) \end{aligned} \tag{3.4.5}$$

Similarly, by substituting (3.4.3) into (3.4.2) and integrating out $\underline{\tilde{a}}^u$, an alternative expression for k^{-1} is obtained:

$$k^{-1} = p(\hat{X}_{1,N}|\hat{Z}_{1,N}, \mathcal{M}_P) = \int_{S(\underline{\tilde{a}}^o)} p(\hat{X}_{1,N}|\underline{\tilde{a}}^o, \hat{Z}_{1,N}, \mathcal{M}_P)p(\underline{\tilde{a}}^o|\mathcal{M}_P)d\underline{\tilde{a}}^o \tag{3.4.6}$$

Equation (3.4.1) may be rewritten using (3.4.3) and (3.4.5):

$$p(\underline{\tilde{a}}|\mathcal{D}_N, \mathcal{M}_P) = p(\underline{\tilde{a}}^o|\mathcal{D}_N, \mathcal{M}_P)p(\underline{\tilde{a}}^u|\underline{\tilde{a}}^o, \mathcal{M}_P) \tag{3.4.7}$$

The last equation implies that:

$$p(\underline{\tilde{a}}^u|\underline{\tilde{a}}^o, \mathcal{D}_N, \mathcal{M}_P) = p(\underline{\tilde{a}}^u|\underline{\tilde{a}}^o, \mathcal{M}_P) \tag{3.4.8}$$

which is simply stating that the observations provide no information to update the conditional pdf of the parameters $\underline{\tilde{a}}^u$, given $\underline{\tilde{a}}^o$. The updated marginal pdf $p(\underline{\tilde{a}}^u|\mathcal{D}_N, \mathcal{M}_P)$ is:

$$\begin{aligned} p(\underline{\tilde{a}}^u|\mathcal{D}_N, \mathcal{M}_P) &= \int_{S(\underline{\tilde{a}}^o)} p(\underline{\tilde{a}}^u|\underline{\tilde{a}}^o, \mathcal{D}_N, \mathcal{M}_P)p(\underline{\tilde{a}}^o|\mathcal{D}_N, \mathcal{M}_P)d\underline{\tilde{a}}^o \\ &= \int_{S(\underline{\tilde{a}}^o)} p(\underline{\tilde{a}}^u|\underline{\tilde{a}}^o, \mathcal{M}_P)p(\underline{\tilde{a}}^o|\mathcal{D}_N, \mathcal{M}_P)d\underline{\tilde{a}}^o \end{aligned} \tag{3.4.9}$$

Notice from the last equation that the data does provide information to update the marginal distribution of $\underline{\tilde{a}}^u$, unless the parameters $\underline{\tilde{a}}^u$ and $\underline{\tilde{a}}^o$ are assumed independently distributed *a priori*.

As can be seen from (3.4.5), the effect of utilizing the available records to update the pdf of the observed model parameters and the observed model-error parameter is contained in the term $kf_N^o(\hat{X}_{1,N};\underline{\tilde{a}}^o,\hat{Z}_{1,N})$, where k serves as a normalizing constant. Assume that $f_N^o(\hat{X}_{1,N};\underline{\tilde{a}}^o,\hat{Z}_{1,N})$, given by (3.3.12), attains its global maximum at a unique set of parameters $\{\underline{\hat{\tilde{a}}}^o\} = \{\underline{\hat{a}}^o,\hat{\sigma}^o\}$; these parameters are also referred to as the "optimal" parameters. If a noninformative prior pdf $\pi_{\underline{\tilde{a}}^o}(\underline{\tilde{a}}^o)$ is assumed locally [Box and Tiao, 1973], in the neighborhood of the optimal parameters, the parameters $\underline{\hat{\tilde{a}}}^o = [\underline{\hat{a}}^{oT},\hat{\sigma}^o]^T$ maximizing $f_N^o(\hat{X}_{1,N};\underline{\tilde{a}}^o,\hat{Z}_{1,N})$ are also maximizing $p(\underline{\tilde{a}}^o|\mathcal{D}_N,\mathcal{M}_P)$, as can be seen by viewing (3.4.5). In this case, the optimal parameters $\underline{\hat{\tilde{a}}}^o$ correspond to the most probable model within the class $\mathcal{M}_P$. The assumption of a locally noninformative prior pdf, in the neighborhood of the optimal parameters, mathematically means that the prior distribution is constant over a neighborhood of radius $O(N^{-1})$. Therefore, for a slowly varying prior distribution and a large number of data points N, this condition is practically always satisfied (see Appendix E). Equation (3.4.5) can be rewritten:

$$\ln p(\underline{\tilde{a}}^o|\mathcal{D}_N,\mathcal{M}_P) = \ln k + \ln f_N(\hat{X}_{1,N};\underline{\tilde{a}}^o,\hat{Z}_{1,N}) + \ln\pi_{\underline{\tilde{a}}^o}(\underline{\tilde{a}}^o) \tag{3.4.10}$$

where from (3.3.12):

$$\ln f_N^o(\hat{X}_{1,N};\underline{\tilde{a}}^o,\hat{Z}_{1,N}) = -c - NN_o\ln\sigma^o - \frac{1}{2(\sigma^o)^2}\sum_{n=1}^{N}\sum_{i=1}^{N_o}\hat{e}_i^o(n;\underline{a}^o)^2 \tag{3.4.11}$$

and $c = -\frac{NN_o}{2}\ln(2\pi)$. Maximizing $f_N^o(\hat{X}_{1,N};\underline{\tilde{a}}^o,\hat{Z}_{1,N})$, with respect to $\underline{\tilde{a}}^o$, is equivalent to maximizing $\ln f_N^o(\hat{X}_{1,N};\underline{\tilde{a}}^o,\hat{Z}_{1,N})$. At $\underline{\tilde{a}}^o = \underline{\hat{\tilde{a}}}^o$ the following conditions hold:

$$\left.\frac{\partial \ln f_N^o(\hat{X}_{1,N};\underline{\tilde{a}}^o,\hat{Z}_{1,N})}{\partial\underline{\tilde{a}}^o}\right|_{\underline{\tilde{a}}^o=\underline{\hat{\tilde{a}}}^o} = 0 \tag{3.4.12}$$

For fixed $\underline{a}^o$, maximizing $\ln f_N^o(\hat{X}_{1,N}; \underline{\tilde{a}}^o, \hat{Z}_{1,N})$ with respect to σ^o requires:

$$\hat{\sigma}^o(\underline{a}^o)^2 = \frac{1}{NN_o}\sum_{n=1}^{N}\sum_{i=1}^{N_o}\hat{e}_i^o(n;\underline{a}^o)^2 = \frac{1}{NN_o}\sum_{n=1}^{N}\sum_{i=1}^{N_o}(\hat{x}_i^o(n) - q_i^o(n;\underline{a}^o))^2 \quad (3.4.13)$$

This shows how the most probable variance $\hat{\sigma}^o(\underline{a}^o)^2$, for given $\underline{a}^o$, depends on the choice of the model parameters $\underline{a}^o$. Obviously, the condition for the overall most probable variance $(\hat{\sigma}^o)^2$ is given by (3.4.13) when $\underline{a}^o = \underline{\hat{a}}^o$. Substituting (3.4.13) into (3.4.11):

$$\ln f_N^o(\hat{X}_{1,N}; \underline{a}^o, \hat{\sigma}^o(\underline{a}^o), \hat{Z}_{1,N}) = -c - NN_o \ln\hat{\sigma}^o(\underline{a}^o) - \frac{NN_o}{2} \quad (3.4.14)$$

Thus $\underline{\hat{a}}^o$ is given by minimizing $\hat{\sigma}^o(\underline{a}^o)$ or, equivalently, minimizing:

$$J(\underline{a}^o) = NN_o\hat{\sigma}^o(\underline{a}^o)^2 = \sum_{n=1}^{N}\sum_{i=1}^{N_o}(\hat{x}_i^o(n) - q_i^o(n;\underline{a}^o))^2 \quad (3.4.15)$$

where the dependence of $J(\underline{a}^o)$ on the input $\hat{Z}_{1,N}$ has been suppressed in the notation. Also, from (3.4.10) and (3.4.14):

$$\ln\left(\frac{p(\underline{a}^o, \hat{\sigma}^o(\underline{a}^o)|\mathcal{D}_N, \mathcal{M}_P)}{p(\underline{\hat{a}}^o, \hat{\sigma}^o(\underline{\hat{a}}^o)|\mathcal{D}_N, \mathcal{M}_P)}\right) = \frac{NN_o}{2}\ln\left(\frac{\hat{\sigma}^o(\underline{\hat{a}}^o)^2)}{\hat{\sigma}^o(\underline{a}^o)^2}\right) + \ln\left(\frac{\pi_{\underline{a}^o,\sigma^o}(\underline{a}^o, \hat{\sigma}^o(\underline{a}^o))}{\pi_{\underline{a}^o,\sigma^o}(\underline{\hat{a}}^o, \hat{\sigma}^o(\underline{\hat{a}}^o))}\right) \quad (3.4.16)$$

where $\pi_{\underline{a}^o,\sigma^o}(\underline{\hat{a}}^o, \hat{\sigma}^o) = \pi_{\underline{\tilde{a}}^o}(\underline{\hat{\tilde{a}}}^o)$. Equation (3.4.16) may be rewritten:

$$\begin{aligned}\frac{p(\underline{a}^o, \hat{\sigma}^o(\underline{a}^o)|\mathcal{D}_N, \mathcal{M}_P)}{p(\underline{\hat{a}}^o, \hat{\sigma}^o(\underline{\hat{a}}^o)|\mathcal{D}_N, \mathcal{M}_P)} &= \frac{\pi_{\underline{a}^o,\sigma^o}(\underline{a}^o, \hat{\sigma}^o(\underline{a}^o))}{\pi_{\underline{a}^o,\sigma^o}(\underline{\hat{a}}^o, \hat{\sigma}^o(\underline{\hat{a}}^o))}\left(\frac{\hat{\sigma}^o(\underline{\hat{a}}^o)}{\hat{\sigma}^o(\underline{a}^o)}\right)^{NN_o} \\ &= \frac{\pi_{\underline{a}^o,\sigma^o}(\underline{a}^o, \hat{\sigma}^o(\underline{a}^o))}{\pi_{\underline{a}^o,\sigma^o}(\underline{\hat{a}}^o, \hat{\sigma}^o(\underline{\hat{a}}^o))}\left(\frac{J(\underline{\hat{a}}^o)}{J(\underline{a}^o)}\right)^{\frac{NN_o}{2}}\end{aligned} \quad (3.4.17)$$

The posterior pdf $p(\underline{\tilde{a}}^o|\mathcal{D}_N, \mathcal{M}_P)$ can be approximated locally, in the neighborhood of $\underline{\hat{\tilde{a}}}^o$, with a multi-dimensional Gaussian distribution with mean $\underline{\hat{\tilde{a}}}^o$ and an $(N_o+1)\times(N_o+1)$ covariance matrix $A_N^{-1}(\underline{\hat{\tilde{a}}}^o)$ (see Appendix E):

$$p(\underline{\tilde{a}}^o|\mathcal{D}_N, \mathcal{M}_P) \simeq p(\underline{\hat{\tilde{a}}}^o|\mathcal{D}_N, \mathcal{M}_P)\exp(-\frac{1}{2}[\underline{\tilde{a}}^o - \underline{\hat{\tilde{a}}}^o]^T A_N(\underline{\hat{\tilde{a}}}^o)[\underline{\tilde{a}}^o - \underline{\hat{\tilde{a}}}^o]) \quad (3.4.18)$$

where the elements $[A_N(\hat{\underline{\tilde{a}}}^o)]_{ij}$ are given by:

$$[A_N(\hat{\underline{\tilde{a}}}^o)]_{ij} = -\frac{\partial^2 \ln f_N^o(\hat{X}_{1,N}^o; \underline{\tilde{a}}^o, \hat{Z}_{1,N})}{\partial \tilde{a}_i^o \partial \tilde{a}_j^o}\bigg|_{\underline{\tilde{a}}^o = \hat{\underline{\tilde{a}}}^o} - \frac{\partial^2 \ln \pi_{\underline{\tilde{a}}^o}(\underline{\tilde{a}}^o)}{\partial \tilde{a}_i^o \partial \tilde{a}_j^o}\bigg|_{\underline{\tilde{a}}^o = \hat{\underline{\tilde{a}}}^o}$$
$$\cong -\frac{\partial^2 \ln f_N^o(\hat{X}_{1,N}^o; \underline{\tilde{a}}^o, \hat{Z}_{1,N})}{\partial \tilde{a}_i^o \partial \tilde{a}_j^o}\bigg|_{\underline{\tilde{a}}^o = \hat{\underline{\tilde{a}}}^o} \tag{3.4.19}$$

The elements of A_N are $O(N)$ and, therefore, for a large number N of available data points, which is usually the case with dynamic tests or earthquake records of structural response, the pdf $p(\underline{\tilde{a}}^o|\mathcal{D}_N, \mathcal{M}_P)$ becomes very peaked at the optimal parameters $\hat{\underline{\tilde{a}}}^o$; this result can also be concluded by viewing Equation (3.4.17). Since the posterior pdf is so peaked at the values of the optimal parameters, predictions can be made using the corresponding most probable model based on the data, assuming it is globally identifiable [Beck 1990]. The property of global identifiability will be explored in Section 3.6, but for now it is understood as the existence of a unique set of optimal parameters.

Consider the case where the optimal parameters are not globally, but locally identifiable; that is, where $f_N^o(\hat{X}_{1,N}; \underline{\tilde{a}}^o, \hat{Z}_{1,N})$ attains its global maximum at a finite number of parameter sets $\{\hat{\underline{\tilde{a}}}_k^o; k = 1, 2, \ldots, K\} = \{\hat{\underline{a}}_k^o, \hat{\sigma}_k^o; k = 1, 2, \ldots, K\}$, where:

$$f_N^o(\hat{X}_{1,N}; \hat{\underline{\tilde{a}}}_k^o, \hat{Z}_{1,N}) = \max_{S(\underline{\tilde{a}}^o)} f_N^o(\hat{X}_{1,N}; \underline{\tilde{a}}^o, \hat{Z}_{1,N}) \; ; \; k = 1, 2, \ldots, K \tag{3.4.20}$$

Following the same steps as in the globally identifiable case, it can be shown that the set of the optimal parameter vectors $\hat{\underline{a}}_k^o$, $k = 1, 2, \ldots, K$ are all the solutions of:

$$J(\hat{\underline{a}}_k^o) = \min_{S(\underline{a}^o)} J(\underline{a}^o) \; ; \; k = 1, \ldots, K \tag{3.4.21}$$

Equation (3.4.21) along with (3.4.15) implies that:

$$(\hat{\sigma}_k^o)^2 = \frac{1}{NN_o} \min J(\underline{a}^o) \equiv (\hat{\sigma}^o)^2 \; ; \; k = 1, 2, \ldots, K \tag{3.4.22}$$

that is, the optimal variances corresponding to the different optimal parameters $\hat{\underline{a}}_k^o$ are all equal. If a uniform, noninformative prior pdf $\pi_{\underline{\tilde{a}}^o}$ is assumed over the

whole domain $S(\underline{\tilde{a}}^o)$, then the above solutions $\underline{\hat{\tilde{a}}}_k^o = [\underline{\hat{a}}_k^{o^T}, \hat{\sigma}^{o^T}]^T$, $k = 1, \ldots, K$ also form the set of solutions that globally maximize $p(\underline{\tilde{a}}^o|\mathcal{D}_N, \mathcal{M}_P)$. For a nonuniform prior, however, it is asymptotically correct that the above solutions are all local maxima of $p(\underline{\tilde{a}}^o|\mathcal{D}_N, \mathcal{M}_P)$ (see Appendix E), while the global maximum is attained only by the solutions $\underline{\hat{\tilde{a}}}_l^o = [\underline{\hat{a}}_l^{o^T}, \hat{\sigma}^o]^T$, such that:

$$\pi_{\underline{\tilde{a}}^o}(\underline{\hat{\tilde{a}}}_l^o) = \max_{k=1,\ldots,K} \pi_{\underline{\tilde{a}}^o}(\underline{\hat{\tilde{a}}}_k^o) \tag{3.4.23}$$

As before, the pdf $p(\underline{\tilde{a}}^o|\mathcal{D}_N, \mathcal{M}_P)$ can be approximated in the neighborhood of each of the optimal parameters $\underline{\hat{\tilde{a}}}_k^o$ with a scaled multi-dimensional Gaussian distribution with mean $\underline{\hat{\tilde{a}}}_k^o$ and a covariance matrix $A_N^{-1}(\underline{\hat{\tilde{a}}}_k^o)$, in accordance with (3.4.18). For large N, the pdf $p(\underline{\tilde{a}}^o|\mathcal{D}_N, \mathcal{M}_P)$ collapses to a few peaks located at the optimal parameters $\underline{\hat{\tilde{a}}}_k^o$, $k = 1, \ldots, K$. Consequently, it is asymptotically correct for prediction purposes to use, out of the class $\mathcal{M}_P$, only the probability models corresponding to the optimal parameters $\underline{\hat{\tilde{a}}}_k^o$, $k = 1, \ldots, K$. Each of these models is weighted proportionally to the volume of the posterior pdf $p(\underline{\tilde{a}}^o|\mathcal{D}_N, \mathcal{M}_P)$ under its Gaussian-shaped peak positioned at the corresponding optimal parameters. The mathematical expression for the weighting coefficient w_k corresponding to the k^{th} vector of optimal parameters $\underline{\hat{\tilde{a}}}_k^o$ is (see Appendix E):

$$w_k = \frac{w_k'}{\sum_{k=1}^K w_k'} \tag{3.4.24}$$

where

$$w_k' = \pi_{\underline{\tilde{a}}^o}(\underline{\hat{\tilde{a}}}_k^o)|A_N^{-1}(\underline{\hat{\tilde{a}}}_k^o)|^{1/2} \tag{3.4.25}$$

The elements of $A_N(\underline{\hat{\tilde{a}}}_k^o)$ can be evaluated numerically through (3.4.19). Numerical examples have shown that these calculations can be very sensitive to roundoff errors if the vector of the observed model parameters $\underline{a}^o$ does not consist of modal quantities exclusively. In addition, independent of the choice of $\underline{a}^o$, the matrix $A_N(\underline{\hat{\tilde{a}}}_k^o)$ is often ill-conditioned, which results in numerical errors when calculating $|A_N^{-1}(\underline{\hat{\tilde{a}}}_k^o)|$. Thus, the weighting effect of $|A_N^{-1}(\underline{\hat{\tilde{a}}}_k^o)|^{\frac{1}{2}}$ cannot be estimated

reliably in general by calculating it directly. A reliable alternative expression is presented later in Section 3.12.3 to overcome this difficulty. Notice that the prior pdf $\pi_{\underline{\tilde{a}}^o}(\underline{\tilde{a}}^o)$ does not need to be specified over the whole domain $S(\underline{\tilde{a}}^o)$. Instead, only the relative values for the optimal parameters $\hat{\underline{\tilde{a}}}_k^o$ need to be specified.

Summarizing the above results, the posterior pdf $p(\underline{\tilde{a}}^o|\mathcal{D}_N, \mathcal{M}_P)$ for a large number N of data points and for the locally or globally identifiable case is given by:

$$p(\underline{\tilde{a}}^o|\mathcal{D}_N, \mathcal{M}_P) \simeq \sum_{k=1}^{K} w_k G\left(\underline{\tilde{a}}^o; \hat{\underline{\tilde{a}}}_k^o, A_N^{-1}(\hat{\underline{\tilde{a}}}_k^o)\right) \tag{3.4.26}$$

where $G\left(\underline{\tilde{a}}^o; \hat{\underline{\tilde{a}}}_k^o, A_N^{-1}(\hat{\underline{\tilde{a}}}_k^o)\right)$ is a multi-dimensional Gaussian distribution for $\underline{\tilde{a}}^o$, with mean $\hat{\underline{\tilde{a}}}_k^o$ and covariance matrix $A_N^{-1}(\hat{\underline{\tilde{a}}}_k^o)$, and w_k is given by (3.4.24). In the globally identifiable case, $K = 1$ and $w_1 = 1$.

Equation (3.4.7), along with (3.4.26) is used to obtain $p(\underline{\tilde{a}}|\mathcal{D}_N, \mathcal{M}_P)$. It is asymptotically correct that:

$$p(\underline{\tilde{a}}|\mathcal{D}_N, \mathcal{M}_P) = \sum_{k=1}^{K} w_k G\left(\underline{\tilde{a}}^o; \hat{\underline{\tilde{a}}}_k^o, A_N^{-1}(\hat{\underline{\tilde{a}}}_k^o)\right) p(\underline{\tilde{a}}^u|\hat{\underline{\tilde{a}}}_k^o, \mathcal{M}_P) \tag{3.4.27}$$

or integrating out $\underline{\tilde{a}}^o$:

$$p(\underline{\tilde{a}}^u|\mathcal{D}_N, \mathcal{M}_P) = \sum_{k=1}^{K} w_k p(\underline{\tilde{a}}^u|\hat{\underline{\tilde{a}}}_k^o, \mathcal{M}_P) \tag{3.4.28}$$

Assuming that $\underline{a}$ and $\underline{\sigma}$ are independently distributed *a priori*:

$$\pi_{\underline{\tilde{a}}}(\underline{\tilde{a}}) \equiv p(\underline{\tilde{a}}|\mathcal{M}_P) = p(\underline{a}|\mathcal{M}_P)p(\underline{\sigma}|\mathcal{M}_P) = \pi_{\underline{a}}(\underline{a})\pi_{\underline{\sigma}}(\underline{\sigma}) \tag{3.4.29}$$

the conditional prior pdf $p(\underline{\tilde{a}}^u|\hat{\underline{\tilde{a}}}_k^o, \mathcal{M}_P)$ in the last two equations can be expressed as:

$$\begin{aligned} \pi_{\underline{\tilde{a}}^u|\underline{\tilde{a}}_k^o}(\underline{\tilde{a}}^u; \hat{\underline{\tilde{a}}}_k^o) \equiv p(\underline{\tilde{a}}^u|\hat{\underline{\tilde{a}}}_k^o, \mathcal{M}_P) &= p(\underline{a}^u|\hat{\underline{a}}_k^o, \mathcal{M}_P)p(\underline{\sigma}^u|\hat{\sigma}^o, \mathcal{M}_P) \\ &= \pi_{\underline{a}^u|\underline{a}^o}(\underline{a}^u; \hat{\underline{a}}_k^o)\pi_{\underline{\sigma}^u|\sigma^o}(\underline{\sigma}^u; \hat{\sigma}^o) \end{aligned} \tag{3.4.30}$$

3.5 Posterior Predictive Probability

The pdf $p(X_{1,M}|Z_{1,M},\mathcal{M}_P)$, before any of the information contained in the data $\hat{X}_{1,N}$ is employed, is given by:

$$\begin{aligned} p(X_{1,M}|Z_{1,M},\mathcal{M}_P) &= \int_{S(\underline{\tilde{a}})} p(X_{1,M}|\underline{\tilde{a}},Z_{1,M},\mathcal{M}_P)p(\underline{\tilde{a}}|\mathcal{M}_P)d\underline{\tilde{a}} \\ &= \int_{S(\underline{\tilde{a}})} g_M(X_{1,M};\underline{\tilde{a}},Z_{1,M})\pi_{\underline{\tilde{a}}}(\underline{\tilde{a}})d\underline{\tilde{a}} \end{aligned} \tag{3.5.1}$$

where $g_M(X_{1,M};\underline{\tilde{a}},Z_{1,M})$ is given by (3.3.11). Also:

$$\begin{aligned} p(X^o_{1,M}|Z_{1,M},\mathcal{M}_P) &= \int_{S(\underline{\tilde{a}}^o)} p(X^o_{1,M}|\underline{\tilde{a}}^o,Z_{1,M},\mathcal{M}_P)p(\underline{\tilde{a}}^o|\mathcal{M}_P)d\underline{\tilde{a}}^o \\ &= \int_{S(\underline{\tilde{a}}^o)} f^o_M(X^o_{1,M};\underline{\tilde{a}}^o,Z_{1,M})\pi_{\underline{\tilde{a}}^o}(\underline{\tilde{a}}^o)d\underline{\tilde{a}}^o \end{aligned} \tag{3.5.2}$$

and

$$\begin{aligned} p(X^u_{1,M}|Z_{1,M},\mathcal{M}_P) &= \int_{S(\underline{\tilde{a}})} p(X^u_{1,M}|\underline{\tilde{a}},Z_{1,M},\mathcal{M}_P)p(\underline{\tilde{a}}|\mathcal{M}_P)d\underline{\tilde{a}} \\ &= \int_{S(\underline{\tilde{a}})} f^u_M(X^u_{1,M};\underline{\tilde{a}},Z_{1,M})\pi_{\underline{\tilde{a}}}(\underline{\tilde{a}})d\underline{\tilde{a}} \end{aligned} \tag{3.5.3}$$

where $f^o_M(X^o_{1,M};\underline{\tilde{a}}^o,Z_{1,M})$ and $f^u_M(X^u_{1,M};\underline{\tilde{a}},Z_{1,M})$ are given by (3.3.12) and (3.3.14), respectively. Notice, however, that $X^o_{1,M}$ and $X^u_{1,M}$ are no longer independently distributed, in contrast to the case where $\underline{\tilde{a}}$ is given:

$$p(X_{1,M}|Z_{1,M},\mathcal{M}_P) \neq p(X^o_{1,M}|Z_{1,M},\mathcal{M}_P)p(X^u_{1,M}|Z_{1,M},\mathcal{M}_P) \tag{3.5.4}$$

The first two moments of the elements $\underline{x}(n)$ can be evaluated according to Equations (2.4.8) and (2.4.9), where the explicit dependence of $\underline{x}$ and $\underline{q}$ on n has been omitted. The high dimensional integrals in these equations can be evaluated using the methodology proposed in Chapter 2.

Utilizing the available data $\hat{X}_{1,N}$, the posterior pdf $p(\underline{\tilde{a}}|\mathcal{D}_N, \mathcal{M}_P)$ is obtained, as discussed in the previous section. This updated pdf can be used to evaluate either (a) $p(X^u_{1,N}|\mathcal{D}_N, \mathcal{M}_P)$, the posterior pdf of the unobserved output quantities for the given excitation, or (b) $p(X_{N+1,M}|\mathcal{D}_N, Z_{N+1,M}, \mathcal{M}_P)$, the posterior predictive pdf of both observed and unobserved output quantities for a future excitation $Z_{N+1,M}$, which is assumed to be specified.

(a) For the former case, $p(X^u_{1,N}|\mathcal{D}_N, \mathcal{M}_P)$ is given by:

$$p(X^u_{1,N}|\mathcal{D}_N, \mathcal{M}_P) = \int_{S(\underline{\tilde{a}})} p(X^u_{1,N}|\underline{\tilde{a}}, \mathcal{D}_N, \mathcal{M}_P) p(\underline{\tilde{a}}|\mathcal{D}_N, \mathcal{M}_P) d\underline{\tilde{a}} \tag{3.5.5}$$

Notice that:

$$p(X^u_{1,N}|\underline{\tilde{a}}, \mathcal{D}_N, \mathcal{M}_P) p(\hat{X}_{1,N}|\underline{\tilde{a}}, \hat{Z}_{1,N}\mathcal{M}_P) = p(\hat{X}_{1,N}, X^u_{1,N}|\underline{\tilde{a}}, \hat{Z}_{1,N}, \mathcal{M}_P) \tag{3.5.6}$$

From (3.3.15), it follows that:

$$p(\hat{X}_{1,N}, X^u_{1,N}|\underline{\tilde{a}}, \hat{Z}_{1,N}, \mathcal{M}_P) = p(\hat{X}_{1,N}|\underline{\tilde{a}}, \hat{Z}_{1,N}, \mathcal{M}_P) p(X^u_{1,N}|\underline{\tilde{a}}, \hat{Z}_{1,N}, \mathcal{M}_P) \tag{3.5.7}$$

Combining (3.5.6) and (3.5.7) leads to:

$$\begin{aligned} p(X^u_{1,N}|\underline{\tilde{a}}, \mathcal{D}_N, \mathcal{M}_P) &= p(X^u_{1,N}|\underline{\tilde{a}}, \hat{Z}_{1,N}, \mathcal{M}_P) \\ &= f^u_N(X^u_{1,N}; \underline{\tilde{a}}, \hat{Z}_{1,N}) \end{aligned} \tag{3.5.8}$$

Substituting (3.5.8) into (3.5.5) leads to:

$$p(X^u_{1,N}|\mathcal{D}_N, \mathcal{M}_P) = \int_{S(\underline{\tilde{a}})} f^u_N(X^u_{1,N}; \underline{\tilde{a}}, \hat{Z}_{1,N}) p(\underline{\tilde{a}}|\mathcal{D}_N, \mathcal{M}_P) d\underline{\tilde{a}} \tag{3.5.9}$$

Utilizing (3.4.27), along with Equation (3.5.9), the following expression, which is asymptotically correct for large N, is obtained:

$$p(X^u_{1,N}|\mathcal{D}_N, \mathcal{M}_P) \simeq \sum_{k=1}^{K} w_k p(X^u_{1,N}|\underline{\hat{\tilde{a}}}^o_k, \hat{Z}_{1,N}, \mathcal{M}_P) \tag{3.5.10}$$

where

$$p(X^u_{1,N}|\hat{\tilde{\underline{a}}}^o_k, \mathcal{D}_N \mathcal{M}_P) = \int_{S(\tilde{\underline{a}}^u)} f^u_N(X^u_{1,N}; \hat{\tilde{\underline{a}}}^o_k, \tilde{\underline{a}}^u, \hat{Z}_{1,N}) \pi_{\tilde{\underline{a}}^u|\tilde{\underline{a}}^o}(\tilde{\underline{a}}^u; \hat{\tilde{\underline{a}}}^o_k) d\tilde{\underline{a}}^u \tag{3.5.11}$$

Equation (3.4.30) can be employed to describe $\pi_{\tilde{\underline{a}}^u|\tilde{\underline{a}}^o}$, if $\underline{a}$ and $\underline{\sigma}$ are independently distributed *a priori*. This equation shows that integration only over the space of the unobserved parameters is required in order to calculate $p(X^u_{1,N}|\mathcal{D}_N, \mathcal{M}_P)$, while $p(X^u_{1,N}|Z_{1,N}, \mathcal{M}_P)$ required integration over the space of all observed and unobserved parameters. The integration over the space of the observed parameters is replaced in the former pdf by a discrete sum over all optimal solutions $\{\hat{\tilde{\underline{a}}}^o_k \ , \ k = 1, \ldots, K\}$. In the special case where $\underline{a} = \underline{a}^o$ and $\underline{\sigma} = \{\sigma^o\}$, Equation (3.5.10) can be written as:

$$p(X^u_{1,N}|\mathcal{D}_N, \mathcal{M}_P) \simeq \sum_{k=1}^{K} w_k f^u_N(X^u_{1,N}; \hat{\tilde{\underline{a}}}^o_k, \hat{Z}_{1,N}) \tag{3.5.12}$$

The expressions for the first two moments of $\underline{x}^u(n)$ after the updating, assuming $\underline{a}$ and $\underline{\sigma}$ are independently distributed, are given by:

$$E[\underline{x}^u(n)|\mathcal{D}_N, \mathcal{M}_P] = \sum_{k=1}^{K} w_k \int_{S(\underline{a}^u)} \underline{q}^u(n; \hat{\underline{a}}^o_k, \underline{a}^u) \pi_{\underline{a}^u|\underline{a}^o}(\underline{a}^u; \hat{\underline{a}}^o_k) d\underline{a}^u \tag{3.5.13}$$

and

$$\begin{aligned} \mathrm{Cov}[\underline{x}^u(n)|\mathcal{D}_N, \mathcal{M}_P] = & \sum_{k=1}^{K} w_k \int_{S(\underline{a}^u)} \underline{q}^u(n; \hat{\underline{a}}^o_k, \underline{a}^u) \underline{q}^{u^T}(n; \hat{\underline{a}}^o_k, \underline{a}^u) \pi_{\underline{a}^u|\underline{a}^o}(\underline{a}^u; \hat{\underline{a}}^o_k) d\underline{a}^u \\ & - E[\underline{x}^u(n)|\mathcal{D}_N, \mathcal{M}_P] E[\underline{x}^u(n)|\mathcal{D}_N, \mathcal{M}_P]^T \\ & + \sum_{k=1}^{K} w_k \int_{S(\underline{\sigma}^u)} \Sigma^u(\hat{\sigma}^o, \underline{\sigma}^u) \pi_{\underline{\sigma}^u|\sigma^o}(\underline{\sigma}^u; \hat{\sigma}^o) d\underline{\sigma}^u \end{aligned} \tag{3.5.14}$$

If the model output $q^u_i(n)$ corresponding to an unobserved output quantity $x^u_i(n)$, $i = 1, \ldots, N_u$ depends only on $\underline{a}^o$, that is $q^u_i(n; \underline{a}) = q^u_i(n; \underline{a}^o)$, then

Equations (3.5.13) and (3.5.14) reduce to:

$$E[x_i^u(n)|\mathcal{D}_N, \mathcal{M}_P] = \sum_{k=1}^{K} w_k q_i^u(n; \underline{\hat{a}}_k^o) \tag{3.5.15}$$

and

$$\begin{aligned} \mathrm{Var}[x_i^u(n)|\mathcal{D}_N, \mathcal{M}_P] = &\sum_{k=1}^{K} w_k q_i^u(n; \underline{\hat{a}}_k^o)^2 - E[x_i^u(n)|\mathcal{D}_N, \mathcal{M}_P]^2 \\ &+ \sum_{k=1}^{K} w_k \int_0^\infty (\sigma_i')^2 \pi_{\sigma_i'|\sigma^o}(\sigma_i'|\hat{\sigma}^o) d\sigma_i' \end{aligned} \tag{3.5.16}$$

where $(\sigma_i')^2 = [\Sigma^u(\underline{\sigma})]_{ii}$. The last term in the right hand side of (3.5.16) can be written as $E[(\sigma_i')^2|\hat{\sigma}^o]$. Additionally, if $\sigma_i' = \sigma^o$, this term reduces to $(\hat{\sigma}^o)^2$.

(b) The expressions for the posterior predictive pdf of the unobserved output quantities $p(X_{N+1,M}^u|\mathcal{D}_N, Z_{N+1,M}, \mathcal{M}_P)$ are obtained through the expression for $p(X_{1,N}^u|\mathcal{D}_N, \mathcal{M}_P)$ by replacing $X_{1,N}^u$ with $X_{N+1,M}^u$ and $f_N^u(X_{1,N}^u; \tilde{\underline{a}}, \hat{Z}_{1,N})$ with $f_{N+1,M}^u(X_{N+1,M}^u; \tilde{\underline{a}}, \hat{Z}_{1,N}, Z_{N+1,M})$ given by:

$$\begin{aligned} f_{N+1,M}^u(X_{N+1,M}^u; \tilde{\underline{a}}, \hat{Z}_{1,N}, Z_{N+1,M}) &= \frac{f_M^u(X_{1,M}^u; \tilde{\underline{a}}, \hat{Z}_{1,N} Z_{N+1,M})}{f_N^u(X_{1,N}^u; \tilde{\underline{a}}, \hat{Z}_{1,N})} \\ &= \frac{1}{(2\pi)^{\frac{(M-N)N_u}{2}} |\Sigma^u(\underline{\sigma})|^{\frac{M-N}{2}}} \\ &\times \exp\left(-\frac{1}{2} \sum_{n=N+1}^{M} \sum_{i=1}^{N_u} \frac{e_i^u(n; \underline{a})^2}{[\Sigma^u(\underline{\sigma})]_{ii}} \right) \end{aligned} \tag{3.5.17}$$

The expressions (3.5.13) through (3.5.16) remain the same, only n is assumed to belong in the set $\{N+1, \ldots, M\}$. As done all along, the dependence of $q_i^u(n; \underline{a})$ and $e_i^u(n; \underline{a})$ on the input $\{\hat{Z}_{1,N}, Z_{N+1,n}\}$ and the theoretical model $\mathcal{M}$, has been suppressed in the notation. The expression for the posterior predictive pdf at the observed dof is:

$$\begin{aligned} p(X_{N+1,M}^o|\mathcal{D}_N, Z_{N+1,M}, \mathcal{M}_P) = &\int_{S(\tilde{\underline{a}}^o)} p(X_{N+1,M}^o|\tilde{\underline{a}}^o, \mathcal{D}_N, Z_{N+1,M}, \mathcal{M}_P) \\ &\times p(\tilde{\underline{a}}^o|\mathcal{D}_N, \mathcal{M}_P) d\tilde{\underline{a}}^o \end{aligned} \tag{3.5.18}$$

Notice that:

$$\begin{aligned} p(X^o_{N+1,M}|\underline{\tilde{a}}^o, \mathcal{D}_N, Z_{N+1,M}, \mathcal{M}_P) &= \frac{p(\hat{X}_{1,N}, X^o_{N+1,M}|\underline{\tilde{a}}^o, \hat{Z}_{1,N}, Z_{N+1,M}, \mathcal{M}_P)}{p(\hat{X}_{1,N}|\underline{\tilde{a}}^o, \hat{Z}_{1,N}, \mathcal{M}_P} \\ &= \frac{f^o_M(\hat{X}_{1,N}, X^o_{N+1,M}; \underline{\tilde{a}}^o, \hat{Z}_{1,N}, Z_{N+1,M})}{f^o_N(\hat{X}_{1,N}; \underline{\tilde{a}}^o \hat{Z}_{1,N})} \\ &\equiv f^o_{N+1,M}(X^o_{N+1,M}; \underline{\tilde{a}}^o, \hat{Z}_{1,N}, Z_{N+1,M}) \\ &= p(X^o_{N+1,M}|\underline{\tilde{a}}^o, \hat{Z}_{1,N}, Z_{N+1,M}, \mathcal{M}_P) \end{aligned} \tag{3.5.19}$$

where

$$\begin{aligned} f^o_{N+1,M}(X^o_{N+1,M}; \underline{\tilde{a}}^o, \hat{Z}_{1,N}, Z_{N+1,M}) \equiv & \frac{1}{(2\pi(\sigma^o)^2)^{\frac{(M-N)N_o}{2}}} \\ & \times \exp\left(-\frac{1}{2(\sigma^o)^2} \sum_{n=N+1}^{M} \sum_{i=1}^{N_o} e^o_i(n; \underline{a}^o)^2\right) \end{aligned} \tag{3.5.20}$$

Substituting (3.5.19) into (3.5.18), we obtain:

$$\begin{aligned} p(X^o_{N+1,M}|\mathcal{D}_N, Z_{N+1,M}, \mathcal{M}_P) = & \int_{S(\underline{\tilde{a}}^o)} f^o_{N+1,M}(X^o_{N+1,M}; \underline{\tilde{a}}^o \hat{Z}_{1,N}, Z_{N+1,M}) \\ & p(\underline{\tilde{a}}^o|\mathcal{D}_N, \mathcal{M}_P) d\underline{\tilde{a}}^o \end{aligned} \tag{3.5.21}$$

Utilizing (3.4.26), the above equation leads to the following approximate expression, which is asymptotically correct for large N:

$$p(X^o_{N+1,M}|\mathcal{D}_N, Z_{N+1,M}, \mathcal{M}_P) \simeq \sum_{R=1}^{K} w_k f^o_{N+1,M}(X^o_{N+1,M}; \hat{\underline{\tilde{a}}}^o_k, \hat{Z}_{1,N}, Z_{N+1,M}) \tag{3.5.22}$$

which is equivalent to the expression given by Beck [1990]. The expected value and the variance of $x^o_i(n)$, $n = N+1, \ldots, M$ are given by:

$$E[x^o_i(n)|\mathcal{D}_N, Z_{N+1,M}, \mathcal{M}_P] = \sum_{k=1}^{K} w_k q^o_i(n; \hat{\underline{a}}^o_k) \tag{3.5.23}$$

and

$$\begin{aligned} \mathrm{Var}[x^o_i(n)|\mathcal{D}_N, Z_{N+1,M}, \mathcal{M}_P] = & \sum_{k=1}^{K} w_k q^o_i(n; \hat{\underline{a}}^o_k)^2 + (\hat{\sigma}^o)^2 \\ & - E[x^o_i(n)|\mathcal{D}_N, Z_{N+1,M}, \mathcal{M}_P]^2 \end{aligned} \tag{3.5.24}$$

Note that in the globally identifiable case, that is $K = 1$, the above equations reduce to:

$$E[x_i^o(n)|\mathcal{D}_N, Z_{N+1,M}, \mathcal{M}_P] = q_i^o(n; \hat{\underline{a}}^o) \tag{3.5.25}$$

$$\mathrm{Var}[x_i^o(n)|\mathcal{D}_N, Z_{N+1,M}, \mathcal{M}_P] = (\hat{\sigma}^o)^2 \tag{3.5.26}$$

3.6 Definitions of Model and System Identifiability

Let $\mathcal{M}$ be a theoretical parametric model, where a particular choice of the values of its parameters $\underline{a} \equiv [\underline{a}^{o^T}, \underline{a}^{u^T}]^T \in S(\underline{a}^o) \times S(\underline{a}^u) \equiv S(\underline{a})$ is assumed to specify a unique model $M(\underline{a})$ within the class $\mathcal{M} = \{M(\underline{a}) : \underline{a} \in S(\underline{a})\}$. Assume that the sampled input $\hat{Z}_{1,N} = \{\hat{z}(n) \in R^{N_I} : n = 1, 2, \ldots N\}$ and output $\hat{X}_{1,N} = \{\hat{\underline{x}}^o(n) \in R^{N_o} : n = 1, 2, \ldots N\}$ histories for a structural system are given, then the basic problem of interest in this section is whether the given input and output specify a unique model within the class $\mathcal{M}$.

Let $Q^o_{1,N}(\underline{a}; \hat{Z}_{1,N}) = \{\underline{q}^o(n; \underline{a}^o, \hat{Z}_{1,N}, \mathcal{M}) \in R^{N_o} : n = 1, 2, \ldots, N\}$ denote the model output history which corresponds to the observed quantities for the given input $\hat{Z}_{1,N}$ and for a model $M(\underline{a}) \in \mathcal{M}$, and let $S(Q^o_{1,N}; \hat{Z}_{1,N})$ denote the space formed by the range of $Q^o_{1,N}(\underline{a}; \hat{Z}_{1,N})$ as $\underline{a}$ ranges over $S(\underline{a})$. There is a natural mapping of the models in the class $\mathcal{M}$ onto $S(Q^o_{1,N}; \hat{Z}_{1,N})$, but it may happen that several models in $\mathcal{M}$ get mapped into the same output under the specified input, making the inverse problem non-unique for that input and output.

First, consider the case where $\hat{X}_{1,N} \in S(Q^o_{1,N}; \hat{Z}_{1,N})$, that is, the observed output is the output of one of the models in the class $\mathcal{M}$. Define an *optimal model* $M(\hat{\underline{a}})$ to be any model in $\mathcal{M}$ such that:

$$Q^o_{1,N}(\hat{\underline{a}}; \hat{Z}_{1,N}) = \hat{X}_{1,N} \tag{3.6.1}$$

The stated hypothesis implies that there is at least one optimal model. If there is more than one optimal model in $\mathcal{M}$, then all such models are "output-equivalent"

for the given input and are therefore indistinguishable on the basis of that input and output alone.

Let $S_{opt}(M(\underline{\hat{a}}); \hat{Z}_{1,N}) \subset \mathcal{M}$ denote the set of all optimal models which are output-equivalent to model $M(\underline{\hat{a}})$ under input $\hat{Z}_{1,N}$. Let $S_{opt}(\underline{\hat{a}}; \hat{Z}_{1,N}) \subset S(\underline{a})$ denote the set of all corresponding optimal parameters. The following definitions are introduced:

M1. A parameter a_j of $\underline{a} \in S(\underline{a})$ is *globally M-identifiable* ("model identifiable") at $\underline{\hat{a}}$ for the input $\hat{Z}_{1,N}$ if $S_{opt}(\underline{\hat{a}}; \hat{Z}_{1,N})$ contains only one optimal parameter or, if not, then for any two optimal parameters $\underline{\hat{a}}^{(1)}$ and $\underline{\hat{a}}^{(2)}$ in $S_{opt}(\underline{\hat{a}}; \hat{Z}_{1,N})$ the following holds:

$$\hat{a}_j^{(1)} = \hat{a}_j^{(2)} \tag{3.6.2}$$

Definition M1 implies that a_j is uniquely specified by $\hat{Z}_{1,N}$ and $\hat{X}_{1,N} = Q^o_{1,N}(\underline{\hat{a}}; \hat{Z}_{1,N})$.

M2. A parameter a_j of $\underline{a} \in S(\underline{a})$ is *locally M-identifiable* at $\underline{\hat{a}}$ for the input $\hat{Z}_{1,N}$ if there exists a positive number ϵ_j such that for any two optimal parameters $\underline{\hat{a}}^{(1)}$ and $\underline{\hat{a}}^{(2)}$ in $S_{opt}(\underline{\hat{a}}; \hat{Z}_{1,N})$ the following holds:

$$|\hat{a}_j^{(1)} - \hat{a}_j^{(2)}| > \epsilon_j \quad \text{or} \quad \hat{a}_j^{(1)} = \hat{a}_j^{(2)} \tag{3.6.3}$$

Definition M2 implies that a_j is uniquely specified within a neighborhood of each of its possible values by $\hat{Z}_{1,N}$ and $\hat{X}_{1,N} = Q^o_{1,N}(\underline{\hat{a}}; \hat{Z}_{1,N})$, and that if $S(\underline{a})$ is a closed-bounded parameter set, there are only a finite number of possible values for a_j under the given input and output. Note that if a_j is globally M-identifiable at $\underline{\hat{a}}$, then it is also locally M-identifiable at $\underline{\hat{a}}$.

M3. A parameter a_j of $\underline{a} \in S(\underline{a})$ is M-identifiable at $\underline{\hat{a}}$ for the input $\hat{Z}_{1,N}$ if it is either locally or globally M-identifiable. For example, the elements of $\underline{a}^u$ are <u>not</u> M-identifiable at any point $\underline{\hat{a}} = [\underline{\hat{a}}^{o^T}, \underline{\hat{a}}^{u^T}]^T$ if the range $S(\underline{a}^u)$ is a dense, non-null set, since, by definition, the model output $Q^o_{1,N}(\underline{\hat{a}}; \hat{Z}_{1,N})$ does not depend on $\underline{a}^u$.

The above definitions can be extended as follows:

The parameter vector $\underline{a}$, or a portion of it, is globally (locally) M-identifiable at $\hat{\underline{a}}$ if all its elements are globally (locally) M-identifiable at $\hat{\underline{a}}$. The parameter vector $\underline{a}$ is not M-identifiable at $\hat{\underline{a}}$ if at least one of its elements is not M-identifiable at $\hat{\underline{a}}$.

If $\underline{a}$ is globally M-identifiable at $\hat{\underline{a}}$, then $S_{opt}(\hat{\underline{a}}; \hat{Z}_{1,N}) = \{\hat{\underline{a}}\}$, that is, $M(\hat{\underline{a}})$ is the only optimal model corresponding to $\hat{Z}_{1,N}$ and $\hat{X}_{1,N} = Q^o_{1,N}(\hat{\underline{a}}; \hat{Z}_{1,N})$. In this case, the model $M(\hat{\underline{a}})$ is said to be *globally identifiable* for the input $\hat{Z}_{1,N}$.

If $\underline{a}$ is locally M-identifiable at $\hat{\underline{a}}$, then $S_{opt}(\hat{\underline{a}}; \hat{Z}_{1,N})$ consists of a countable number of optimal parameters, that is, $S_{opt}(\hat{\underline{a}}; \hat{Z}_{1,N}) = \{\hat{\underline{a}}^{(k)} : k = 1, 2, \ldots\}$. If the parameter space $S(\underline{a})$ is closed and bounded, then $S_{opt}(\hat{\underline{a}}; \hat{Z}_{1,N})$ will actually consist of a finite number K of optimal parameters, that is, $S_{opt}(\hat{\underline{a}}; \hat{Z}_{1,N}) = \{\hat{\underline{a}}^{(k)} : k = 1, 2, \ldots, K\}$. In this case, each model $M(\hat{\underline{a}}^{(k)})$ is said to be *locally identifiable* for the input $\hat{Z}_{1,N}$.

If $\underline{a}$ is not M-identifiable at $\hat{\underline{a}}$, then $S_{opt}(\hat{\underline{a}}; \hat{Z}_{1,N})$ is a dense set, so there is an infinite number of optimal parameters. Each model in the infinite set $S_{opt}(M(\hat{\underline{a}}); \hat{Z}_{1,N})$ is said to be *unidentifiable* for the input $\hat{Z}_{1,N}$.

The above definitions of identifiability can be extended for the case of real data $\mathcal{D}_N = \{\hat{Z}_{1,N}, \hat{X}_{1,N}\}$, where $\hat{X}_{1,N} \notin S(Q^o_{1,N}; \hat{Z}_{1,N})$, that is, the case where the observed system output is not the output of any of the models in the class $\mathcal{M}$ because of the existence of model-error and measurement noise. In this case, the class $\mathcal{M}$ is extended to a class of probability models $\mathcal{M}_P$, as discussed in Section 3.2, where a particular choice of its parameters $\tilde{\underline{a}} = [\underline{a}^T, \underline{\sigma}^T]^T \in S(\underline{a}) \times S(\underline{\sigma}) \equiv S(\tilde{\underline{a}})$ is assumed to specify a unique probability model $M_P(\tilde{\underline{a}})$ within the class $\mathcal{M}_P$. As discussed in Section 3.2, $\mathcal{M}_P$ prescribes, among others, a function f^o_N such that:

$$p(X^o_{1,N} | \tilde{\underline{a}}, Z_{1,N}, \mathcal{M}_P) = f^o_N(X^o_{1,N}; \tilde{\underline{a}}, Z_{1,N}) \tag{3.6.4}$$

that is, it prescribes the probability for all possible observable output histories

for given probability model parameters $\underline{\tilde{a}}$. It was also shown that f_N^o depends only on the parameters $\underline{\tilde{a}}^o = [\underline{a}^{oT}, \sigma^o]^T$, that is:

$$f_N^o(X_{1,N}^o; \underline{\tilde{a}}, Z_{1,N}) = f_N^o(X_{1,N}^o; \underline{\tilde{a}}^o, Z_{1,N}) \tag{3.6.5}$$

An *optimal model* $M_P(\underline{\hat{\tilde{a}}})$ for given data $\mathcal{D}_N$ is defined to be any model in $\mathcal{M}_P$ such that:

$$f_N^o(\hat{X}_{1,N}; \underline{\hat{\tilde{a}}}, \hat{Z}_{1,N}) = \max_{\underline{\tilde{a}} \in S(\underline{\tilde{a}})} f_N^o(\hat{X}_{1,N}; \underline{\tilde{a}}, \hat{Z}_{1,N}) \tag{3.6.6}$$

where the parameters $\underline{\hat{\tilde{a}}} = [\underline{\hat{a}}^T, \hat{\underline{\sigma}}^T]^T$ are called optimal parameters. Let $S_{opt}(M_P(\underline{\hat{\tilde{a}}}); \mathcal{D}_N) \subseteq \mathcal{M}_P$ denote the set of all optimal models in the class $\mathcal{M}_P$ and $S_{opt}(\underline{\hat{\tilde{a}}}; \mathcal{D}_N) \subseteq S(\underline{\tilde{a}})$ denote the set of all corresponding optimal parameters. All the earlier definitions of identifiability can be generalized simply by extending the parameter vector $\underline{\hat{a}}$ to $\underline{\hat{\tilde{a}}}$ as follows:

S1. A parameter $\tilde{a}_j$ of $\underline{\tilde{a}} \in S(\underline{\tilde{a}})$ is *globally S-identifiable* ("system identifiable") at $\underline{\hat{\tilde{a}}}$ for the input and output data $\mathcal{D}_N$ if $S_{opt}(\underline{\hat{\tilde{a}}}; \mathcal{D}_N)$ contains only one optimal parameter, or, if not, then:

$$\underline{\hat{\tilde{a}}}^{(1)}, \underline{\hat{\tilde{a}}}^{(2)} \in S_{opt}(\underline{\hat{\tilde{a}}}; \mathcal{D}_N) \Rightarrow \hat{\tilde{a}}_j^{(1)} = \hat{\tilde{a}}_j^{(2)} \tag{3.6.7}$$

S2. A parameter $\tilde{a}_j$ of $\underline{\tilde{a}}$ is *locally S-identifiable* at $\underline{\hat{\tilde{a}}}$ for data $\mathcal{D}_N$ if there exists a positive number ϵ_j such that:

$$\underline{\hat{\tilde{a}}}^{(1)}, \underline{\hat{\tilde{a}}}^{(2)} \in S_{opt}(\underline{\hat{\tilde{a}}}; \mathcal{D}_N) \Rightarrow |\hat{\tilde{a}}_j^{(1)} - \hat{\tilde{a}}_j^{(2)}| > \epsilon_j \text{ or } \hat{\tilde{a}}_j^{(1)} = \hat{\tilde{a}}_j^{(2)} \tag{3.6.8}$$

S3. A parameter $\tilde{a}_j$ of $\underline{\tilde{a}}$ is not S-identifiable at $\underline{\hat{\tilde{a}}}$ for data $\mathcal{D}_N$ if it is not locally S-identifiable.

As was shown in Section 3.4 and 3.5, it is of particular importance to investigate the identifiability of the optimal observed parameter vector $\underline{\hat{a}}^o$ based on input and output data from the structural system. If $\underline{\hat{a}}^o$ is globally or locally S-identifiable, simplified expressions hold for calculating the posterior pdf

of the uncertain parameters or the posterior predictive probability of the output quantities of interest, when the sample size N is large.

A major complication in the case of real data is the following. While in the case of M-identifiability all optimal models $M(\underline{a}) \in S_{opt}(M(\hat{\underline{a}}); \hat{Z}_{1,N})$ have, by definition, the same model output $Q^o_{1,N}(\hat{\underline{a}}; \hat{Z}_{1,N})$, this is not necessarily true when identifying the optimal models $M_P(\underline{\tilde{a}}) \in S_{opt}(M_P(\hat{\underline{\tilde{a}}}); \mathcal{D}_N)$ in the case of real data. That is:

$$\hat{\underline{\tilde{a}}}^{(1)} = [\hat{\underline{a}}^{(1)^T}, \hat{\underline{\sigma}}^{(1)^T}]^T \in S_{opt}(\hat{\underline{\tilde{a}}}; \mathcal{D}_N) \quad \text{and} \quad \hat{\underline{\tilde{a}}}^{(2)} = [\hat{\underline{a}}^{(2)^T}, \hat{\underline{\sigma}}^{(2)^T}]^T \in S_{opt}(\hat{\underline{\tilde{a}}}; \mathcal{D}_N)$$
$$\not\Rightarrow Q^o_{1,N}(\hat{\underline{a}}^{(1)}; \hat{Z}_{1,N}) = Q^o_{1,N}(\hat{\underline{a}}^{(2)}; \hat{Z}_{1,N}) \tag{3.6.9}$$

It is true, however, that given a model $M_P(\hat{\underline{a}}, \hat{\underline{\sigma}})$ in the class $\mathcal{M}_P$, all other models $M(\underline{a}^*) \in S_{opt}(M(\hat{\underline{a}}); \hat{Z}_{1,N})$, if any, having the same observed model output as $M(\hat{\underline{a}})$, correspond to an optimal model $M_P(\underline{a}^*, \hat{\underline{\sigma}}) \in S_{opt}(M_P(\hat{\underline{a}}, \hat{\underline{\sigma}}); \mathcal{D}_N)$ in the class $\mathcal{M}_P$. That is:

$$Q^o_{1,N}(\hat{\underline{a}}; \hat{Z}_{1,N}) = Q^o_{1,N}(\underline{a}^*; \hat{Z}_{1,N}) \quad \text{and} \quad [\hat{\underline{a}}^T, \hat{\underline{\sigma}}^T]^T \in S_{opt}(\hat{\underline{\tilde{a}}}; \mathcal{D}_N)$$
$$\Rightarrow [\underline{a}^{*^T}, \hat{\underline{\sigma}}^T]^T \in S_{opt}(\hat{\underline{\tilde{a}}}; \mathcal{D}_N) \tag{3.6.10}$$

Another way of looking at this result is that if the parameter vector $\underline{a}$ is not globally M-identifiable at $\hat{\underline{a}}$, then $\underline{a}$ cannot be globally S-identifiable at $[\hat{\underline{a}}^T, \hat{\underline{\sigma}}^T]^T$. Furthermore, the number of optimal probability models in $S_{opt}(M_P(\hat{\underline{a}}, \hat{\underline{\sigma}}); \mathcal{D}_N) \subset \mathcal{M}_P$ must be at least as large as the number of optimal models in $S_{opt}(M(\hat{\underline{a}}); \hat{Z}_{1,N}) \subset \mathcal{M}$.

In the next section, some M-identifiability results presented by Beck [1978] for the class $\mathcal{M}_{N_d}$ of N_d-degree of freedom linear structural models are reviewed. A modal form of the theoretical model is studied.

3.7 Identifiability of Some Modal Parameters

Assume the modal form of the theoretical model defining the class $\mathcal{M}_{N_d}$ of N_d-degree-of-freedom (dof) linear structural models (see Section 2.6). The

parameters of this theoretical model, assuming zero initial conditions, are the modal frequencies ω_r, the damping ratios ζ_r, and the effective participation factors $\beta_i^{(r)}$ where $i, r = 1, 2, \ldots, N_d$. Let $\mathcal{L}^o$ and $\mathcal{L}^u$ denote the set of integers corresponding to the observed and unobserved degrees of freedom, respectively. The two sets are related as follows:

$$\mathcal{L}^u = \{1, 2, \ldots, N_d\} - \mathcal{L}^o \tag{3.7.1}$$

It has been shown [Beck 1978] that the parameters $\{\omega_r, \zeta_r, \beta_i^{(r)}, r = 1, 2, \ldots, N_d, i \in \mathcal{L}^o\}$ which comprise the elements of $\underline{a}^o$ are globally M-identifiable from the input and output if the following conditions are met: (a) the model has no repeated modes, that is, no two modes have the same modal frequencies and damping ratios, (b) there are no modes with a zero participation factor, and (c) no mode has a node at each coordinate at which the response is measured. Conditions (b) and (c) can be stated as follows: for each mode $r = 1, 2, \ldots, N_d$, there exists at least one $i \in \mathcal{L}^o$, such that $\beta_i^{(r)} \neq 0$. Notice that if this condition is not satisfied, that is, if $\beta_i^{(r)} = 0$ for each $i \in \mathcal{L}^o$, the r^{th} mode will be missing from the output and hence ω_r and ζ_r will not be able to be determined from the input and output.

A practical way of obtaining the globally identifiable optimal vector $\hat{\underline{a}}^o$ has been developed [Beck 1978]. In the case of real data, the existence of model error and measurement noise does not allow for global S-identifiability of the modal parameters in $\underline{a}^o$ corresponding to the higher modes. However, these higher modes do not have an important contribution when predicting the structural response at the observed degrees of freedom for a future excitation of similar spectral content.

The property of global M-identifiability of the elements of $\underline{a}^o$ and the efficiency of the above-referenced numerical algorithm for obtaining the optimal parameters makes it very convenient to apply this modal identification. However, there are also several drawbacks associated with it.

The first drawback associated with the modal identification becomes apparent if the class of linear models considered is a subclass of the class $\mathcal{M}_{N_d}$ of linear classically-damped N_d-dof structural models. Notice that in the case where the whole class $\mathcal{M}_{N_d}$ is considered, the space of permissible values $S(\underline{a})$ for the modal parameters $\underline{a}$ is regular and well defined, since the only constraints are $0 \leq \omega_r$, $\omega_s \leq \omega_r$ for $s < r$, $0 \leq \zeta_r < 1$, and $\sum_{r=1}^{N} \beta_i^{(r)} = b_i$. The condition $\omega_s \leq \omega_r$ for $s < r$ is imposed by defining the r^{th} mode to be the mode whose corresponding modal frequency is the r^{th} of the modal frequencies when they are placed in an ascending order. Consider now a subclass of $\mathcal{M}_{N_d}$ specified by imposing certain constraints on the stiffness matrix K. For example, the class of planar shear structural models constitutes a subclass of $\mathcal{M}_{N_d}$ with the stiffness matrix of its models having a specific tridiagonal structure. For such a subclass of models, the space $S(\underline{a}^o)$ of permissible values for $\underline{a}^o$ is no longer regular shaped, but instead can become very irregular and difficult to define. Therefore, an optimization algorithm searching for the optimal parameters in $S(\underline{a}^o)$ can become extremely cumbersome. Thus, although usually the lack of need to specify a structural model other than it be linear is a major advantage of the modal identification approach, it becomes a drawback when it is desirable to use more detailed information about the structural system.

Another closely related drawback is that when applying the modal identification, no information is extracted from the available data to directly update the remaining unobserved modal parameters $\{\beta_i^{(r)}, r = 1, \ldots, N, i \in \mathcal{L}^u\}$, which comprise the elements in $\underline{a}^u$. The elements of $\underline{a}^u$ are updated through (3.4.28), which for the special case where $K = 1$ gives:

$$p(\underline{a}^u | \mathcal{D}_N, \mathcal{M}_P) = p(\underline{a}^u | \hat{\underline{a}}^o, \mathcal{M}_P) \tag{3.7.2}$$

In the case where the whole class $\mathcal{M}_{N_d}$ is considered, the elements of $\underline{a}^u$ remain unidentifiable after using the available data, since the domain of permissible values for the elements of $\underline{a}^u$ given $\hat{\underline{a}}^o$ is a whole continuum restricted only by

the constraints $\sum_{r=1}^{N} \beta_i^{(r)} = b_i, i \in \mathcal{L}^u$. This unidentifiability can result in large uncertainties when predicting the values of output quantities at the unobserved degrees of freedom. On the other hand, if a particular subclass of $\mathcal{M}_{N_d}$ is considered, then the domain of permissible values for $\underline{a}^u$ given $\hat{\underline{a}}^o$ might consist of one or a finite set of isolated points, in which case $\underline{a}^u$ is globally or locally identifiable, respectively. These questions of identifiability of $\underline{a}^u$ cannot be answered directly by using modal identification alone without reference to the particular structure of the considered subclass. Another situation where unidentifiability might be avoided by utilizing the particular structure of the subclass of consideration is the case where some of the conditions for global identifiability, stated earlier, are violated, resulting in unidentifiability of some of the elements of $\underline{a}^o$ when modal identification is utilized alone.

Another drawback of modal identification is that it does not provide information regarding the identifiability and the optimal values of structural properties, such as stiffnesses, which can be of great interest to the engineer, unless a subsequent stage of identification is performed using the identified modal parameters.

To overcome these weaknesses of modal identification, the identification of a different set of parameters, not all modal, will be addressed.

3.8 A Combined Set of Modal and Structural Parameters

Consider again the class $\mathcal{M}_{N_d}$ of linear, classically damped structural models. Assume that the mass matrix M is known, while the stiffness matrix K and the damping matrix C are unknown. Let the stiffness matrix be parameterized by a set of dimensionless parameters $\{\theta_i, i = 1, \ldots, N_\theta\}$, as prescribed by (2.6.10), where each θ_i scales the stiffness contribution K_i of a certain substructure to the total stiffness matrix. The set of permissible values for each θ_i is $S(\theta_i) = [0, \infty)$. Notice that if K has a particular structure, such as being tridiagonal, this structure is preserved and K remains physically interpretable and consistent through

such a parameterization. The damping matrix C is assumed to be specified by using the set of its modal damping ratios $\{\zeta_r, r = 1, \ldots, N_d\}$ and the set of the stiffness parameters $\underline{\theta}$. This becomes possible by utilizing (2.6.33b), where the vector of modal frequencies $\underline{\omega}$ and the matrix B of the effective participation factors can be obtained for the given $\underline{\theta}$ by solving the appropriate eigenvalue problem involving the resulting stiffness matrix K and the known mass matrix M, as discussed in Section 2.6.2. Therefore, the resulting parameter vector $\underline{a} = [\underline{\theta}^T, \underline{\zeta}^T]^T$, consisting of the structural parameters $\underline{\theta}$ and the modal parameters $\underline{\zeta}$, completely parameterizes the class or subclass of $\mathcal{M}_{N_d}$ of interest, and will be the target of identification. It is interesting to note that this choice of parameters leads to $\underline{a}^o = \underline{a}$, that is, all parameters in $\underline{a}$ become involved in any observed output, and, therefore, all parameters in $\underline{a}$ will be updated directly from any observed data. This is due to the fact that the output at the i^{th} degree of freedom depends on the set of modal quantities $\{\omega_r, \zeta_r, \beta_i^{(r)}, r = 1, \ldots, N_d\}$, out of which the set $\{\zeta_r, r = 1, \ldots, N_d\}$ is directly contained in $\underline{a}$ and the remaining set $\{\omega_r, \beta_i^{(r)}, r = 1, \ldots, N_d\}$ is directly dependent on the remaining parameters $\underline{\theta}$.

According to the discussion of Section 3.7, the parameters $\underline{\zeta} = [\zeta_1, \ldots, \zeta_{N_d}]^T$ are globally M-identifiable if certain conditions are met. Therefore, the problem of model identifiability of the optimal parameters reduces to the model identifiability of $\underline{\theta}$. The goals of the remaining sections of this chapter are: (a) to present an efficient algorithm for obtaining the optimal parameters $(\hat{\underline{\theta}}, \hat{\underline{\zeta}})$ by minimizing a function $J(\underline{\theta}, \underline{\zeta})$ and (b) to investigate the model identifiability of the optimal parameters $\hat{\underline{\theta}}$.

3.9 Recovery of Optimal Parameters

By definition, the optimal parameters globally maximize the function $f_N^o(\hat{X}_{1,N}; \underline{a}^o, \sigma^o, \hat{Z}_{1,N})$. It was shown in Section 3.4 that the optimal parameters

$\hat{\underline{a}}^o$ globally minimize $J(\underline{a}^o)$, given by (3.4.15), where the dependence of $J(\underline{a}^o)$ on the input and output data and the theoretical model is suppressed in the notation. Notice that $J(\underline{a}^o)$ is a nonlinear function in the parameters $\underline{a}^o$. This is because $\underline{q}^o$ is a nonlinear function of $\underline{a}^o$, even if the model is linear in the parameters. The task of finding all the global minima of a nonlinear function of one or more variables, subject to possible constraints, is extremely difficult. The difficulties encountered are associated with the following two steps:

1. Choosing an algorithm that will converge to at least a true local minimum of J. In addition, the desired algorithm is required to be computationally efficient, that is, converge to the minimum quickly without using too much memory. The choice of an appropriate algorithm clearly depends on the function to be minimized. An inappropriate algorithm may not converge at all, or may exhibit premature convergence, that is, it may indicate that convergence has been achieved before a local minimum has been reached. This is often the case if the function to be minimized is very slowly varying along some twisted "valley floor" in the multi-dimensional parameter space. The property of computational efficiency is equally important as the property of convergence, since a theoretically converging, but very slow algorithm, may require an unrealistic amount of time and computational cost, so that it has to be viewed as practically non-converging.

2. Examining if the attained minimum of J is a global one or just a local minimum, and if it is global, examining its uniqueness. In the case of nonuniqueness, the additional task of finding all global minima is required. Virtually nothing is available for finding all global extrema of non-convex functions. The approach usually followed is to find the local minima reached by starting from widely varying starting values of the independent variables and then to pick the most extreme of these. There is no systematic way of assuring that all global minima have been reached other than an exhaustive search through the whole parameter space, which is computationally prohibitive in

most applications in higher dimensions.

In the next sections, an efficient algorithm for finding all global minima of $J(\underline{a}^o)$ will be presented for a particular case where $\underline{a}^o = \underline{a} = [\underline{\theta}^T, \underline{\zeta}^T]^T$.

3.9.1 Comments on the Performance of Existing Minimization Algorithms when Applied to Minimizing $J(\underline{\theta}, \underline{\zeta})$

A review of well-established minimization algorithms can be found in [Press H.W. et al., 1989]. The performance of these algorithms when applied to minimize $J(\underline{\theta}, \underline{\zeta})$ is evaluated in this section.

As a first step, it is important to realize the amount of calculations involved in evaluating $J(\underline{\theta}, \underline{\zeta})$, given by:

$$J(\underline{\theta}, \underline{\zeta}) = \sum_{n=1}^{N} \sum_{i=1}^{N_o} (\hat{x}_i^o(n) - q_i^o(n; \underline{\theta}, \underline{\zeta}))^2 \tag{3.9.1}$$

The dependence of J and q_i^o on the input has been suppressed in the notation. In order to evaluate the model response q_i^o, the necessary modal quantities have to be calculated first by solving the appropriate eigenvalue problem. Next, the histories of each of the modal contributions $\{q_i^{o^{(r)}}(n; \omega_r(\underline{\theta}), \beta_i^{(r)}(\underline{\theta}), \zeta_r), n = 1, 2, \ldots, N\}, r = 1, \ldots, N_d$ must be calculated. If q_i^o represents a displacement quantity, that is achieved by numerically solving (2.6.29). If q_i^o represents velocity or acceleration, it is calculated through appropriate differentiation of the corresponding displacement. Finally, q_i^o is calculated as a superposition of its modal contributions by (2.6.28). Hence, it follows that evaluating the function $J(\underline{\theta}, \underline{\zeta})$ is computationally expensive and, therefore, it is desirable to evaluate it as few times as possible.

All minimization algorithms perform a sequence of one-dimensional minimizations. The difference between the various methods lies in the choice of the directions along which the one-dimensional minimizations are performed. In choosing the directions of 1-D minimizations, some of the methods require only

evaluation of the function to be minimized, while others also require evaluation of its gradient. Independent of whether or not derivative information is used, an algorithm may become very inefficient for certain configurations of contour maps, if no information accumulated during the preceding one-dimensional minimizations is utilized to influence the choice of the future directions. An example of an inefficient algorithm without the use of derivative information is demonstrated in Figure 3.1, where the convergence path followed by successive minimizations along the coordinate directions for a function with a contour map containing a long, narrow valley is depicted. Unless the valley is optimally oriented, this method is extremely inefficient, taking many steps to get to the minimum. On the other hand, the method of steepest descent is an example of an algorithm using derivative information, which is very inefficient for obtaining the minimum in the case of the function of Figure 3.1. Actually, in the case of a function of two variables, the method of successive minimizations along the coordinate directions is equivalent to the method of steepest descent after the first 1-D minimization has been performed [Beck 1978].

Among the best-established categories of algorithms that include updating of the directions along which 1-D minimizations are to be performed, using information extracted from the preceding 1-D minimizations, are the following:

a) The direction-set methods among which Powell's method is the prototype. This is a method not requiring calculation of derivatives.

b) The conjugate gradient methods, which require derivative calculations. The best known members of this family are the Fletcher-Reeves algorithm and the closely related Polak-Ribiere algorithm.

c) The quasi-Newton or variable metric methods, which also require derivative information. The best known algorithms in this category are the Davidon-Fletcher-Powell (DFP) algorithm, and the closely related Broyden- Fletcher-Goldfarb-Sharma (BFGS) algorithm.

For the case where a method requiring derivative information is chosen, it is important to emphasize that numerically approximating the derivatives $\frac{\partial J}{\partial \theta_i}$ using a central difference method does not allow for reliable estimates due to significant numerical errors. Instead, the derivatives ought to be calculated by using the analytical expression:

$$\frac{\partial J}{\partial \theta_i} = \sum_{r=1}^{N_d} \frac{\partial J}{\partial \omega_r} \frac{\partial \omega_r}{\partial \theta_i} = -2 \sum_{r=1}^{N_d} \sum_{n=1}^{N} \sum_{i=1}^{N_o} (\hat{x}_i^o(n) - q_i^o(n; \underline{\theta}, \underline{\zeta})) \frac{\partial q_i^{o(r)}(n; \omega_r(\underline{\theta}), \zeta_r)}{\partial \omega_r} \tag{3.9.2}$$

where $\frac{\partial \omega_r}{\partial \theta_i}$ is calculated analytically by (See Appendix B):

$$\frac{\partial \omega_r}{\partial \theta_i} = \frac{1}{2\omega_r} \underline{\phi}^{(r)^T} K_i \underline{\phi}^{(r)} \tag{3.9.3}$$

and $\frac{\partial q_i^{o(r)}(n; \omega_r(\underline{\theta}), \zeta_r)}{\partial \omega_r}$ is calculated by solving an appropriate differential equation, analogous to (2.5.11), if q_i^o represents displacement. The additional computational cost for calculating the derivatives of J is usually not compensated for by a proportional increase in the performance of the algorithms making use of them.

All three categories of algorithms mentioned earlier were tested using simulated data. The input was chosen to be the 1940 El Centro earthquake record, NS component. The observed output was chosen to be the response at the roof of a N_d-dof planar shear structural model with uniform distribution of mass, $m_i = m_o$, $i = 1, \ldots, N_d$, and interstory stiffness, $k_i = k_o$, $i = 1, 2, \ldots N_d$, and equal modal damping ratios, $\zeta_r = \zeta_o$, $r = 1 \ldots N_d$. Assuming the damping ratios to be known and fixed, the function J to be minimized becomes only a function of the parameters $\underline{\theta}$, that is, $J = J(\underline{\theta})$, where θ_i is assumed to scale the i^{th} interstory stiffness, that is, $k_i = \theta_i k_o$. Obviously, in this case of ideal data, the minimum value that $J(\underline{\theta})$ attains is zero. Also, it is known that $\hat{\underline{\theta}} = [1, 1, \ldots, 1]^T$ is an optimal vector. The convergence of each algorithm was tested for different numbers of degrees of freedom N_d, varying from two to six, and using different starting points in each case. The values for k_o and ζ_o were chosen arbitrarily to

be $k_0 = 2000 m_o \text{sec}^{-2}$ and $\zeta_o = 0.05$. Table 3.1 shows some of the results obtained for a small representative sampling of this numerical testing for the case where $N_d = 4$. The point $\underline{\theta}^o$ corresponds to the chosen starting point, while the point $\underline{\theta}^*$ corresponds to the point to which each algorithm converged. It can be seen that although the values of $J(\underline{\theta}^*)$, normalized by $\sum_{n=1}^{N} \sum_{i=1}^{N_o} \hat{x}_i^o(n)^2$, are small, the values of the final estimates θ_i^* are up to 20% different from the exact optimal values $\hat{\theta}_i = 1$. In the following, the conclusions drawn from these numerical studies are summarized.

The most important and general conclusion is that none of the applied algorithms guaranteed convergence to the real local minimum, especially as cases with a higher number N_d of dof were considered. Although Powell's method converged slightly faster, in general, than the methods using derivative information, all algorithms reached their convergence criterion of a relative change in J being below a prescribed threshold taken to be 10^{-4}, before reaching the optimal solution $\hat{\underline{\theta}} = [1, 1, \ldots, 1]^T$. However, the corresponding minimum value of J achieved was close to zero. The fact that a value of J so close to zero is achieved without reaching the optimal solution, where J reaches its global minimum value of zero, implies that the contour-map of J contains a very "flat valley floor" on which the reached solutions, as well as the targeted optimal solution, lie. The solution in the neighborhood of $\hat{\underline{\theta}}$, to which each algorithm converged, was dependent on the starting point, which usually was chosen to be relatively close to the targeted optimal solution, and on the algorithm used. However, the larger the number N_d of degrees of freedom considered, the farther the obtained solution was from the optimal solution in general. In some cases, where the starting point was chosen to be far apart from the optimal solution, the convergence criterion was reached at a point distant from the optimal solution $\hat{\underline{\theta}} = [1, 1, \ldots, 1]^T$, but with a corresponding value for J still close to zero. The explanation for this is that in these cases the algorithm converged to a solution close to another global minimum. However, since the algorithms proved to be converging prematurely, the exact

value of the corresponding optimal solution is not known.

Figure 3.2 depicts the contour-map of $J(\underline{\theta})$, corresponding to the particular case of the above-described numerical studies where a two-story planar shear structure is considered. $J(\underline{\theta})$ has been normalized by dividing it with $\sum_{n=1}^{N}\sum_{i=1}^{N_o}\hat{x}_i^o(n)^2$. This figure is instructive in understanding the reasons that cause difficulty in convergence, although it must be kept in mind that these reasons become much more pronounced when dealing with higher-dimensional problems. It can be verified by looking at this figure that there really exists, as expected, a very flat valley floor. The topology of this valley floor, being very flat along some curving direction, while being very steep along the perpendicular direction, is the reason for the difficulty of convergence that all the above algorithms exhibit. All of the algorithms, designed to exhibit quadratic convergence, have difficulty following this twisting valley floor. The reason for this is that at any point along this floor a quadratic approximation of the J function is acceptably valid only over a very small neighborhood of this point. As a result, the convergence criterion of J changing below a prescribed tolerance is satisfied when a one-dimensional minimization along a straight direction is performed, even if this direction is the best direction based on a quadratic approximation. Decreasing the threshold for the convergence criterion helps reach a slightly closer solution, but convergence becomes prohibitively slow. It can also be seen by looking at Figure 3.2 that there exists another global minimum, which can be proven to be located at $\underline{\hat{\theta}}_2 = [2.0, 0.5]^T$. If a starting point is chosen closer to this optimal solution, then the minimum reached will lie in the neighborhood of $\underline{\hat{\theta}}_2$, and not in the neighborhood of $\underline{\hat{\theta}}_1 = [1.0, 1.0]^T$.

From the above discussion it can be concluded that the available minimization algorithms are incapable of guaranteeing convergence to a local minimum of $J(\underline{\theta})$. Instead, they prematurely converge to a solution lying on a twisted and almost flat valley floor on the corresponding contour map. This premature convergence can be interpreted as the inability of these algorithms to follow a

very slowly descending path along this twisting valley floor all the way to the optimal solution. The solutions at which these algorithms prematurely converge might differ quite significantly from the targeted optimal solutions, although the corresponding values of $J(\underline{\theta})$ might differ only slightly in absolute value. Recall from (3.4.17) that the ratio of posterior probabilities of two sets of parameters is proportional to the inverse ratio of their corresponding J values, raised to a power proportional to the number of available data points. This result implies that a reached solution $\underline{\theta}$ is relatively very improbable compared to the optimal solution $\hat{\underline{\theta}}$, unless the relative difference of their corresponding J values, defined as $\frac{J(\underline{\theta})-J(\hat{\underline{\theta}})}{J(\underline{\theta})}$, is below a certain threshold. For example, assume that 20 sec of output sampled at 0.02 sec is used, and that only one output quantity is observed. In this case, $N = 1000, N_o = 1$ and, assuming a noninformative prior distribution, it follows that a solution is 100 times more improbable than the optimal solution if the relative difference of their J values is $\sim 9.25 \times 10^{-3}$, while it is 10 times more improbable if the relative difference of their J values is $\sim 4.62 \times 10^{-3}$. Such a criterion would be a rational criterion for judging covergence to an optimal solution. Note that in the particular case where $J(\hat{\underline{\theta}}) = 0$, any solution $\underline{\theta} \neq \hat{\underline{\theta}}$ has a relatively small probability compared to the probability of the optimal solution $\hat{\underline{\theta}}$, and therefore convergence under such a criterion is not achieved unless the actual optimal vector $\hat{\underline{\theta}}$ is reached. However, since the extremal value of $J(\underline{\theta})$ is in general not known *a priori*, applying such a criterion is not possible. Instead, the criterion for convergence used by the above algorithms, defined as the relative change in J during one iteration being below a certain threshold, is a rational criterion for judging convergence, but, at the same time, it does not guarantee convergence to an optimal solution as desired.

One of the objectives of this chapter is to present an efficient algorithm which is capable of converging to an optimal solution. Such an algorithm was developed and is presented in Section 3.11, based on a transformation of variables discussed next.

3.10 A Useful Transformation of Variables

Consider an N_d-degree of freedom theoretical model $\mathcal{M} \subseteq \mathcal{M}_{N_d}$, parameterized by $\underline{a} = [\underline{\theta}^T, \underline{\zeta}^T]^T$, where $\underline{\theta} \in S(\underline{\theta}) = [0, \infty)^{N_\theta}$ and $\underline{\zeta} \in S(\underline{\zeta}) = [0, 1]^{N_d}$. Assuming that the mass matrix $\mathcal{M}$ and the stiffness matrices $K_i, i = 0, 1, \ldots, N_\theta$ of (2.6.10) are known, each $\underline{\theta} \in S(\underline{\theta})$ uniquely specifies the vector of modal frequencies $\underline{\omega} = \underline{\omega}(\underline{\theta}) \in S(\underline{\omega}) \subset [0, \infty)^{N_d}$, where its elements $\omega_r, r = 1, \ldots, N_d$ are assumed to be in ascending order, that is, $\omega_s \leq \omega_r$ for $s < r \leq N_d$. It is shown with a particular example, in Section 3.10.1, that such a transformation $\underline{\theta} \rightarrow \underline{\omega}(\underline{\theta})$ leads to an almost ellipsoidal contour map for J, with the principal directions aligned almost along the straight coordinate directions of the transformed variables $\underline{\omega}$. Such a property is very important, since it provides a tool for dealing with the highly complex contour map of $J(\underline{\theta}; \underline{\zeta})$ in a straightforward manner. To provide better insight into this powerful mapping, some definitions and properties concerned with this transformation $\underline{\theta} \rightarrow \underline{\omega}(\underline{\theta})$ are highlighted.

The space $S(\underline{\omega})$ is the image of $S(\underline{\theta})$ under the mapping $\underline{\theta} \rightarrow \underline{\omega}(\underline{\theta})$. The conditions $0 < \omega_r$ and $\omega_s \leq \omega_r, 1 \leq s < r \leq N_d$ alone are generally not enough to specify the boundaries of $S(\underline{\omega})$, since more restrictions, whose explicit form is not always easily determined, are imposed by the particular theoretical model $\mathcal{M}$ considered. Although each $\underline{\theta} \in S(\underline{\theta})$ is uniquely mapped into an $\underline{\omega} \in S(\underline{\omega})$, the converse is not necessarily true, that is, there might be more than one $\underline{\theta} \in S(\underline{\theta})$ corresponding to the same $\underline{\omega} \in S(\underline{\omega})$. Assume from now on, unless otherwise specified, the particular case where $N_\theta = N_d$, that is, the case where the dimension of the vector $\underline{\theta}$ is equal to the number of degrees of freedom of the theoretical model. The cases where $N_\theta < N_d$ and $N_\theta > N_d$ will also be addressed later in Section 3.11.4.

A sufficient condition for the mapping of a subspace $\Theta \subseteq S(\underline{\theta})$ onto the subspace $\Omega \subseteq S(\underline{\omega})$ to be locally one-to-one is:

$$\mathcal{J}(\underline{\theta}) \equiv | \nabla \underline{\omega}(\underline{\theta})| \neq 0, \ \forall \underline{\theta} \in \Theta \tag{3.10.1}$$

where

$$\nabla\underline{\omega}(\underline{\theta}) \equiv \frac{\partial \underline{\omega}}{\partial \underline{\theta}} = \begin{bmatrix} \frac{\partial \omega_1}{\partial \theta_1} & \cdots & \frac{\partial \omega_1}{\partial \theta_{N_\theta}} \\ \vdots & & \\ \frac{\partial \omega_{N_d}}{\partial \theta_1} & \cdots & \frac{\partial \omega_{N_d}}{\partial \theta_{N_\theta}} \end{bmatrix} \tag{3.10.2}$$

Note that the above matrix is a square matrix, since it was assumed that $N_\theta = N_d$. If at a point $\tilde{\underline{\theta}} \in S(\underline{\theta})$ the above defined Jacobian $\mathcal{J}(\tilde{\underline{\theta}})$ is nonzero, then there exists a neighborhood $\mathcal{H}(\underline{\theta}; \tilde{\underline{\theta}}, \epsilon) = \{|\underline{\theta} - \tilde{\underline{\theta}}| < \epsilon, \underline{\theta} \in S(\underline{\theta}); \epsilon > 0\}$, such that no two points of this neighborhood correspond to the same $\underline{\omega}$. The condition, of the Jacobian being nonzero for such a neighborhood to exist, is only a sufficient and not a necessary condition. Let $S_I \subset S(\underline{\theta})$ denote the set of all such points $\underline{\theta}$ for which the transformation $\underline{\theta} \rightarrow \underline{\omega}(\underline{\theta})$ is locally invertible.

If there does not exist any $\epsilon > 0$, such that the neighborhood $\mathcal{H}(\underline{\theta}; \tilde{\underline{\theta}}, \epsilon)$ has the property of being mapped one-to-one under the mapping $\underline{\theta} \rightarrow \underline{\omega}(\underline{\theta})$, then the corresponding Jacobian $\mathcal{J}(\tilde{\underline{\theta}})$ is zero. Let $S_B(\underline{\theta}) \subset S(\underline{\theta})$ denote the set of all such points $\underline{\theta}$ for which the transformation $\underline{\theta} \rightarrow \underline{\omega}(\underline{\theta})$ is locally non-invertible. It follows from the above definition that:

$$\mathcal{J}(\underline{\theta}) = 0 \quad ; \quad \forall \underline{\theta} \in S_B(\underline{\theta}) \tag{3.10.3}$$

Also, the above definitions imply that:

$$S_I(\underline{\theta}) \cup S_B(\underline{\theta}) = S(\underline{\theta}) \quad \text{and} \quad S_I(\underline{\theta}) \cap S_B(\underline{\theta}) = \{\emptyset\} \tag{3.10.4}$$

The continuity of the mapping $\underline{\theta} \rightarrow \underline{\omega}(\underline{\theta})$ implies that if the set $S_B(\underline{\theta})$ is empty, then the overall mapping $S(\underline{\theta}) \rightarrow S(\underline{\omega})$ is one-to-one. Conversely, if the latter overall mapping is not one-to-one, then the set $S_B(\underline{\theta})$ is not empty, but defines the boundaries separating the space $S_I(\underline{\theta})$ into different subregions $\Theta_i \subseteq S_I(\underline{\theta}) \subset S(\underline{\theta}), i = 1, \ldots, N_\Theta$. These subregions satisfy the following three properties:

$$1) \bigcup_{i=1}^{N_\Theta} \Theta_i = S_I(\underline{\theta}) \quad , \quad 2) \; \Theta_i \bigcap \Theta_j = \{\emptyset\} \quad ; \quad i \neq j$$

and 3) $\Theta_i \bigcup \Theta_j \quad ; \quad i \neq j$ is a non-connected set,

where $i, j \in \{1, 2, \ldots, N_\Theta\}$. The subregions $\Theta_i, i = 1, \ldots, N_\Theta$ should be viewed as the largest connected subsets of $S_I(\underline{\theta})$, so that any connected subset of $S_I(\underline{\theta})$ is a subset of one of the above subregions Θ_i. The boundary set $S_B(\underline{\theta})$, separating the above subregions Θ_i from each other, consists of continuous $(N_\theta - 1)$-dimensional surfaces. At a point $\underline{\theta}$ of $S_B(\underline{\theta})$, where the nullity (dimension of the null space) of the corresponding matrix $\nabla\underline{\omega}(\underline{\theta})$ is equal to one, only one such surface is passing through. If, on the other hand, the nullity is $N_n > 1$, then this point has to be viewed as the intersection of N_n of these $(N_\theta - 1)$-dimensional surfaces.

Define the multiplicity $N_\mu = N_\mu(\tilde{\underline{\omega}})$ of a point $\tilde{\underline{\omega}} \in S(\underline{\omega})$ to be the number of elements contained in the set $\{\underline{\theta} \in S(\underline{\theta}) : \underline{\omega}(\underline{\theta}) = \tilde{\underline{\omega}}\}$. Obviously, the multiplicity of any point $\tilde{\underline{\omega}} \in S(\underline{\omega})$ is smaller or equal to the number N_Θ of the subregions Θ_i. The multiplicity of a point $\underline{\omega}$ belonging in the set $S_B(\underline{\omega}) = \{\underline{\omega}(\underline{\theta}), \underline{\theta} \in S_B(\underline{\theta})\} \subset S(\underline{\omega})$ is generally smaller than that of a point belonging in the set $S_I(\underline{\omega}) = \{\underline{\omega}(\underline{\theta}), \underline{\theta} \in S_I(\underline{\theta})\} \subset S(\underline{\omega})$. For the points $\underline{\theta} \in S_B(\underline{\theta})$, the larger the nullity of the matrix $\nabla\underline{\omega}(\underline{\theta})$ is, or equivalently, the smaller its rank is, the smaller the multiplicity of the corresponding $\underline{\omega} = \underline{\omega}(\underline{\theta}) \in S_B(\underline{\omega})$. It can also be shown that the eigenvectors corresponding to the nonzero eigenvalues of $\nabla\underline{\omega}(\underline{\theta}), \underline{\theta} \in S_B(\underline{\theta})$ form a basis spanning locally, in the neighborhood of $\underline{\omega}(\underline{\theta})$, the space $S_B(\underline{\theta})$. The higher the rank of $\nabla\underline{\omega}(\underline{\theta})$, the higher the dimension of the space $S_B(\underline{\theta})$.

In order to clarify ideas, the above concepts will be demonstrated using a particular example.

3.10.1 An Example: Two Degree of Freedom Shear Model

Consider the theoretical model of a two degree of freedom planar shear building. Such a structure is shown for the general N-dof case in Figure 2.7. Assume a known uniform mass distribution, $m_1 = m_2 = m_0$. Let the stiffness matrix K be parameterized by $\underline{\theta} = [\theta_1, \theta_2]^T$ such that the interstory stiffnesses

are given by $k_1 = \theta_1 k_0$ and $k_2 = \theta_2 k_0$. The mass and stiffness matrix are, therefore:

$$M = \begin{bmatrix} m_0 & 0 \\ 0 & m_0 \end{bmatrix} \quad \text{and} \quad K = k_0 \begin{bmatrix} (\theta_1 + \theta_2) & -\theta_2 \\ -\theta_2 & \theta_2 \end{bmatrix} \tag{3.10.5}$$

The eigenfrequencies ω_r and the eigenvectors $\phi^{(r)}, r = 1, 2$ are found by solving the eigenvalue problem:

$$[M^{-1}K - \omega_r^2 I] \begin{bmatrix} \phi_1^{(r)} \\ \phi_2^{(r)} \end{bmatrix} = \begin{bmatrix} 0 \\ 0 \end{bmatrix} \quad ; \quad r = 1, 2 \tag{3.10.6}$$

where I is a 2×2 identity matrix. The solutions for $\omega_r^2, r = 1, 2$, obtained by requiring $|M^{-1}K - \omega_r^2 I|$ to be zero, lead to the vector of modal frequencies $\underline{\omega}$:

$$\underline{\omega} = \begin{bmatrix} \omega_1 \\ \\ \omega_2 \end{bmatrix} = \sqrt{\frac{k_0}{2m_0}} \begin{bmatrix} \sqrt{\theta_1 + 2\theta_2 - \sqrt{\theta_1^2 + 4\theta_2^2}} \\ \sqrt{\theta_1 + 2\theta_2 + \sqrt{\theta_1^2 + 4\theta_2^2}} \end{bmatrix} \tag{3.10.7}$$

and the modeshape matrix Φ, normalized so that $\phi_2^{(r)} = 1, r = 1, 2$:

$$\Phi = \begin{bmatrix} \dfrac{\theta_1 + \sqrt{\theta_1^2 + 4\theta_2^2}}{2\theta_2} & \dfrac{\theta_1 - \sqrt{\theta_1^2 + 4\theta_2^2}}{2\theta_2} \\ 1 & 1 \end{bmatrix} = \begin{bmatrix} \dfrac{\lambda + \sqrt{\lambda^2 + 4}}{2} & \dfrac{\lambda - \sqrt{\lambda^2 + 4}}{2} \\ 1 & 1 \end{bmatrix} \tag{3.10.8}$$

where $\lambda = \frac{\theta_1}{\theta_2}$. The resulting vector of modal participation factors for this choice of Φ is:

$$\underline{\alpha} = \begin{bmatrix} \frac{1}{2}(1 + \dfrac{2 - \lambda}{\sqrt{\lambda^2 + 4}}) \\ \frac{1}{2}(1 - \dfrac{2 - \lambda}{\sqrt{\lambda^2 + 4}}) \end{bmatrix} \tag{3.10.9}$$

Finally, the matrix of effective participation factors B, which is independent of the normalization chosen for Φ, is:

$$B = \begin{bmatrix} \dfrac{1}{2}\left(1 + \dfrac{2 - \lambda}{\sqrt{\lambda^2 + 4}}\right) & \dfrac{1}{2}\left(1 - \dfrac{2 - \lambda}{\sqrt{\lambda^2 + 4}}\right) \\ \dfrac{1}{2}\left(1 + \dfrac{2 + \lambda}{\sqrt{\lambda^2 + 4}}\right) & \dfrac{1}{2}\left(1 - \dfrac{2 + \lambda}{\sqrt{\lambda^2 + 4}}\right) \end{bmatrix} \tag{3.10.10}$$

The set of allowable values for $\underline{\theta}$ is $S(\underline{\theta}) = [0, \infty) \times [0, \infty]$. For each $\underline{\theta} \in S(\underline{\theta})$, a unique vector $\underline{\omega} = [\omega_1, \omega_2]^T$ is specified through (3.10.7). The space $S(\underline{\omega})$, defined as the image of $S(\underline{\theta})$ under the mapping $\underline{\theta} \rightarrow \underline{\omega}(\underline{\theta})$, must satisfy the constraint: $0 \leq \omega_1 \leq \omega_2$. However, this general constraint alone proves to be inadequate to determine the boundaries of $S(\underline{\omega})$, since there are additional constraints imposed by the particular class of models $\mathcal{M}$ considered. To determine any additional constraint, consider the inverse mapping $\underline{\omega} \rightarrow \underline{\theta}(\underline{\omega})$ by solving Equation (3.10.7) for $\underline{\theta}$, given $\underline{\omega}$. There are generally two such solutions, $\underline{\theta}_1$ and $\underline{\theta}_2$, proving that the mapping $\underline{\omega} \rightarrow \underline{\omega}(\underline{\theta})$ is not one-to-one, given by:

$$\underline{\theta}_1, \underline{\theta}_2 = \frac{m_0}{4k_0} \begin{bmatrix} 2(\omega_1^2 + \omega_2^2 \mp \sqrt{(\omega_1^2 + \omega_2^2)^2 - 8\omega_1^2\omega_2^2}) \\ \omega_1^2 + \omega_2^2 \pm \sqrt{(\omega_1^2 + \omega_2^2)^2 - 8\omega_1^2\omega_2^2} \end{bmatrix} \tag{3.10.11}$$

For the solutions given by (3.10.11) to be real, the following constraint must be satisfied:

$$\omega_1^2 + \omega_2^2 \geq \sqrt{8}\omega_1\omega_2 \tag{3.10.12}$$

The latter inequality implies that ω_2 lies outside the roots of the quadratic $\omega_1^2 - \sqrt{8}\omega_1\omega_2 + \omega_2^2 = 0$, that is:

$$\omega_2 \leq \omega_1(\sqrt{2} - 1) \tag{3.10.13a}$$

or

$$\omega_2 \geq \omega_1(\sqrt{2} + 1) \tag{3.10.13b}$$

Inequality (3.10.13a) contradicts the general requirement $\omega_2 \geq \omega_1$; therefore, the only constraint left is (3.10.13b). The space $S(\underline{\omega})$, being the subspace of R^2 satisfying the constraints $\omega_1 \geq 0$ and $\omega_2 \geq \omega_1(\sqrt{2} + 1)$, is schematically shown in Figure 3.3b. It can be seen from (3.10.11) that for each $\underline{\omega} \in S(\underline{\omega})$, such that $\omega_2 > \omega_1(\sqrt{2}+1)$, there exist two different solutions corresponding to this $\underline{\omega}$, and, therefore, the multiplicity of each such $\underline{\omega}$ is equal to two. In the special case where $\omega_2 = \omega_1(\sqrt{2} + 1)$, the two solutions $\underline{\theta}_1$ and $\underline{\theta}_2$ collapse to one, that is,

$\underline{\theta}_1 = \underline{\theta}_2$ with a corresponding ratio $\lambda_1 = \lambda_2 = 2$. Therefore, the multiplicity of the points $\underline{\omega} \in S(\underline{\omega})$ with $\omega_2 = \omega_1(\sqrt{2}+1)$ is equal to one. It can be observed from (3.10.11) that the two solutions $\underline{\theta}_1$ and $\underline{\theta}_2$ satisfy the following relationship:

$$\underline{\theta}_i = \begin{bmatrix} 0 & 2 \\ 0.5 & 0 \end{bmatrix} \underline{\theta}_j \quad i \neq j,\ i,j \in \{1,2\} \tag{3.10.14}$$

Equation (3.10.14) implies that:

$$\lambda_1 = \frac{4}{\lambda_2} \tag{3.10.15}$$

By substituting (3.10.15) into (3.10.10) it can be seen that the two solutions $\underline{\theta}_i, i = 1,2$, corresponding to the same vector $\underline{\omega}$, have the same effective participation factors for each mode at the second floor, that is:

$$\beta_2^{(r)}(\underline{\theta}_1) = \beta_2^{(r)}(\underline{\theta}_2)\ ;\ r = 1,2 \tag{3.10.16a}$$

At the first floor, the effective participation factors for each mode corresponding to the two solutions are not equal, but switch order, namely, the effective participation factors for the first and second mode corresponding to $\underline{\theta}_1$ are equal to the effective participation factors for the second and first mode corresponding to $\underline{\theta}_2$, respectively:

$$\beta_1^{(r)}(\underline{\theta}_1) = \beta_1^{(3-r)}(\underline{\theta}_2)\ ;\ r = 1,2 \tag{3.10.16b}$$

The matrix $\nabla\underline{\omega}(\underline{\theta})$ is given by:

$$\nabla\underline{\omega}(\underline{\theta}) = \frac{\partial\underline{\omega}}{\partial\underline{\theta}} = c \begin{bmatrix} \dfrac{\sqrt{\theta_1^2+4\theta_2^2}-\theta_1}{\sqrt{\theta_1+2\theta_2-\sqrt{\theta_1^2+4\theta_2^2}}} & \dfrac{2\sqrt{\theta_1^2+4\theta_2^2}-4\theta_2}{\sqrt{\theta_1+2\theta_2-\sqrt{\theta_1^2+4\theta_2^2}}} \\ \dfrac{\sqrt{\theta_1^2+4\theta_2^2}+\theta_1}{\sqrt{\theta_1+2\theta_2+\sqrt{\theta_1^2+4\theta_2^2}}} & \dfrac{2\sqrt{\theta_1^2+4\theta_2^2}+4\theta_2}{\sqrt{\theta_1+2\theta_2+\sqrt{\theta_1^2+4\theta_2^2}}} \end{bmatrix} \tag{3.10.17}$$

where $c = \frac{1}{2}\sqrt{\frac{k_0}{2m_0}}\frac{1}{\sqrt{\theta_1^2+4\theta_2^2}}$. The Jacobian $\mathcal{J}(\underline{\theta})$ is then:

$$\mathcal{J}(\underline{\theta}) = |\nabla\underline{\omega}(\underline{\theta})| = \frac{k_0}{4m_0}\frac{2\theta_2-\theta_1}{\sqrt{\theta_1\theta_2(\theta_1^2+4\theta_2^2)}} \tag{3.10.18}$$

The condition $\mathcal{J}(\underline{\theta}) \neq 0$ is satisfied everywhere in $S(\underline{\theta})$ except for the points $\underline{\theta}$ for which $\theta_1 = 2\theta_2$. For any neighborhood $\mathcal{H}(\underline{\theta}; \tilde{\underline{\theta}}, \epsilon)$ of $\tilde{\underline{\theta}} = [2\theta^*, \theta^*]^T$, there exist at least two points corresponding to the same $\underline{\omega}$. Such points, for example, are the points $\underline{\theta}_1 = [2\theta^* + 0.5\epsilon, \theta^*]$ and $\underline{\theta}_2 = [2\theta^*, \theta^* + 0.25\epsilon]$, since they satisfy (3.10.14). Hence, all solutions $\underline{\theta}$ such that $\mathcal{J}(\underline{\theta}) = 0$ belong, according to the definitions of the previous section, to the set of boundary points $S_B(\underline{\theta})$:

$$S_B(\underline{\theta}) = \{\underline{\theta} \in S(\underline{\theta}),\ \theta_1 = 2\theta_2\} \tag{3.10.19a}$$

while all the remaining points of $S(\underline{\theta})$, where $\mathcal{J}(\underline{\theta})$ is nonzero, and the transformation is locally invertible, belong to the set $S_I(\underline{\theta})$:

$$S_I(\underline{\theta}) = \{\underline{\theta} \in S(\underline{\theta}),\ \theta_1 \neq 2\theta_2\} \tag{3.10.19b}$$

Figure 3.3a schematically shows $S_B(\underline{\theta})$ and the two regions Θ_1 and Θ_2, in which it separates the remaining space $S_I(\theta)$. The corresponding sets $S_B(\underline{\omega})$ and $S_I(\underline{\omega})$, shown schematically in Figure 3.3b, are:

$$S_B(\underline{\omega}) = \{\underline{\omega} \in S(\underline{\omega}), \omega_2 = \omega_1(\sqrt{2}+1)\} \tag{3.10.20a}$$

$$S_I(\underline{\omega}) = \{\underline{\omega} \in S(\underline{\omega}), \omega_2 \neq \omega_1(\sqrt{2}+1)\} \tag{3.10.20b}$$

The multiplicity of the points of $S_B(\underline{\omega})$ is equal to one, while the multiplicity of the points of $S_I(\underline{\omega})$ is equal to two. Of the two solutions $\underline{\theta}_i, i = 1, 2$, satisfying $\underline{\omega}(\theta_i) = \underline{\omega}^* \in S_I(\underline{\omega})$, one belongs in the region Θ_1, and the other in the region Θ_2. At a point $\underline{\theta}' \in S_B(\underline{\theta})$ corresponding to $\underline{\omega}' \in S_B(\underline{\omega})$, the matrix $\nabla\underline{\omega}(\underline{\theta}')$ of (3.10.17) becomes singular. The eigenvector corresponding to the zero eigenvalue of $\nabla\underline{\omega}(\underline{\theta}')$ is $\delta\underline{\theta}_1 = [+2, -1]^T$. This eigenvector corresponds to the common tangent of the curves $\omega_1(\underline{\theta}) = \omega_1'$ and $\omega_2(\underline{\theta}) = \omega_2'$ at the point $\underline{\theta}'$. The eigenvector corresponding to the nonzero eigenvalue is $\delta\underline{\theta}_2 = [1, (1+\sqrt{2})]$. Notice that this eigenvector spans the space $S_B(\omega)$ given by (3.10.20).

It is important to note, by comparing Figure 3.2 with Figure 3.4, that the contour curves of $J(\underline{\theta})$ of Figure 3.2 look extremely similar to the curves $\omega = \omega_1$

of Figure 3.4. This observation suggests that the long and narrow curved valley floor of $J(\underline{\theta})$, when plotted in the $\omega_1 - \omega_2$ plane, should correspond to a long and narrow but straight valley floor along the ω_2 coordinate direction. The function $J(\underline{\omega}) = J(\underline{\theta}(\underline{\omega})), \underline{\omega} \in S(\underline{\omega})$ is generally multi-valued, since the function $\underline{\theta} = \underline{\theta}(\underline{\omega})$ is multi-valued, with solutions $\underline{\theta}_i = \underline{\theta}(\underline{\omega})$, $i = 1, \ldots, N_\mu(\underline{\omega})$ generally corresponding to different values of J. The function $J(\underline{\omega}), \underline{\omega} \in S(\underline{\omega})$ can become single-valued if a subregion Θ_i is specified, since then for a given point $\underline{\omega}^*$ with multiplicity $N_\mu(\underline{\omega}^*) > 1$, for which the mapping $\underline{\theta} = \underline{\theta}(\underline{\omega}^*)$ is multi-valued, the uniquely defined point $\underline{\theta}_i \in \Theta_i$, satisfying $\underline{\omega}(\underline{\theta}_i) = \underline{\omega}^*$, can be used to evaluate a single value for J, that is, $J(\underline{\omega}^*|\Theta_i) = J(\underline{\theta}_i)$. However, in the particular example of Figure 3.2, the so specified single-valued functions $J(\underline{\omega}^*|\Theta_1)$ and $J(\underline{\omega}^*|\Theta_2)$ are identical, since the two solutions $\underline{\theta}_1 \in \Theta_1$ and $\underline{\theta}_2 \in \Theta_2$, corresponding to the same $\underline{\omega}$ and given by (3.10.11), have also, according to (3.10.16a), the same effective participation factors at the second floor, which results in identical modal responses at that floor, that is, $q_2(t; \underline{\theta}_1) = q_2(t; \underline{\theta}_2)$, therefore leading to $J(\underline{\theta}_1) = J(\underline{\theta}_2)$. Figure 3.5(a) and (b) show the contour map of this function $J(\underline{\omega}|\Theta_1) = J(\underline{\omega}|\Theta_2)$. As expected, the contour map of $J(\underline{\omega}|\Theta_i), i = 1, 2$ consists of ellipse-like contour curves, with a long axis oriented along the ω_2-coordinate direction and a much shorter axis oriented along the ω_1-coordinate direction. The global minimum is attained at a unique point $\hat{\underline{\omega}}$ in this $\omega_1 - \omega_2$ plot. This point $\hat{\underline{\omega}}$, when viewed as the minimum of $J(\underline{\omega}|\Theta_1)$, corresponds to the optimal solution $\hat{\underline{\theta}}_1 = [1.0, 1.0]^T$, while when viewed as the minimum of $J(\underline{\omega}|\Theta_2)$, corresponds to the optimal solution $\hat{\underline{\theta}}_2 = [2.0, 0.5]^T$.

To illustrate a case where $J(\underline{\omega}|\Theta_1) \neq J(\underline{\omega}|\Theta_2)$, assume that in the example of Figure 3.2 the observed data consists of the response at the first floor instead of the response at the second floor. Figure 3.6 depicts the contour map of $J(\underline{\theta})$ for this case. It can be seen that, in this case, there exists a unique global minimum located at $\hat{\underline{\theta}} = [1.0, 1.0]^T$. Figure 3.7(a) uses the $\omega_1 - \omega_2$ plane to depict the contour maps of $J(\underline{\omega}|\Theta_1)$ and $J(\underline{\omega}|\Theta_2)$. Figure 3.7(b) provides a

magnified view of these contour maps in the neighborhood of $\underline{\omega}(\hat{\underline{\theta}})$. These two functions are no longer identical, since the modal effective participation factors at the first floor, corresponding to the $\underline{\theta}$ solutions with the same $\underline{\omega}$, are not equal, as stated in (3.10.16b). It can be seen that only $J(\underline{\omega}|\Theta_1)$ contains close contour curves enclosing a global minimum corresponding to the unique optimal solution $\hat{\underline{\theta}} = [1.0, 1.0]^T \in \Theta_1$. Again, the axes of these curves are oriented along the ω-coordinate directions, the longer one along the ω_2 coordinate and the shorter one along the ω_1 coordinate. The contour map of $J(\underline{\omega}|\Theta_2)$ does not contain any closed contour curves enclosing a local minimum, and, therefore, there exists no optimal solution belonging in Θ_2. However, it can be seen that there exists a long and narrow valley floor oriented along the ω_2 direction. The property of the valley floors being oriented along one of the ω-coordinate directions is what makes the mapping $\underline{\theta} \rightarrow \underline{\omega}(\underline{\theta})$ so powerful.

3.11 Proposed Algorithm to Minimize $J(\underline{\theta}, \underline{\zeta})$

A new method is proposed to minimize the function $J(\underline{\theta}, \underline{\zeta})$ to overcome the difficulties in convergence of the existing algorithms. This new algorithm will be presented in two steps. In the first step, it will be assumed that the parameter vector $\underline{\zeta}$ is fixed and known, reducing the problem to the minimization of $J(\underline{\theta})$. The second step is a natural extension of the first step, where the parameter vector $\underline{\zeta}$ will be assumed unknown and will, therefore, be included in the argument of J.

3.11.1 Minimization of $J(\underline{\theta})$

Assume that the length N_θ of the uncertain parameter vector $\underline{\theta}$ is equal to the number of modes N_m included in the model response. The idea behind the new minimization algorithm is to perform a series of one-dimensional curve minimizations in the $\underline{\theta}$-space, which in the $\underline{\omega}$-space correspond to a series of

one-dimensional straight line minimizations in the ω-coordinate directions.

Let $c_k(\underline{\theta};\underline{\theta}^*)$ denote a one-dimensional curve in the space $S(\underline{\theta})$, passing through a point $\underline{\theta}^*$, with the property that along this curve all of the first N_m modal frequencies remain fixed except for the k^{th} modal frequency, which is allowed to vary, that is:

$$\begin{aligned} c_k(\underline{\theta};\underline{\theta}^*) = &\text{the largest connected subset of} \\ &\{\underline{\theta} \in S(\underline{\theta}) : \omega_r(\underline{\theta}) = \omega_r(\underline{\theta}^*); r = 1,\ldots,k-1,k+1,\ldots,N_m\} \\ &\text{containing } \underline{\theta}^* \end{aligned} \tag{3.11.1}$$

Performing a one-dimensional curve minimization in the $\underline{\theta}$-space along the curve $c_k(\underline{\theta};\underline{\theta}^*)$, starting at $\underline{\theta}^*$, corresponds to a one-dimensional minimization in the $\underline{\omega}$-space along a straight line parallel to the ω_k-coordinate direction and passing through the point $\underline{\omega}(\underline{\theta}^*)$.

The proposed minimization algorithm consists of successive sweeps of the modal frequencies. Each modal sweep consists of a sequence of N_m one-dimensional minimizations in the $\underline{\theta}$-space, along curves $c_k(\underline{\theta};\underline{\theta}^{s,k-1}), k = 1\ldots,N_m$. The superscript s denotes the number of modal sweeps already performed. Each one-dimensional minimization along the curve $c_k(\underline{\theta};\underline{\theta}^{s,k-1})$ starts at the point $\underline{\theta}^{s,k-1}$, which is the point where the minimum was attained during the previous one-dimensional minimization along the curve $c_{k-1}(\underline{\theta};\underline{\theta}^{s,k-2})$. The point $\underline{\theta}^{s,N_m}$ corresponding to the minimum of J during the last one-dimensional minimization of the $(s+1)^{th}$ sweep, that is, when minimizing along $c_{N_m}(\underline{\theta};\underline{\theta}^{s,N_m-1})$, serves as a starting point for the next sweep, that is:

$$c_1(\underline{\theta};\underline{\theta}^{s+1,0}) = c_1(\underline{\theta};\underline{\theta}^{s,N_m}) \tag{3.11.2}$$

According to this general description, the algorithm works as follows. Let $\underline{\theta}^{0,0}$ denote the starting point of the minimization algorithm. The first modal sweep starts with a one-dimensional minimization of $J(\underline{\theta})$, performed along the

curve $c_1(\underline{\theta};\underline{\theta}^{0,0})$, and starting at $\underline{\theta}^{0,0}$. Let $\underline{\theta}^{0,1}$ denote the point of $c_1(\underline{\theta};\underline{\theta}^{0,0})$ at which a local minimum is attained. This point serves as a starting point for the second one-dimensional minimization of $J(\underline{\theta})$, performed along the curve $c_2(\underline{\theta};\underline{\theta}^{0,1})$, and starting at $\underline{\theta}^{0,1}$. The minimum of this second one-dimensional minimization is denoted by $\underline{\theta}^{0,2}$, and serves as a starting point for the one-dimensional minimization along the curve $c_3(\underline{\theta};\underline{\theta}^{0,2})$. This procedure is repeated until the last minimization of the first sweep along the curve $c_{N_m}(\underline{\theta};\underline{\theta}^{0,N_m-1})$ is performed, with a minimum attained at a point $\underline{\theta}^{0,N_m}$. This completes the first modal sweep. The last point $\underline{\theta}^{0,N_m}$ serves as a starting point for the first one-dimensional minimization along the curve $c_1(\underline{\theta};\underline{\theta}^{1,0})$ of the second modal sweep, that is, $\underline{\theta}^{1,0} = \underline{\theta}^{0,N_m}$. The second modal sweep is performed by applying N_m successive one-dimensional curve minimizations in a similar manner as was done during the first modal sweep. Modal sweeps are continued similarly until the function $J(\underline{\theta})$ is unable to decrease during a modal sweep more than a prescribed fractional tolerance, in which case convergence is achieved.

Figure 3.8 shows schematically the minimization path followed in the $\underline{\theta}$-space, when this proposed algorithm is employed, for the two-degree of freedom shear building example of Section 3.10.1. In this example, two modal sweeps are sufficient to reach the optimal solution $\hat{\underline{\theta}}_1 = [1.0, 1.0]^T$.

The key step of the proposed minimization algorithm is performing the one-dimensional minimizations along the curves $c_k(\underline{\theta};\underline{\theta}^{s,k-1})$. This step is described next.

3.11.2 Minimization of $J(\underline{\theta})$ Along the Curve $c_k(\underline{\theta};\underline{\theta}^{s,k-1})$

The point $\underline{\theta}^{s,k-1}$, obtained during the last performed one-dimensional curve minimization, is assumed known. If the algorithm is in its beginning and none of the one-dimensional curve minimizations have been performed, then the starting point $\underline{\theta}^{0,0}$ for the first one-dimensional minimization along $c_1(\underline{\theta};\underline{\theta}^{0,0})$

is chosen to be the most probable point in the space $S(\underline{\theta})$, based on the prior probability distribution. The task here is, starting at $\underline{\theta}^{s,k-1}$, to follow the curve $c_k(\underline{\theta};\underline{\theta}^{s,k-1})$; along which all but the k^{th} modal frequency remain constant, that is:

$$\omega_j(\underline{\theta}) = \omega_j(\underline{\theta}^{s,k-1}) \quad ; \quad j = 1,\ldots,k-1,k+1,\ldots,N_m, \tag{3.11.3}$$

The curve $c_k(\underline{\theta};\underline{\theta}^{s,k-1})$ must be followed in the direction of decreasing vaues of J until the point $\underline{\theta}^{s,k}$ is reached, where a local minimum of J is attained. In order to do so, the following steps are taken.

The curve $c_k(\underline{\theta};\underline{\theta}^{s,k-1})$ is followed through a sequence of points $\underline{\theta}^i, i = 0,1,2,\ldots$, where $\underline{\theta}^o = \underline{\theta}^{s,k-1}$. Each point $\underline{\theta}^i$ must lie on the curve c_k. This requirement is, however, relaxed to:

$$|\omega_j(\underline{\theta}^i) - \omega_j(\underline{\theta}^o)|/\omega_j(\underline{\theta}^o) \leq \epsilon \quad ; \quad j = 1,\ldots,k-1,k+1,\ldots,N_m \tag{3.11.4}$$

The fractional frequency tolerance ϵ controls how close to the curve c_k the points lie. A direction parameter γ is introduced controlling the direction in which c_k must be followed to decrease J. Initially, γ is chosen arbitrarily to $+1$, but during the one-dimensional minimization it might switch several times between its possible values of ± 1. A fractional frequency step α specifies the desired change in the value of w_k from one point $\underline{\theta}^i$ to the next point $\underline{\theta}^{i+1}$. Given the point $\underline{\theta}^i$, a point $\tilde{\underline{\theta}}^{i+1}$ is obtained through:

$$\tilde{\underline{\theta}}^{i+1} = \underline{\theta}^i + \delta\tilde{\underline{\theta}}^i \tag{3.11.5}$$

The vector $\delta\tilde{\underline{\theta}}^i$ is calculated from the following linear algebraic system:

$$\nabla\underline{\omega}^i \delta\tilde{\underline{\theta}}^i = \delta\underline{\omega}^i \tag{3.11.6}$$

where

$$\nabla\underline{\omega}^i = \nabla\underline{\omega}(\underline{\theta}^i) \tag{3.11.7}$$

with $\nabla\underline{\omega}(\underline{\theta})$ given in (3.10.2), and

$$\begin{aligned} \delta\omega_j^i &= \omega_j(\underline{\theta}^{s,k-1}) - \omega_j(\underline{\theta}^i) \quad ; \quad j = 1,\ldots,k-1,k+1,\ldots,N_m \\ \delta\omega_k^i &= \gamma\alpha\omega_k(\underline{\theta}^{s,k-1}) \end{aligned} \tag{3.11.8}$$

Equation (3.11.6) is solved using the singular value decomposition technique, since this method gives satisfactory results even when $\nabla\underline{\omega}^i$ is almost singular. To avoid large steps in the $\underline{\theta}$-space, $\delta\tilde{\underline{\theta}}^i$ is required to satisfy:

$$|\delta\tilde{\underline{\theta}}^i| \leq d \tag{3.11.9}$$

where d is the selected maximum step size. If the vector $\delta\tilde{\underline{\theta}}^i$ obtained from solving (3.11.6) does not satisfy the constraint (3.11.9), then it is scaled appropriately so that $\delta\tilde{\underline{\theta}}^i = d$. After $\delta\tilde{\underline{\theta}}^i$ is calculated, and if $i > 0$, that is, if at least one point has been found along c_k with corresponding J value smaller than that of $J(\underline{\theta}^o)$, the following condition is checked:

$$(\delta\tilde{\underline{\theta}}^i)^T\delta\tilde{\underline{\theta}}^{i-1} > 0 \tag{3.11.10}$$

This constraint helps avoid an undesired change in the direction in which c_k is followed. Such an undesired change might occur when c_k is followed in an established direction, in which J is decreasing, and when the value of ω_k passes through an extremum. If (3.11.10) is not satisfied, then $\delta\tilde{\underline{\theta}}^i$ is set equal to $-\delta\tilde{\underline{\theta}}^i$ and the sign of the direction parameter γ is changed. After $\delta\tilde{\underline{\theta}}^i$ satisfying both constraints (3.11.9) and (3.11.10) has been established, $\tilde{\underline{\theta}}^{i+1}$ is calculated through (3.11.5). Next, it is checked if $\tilde{\underline{\theta}}^{i+1}$ satisfies the constraints imposed by (3.11.4), that is:

$$|\omega_j(\tilde{\underline{\theta}}^{i+1}) - \omega_j(\underline{\theta}^o)|/\omega_j(\underline{\theta}^o) \leq \epsilon \quad ; \quad j = 1,\ldots,k-1,k+1,\ldots,N_m \tag{3.11.11}$$

If (3.11.11) is satisfed, then $\underline{\theta}^{i+1} = \tilde{\underline{\theta}}^{i+1}$. If (3.11.11) is not satisfied, which means that $\tilde{\underline{\theta}}^{i+1}$ is not close enough to the curve c_k, then $\tilde{\underline{\theta}}^{i+1}$ is adjusted properly through:

$$\underline{\theta}^* = \tilde{\underline{\theta}}^{i+1} \quad , \quad \tilde{\underline{\theta}}^{i+1} = \underline{\theta}^* + \delta\underline{\theta}^* \tag{3.11.12}$$

where $\delta\underline{\theta}^*$ is obtained by solving the following linear system:

$$\left(\left.\frac{\partial\omega_j(\underline{\theta})}{\partial\underline{\theta}}\right|_{\underline{\theta}=\underline{\theta}^*}\right)^T \delta\underline{\theta}^* = \omega_j(\underline{\theta}^o) - \omega_j(\underline{\theta}^*) \quad ; \quad j = 1,\ldots,k-1,k+1,\ldots,N_m$$
$$(\underline{\theta}^* - \underline{\theta}^i)\delta\underline{\theta}^* = 0 \tag{3.11.13}$$

Steps (3.11.12) and (3.11.13) are repeated, if necessary, until the adjusted point $\tilde{\underline{\theta}}^{i+1}$ satisfies (3.11.11), in which case $\underline{\theta}^{i+1} = \tilde{\underline{\theta}}^{i+1}$, as already mentioned. Finally, $\delta\underline{\theta}^i$ is calculated by:

$$\delta\underline{\theta}^i = \underline{\theta}^{i+1} - \underline{\theta}^i \tag{3.11.14}$$

After the point $\underline{\theta}^{i+1}$ has been determined, its corresponding J value is calculated and it is checked if:

$$J(\underline{\theta}^{i+1}) < J(\underline{\theta}^i) \tag{3.11.15}$$

If (3.11.15) is satisfied, then the curve c_k continues to be followed in the same direction, using the same steps to determine the next point $\underline{\theta}^{i+2}$ as those followed earlier to determine the point $\underline{\theta}^{i+1}$. On the other hand, if (3.11.15) is not satisfied, then two different cases must be considered, depending on whether i is greater than or equal to zero. If $i = 0$, then the condition $J(\underline{\theta}^1) > J(\underline{\theta}^0)$ suggests to start looking in the opposite direction by changing the sign of the direction parameter γ. If the new point $\underline{\theta}^1$, obtained by following the opposite direction, still does not satisfy (3.11.15), it can be concluded that the minimum of J is attained at a point within the segment of c_k specified by the two points $\underline{\theta}^1$ lying on opposite sides of $\underline{\theta}^0$. In this case, one of the two $\underline{\theta}^1$ points is renamed to $\underline{\theta}^{-1}$ and the minimization algorithm is restarted at the same $\underline{\theta}^0$, but with a reduced fractional frequency step α, in a way similar to that discussed next, for the case where $i \neq 0$.

If $i \neq 0$ and the condition (3.11.15) is not satisfied, it can be concluded that a minimum of J is attained at a point lying within the segment of the curve c_k specified by the points $\underline{\theta}^{i-1}$ and $\underline{\theta}^{i+1}$ and containing $\underline{\theta}^i$. In this case, $\underline{\theta}^i$ is set equal to $\underline{\theta}^0$, and the one-dimensional minimization algorithm is restarted at

this new point $\underline{\theta}^0$ using a reduced fractional frequency step α, dictated by the fractional difference of $\omega_k(\underline{\theta}^i)$ and ω_k^*, where ω_k^* is the estimated value of ω_k at the point where the minimum of J is attained. The value of ω_k^* is approximated by interpolating a parabola for J through the values of ω_k corresponding to the last three points $\underline{\theta}^{i-1}, \underline{\theta}^i, \underline{\theta}^{i+1}$. However, it is recommended that:

$$\alpha < \frac{\underline{\omega}(\underline{\theta}^{i+1}) - \underline{\omega}(\underline{\theta}^{i-1})}{2(\underline{\omega}(\underline{\theta}^{i+1}) + \underline{\omega}(\underline{\theta}^{i-1}))} \tag{3.11.16}$$

Convergence of this one-dimensional minimization is achieved when starting at the current point $\underline{\theta}^0$, and, using a fractional frequency step α smaller than the fractional frequency tolerance ϵ, the value of J is unable to decrease when following the curve c_k in either direction. In this case, this current $\underline{\theta}^o$ corresponds to the sought point $\underline{\theta}^{s,k}$, from which a new one-dimensional minimization will start along the new curve $c_{k+1}(\underline{\theta}; \underline{\theta}^{s,k})$.

3.11.3 Some Comments Regarding the One-Dimensional Minimization Algorithm

The computational effort of the proposed one-dimensional minimization is mainly due to the following steps:

a) Solving an eigenvalue problem at each point $\underline{\theta}^i$. This step must be taken even when a straight line minimization is performed.

b) Evaluating the value of $J(\underline{\theta}^i)$. The proposed one-dimensional curve minimizations are computationally superior to straight line minimizations because of their efficiency in performing these function evaluations. The key point here is that the modal contributions to the output, corresponding to all modal frequencies except the k^{th} one, do not need to be calculated from scratch at every new point along the curve c_k, but need only to be scaled proportionally to the corresponding current effective participation factors, if zero initial conditions are assumed. This is because $q_i^{(r)}$, the r^{th} modal contribution to the response at the i^{th} degree of freedom, is then equal to the

response of a SDOF oscillator with frequency $\omega_r(\underline{\theta})$, scaled by the effective participation factor $\beta_i^{(r)}(\underline{\theta})$. The stated result becomes obvious by noticing that the value of ω_r remains constant along the curve c_k, when $r \neq k$.

c) Forming and solving the equations involving $\nabla\underline{\omega}$. This step is performed efficiently, since the elements $\frac{\partial\omega_r}{\partial\theta_i}$ can be calculated analytically through (3.9.3).

The computational efficiency when performing these one-dimensional curve minimizations, along with the fact that these curved minimizations are much more powerful than any straight line minimization performed in the $\underline{\theta}$-space, are the reasons for the superiority of the proposed minimization algorithm.

3.11.4 Minimization Algorithm when $N_\theta \neq N_m$

It was assumed, when presenting the proposed minimization algorithm for $J(\underline{\theta})$, that $N_\theta = N_m$. This assumption allowed for the intersection of the $(N_m - 1)$ hypersurfaces $\omega_r(\underline{\theta}) = \text{constant}$, $r = 1, \ldots, k-1, k+1, \ldots, N_m$ to be a one-dimensional curve c_k (along which one-dimensional minimizations can be performed as was shown). If $N_\theta \neq N_m$, then the approach taken to obtain such curves, along which one-dimensional minimizations can be performed, must be modified appropriately.

Consider first the case where $N_\theta < N_m$. In this case, only the first N_θ modal frequencies are included to define the curves $c_k, k = 1, \ldots, N_\theta$. Along each such curve, all first N_θ modal frequencies, except the k^{th} one, are kept fixed, while the k^{th} modal frequency, as well as the last $(N_m - N_\theta)$ modal frequencies, are allowed to vary. Therefore, when a one-dimensional minimization along c_k is performed, the modal contributions of the k^{th} mode and of the $(N_m - N_\theta)$ last modes must be calculated from scratch at each new point.

In the case where $N_\theta > N_m$, the intersection of the $(N_m - 1)$ hypersurfaces $\omega_r(\underline{\theta}) = \text{constant}$, $r = 1, \ldots, k-1, k+1, \ldots, N_m$ is an $(N_\theta - N_m + 1)$-dimensional

surface in the space $S(\underline{\theta})$. Let $\underline{\tilde{\theta}}$ denote a vector consisting of $(N_\theta - N_m)$ elements of $\underline{\theta}$. The proposed minimization algorithm searches the space $S(\underline{\theta})$ by performing sweeps, each consisting of N_θ one-dimensional minimizations. N_m of these one-dimensional minimizations are performed along the curves c_k where the vector $\underline{\tilde{\theta}}$, as well as all N_m modal frequencies except the k^{th} one, remain constant. The remaining $(N_\theta - N_m)$ one-dimensional minimizations are performed along curves where all modal frequencies, as well as all elements of $\underline{\tilde{\theta}}$ except one, are kept fixed. During these last $(N_\theta - N_m)$ minimizations, none of the modal contributions needs to be calculated from scratch.

3.11.5 Minimization of $J(\underline{\theta}, \underline{\zeta})$

Including the parameter vector $\underline{\zeta}$ in the argument of J increases the dimension of the minimization problem by N_m. The most efficient way of performing the minimization of J in the augmented parameter space $S(\underline{\theta}) \times S(\underline{\zeta})$ is the following. While the one-dimensional curve c_k is followed, none of the modal damping ratios $\zeta_r, r = 1, \ldots, k-1, k+1, \ldots, N_m$ is allowed to vary. This way, only the k^{th} modal contribution to the observed output needs to be calculated from scratch along c_k, thus preserving the computational efficiency of the algorithm performing the one-dimensional curve minimizations. The minimization of J with respect to ζ_k as the curve c_k is followed is not performed at every point of the curve. It is only performed when the tracking of the curve in an established direction is finally interrupted after a point $\underline{\theta}^i$, where $J(\underline{\theta}^{i-1}) > J(\underline{\theta}^i) < J(\underline{\theta}^{i+1})$. In this case, before the fractional frequency step α is reduced, a one-dimensional minimization with respect to ζ_k is performed at $\underline{\theta} = \underline{\theta}^i$, keeping the remaining modal damping ratios fixed at their current values. This is done hoping that after optimizing ζ_k, the curve c_k can be followed further keeping the same fractional frequency step α; it is only if this is not possible that the step α is reduced according to the discussion in Section 3.11.3.

The proposed algorithm was tested using simulated data for both cases, where the damping $\underline{\zeta}$ is kept fixed and where it is not, and it was found to always converge to the known minimum. Table 3.1 compares the results obtained using the proposed method to the ones obtained using existing methods, when simulated data corresponding to the response measured at the roof of a four-story uniform shear building excited by the 1940 El Centro NS record are utilized. The damping ratios $\underline{\zeta}_r, r = 1, \ldots, 4$ are assumed fixed at 5% in this example. It can be seen that the proposed algorithm reaches the optimal point $\hat{\underline{\theta}} = [1, 1, 1, 1]^T$, while both Powell and Fletcher-Reeves algorithms were unable to do so.

3.12 Identifiability of the Optimal Parameters $\hat{\underline{\theta}}$ and $\hat{\underline{\zeta}}$

It has been shown in the earlier sections of this chapter that the system identifiability of the optimal parameters from the available data $\mathcal{D}_N$ is a very important issue that needs to be resolved. In Section 3.6, it was shown that a first step for resolving this problem is to resolve the model identifiablity of the optimal parameters under the given input, that is, to find all models in the class $\mathcal{M}$ that have identical output at the observed degrees of freedom under the given input. Finding all the corresponding "output-equivalent" optimal parameters is the subject of this section.

It was shown in Section 3.8 that the problem of the model identifiability of the optimal parameters is reduced to finding if the parameter vector $\underline{\theta}$ is M-identifiable at $\hat{\underline{\theta}}$ under the given input $\hat{Z}_{1,N}$, since the parameter vector $\underline{\zeta}$ is known to be globally identifiable at $\hat{\underline{\zeta}}$ under this input. In the case where the parameters $\underline{\theta}$ are only locally M-identifiable at $\hat{\underline{\theta}}$ under the input $\hat{Z}_{1,N}$, the whole set of optimal parameters $S_{opt}(\hat{\underline{\theta}}; \hat{Z}_{1,N}) = \{\hat{\underline{\theta}}^{(k)} : k = 1, 2, \ldots, K\}$ needs to be evaluated. The models $M(\hat{\underline{\theta}}^{(k)}, \hat{\underline{\zeta}}); k = 1, 2, \ldots, K$ are then all "output-equivalent" models in the class $\mathcal{M}$ under the given input. Here it is assumed that a closed, bounded region of $S(\underline{\theta})$ is selected as the subset consisting of

possible values of $\underline{\theta}$, so there is only a finite number of optimal solutions.

Resolving the model identifiability of the optimal parameters $\hat{\underline{\theta}}$ is a problem that had not been fully solved. Udwadia [1978a] has shown that the stiffness distribution of an N_d-degree of freedom planar shear building model with known mass distribution and modal damping ratios, cannot be identified uniquely from the data, if that data consist of the input at the base and the model response at a degree of freedom other than the first floor. If the base input and the response at the roof only are known, an upper bound of $(N_d!)$ is given for the number of possible stiffness distribution solutions. However, addressing the problem of finding the exact number, as well as the values of these "output-equivalent" stiffness distribution solutions, seemed hopeless, since it required an exhaustive search of the stiffness parameter space, which for high dimensions becomes computationally prohibitive.

A new methodology has been developed to make such an exhaustive search of the high-dimensional space $S(\underline{\theta})$, for finding all elements in $S_{opt}(\hat{\underline{\theta}}; \hat{Z}_{1,N})$, feasible.

3.12.1 Proposed Methodology for Finding $S_{opt}(\hat{\underline{\theta}}; \hat{Z}_{1,N})$

All models $M(\underline{\hat{\theta}}^{(k)}, \underline{\hat{\zeta}})$; $k = 1, 2, \ldots, K$, where $\underline{\hat{\theta}}^{(k)} \in S_{opt}(\hat{\underline{\theta}}; \hat{Z}_{1,N})$ are by definition "output equivalent." Therefore, as discussed in Section 3.7, they all have identical corresponding modal frequenices, damping ratios, and effective modal participation factors for the set $\mathcal{L}^o$ of observed degrees of freedom. Let $\{\hat{\omega}_r, \hat{\zeta}_r, \hat{\beta}_i^{(r)}, r = 1, \ldots, N_m, i \in \mathcal{L}^o\}$ denote these common optimal modal parameters. It is obvious that every $\underline{\hat{\theta}}^{(k)} \in S_{opt}(\hat{\underline{\theta}}; \hat{Z}_{1,N}), k \in \{k, \ldots, K\}$ satisfies:

$$\omega_r(\underline{\hat{\theta}}^{(k)}) = \hat{\omega}_r \quad ; \quad r = 1, \ldots, N_m \quad , \quad k \in \{k, \ldots, K\} \tag{3.12.1}$$

$$\beta_i^{(r)}(\underline{\hat{\theta}}^{(k)}) = \hat{\beta}_i^{(r)} \quad ; \quad r = 1, \ldots, N_m \quad , \quad i \in \mathcal{L}^o \quad , \quad k \in \{k, \ldots, K\} \tag{3.12.2}$$

Let $\Theta_{\hat{\Omega}}$ denote the set of all parameters $\underline{\tilde{\theta}}^{(k)} \in S(\underline{\theta})$ with corresponding modal

frequencies $\hat{\omega}_r, r = 1, \ldots, N_m$, that is:

$$\Theta_{\hat{\Omega}} = \{\underline{\tilde{\theta}} \in S(\underline{\theta}) : \omega_r(\underline{\tilde{\theta}}) = \hat{\omega}_r; r = 1, \ldots, N_m\} \tag{3.12.3}$$

It is obvious from the definition of $\Theta_{\hat{\Omega}}$ that it is a superset of $S_{opt}(\underline{\hat{\theta}}, \hat{Z}_{1,N})$:

$$S_{opt}(\underline{\hat{\theta}}, \hat{Z}_{1,N}) \subseteq \Theta_{\hat{\Omega}} \tag{3.12.4}$$

The methodology for finding the set $S_{opt}(\underline{\hat{\theta}}; \hat{Z}_{1,N})$ consists of two steps. First, the parameter space $S(\underline{\theta})$ is searched methodically, using a new proposed algorithm, to find all elements of $\Theta_{\hat{\Omega}}$. After $\Theta_{\hat{\Omega}}$ has been found, the second step is taken, consisting of an elimination process, to determine which elements of $\Theta_{\hat{\Omega}}$ satisfy (3.12.2), belonging, therefore, in the desired set $S_{opt}(\underline{\hat{\theta}}, \hat{Z}_{1,N})$.

3.12.2 Proposed Algorithm for Finding $\Theta_{\hat{\Omega}}$

Utilizing the minimization algorithm proposed earlier, an optimal parameter $\underline{\hat{\theta}} = \underline{\tilde{\theta}}^{(1)}$ is obtained with corresponding modal frequencies $\underline{\hat{\omega}} = \underline{\omega}(\underline{\hat{\theta}})$. The goal of this section is to present an algorithm that searches the parameter space $S(\underline{\theta})$ to find the whole set $\Theta_{\hat{\Omega}}$ of all "modal frequency equivalent" parameters $\underline{\tilde{\theta}}^{(i)} \in S(\underline{\theta})$, that is, $\Theta_{\hat{\Omega}} = \{\underline{\tilde{\theta}}^{(i)} \in S(\underline{\theta}) : \omega_r(\underline{\tilde{\theta}}^{(i)}) = \hat{\omega}_r \; ; \; r = 1, 2, \ldots, N_m, i = 1, 2, \ldots, K_{\hat{\Omega}}\}$, where $K_{\hat{\Omega}} \geq K$.

Assuming that $N_\theta = N_m$, an approach similar to the one used in the proposed minimization algorithm for $J(\underline{\theta})$ is followed. The basic idea is to follow the different curves $c_k(\underline{\theta}; \underline{\hat{\theta}})$, $k = 1, 2, \ldots, N_m$, and monitor when the value of the freed modal frequency ω_k becomes equal to $\hat{\omega}_k$. Every point $\underline{\theta}^* \in c_k(\underline{\theta}; \underline{\hat{\theta}})$, satisfying $\omega_k(\underline{\theta}^*) = \hat{\omega}_k$, belongs in $\Theta_{\hat{\Omega}}$, since it also satisfies $\omega_r(\underline{\theta}^*) = \omega_r(\underline{\theta}) = \hat{\omega}_r, r \neq k$, the latter, by definition, being the property of all points of $c_k(\underline{\theta}; \underline{\hat{\theta}})$.

The algorithm for following the curves c_k is very similar to the one described in 3.11.2. The only differences are: (a) instead of checking when J goes through a minimum, it is checked when $(\omega_k(\underline{\theta}) - \hat{\omega}_k)$ changes sign, and (b) instead of

stopping when a desired point $\underline{\theta}^* = \underline{\tilde{\theta}}^{(i)}$ is found, the curve c_k continues to be followed, searching for another possible point $\underline{\tilde{\theta}}^{(i+1)}$, and then another, and so on.

If the curve c_k is closed, it is followed all the way around to its starting point $\underline{\hat{\theta}}$. If the curve c_k is open, it is followed in both directions, starting always from $\underline{\hat{\theta}}$, and only up to a specified distance from $\underline{\hat{\theta}}$. The reason for this is that if the curve c_k is open, its length is infinite, and, therefore, its tracking must be confined over a finite length for the algorithm to converge. This finite length is, in effect, set by the chosen closed, bounded subset of all possible parameter values.

It is important to notice that following only one of the curves $c_k(\underline{\theta}; \underline{\hat{\theta}})$ does not provide the whole set $\Theta_{\hat{\Omega}}$. The reason for this is that the set:

$$\Theta_k = \{\underline{\theta} \in S(\underline{\theta}) : \omega_r(\underline{\hat{\theta}}) = \hat{\omega}_r, r = 1, \ldots, k-1, k+1, \ldots, N_m\} \qquad (3.12.5)$$

might be a non-connected set, while the curve $c_k(\underline{\theta}; \underline{\hat{\theta}}) \subseteq \Theta_k$ is by its definition in (3.11.1), the largest connected subset of Θ_k containing $\underline{\tilde{\theta}}$. Although it is obvious from the above definitions that $\Theta_{\hat{\Omega}} \subset \Theta_k$, implying that if the whole set Θ_k is searched, the whole set $\Theta_{\hat{\Omega}}$ can be recovered, this search is not possible when $c_k(\underline{\theta}; \underline{\hat{\theta}}) \neq \Theta_k$, since the proposed algorithm is based on the tracking of the continuous curve c_k, and it has no direct way of jumping to the portions of Θ_k that are not connected to $c_k(\underline{\theta}; \underline{\hat{\theta}})$.

However, there is an indirect way of finding any other curves belonging in Θ_k different than $c_k(\underline{\theta}; \underline{\hat{\theta}})$. This is done by requiring all curves $c_k(\underline{\theta}; \underline{\tilde{\theta}}^{(i)}), k = 1, 2, \ldots, N_m$, passing through all found points $\underline{\tilde{\theta}}^{(i)} \in \Theta_{\hat{\Omega}}$, to be followed. For example, assume that a point $\underline{\tilde{\theta}}^{(i)} \in \Theta_{\hat{\Omega}}$ is found by following the curve $c_r(\underline{\theta}; \underline{\hat{\theta}})$, while at the same time it is not found when the curve $c_k(\underline{\theta}; \underline{\hat{\theta}})$ is followed. Then, the curve $c_k(\underline{\theta}; \underline{\tilde{\theta}}^{(i)})$, satisfying $c_k(\underline{\theta}; \underline{\hat{\theta}}) \cap c_k(\underline{\theta}; \underline{\tilde{\theta}}^{(i)}) = \{\emptyset\}$, is another subset of Θ_k, and must, therefore, be followed.

Notice that although the above methodology requires all curves $c_k(\underline{\theta}; \underline{\tilde{\theta}}^{(i)})$, $i = 1, 2, \ldots, K$, $k = 1, 2, \ldots, N_m$ to be followed, the total number of curves

followed is much smaller than KN_m. This is because, for all points $\tilde{\underline{\theta}}^{(i)}$ lying on a particular curve $c_k(\underline{\theta}; \tilde{\underline{\theta}}^{(j)})$, the corresponding curve $c_k(\underline{\theta}; \tilde{\underline{\theta}}^{(i)})$ is identical to $c_k(\underline{\theta}; \tilde{\underline{\theta}}^{(j)})$ and, therefore, it needs to be followed only once.

Figure 3.9 demonstrates the proposed algorithm for the two-story building example of Section 3.10.1. Starting at the point $\hat{\underline{\theta}}^{(1)} = [1.0, 1.0]^T$ and following the curves $c_1(\underline{\theta}; \hat{\underline{\theta}}^{(1)})$ and $c_2(\underline{\theta}; \hat{\underline{\theta}}^{(1)})$, the set $\Theta_{\hat{\Omega}} = \{\tilde{\underline{\theta}}^{(1)}, \tilde{\underline{\theta}}^{(2)}\}$ is found, where $\tilde{\underline{\theta}}^{(1)} = \hat{\underline{\theta}}^{(1)}$ and $\tilde{\underline{\theta}}^{(2)} = [2.0, 0.5]^T$. In order to evaluate the set $S_{opt}(\hat{\underline{\theta}}; \hat{Z}_{1,N})$, it is checked if $\tilde{\underline{\theta}}^{(2)}$ satisfies (3.12.2), that is, if it has the same effective participation factors at the observed degrees of freedom as $\tilde{\underline{\theta}}^{(1)}$. This is true in the case where the only observed degree of freedom corresponds to the roof, resulting in $S_{opt}(\hat{\underline{\theta}}; \hat{Z}_{1,N}) = \{\hat{\underline{\theta}}^{(1)}, \hat{\underline{\theta}}^{(2)}\}$, where $\hat{\underline{\theta}}^{(2)} = \tilde{\underline{\theta}}^{(2)}$. In the case where the observed degree of freedom corresponds to the first floor, the solution $\tilde{\underline{\theta}}^{(2)}$ does not satisfy (3.12.2), and, therefore, it is not included in the set $S_{opt}(\hat{\underline{\theta}}; \hat{Z}_{1,N})$, which is left with only one element $\{\hat{\underline{\theta}}^{(1)}\}$, proving that the parameter $\hat{\underline{\theta}}^{(1)}$ is, in this case, globally M-identifiable.

3.12.3 A Simplified Expression for the Weighting Coeffiient w_k

At this point, an alternative expression for the weighting coefficient w_k, weighting the optimal parameter $\hat{\underline{\theta}}^{(k)}$, is given for the case where $N_\theta = N_m$, simplifying the earlier expression given by (3.4.24) and (3.4.25). The difficulty in these earlier expressions is due to the term $|A_N^{-1}(\hat{\underline{a}}_k^o)|^{\frac{1}{2}}$, which requires large computational effort to be evaluated, while at the same time it is vulnerable to numerical errors, especially when the matrix $A_N^{-1}(\hat{\underline{a}}_k^o)$ is ill-conditioned, which is often the case in practice. The introduced simplification stems from the fact that the matrix $A_N(\hat{\underline{a}}_k^o)$, given by (3.4.19), can be rewritten as follows, if the transformed variables $\underline{b} = [\omega_1, \ldots, \omega_{N_m}, \zeta_1, \ldots, \zeta_{N_m}, \sigma^o]^T$ are employed instead

of $\underline{\tilde{a}}^o = [\theta_1, \ldots, \underline{\theta}_{N_\theta}, \zeta_1, \ldots, \zeta_{N_m}, \sigma^o]^T$:

$$A_N^{-1}(\hat{\underline{\tilde{a}}}_k^o) \simeq -\frac{\partial^2 \ln f_N^o(\hat{X}_{1,N}^o; \underline{\tilde{a}}^o, \hat{Z}_{1,N})}{\partial \underline{\tilde{a}}^o \partial \underline{\tilde{a}}^o}\Bigg|_{\underline{\tilde{a}}^o = \hat{\underline{\tilde{a}}}_k^o}$$

$$= -\left[\frac{\partial \underline{b}}{\partial \underline{\tilde{a}}^o}\Big|_{\underline{b}=\hat{\underline{b}}_k}\right]^T \left[\frac{\partial^2 \ln f_N^o(\hat{X}_{1,N}^o; \underline{b}, \hat{Z}_{1,N})}{\partial \underline{b} \partial \underline{b}}\Big|_{\underline{b}=\hat{\underline{b}}_k}\right] \left[\frac{\partial \underline{b}}{\partial \underline{\tilde{a}}^o}\Big|_{\underline{b}=\hat{\underline{b}}_k}\right] \tag{(3.12.6)}$$

where

$$\hat{\underline{b}}_k = [\underline{\omega}^T(\hat{\underline{\theta}}^{(k)}), \hat{\underline{\zeta}}^T, \hat{\sigma}^o]^T \tag{3.12.7}$$

and

$$\frac{\partial \underline{b}}{\partial \underline{\tilde{a}}^o} = \begin{bmatrix} \frac{\partial \underline{\omega}}{\partial \underline{\theta}} & 0 \\ 0 & I \end{bmatrix} \tag{3.12.8}$$

where I is an $(N_m+1)\times(N_m+1)$ identity matrix. Utilizing (3.12.6) and (3.12.8), and recognizing that $\hat{\underline{b}}_k = \hat{\underline{b}}_l$, $\forall\ k, l \in \{1, 2, \ldots, K\}$, it can be seen that:

$$\frac{|A_N^{-1}(\hat{\underline{\tilde{a}}}_k^o)|^{\frac{1}{2}}}{|A_N^{-1}(\hat{\underline{\tilde{a}}}_l^o)|^{\frac{1}{2}}} = \frac{\mathcal{J}(\hat{\underline{\theta}}^{(l)})}{\mathcal{J}(\hat{\underline{\theta}}^{(k)})} \tag{3.12.9}$$

where

$$\mathcal{J}(\hat{\underline{\theta}}^{(k)}) = |\nabla \underline{\omega}(\hat{\underline{\theta}}^{(k)})| \tag{3.12.10}$$

is the Jacobian of the transformation $\underline{\theta} \rightarrow \underline{\omega}(\underline{\theta})$ at the optimal parameter $\hat{\underline{\theta}}^{(k)}$. The elements of the matrix $\nabla \underline{\omega}(\underline{\theta}^{(k)})$ can be calculated easily utilizing the analytic expression (3.9.3). Employing (3.12.9), the resulting simplified expression for w_k is

$$w_k = \frac{w_k'}{\sum_{k=1}^K w_k'} \tag{3.12.11}$$

where

$$w_k' = \pi_{\underline{\theta}}(\hat{\underline{\theta}}^{(k)}) \mathcal{J}^{-1}(\hat{\underline{\theta}}^{(k)}) \tag{3.12.12}$$

Notice (3.12.11) is identical to (3.4.24), and (3.12.12) is a simplified version of (3.4.25), where $|A_N^{-1}(\hat{\underline{\tilde{a}}}_k^o)|^{\frac{1}{2}}$ has been replaced by $\mathcal{J}^{-1}(\hat{\underline{\theta}}^{(k)})$ and $\pi_{\underline{\tilde{a}}^o}(\hat{\underline{\tilde{a}}}_k^o)$ has been replaced by $\pi_{\underline{\theta}}(\hat{\underline{\theta}}^{(k)})$. The latter is possible because all parameters in $\underline{\tilde{a}}^o$, except

for the parameters $\underline{\theta}$, that is, the parameters $\underline{\zeta}$ and σ^o, are globally identifiable, while at the same time, the parameters $\underline{\theta}$ and the parameters $\underline{\zeta}$ and σ^o are assumed to be independently distributed. It is interesting to notice that the weighting coefficient w_k, given by the expressions (3.12.11) and (3.12.12), does not depend explicitly on the measured output. This is surprising at first, since the term $|A_N^{-1}(\hat{\underline{\alpha}}_k^o)|^{\frac{1}{2}}$ in the earlier expression (3.4.25) for w_k' clearly depended on the measured output.

3.12.4 Identifiability of $\underline{\theta}$: Some Test Results

The proposed algorithm for investigating the model identifiability of the parameters $\underline{\theta}$ was tested extensively, and some of the results obtained are presented in this section.

Table 3.2 shows the number of stiffness distribution solutions $\hat{\underline{\theta}}^{(i)}$ that are obtained for planar shear buildings with different degrees of freedom N_d, when the observed degree of freedom is the one corresponding to the roof. The mass distribution is assumed to be uniform and known. It can be seen that the number K of "output-equivalent" solutions that were found is much smaller than the upper bound of $(N_d!)$ placed by Udwadia [1978a]. For the tested cases, this number is given by $K = 2^{\mathrm{INT}(\frac{N_d}{2})}$.

Table 3.3 shows the eight "output-equivalent" solutions for a six-story ($N_d = 6$) uniform shear building, when the observed degree of freedom is the one corresponding to the roof. Figure 3.10 shows all the effective participation factors of the different modes at the different floor levels corresponding to all the different solutions $\hat{\underline{\theta}}^{(i)}, i = 1, \ldots, 8$, shown in Table 3.3. It can be seen that while all these different solutions have the exact same effective participation factors at the observed degree of freedom corresponding to the roof, their values at the lower degrees of freedom become increasingly scattered. It can be concluded that if predictions are to be made at the roof, then any of these optimal solutions is

going to give the same results, while if the response at a lower degree of freedom is to be predicted, all optimal models must be included, appropriately weighted through the coefficients w_k. The weighting factors w_k for each model are given in the last column of Table 3.3, based on (3.12.11) and (3.12.12), and under the assumption that the models are equally plausible *a priori*, so that the factors $\pi_{\underline{\theta}}(\underline{\hat{\theta}}^{(k)})$ can be omitted.

3.13 Summary and Conclusions

The problems of model updating when records of measured input and output are available, and the use of the updated model to predict the uncertainties in the structural response during a future excitation, have been discussed in this chapter.

Using a Bayesian probabilistic approach, the problem of model updating translates into calculating the posterior probability distribution of the uncertain model parameters $\underline{a}$, and the model-error parameters $\underline{\sigma}$. It has been shown that only the parameters $\underline{a}^o$ and σ^o, associated with the observed output quantities, are directly updated using the available data $\mathcal{D}_N$. The posterior pdf of these observed parameters $\underline{a}^o$ and σ^o is found to be very peaked at the values of some optimal values $(\underline{\hat{a}}^o, \hat{\sigma}^o) \in S_{opt}(\underline{\hat{a}}^o, \hat{\sigma}^o; \mathcal{D}_N)$. An asymptotic result [Beck 1990] has been extended to calculate the uncertainties in the predictive response at both the observed and the unobserved degrees of freedom. This result states that if the number of available data points is large, the uncertainties in the predictive response can be calculated by considering only the optimal models with parameters $(\underline{\hat{a}}^o, \hat{\sigma}^o)$ belonging in the set $S_{opt}(\underline{\hat{a}}^o, \hat{\sigma}^o; \mathcal{D}_N)$. If the number of the optimal parameters contained in this set is finite, then the pdf of the predictive response at the observed degrees of freedom is given by the sum of the pdf's corresponding to each of these optimal parameters, each being appropriately weighted. This result, assuming the set of optimal parameters $S_{opt}(\underline{\hat{a}}^o, \hat{\sigma}^o; \mathcal{D}_N)$ is known, is very

significant, since it simplifies the response prediction problem by replacing the required high-dimensional integrations over the domain of the observed parameters $\underline{a}^o$ and σ^o with a finite sum. The pdf of the predictive response at the unobserved degrees of freedom is given by a similar sum expression, where each of the terms in the sum, corresponding to one of the optimal observed parameters, involves integrations over the space of the "unobserved" parameters $\underline{a}^u$ and $\underline{\sigma}^u$. In this case, the simplification amounts to reducing the originally required integrations over the space of all parameters $\underline{a}$ and $\underline{\sigma}$ to integrations over the reduced space of the unobserved parameters. The implementation of these asymptotic results assumes that the set of all optimal parameters $S_{opt}(\hat{\underline{a}}^o, \hat{\sigma}^o; \mathcal{D}_N)$ has been found. It was shown that the optimal value $\hat{\sigma}^o$ is globally identifiable, reducing the problem to finding all optimal observed model parameters $\hat{\underline{a}}^o \in S_{opt}(\hat{\underline{a}}^o; \mathcal{D}_N)$.

The definitions of model and system identifiability are introduced. Resolving the system identifiability of the optimal parameters $\hat{\underline{a}}^o$ is a very difficult problem, and amounts to finding the whole set $S_{opt}(\hat{\underline{a}}^o; \mathcal{D}_N)$. Resolving the model identifiability of the optimal parameters $\hat{\underline{a}}^o$ amounts to finding if there are other models in the class, corresponding to different values of $\hat{\underline{a}}^o$, and having identical output at the observed degrees of freedom under the given input as the optimal model corresponding to $\hat{\underline{a}}^o$. It was shown that the set $S_{opt}(\hat{\underline{a}}^o; \hat{Z}_{1,N})$ of the optimal parameters $\hat{\underline{a}}^o$ corresponding to all such "output-equivalent" optimal models satisfies $S_{opt}(\hat{\underline{a}}^o; \hat{Z}_{1,N}) \subseteq S_{opt}(\hat{\underline{a}}^o; \mathcal{D}_N)$, implying that resolving the model identifiability of the optimal parameters is a first step towards resolving the system identifiability.

The optimal parameters $\hat{\underline{a}}^o$ globally minimize a positive-definite measure-of-fit function $J(\underline{a}^o)$. For the case where $\underline{a}^o = \underline{a} = [\underline{\theta}^T, \underline{\zeta}^T]^T$, a new minimization algorithm has been presented to obtain an optimal set of parameters $\hat{\underline{\theta}}$ and $\hat{\underline{\zeta}}$ by minimizing the corresponding function $J(\underline{\theta}, \underline{\zeta})$. This algorithm was developed to overcome problems of convergence that the existing algorithms were found to exhibit, and it is based on performing a series of one-dimensional curve min-

imizations. It was shown that the proposed minimization algorithm not only converges to a minimum of J, but it does so very efficiently.

The model identifiability of the optimal parameters $\hat{\underline{\theta}}$ and $\hat{\underline{\zeta}}$, obtained using the proposed minimization algorithm, was addressed. The modal damping ratios $\hat{\underline{\zeta}}$ are globally M-identifiable [Beck 1978], and, therefore, only the model identifiability of the parameters $\underline{\theta}$ remains to be resolved, that is, finding the set $S_{opt}(\hat{\underline{\theta}}, \hat{Z}_{1,N})$ of all "output-equivalent" $\underline{\theta}$-distributions. This problem has been solved here, for the first time, by presenting a new algorithm that efficiently and systematically searches the parameter space $S(\underline{\theta})$ to find all elements $\hat{\underline{\theta}} \in S_{opt}(\hat{\underline{\theta}}; \hat{Z}_{1,N})$. A simplified expression for the weighting coefficients corresponding to these optimal "output-equivalent" parameters is also derived to be used in the asymptotic expression for the pdf for the predictive response.

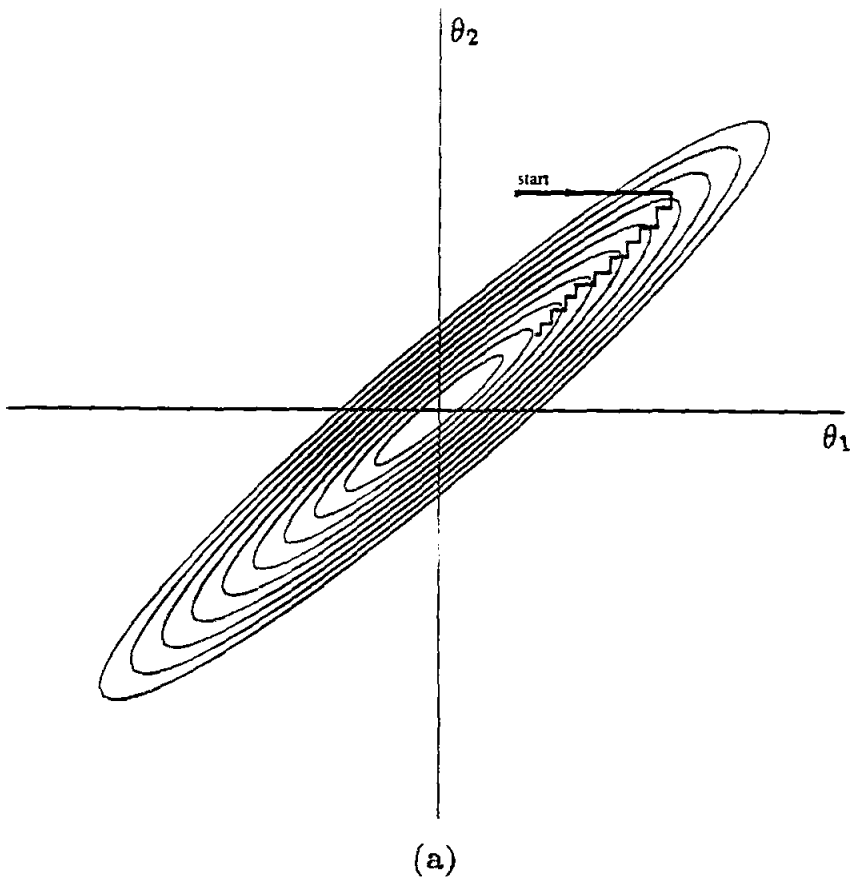

Figure 3.1 (a) Successive minimizations along coordinate directions in a long, narrow "valley." Unless the valley is optimally oriented, this method is extremely inefficient, requiring many steps to get to the minimum.

(b) Magnified view of a 1-D minimization step.

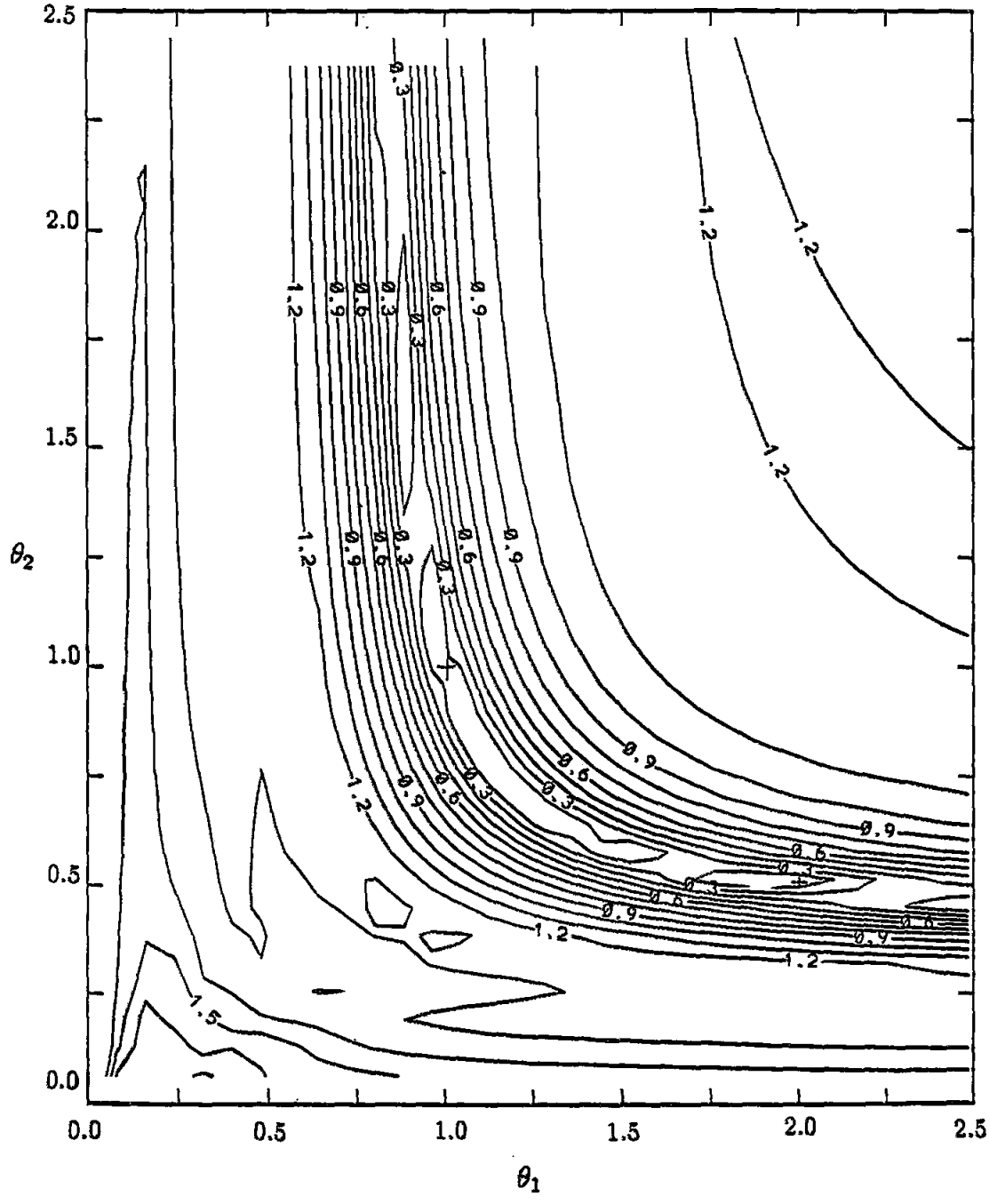

Figure 3.2 Contour map of $J(\theta_1, \theta_2)$, appropriately normalized, for the example of Section 3.10.1, where simulated data corresponding to the response at the roof of a uniform two-story planar shear structure are used. (Lack of smoothness in some of the contours is due to the finite resolution of the grid used.)

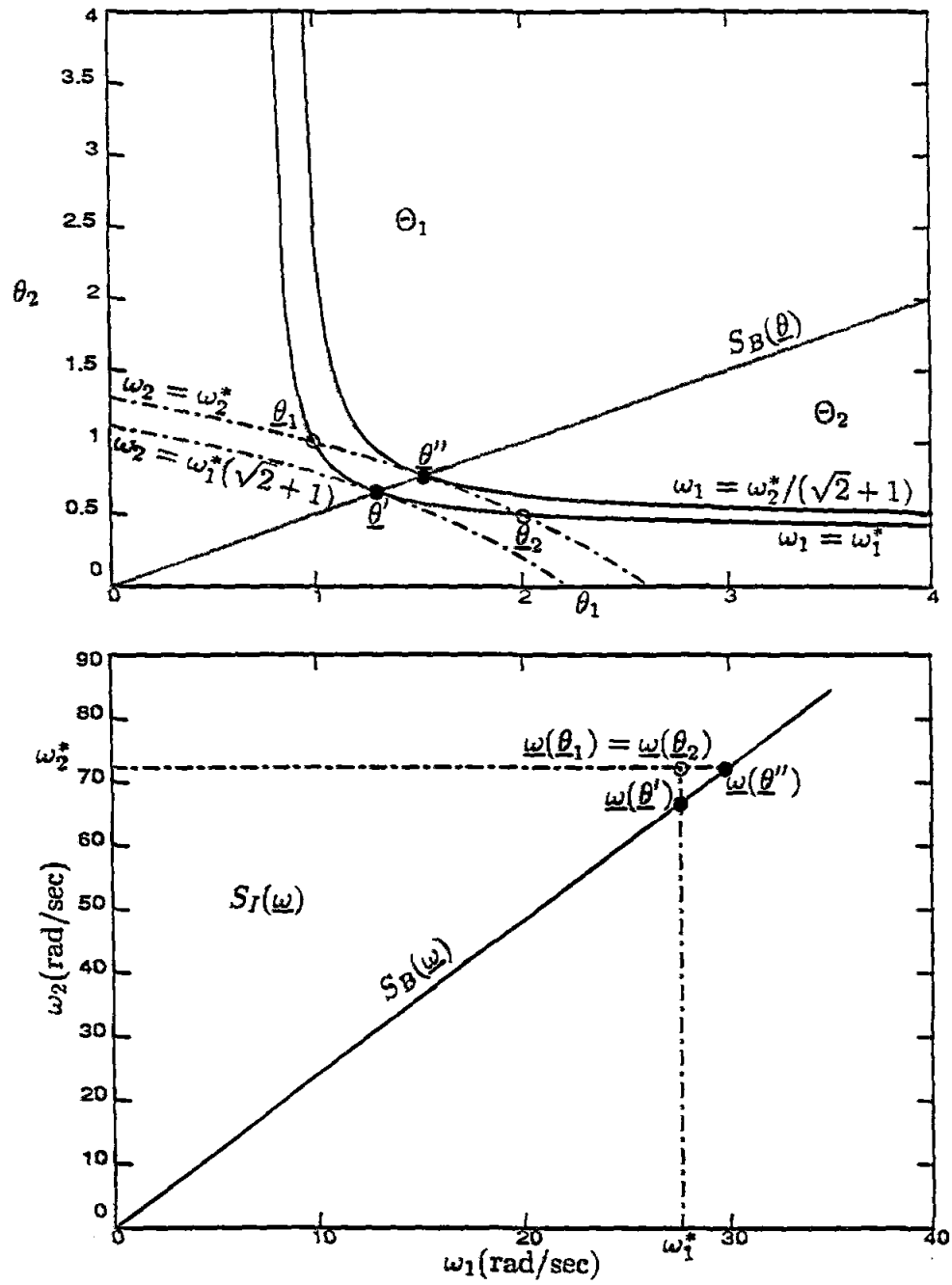

Figure 3.3 (a) Space $S(\underline{\theta})$ for the example of Section 3.10.1.

(b) Space $S(\underline{\omega})$ for the same example. Each point $\underline{\omega} \in S_I(\underline{\omega})$ is the image of two points in $S(\underline{\theta})$, one belonging in the region Θ_1 and the other in the region Θ_2, while each point in the boundary $S_B(\underline{\omega})$ is the image of only one point in $S(\underline{\theta})$, belonging on the straight line $S_B(\underline{\theta})$ separating Θ_1 and Θ_2.

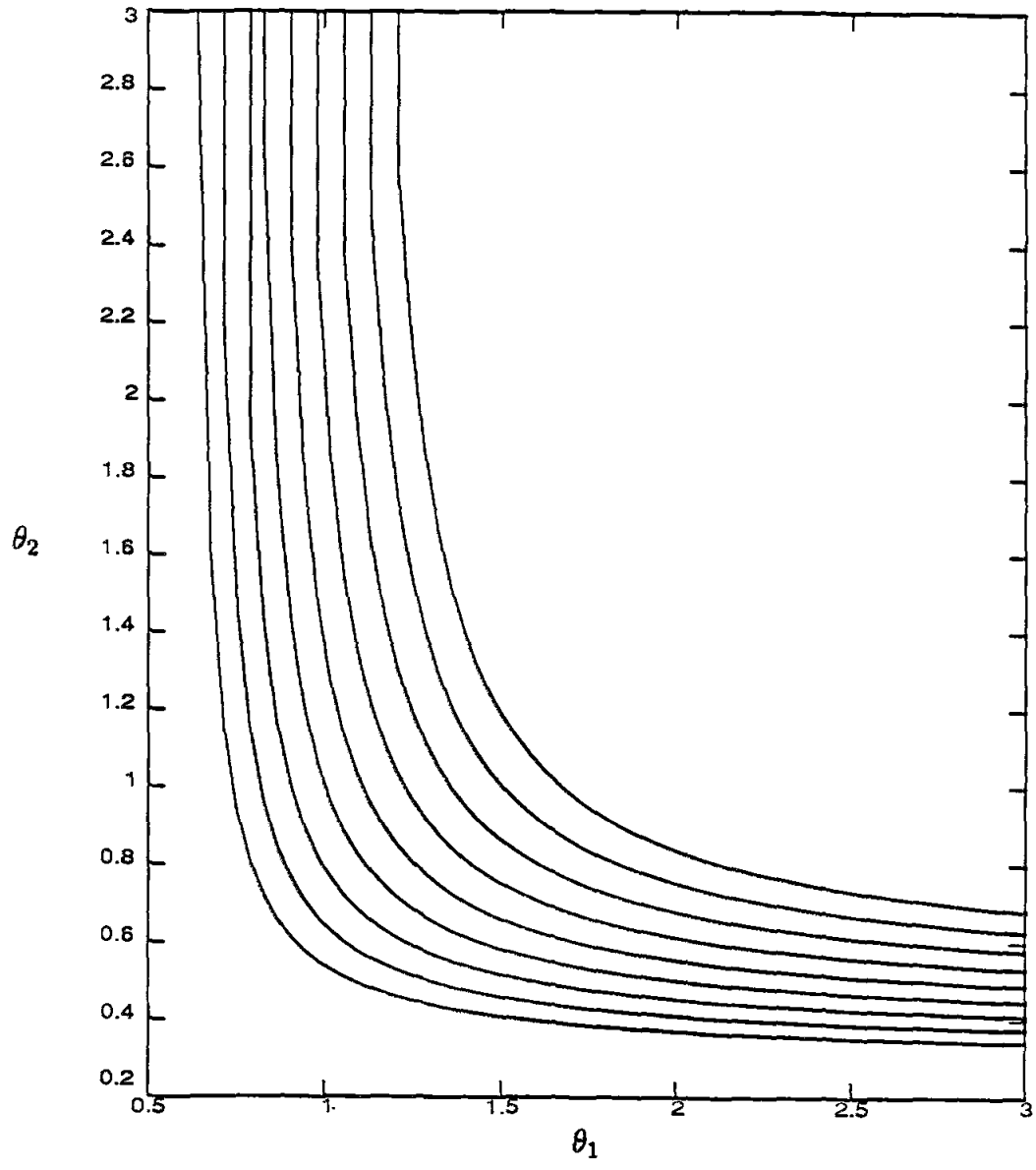

Figure 3.4 Curves in the $\underline{\theta}$-space along which ω_1 is constant, for the case of the two degree of freedom shear model of Section 3.10.1.

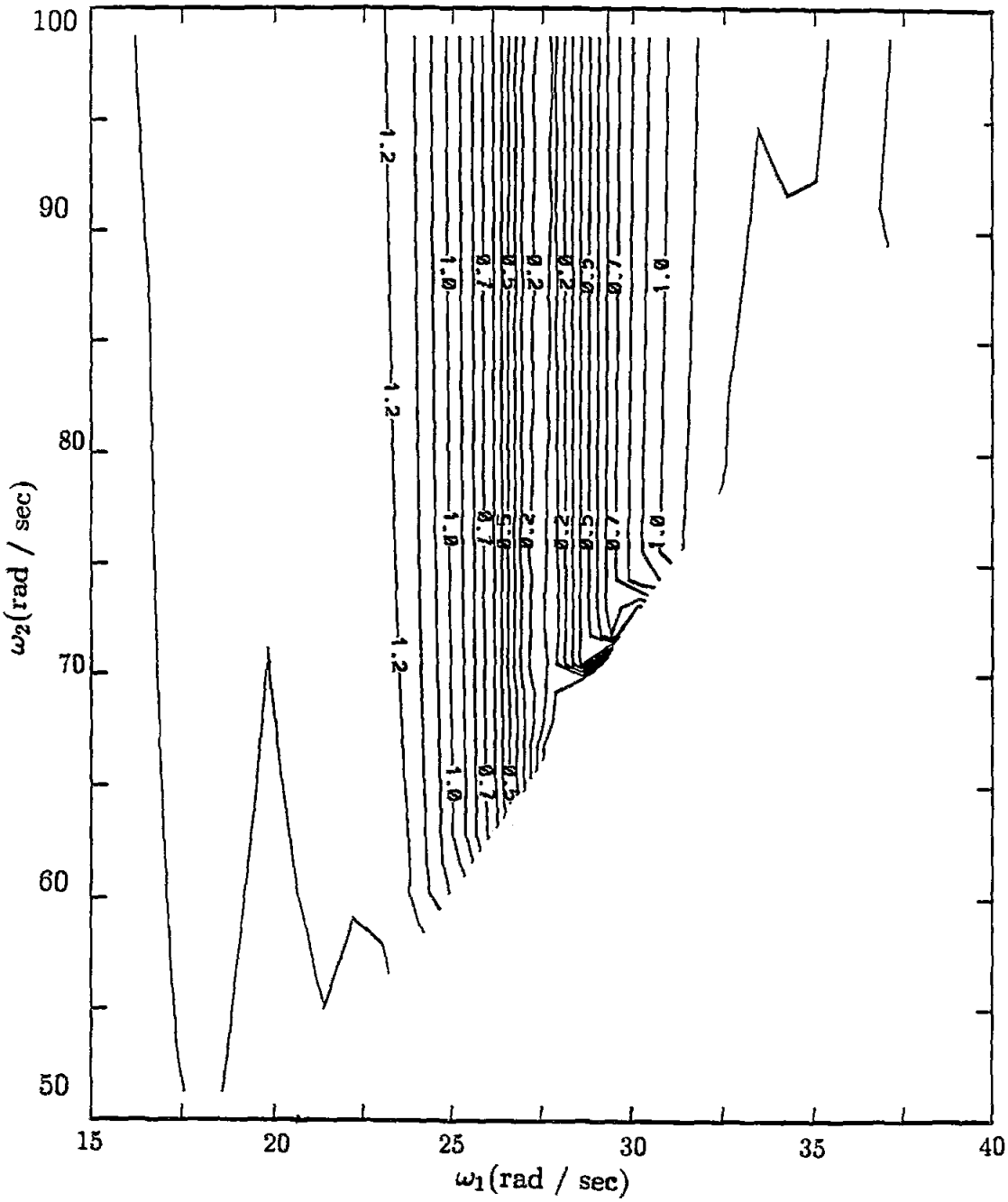

Figure 3.5(a) Contour map of $J(\underline{\omega}|\Theta_1) = J(\underline{\omega}|\Theta_2)$, appropriately normalized, for the example used in Figure 3.2.

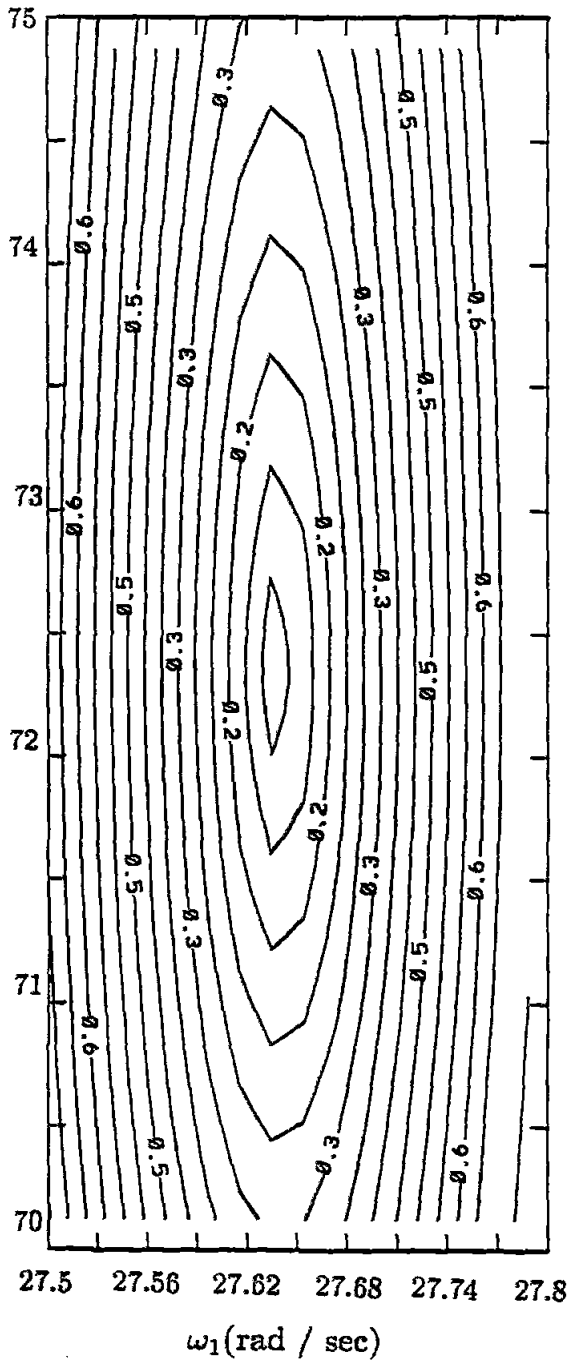

Figure 3.5(b) Magnified view of the contour map of Figure 3.5(a) in the neighborhood of $\underline{\omega}(\underline{\hat{\theta}}) = (27.64, 72.36)$ rad/sec.

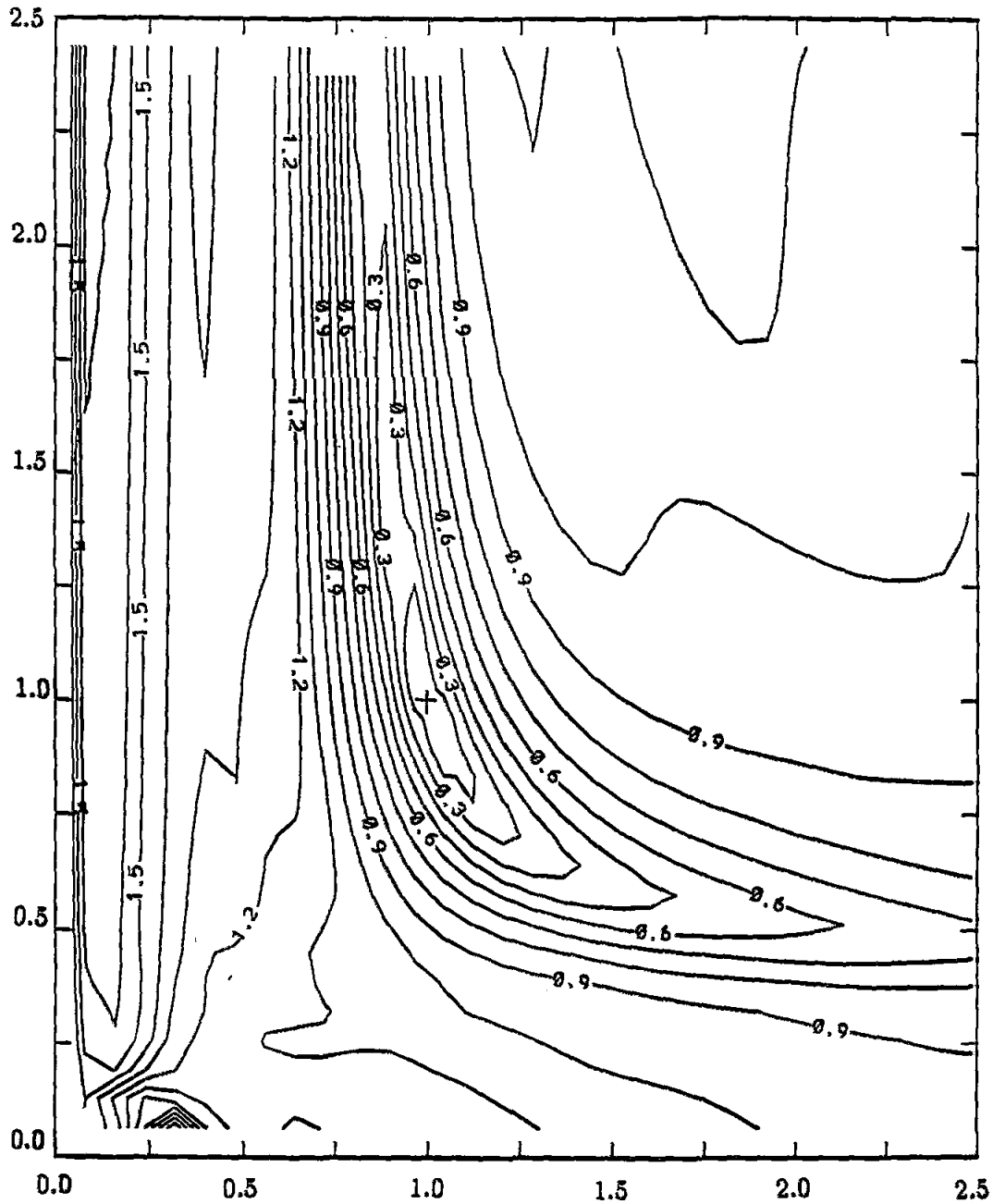

Figure 3.6 Contour map of $J(\theta_1, \theta_2)$, appropriately normalized, for the example of Section 3.10.1, where simulated data corresponding to the response at the first floor of a uniform two-story planar shear structure are used.

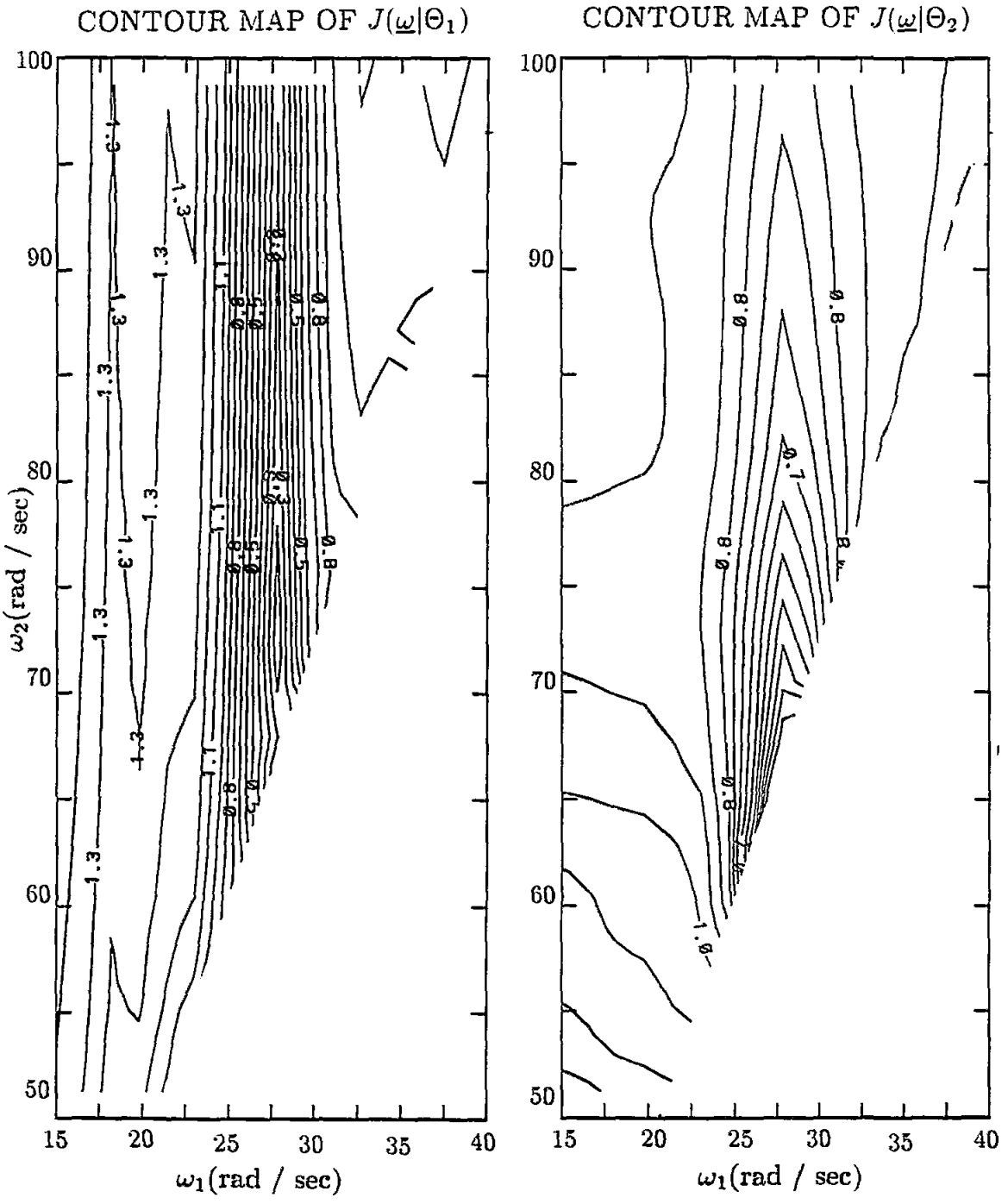

Figure 3.7(a) Contour map of $J(\underline{\omega}|\Theta_1)$ (left) and $J(\underline{\omega}|\Theta_2)$ (right) for the example used in Figure 3.6.

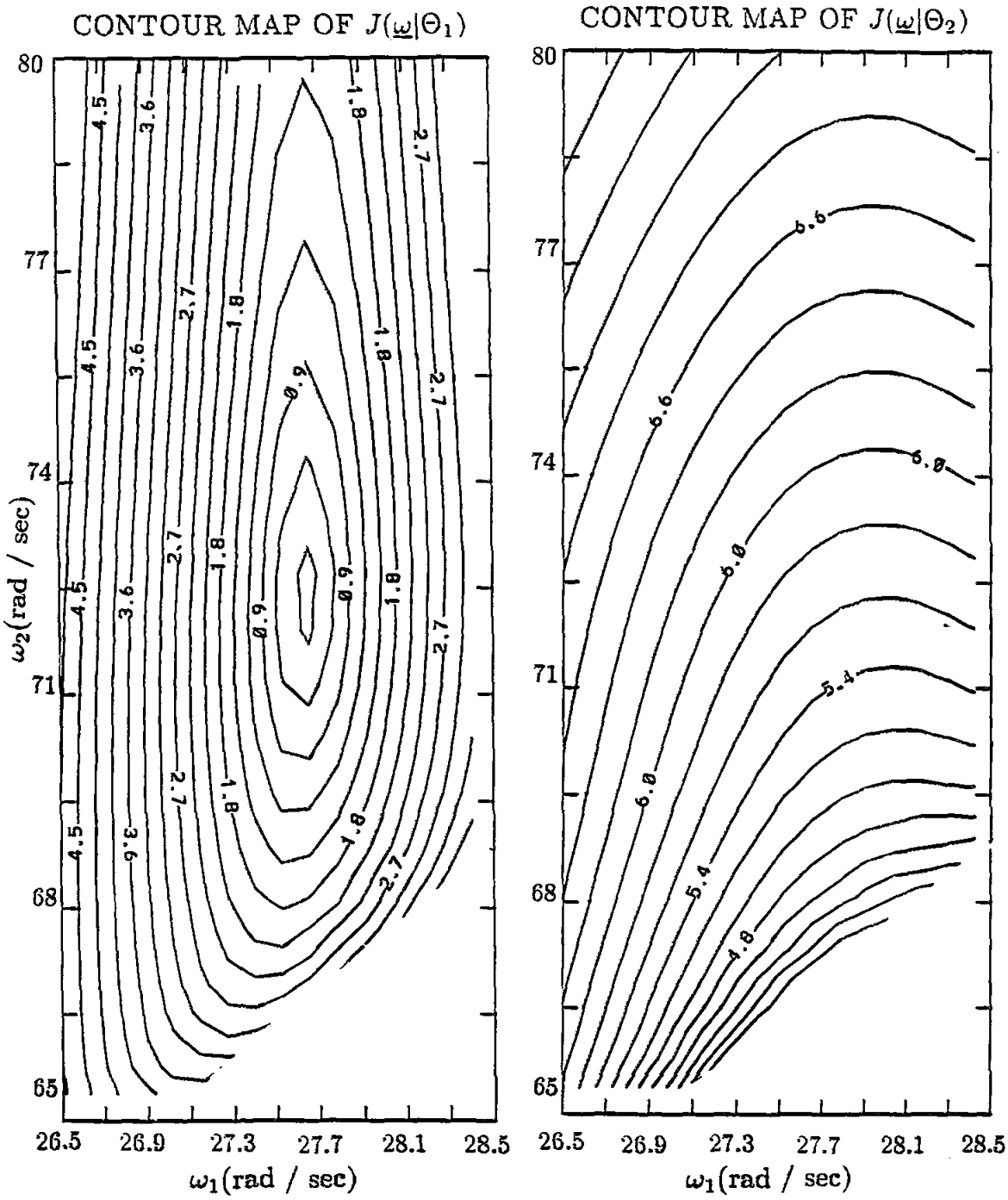

Figure 3.7(b) Magnified views of the contour map of $J(\underline{\omega}|\Theta_1)$ (left) and $J(\underline{\omega}|\Theta_2)$ (right), in the neighborhood of $\underline{\omega}(\hat{\underline{\theta}}) = (27.64, 72.36)$ rad/sec for the example used in Figure 3.6.

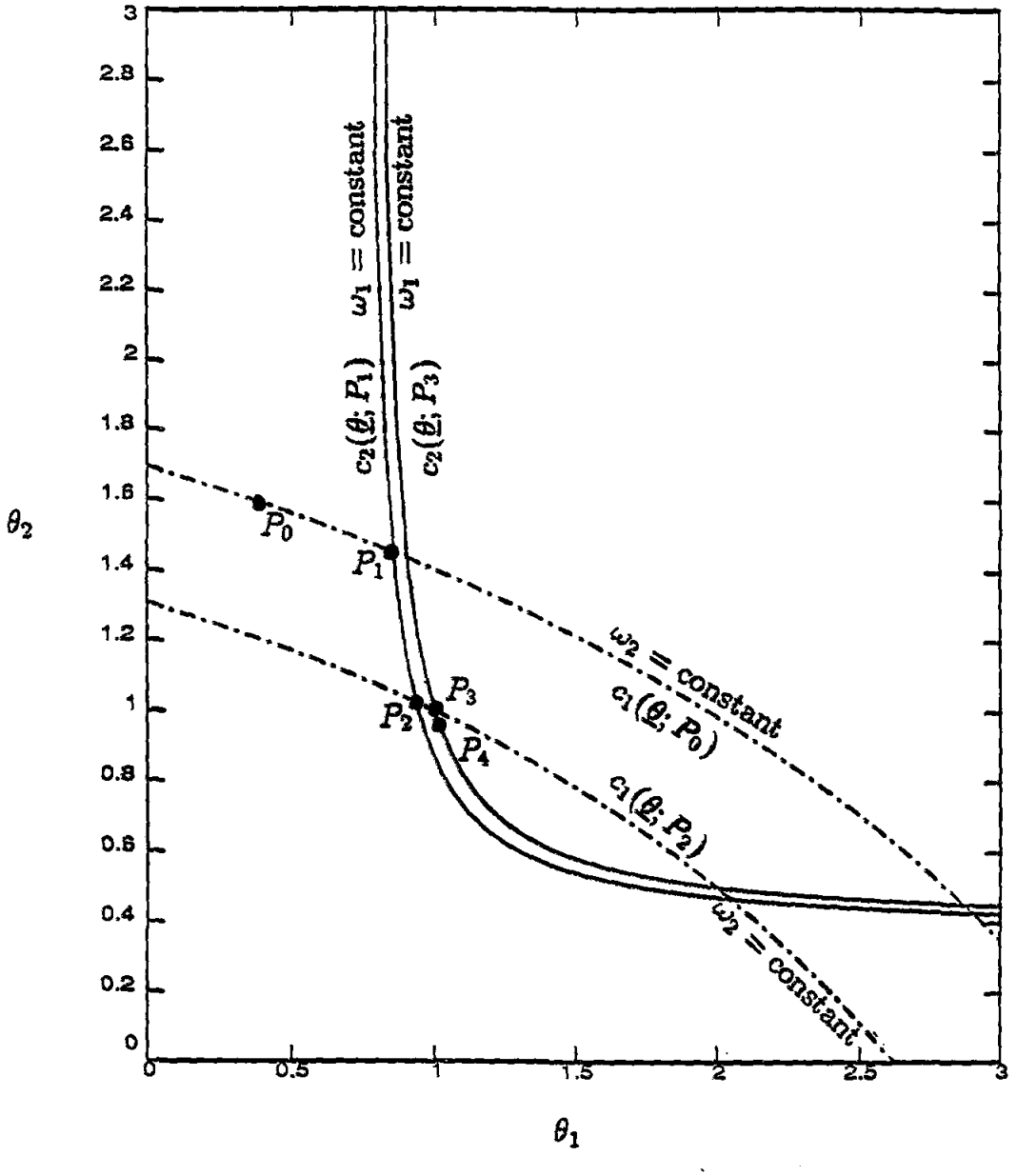

Figure 3.8 Path followed by the minimization algorithm proposed in Section 3.11 for the two-story shear building of Section 3.10.1. Two modal sweeps are sufficient to reach the optimal solution $\hat{\underline{\theta}}_1 = [1.0, 1.0]^T$. ($P_0 = \underline{\theta}^{0,0}, P_1 = \underline{\theta}^{0,1}, P_2 = \underline{\theta}^{0,2} = \underline{\theta}^{1,0}, P_3 = \underline{\theta}^{1,1}, P_4 = \underline{\theta}^{1,,2} = \hat{\underline{\theta}} = [1, 1]^T$.)

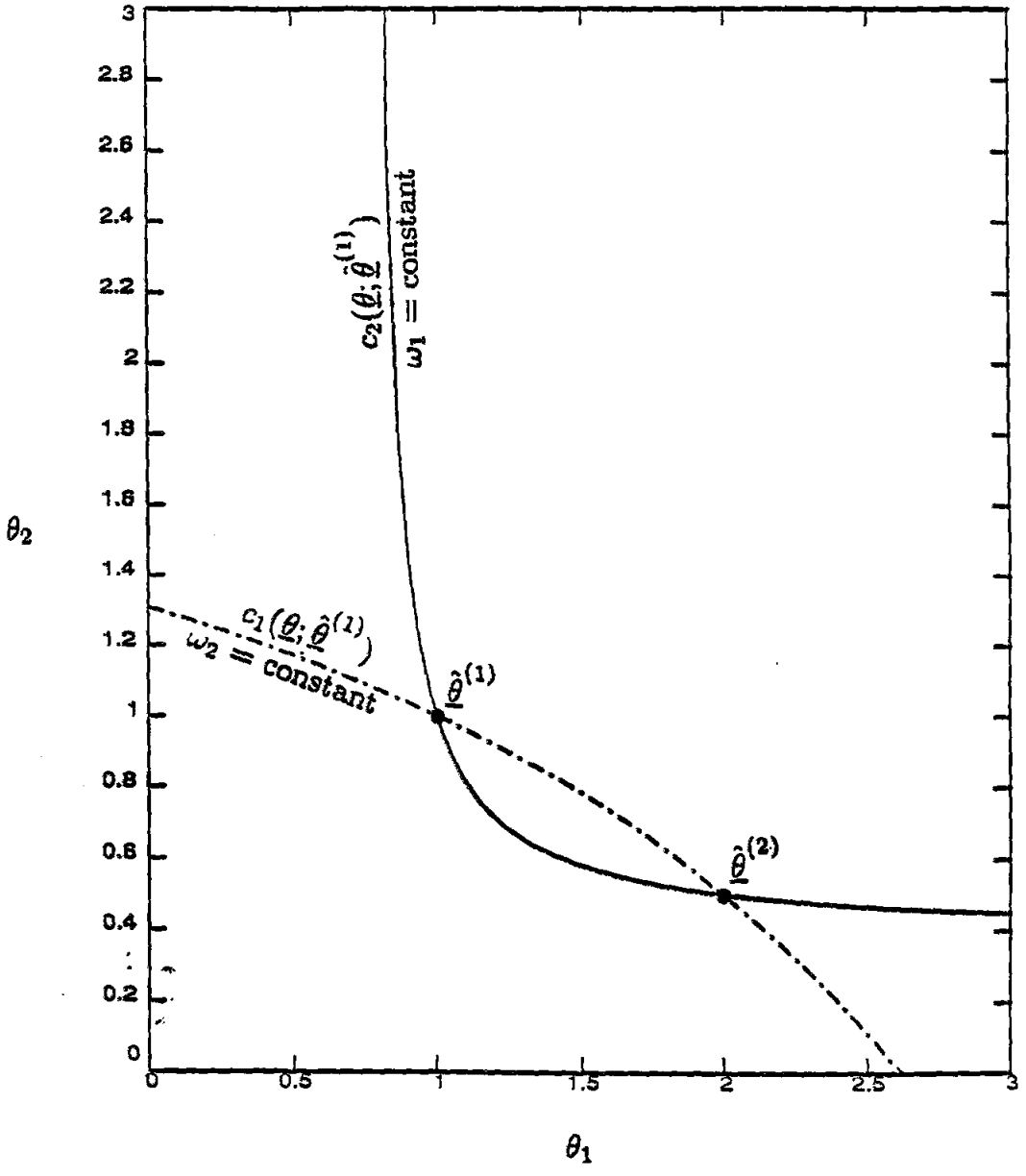

Figure 3.9 Schematic representation of the algorithm proposed in Section 3.12 to investigate the model identifiability of the stiffness parameters $\underline{\theta}$ for the two-story shear building example of Section 3.10.1.

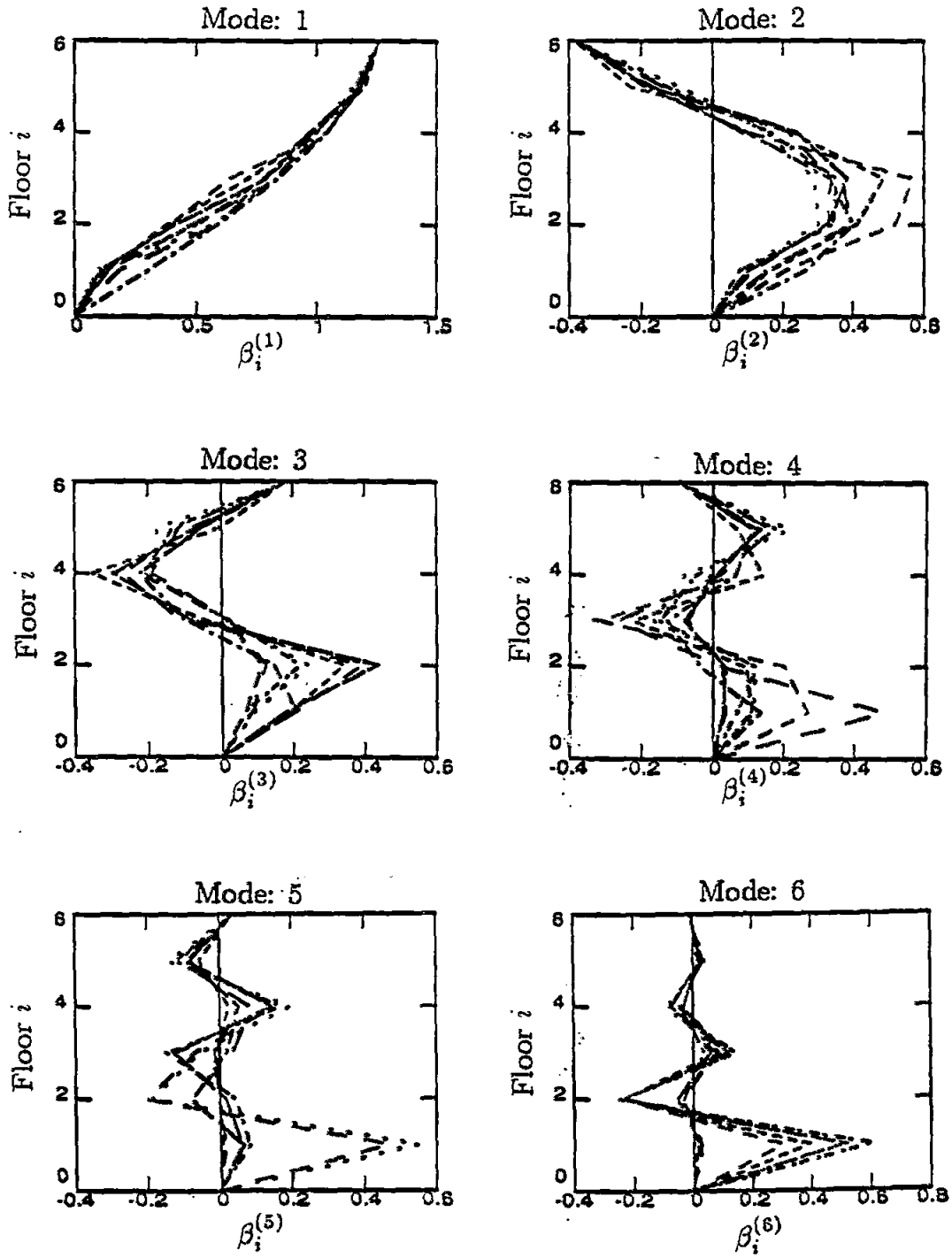

Figure 3.10 Effective participation factors $\beta_i^{(r)}$ corresponding to the six-story shear buildings with parameters $\underline{\theta}$ given by the equivalent $\hat{\underline{\theta}}$ parameters shown in Table 3.3. The values of $\beta_i^{(r)}$ are plotted against the floor number $i = 1, \ldots, 6$ and for all modes $r = 1, \ldots, 6$.

ALGORITHM	θ_1^0	θ_2^0	θ_3^0	θ_4^0	θ_1^*	θ_2^*	θ_3^*	θ_4^*	$J(\underline{\theta}^*)$
POWELL	1.2	1.2	1.2	1.2	0.85	1.20	1.17	0.95	3.94×10^{-3}
POWELL	1.2	1.0	0.8	0.6	1.11	0.96	0.86	1.06	5.96×10^{-4}
FLETCHER-REEVES	1.2	1.2	1.2	1.2	0.96	1.06	0.98	1.04	1.71×10^{-3}
FLETCHER-REEVES	1.2	1.0	0.8	0.6	1.20	0.90	0.83	1.04	1.94×10^{-3}
PROPOSED	1.2	1.2	1.2	1.2	1.00	1.00	1.00	1.00	1.76×10^{-5}
PROPOSED	1.2	1.0	0.8	0.6	1.00	1.00	1.00	1.00	1.42×10^{-5}

Table 3.1 Comparison of convergence of different minimization algorithms using simulated data corresponding to a four-story uniform shear building. $\underline{\theta}^o$ is the chosen starting point and $\underline{\theta}^*$ is the point to which each algorithm converged. The values of J have been normalized by dividing it with $\sum_{n=1}^{N} \hat{x}^o(n)^2$.

No. of Stories	No. of Equiv. Soln.
2	2
3	2
4	4
5	4
6	8
7	8
8	16

Table 3.2 Number of "output-equivalent" stiffness distributions of an N_d-story uniform planar shear building, when the only observed degree of freedom is the one corresponding to the roof.

No.	$\hat{\theta}_1$	$\hat{\theta}_2$	$\hat{\theta}_3$	$\hat{\theta}_4$	$\hat{\theta}_5$	$\hat{\theta}_6$	$w_k(\%)$
1	1.0000	1.0000	1.0000	1.0000	1.0000	1.0000	21.35
2	1.5848	0.6963	1.2875	0.7574	1.1766	0.7898	13.49
3	1.9970	0.7980	0.7095	1.3848	0.7113	0.8980	4.91
4	2.0000	1.0000	1.0000	0.5000	1.0000	1.0000	21.35
5	2.0932	1.0476	0.7240	0.7374	0.6705	1.2738	17.07
6	2.2911	0.6304	0.9321	1.1774	0.9515	0.6631	6.46
7	2.4913	0.8777	0.6514	1.1106	0.6672	0.9475	7.40
8	2.8252	0.6753	0.8826	0.9021	0.8753	0.7520	7.97

Table 3.3 "Output-equivalent" stiffness distributions $\underline{\hat{\theta}}$ for a six-story uniform planar shear building, when the only observed degree of freedom is the one corresponding to the roof. $w_k(\%)$ is the weighting factor of $\underline{\hat{\theta}}^{(k)}$, $k = 1, \ldots, 8$, calculated through (3.12.11) and (3.12.12).

Chapter 4

Conclusions

The uncertainties related to the modeling of the dynamic behavior of a structure have been studied in this dissertation. Two major categories of uncertainties are encountered in such a modelling: (a) uncertainties in the model parameters specifying a particular model in a chosen class and (b) uncertainties in the model error parameters quantifying the model error, which refers to the discrepancies between the model and real system responses. A Bayesian probablistic approach has been followed to analyze these parameter uncertainties and to account for them when investigating the resulting uncertainties in the predictive structural response. Two different cases have been addressed, depending on whether or not records of structural response are available.

In Chapter 2, the case of preliminary design has been studied, where the structure has not yet been built, or, more generally, where no records of structural response are available. In this case, the uncertainties in the structural model parameters, as well as in the model-error parameters, are estimated subjectively, based on any information available and on the engineer's past experience in dealing with similar structures. Calculating the statistics of the resulting uncertainties in the structural response due to the uncertainties in the model and the model-error parameters is a conceptually easy problem, and can be formulated mathematically as an integral over the domain of all the uncertain parameters. The difficulty of the problem lies in the evaluation of these high-dimensional integrals. which cannot be done analytically, in general. The existing numerical methods for approximating these integrals can either become computationally

prohibitive (simulations, numerical integrations), or are shown to be potentially very inaccurate ("second moment" approach). A new, efficient and accurate approximate method has been presented to overcome the difficulties of the existing methods. Most of the computational effort required by this new method depends only on the number of modes included in the model response and on the time length over which the response statistics are to be calculated, and is independent of the number of uncertain parameters involved. This is in contrast to the numerical integration method, where the computational effort grows exponentially with the dimension of the integrals to be calculated, being specified by the number of the uncertain parameters. The new method provides the engineer with a tool to go beyond checking the nominal dynamic response to specified excitations for a preliminary design by examining the resulting uncertainties in the structural response due to uncertainties in the modeling process.

In Chapter 3, the case where records of the input and the corresponding output of a structural system are available was considered. The output is assumed to be measured only at certain "observed" degrees of freedom. Using Bayes' Theorem, the information contained in the available data is extracted and used to update the initial estimates of the uncertainties of the structural model parameters and the model-error parameters. It was shown that only the "observed" portions of the uncertain parameters are updated directly from the data, and that the corresponding updated posterior probability density function of these observed parameters is very peaked at the values of some optimal parameters. The larger the number of available data, the more peaked the posterior probability distribution becomes at the values of the optimal parameters. An asymptotic result [Beck 1990] can be applied in an extended form, allowing for any integrations over the domain of the observed parameters to be replaced by a weighted sum over all optimal observed parameters, assuming their number is finite. This result is very important, since the high-dimensional integrations can be completely avoided when calculating the uncertainties in the predictive response

at the observed degrees of freedom. It also means that only integrations over the lower-dimensional space of the "unobserved" parameters is necessary when calculating the uncertainties in the predictive response at the unobserved degrees of freedom.

However, the implementation of these asymptotic results assumes that the problem of finding the set of all optimal observed parameters has been solved. The optimal observed parameters can be recovered by solving a minimization problem of a positive-definite measure-of-fit function of the observed model parameters. It was shown that the optimal observed model-error parameter depends only on the global minimum value of this function, and is therefore specified uniquely, while the optimal observed structural model parameters correspond to all the points in the observed model parameter space at which this global minimum is attained. Solving this minimization problem is extremely difficult because the observed model parameter space is high-dimensional and the function to be minimized is not convex, so that its global minimum cannot be guaranteed to be attained only at a unique point. Therefore, a minimization algorithm capable of converging to the minimum at the values of some optimal parameters is needed, along with a tool to investigate the identifiability of the calculated optimal parameters.

The existing minimization algorithms were tested and were found to spuriously indicate convergence before reaching a local minimum. The reasons for this behavior were shown, and a new minimization algorithm was proposed to overcome this convergence difficulty. The proposed algorithm, based on performing a series of minimizations along one-dimensional curves in the parameter space and not straight lines as usually done, was tested for cases where the number of uncertain parameters is equal to the number of modes included in the response, and was found to efficiently converge to the minimum.

The concepts of model and system identifiability were introduced to inves-

tigate the uniqueness of the reached optimal parameters. It was shown that resolving the model identifiability, that is, finding all optimal models with identical output at the observed degrees of freedom under the given input, is an important first step toward reaching the final goal of resolving the system identifiability. In the case of no model error and measurement noise, the problems of system and model identifiability are identical. The problem of model identifiability had been previously solved for "shear-building" mdels up to the point of finding upper bounds regarding the number of "output-equivalent" optimal parameters. An algorithm was proposed in this work to search the high-dimensional parameter space systematically and efficiently by following certain curves in the space to find the whole set of these "output-equivalent" optimal parameters. Although it has not been proven theoretically that the proposed algorithm guarantees the recovery of all "output-equivalent" optimal parameters, there is confidence that it does so in practice. The case where the number of uncertain parameters is equal to the number of modes included in the response was treated. Also, a simplified expression was derived in this case, giving the weighting coefficients of each of these optimal parameters to be used in the asymptotic expression for the pdf for the predictive response. The algorithm was tested extensively to identify the stiffness distributions of "shear-building" models having identical response at various specified degrees of freedom. It was found that the existing theoretical upper bounds for the number of optimal solutions being "output equivalent," when the response is measured only at the roof, are extremely conservative when the number of stories is large.

The work presented in Chapter 3 is the first step toward properly updating a probabilistic model for the dynamic behavior of a structural system using available data. This problem, also referred to as statistical system identification Beck [1990], is extremely important, with applications in response predictions, structural control, and "damage detection" or "health monitoring" of structures. Notice that, unlike deterministic system identification which usually produces a

single optimal model without a clear picture of the associated modeling uncertainties, the results obtained using statistical system identification quantify these uncertainties in a way which can be easily interpreted. For example, the value of the measure-of-fit function is related to the observed model-error parameter, describing how large the model error of the observed output quantities is, and, therefore it comments on the reliability of the response predictions by the model.

Since the study of statistical system identification within the Bayesian framework used here is a relatively new area of research, there is still a lot of work that needs to be devoted to this subject. In continuing the work presented in this dissertation, future research should be focused in the following directions. The proposed minimization algorithm should be tested using simulated data for the case where the number of uncertain parameters is different from the number of modes included in the response. Also, this algorithm needs to be tested extensively using real data. The algorithm that was proposed to investigate the model identifiability of the optimal stiffness parameters, as well as the derived expressions for the corresponding weighting factors, needs to be extended and tested for the case where the number of uncertain parameters is different from the number of modes included in the response. Finally, a methodology must be developed to explore the system identifiability of the optimal parameters.

Because of the difficulty of the problems encountered, the task of resolving the problem of statistical system identification is a very challenging one. The work presented in this dissertation constitutes an important step towards resolving this problem, and reinforces that the Bayesian approach is a profitable one for future work in this area. The potential rewards of resolving this problem are tremendous, due to the many practical applications.

References

Bazant, Z.P., "Response of Aging Linear Systems to Ergodic Random Input," *ASCE J. Eng. Mech.* 112(3), 322-342, 1986.

Bazant, Z.P. and Wang, T.S., "Spectral Finite Element Analysis of Random Shrinkage in Concrete," *ASCE Struct. Eng.* 110(9), 2196-2111, 1984.

Beck, J.L., "Determining Models of Structures from Earthquake Records," EERL Report No, 78-01, California Institute of Technology, 1978.

Beck, J.L., "Statistical System Identification of Structures," *Structural Safety and Reliability*, ASCE, II, 1395-1402, 1990.

Beck, J.L. and Katafygiotis, L.S., "Treating Model Uncertainties in Structural Dynamics," *Proceedings 9th World Conference on Earthquake Engineering*, 5, Tokyo-Kyoto, Japan, 1989.

Benaroya, H. and Rehak, M., "Finite Element Methods in Probabilistic Structural Analysis: A Selective Review," *Applied Mechanics Reviews*, 41(5), 201-213, 1988.

Bendiksen, O.O., "Mode Localization Phenomena in Large Space Structures," AIAA Paper 86-0903, *Proceedings of the 27th* AIAA/ASME/ASCE/AHS *Structures, Structural Dynamics, and Materials Conference*, San Antonio, TX, 1986.

Box, G.E.P., and Tiao, G.C., "Bayesian Inference in Statistical Analysis," *Addison-Wesley*, Reading, Massachusetts, 1973.

Branstetter, L. and Paez, T., "Dynamic Response Moments of Random Parametered Structures with Random Excitations," *Proceedings 3rd Conference on the Dynamic Response of Structures*, Los Angeles, ASCE, New York, 1986.

Caughey, T.K. and O'Kelly, M.E.J., "Classical Normal Modes in Damped Linear Dynamic Systems," Journal of Applied Mechanics, ASME, 32, 583-588.

1965.

Chen, P.C. and Soroka, W.W., "Impulse Response of a Dynamic System with Statistical Properties," *Journal of Sound and Vibration*, 31, 309-314, 1973.

Collins, J.D. and Thomson, W.T., "The Eigenvalue Problem or Structural Systems with Statistical Properties," *AIAA J* 7(4), 642-648, 1969.

Contreras, H., "The Stochastic Finite Element Model," *Computers and Structures,* 12, 341-348, 1980.

Cox, R.T., "The Algebra of Probable Inference," *John Hopkins Press*, Baltimore, 1961.

Ditlevsen, O., "Uncertainty Modeling," *Mc-Graw Hill*, New York, 1981.

Hall, J.F., "An FFT Algorithm for Structural Dynamics," Earthquake Engineering and Structural Dynamics, Vol. 10, 797-811, 1982.

Hisada, T. and Nakagiri, S., "Stochastic Finite Element Analysis of Uncertain Structural Systems," *4th International Conference on Finite Element Methods*, Melbourne, Australia, 1982.

Hisada, T. and Nakagiri, S., "Stochastic Finite Element Method Developed for Structural Safety and Reliability," *3rd International Conference on Structural Safety and Reliability*, Trandheim, Norway, 1981.

Hodges, C.H., "Confinement of Vibration by Structural Irregularity," *Journal of Sound and Vibration*, Vol. 82, 411-424, 1982.

Ibrahim, R., "Random Parametric Vibrations," *Research Studies Press*, London, 1983.

Jaynes, E.T., "Prior Probabilities," *IEEE Trans. Syst. Sci. & Cybernetics*, SSC-4, 227-241, 1968.

Jensen, H.A., "Dynamic Response of Structures with Uncertain Parameters," EERL Report No. 89-02, California Institute of Technology, 1989.

Jeffreys, H., "Theory of Probability," *Oxford Clarendon Press*, 3rd Ed., 1961.

Larson, H.J., "Probabilistic Models in Engineering," V1-2, *John Wiley*, 1979.

Liu, W.K., Belytschko, T., Mani, A., and Besterfield, G.A., "A Variational Formulatiuon for Probabilistic Mechanics," *Finite Element Methods for Plate and Shell Structures, Vol. 2: Formulations and Algorithms*, T. Hughes and E. Hinton, Eds., Pineridge. U.K., 1988a.

Liu, W.K., Besterfield, G.H., and Belytschko, T., "Variational Approach to Probabilistic Finite Elements," *Journal of Engineering Mechanics*, 114(12), 2115-2133, 1988b.

Liu, W.K., Mani, and Belytschko, T., "Finite Element Methods in Probabilistic Mechanics," *Probabilistic Engineering Methods*, 2(4), 201-213, 1987.

Meirovitch, L, Baruh, H., and Oz, H., "A Comparison of Control Techniques for Large Flexible Systems," *J. Guidance Control Dyn.* 6 302-310, 1983.

Peterka, V., "Bayesian Approach to System Identification," *Trends and Progress in System Identification*, P. Eykhoff (Ed.), Permagon Press, New York, 1981.

Prasthofer, P.H., and Beadle, C.W., "Dynamic Response of Structures with Statistical Uncertainties in Their Stiffness," *Journal of Sound and Vibration*, 42(4), 477-493, 1975.

Press, W.H., Flannery, B.P., Teukolsky, W.T., Vetterling, S.A., "Numerical Recipes," Cambridge University Press, 1989.

Scheidt, J. and Purkert, W., "Random Eigenvalue Problems," Elsevier, New York, 1983.

Schiff, A.J. and Bagdanoff, J.L., "An Estimator for the Standard Deviation of a Natural Frequency - Part 1," *ASME Journal of Applied Mechanics*, 39, 535-538, 1972a.

Schiff, A.J. and Bagdanoff, J.L., "An Estimator for the Standard Deviation of a Natural Frequency - Part 2," *ASME Journal of Applied Mechanics*, 39, 539-544, 1972b.

Shinozuka, M., "Monte Carlo Solution of Structural Dynamics," *International Journal of Computers and Structures*, 2, 885-874, 1972.

Shinozuka, M., "Structural Response Variability," *Journal of Engineering Mechanics*, 113(6), 825-842, 1987.

Shinozuka, M. and Deodatis, G., "Response Variability of Stochastic Finite Element Systems," *Journal of Engineering Mechanics*, 114(3), 499-519, 1988.

Shinozuka, M. and Jan, C.M., "Digital Simulation of Random Processes and Its Aplications," *Journal of Sound and Vibration*, 25, 111-128, 1972.

Udwadia, F.E. and Shah, P.C., "Some Uniqueness Results Related to Building Structural Identification," *SIAM Journal of Applied Mathematics*, Vol. 24, No. 1, 1978a.

Udwadia, F.E., Sharma, D.K., Shah, P.C., "Uniqueness of Damping and Stiffness Distributions in the Identification of Soil and Structural Systems," *Journal of Applied Mechanics*, 45, 181-187, 1978b.

Vanmarcke, E. and Grigoriou, M., "Stochastic Finite Element Analysis of Simple Beams," *Journal of Engineering Mechanics*, 109(5), 1203-1214, 1983.

Vanmarcke, E., Shinozuka, M., Nakagiri, S., Shueller, G.I., and Grigoriou, M.,"Random Fields and Stochastic Finite Elements," *Structural Safety*, 3, 143-166, 1986.

Appendix A: Proof of Equations (2.4.8) and (2.4.9)

Let $S(\cdot)$ denote the domain of the quantity in the parenthesis. The pdf $p(\underline{x}|\mathcal{M}_P)$ of the response $\underline{x}(t)$, based on the axioms of probability logic, is expressed as:

$$p(\underline{x}|\mathcal{M}_P) = \int_{S(\underline{a})} \int_{S(\underline{\sigma})} f(\underline{x};\underline{a},\underline{\sigma})\pi_{\underline{a}}(\underline{a})\pi_{\underline{\sigma}}(\underline{\sigma})d\underline{a}d\underline{\sigma} \tag{2.4.7}$$

where $f(\underline{x};\underline{a},\underline{\sigma})$ is assumed to be given by:

$$f(\underline{x};\underline{a},\underline{\sigma}) = \frac{1}{(2\pi)^{\frac{N_R}{2}}|\Sigma(\underline{\sigma})|^{\frac{1}{2}}}\exp\left[-\frac{1}{2}[\underline{x}-\underline{q}(\underline{a})]^T\Sigma^{-1}(\underline{\sigma})[\underline{x}-\underline{q}(\underline{a})]\right]$$

The expected value $\bar{\underline{x}}$ of the response is given by:

$$\begin{aligned}
\bar{\underline{x}} \equiv E[\underline{x}|\mathcal{M}_P] &= \int_{S(\underline{x})} \underline{x}p(\underline{x}|\mathcal{M}_P)d\underline{x} \\
&= \int_{S(\underline{x})}\int_{S(\underline{a})}\int_{S(\underline{\sigma})} \underline{x}f(\underline{x};\underline{a},\underline{\sigma})\pi_{\underline{a}}(\underline{a})\pi_{\underline{\sigma}}(\underline{\sigma})d\underline{a}d\underline{\sigma}d\underline{x} \\
&= \int_{S(\underline{\sigma})}\left[\int_{S(\underline{a})}\left[\int_{S(\underline{x})} \underline{x}f(\underline{x};\underline{a},\underline{\sigma})d\underline{x}\right]\pi_{\underline{a}}(\underline{a})d\underline{a}\right]\pi_{\underline{\sigma}}(\underline{\sigma})d\underline{\sigma} \\
&= \int_{S(\underline{\sigma})}\left[\int_{S(\underline{a})} \underline{q}(\underline{a})\pi_{\underline{a}}(\underline{a})d\underline{a}\right]\pi_{\underline{\sigma}}(\underline{\sigma})d\underline{\sigma} \\
&= \int_{S(\underline{\sigma})} \pi_{\underline{\sigma}}(\underline{\sigma})d\underline{\sigma}\int_{S(\underline{a})} \underline{q}(\underline{a})\pi_{\underline{a}}(\underline{a})d\underline{a} \\
&= \int_{S(\underline{a})} \underline{q}(\underline{a})\pi_{\underline{a}}(\underline{a})d\underline{a}
\end{aligned} \tag{2.4.8}$$

since

$$\int_{S(\underline{\sigma})} \pi_{\underline{\sigma}}(\underline{\sigma})d\underline{\sigma} = 1$$

Similarly the covariance matrix of $\underline{x}$ can be expressed as follows:

$$\begin{aligned}
\text{Cov}(\underline{x}) &\equiv E\left[[\underline{x}-\bar{\underline{x}}][\underline{x}-\bar{\underline{x}}]^T|\mathcal{M}_P\right] \\
&= E[\underline{x}\underline{x}^T|\mathcal{M}_P] - \bar{\underline{x}}\bar{\underline{x}}^T
\end{aligned} \tag{.4.1}$$

and

$$
\begin{aligned}
E[\underline{x}\underline{x}^T|\mathcal{M}_P] &= \int_{S(\underline{x})} \underline{x}\underline{x}^T p(\underline{x}|\mathcal{M}_P) d\underline{x} \\
&= \int_{S(\underline{x})} \int_{S(\underline{a})} \int_{S(\underline{\sigma})} \underline{x}\underline{x}^T f(\underline{x};\underline{a},\underline{\sigma}) \pi_{\underline{a}}(\underline{a}) \pi_{\underline{\sigma}}(\underline{\sigma}) d\underline{a} d\underline{\sigma} d\underline{x} \\
&= \int_{S(\underline{\sigma})} \left[\int_{S(\underline{a})} \left[\int_{S(\underline{x})} \underline{x}\underline{x}^T f(\underline{x};\underline{a},\underline{\sigma}) d\underline{x} \right] \pi_{\underline{a}}(\underline{a}) d\underline{a} \right] \pi_{\underline{\sigma}}(\underline{\sigma}) d\underline{\sigma} \\
&= \int_{S(\underline{\sigma})} \left[\int_{S(\underline{a})} \left(\underline{q}(\underline{a})\underline{q}(\underline{a})^T + \Sigma(\underline{\sigma}) \right) \pi_{\underline{a}}(\underline{a}) d\underline{a} \right] \pi_{\underline{\sigma}}(\underline{\sigma}) d\underline{\sigma} \qquad (A.2) \\
&= \int_{S(\underline{\sigma})} \pi_{\underline{\sigma}}(\underline{\sigma}) d\underline{\sigma} \int_{S(\underline{a})} \underline{q}(\underline{a})\underline{q}(\underline{a})^T \pi_{\underline{a}}(\underline{a}) d\underline{a} \\
&\quad + \int_{S(\underline{\sigma})} \Sigma(\underline{\sigma}) \pi_{\underline{\sigma}}(\underline{\sigma}) d\underline{\sigma} \int_{S(\underline{a})} \pi_{\underline{a}}(\underline{a}) d\underline{a} \\
&= \int_{S(\underline{a})} \underline{q}(\underline{a})\underline{q}(\underline{a})^T \pi_{\underline{a}}(\underline{a}) d\underline{a} + \int_{S(\underline{\sigma})} \Sigma(\underline{\sigma}) \pi_{\underline{\sigma}}(\underline{\sigma}) d\underline{\sigma}
\end{aligned}
$$

since

$$
\int_{S(\underline{\sigma})} \pi_{\underline{\sigma}}(\underline{\sigma}) d\underline{\sigma} = 1 \quad \text{and} \quad \int_{S(\underline{a})} \pi_{\underline{a}}(\underline{a}) d\underline{a} = 1
$$

It follows directly from (A.1) and (A.2), that:

$$
\mathrm{Cov}(\underline{x}) = \int_{S(\underline{a})} \underline{q}(\underline{a})\underline{q}(\underline{a})^T \pi_{\underline{a}}(\underline{a}) d\underline{a} - \bar{\underline{x}}\bar{\underline{x}}^T + \int_{S(\underline{\sigma})} \Sigma(\underline{\sigma}) \pi_{\underline{\sigma}}(\underline{\sigma}) d\underline{\sigma} \qquad (2.4.9)
$$

Appendix B: An Analytical Expression for $\frac{\partial \omega_r}{\partial \theta_i}$.

Recall from Chapter 2:

$$K\underline{\phi}^{(r)} = \omega_r^2 M\underline{\phi}^{(r)} \quad ; \quad r = 1, \ldots, N_d \tag{2.6.13a}$$

where

$$K = K_0 + \sum_{i=1}^{N_\theta} \theta_i K_i \tag{2.6.10}$$

Assume also that the modeshapes have been normalized so that they constitute an orthonormal basis for R^{N_d} with respect to M:

$$\underline{\phi}^{(r)^T} M \underline{\phi}^{(s)} = \delta_{rs} \tag{2.6.16}$$

Differentiating (2.6.13a) with respect to θ_i, we obtain:

$$\frac{\partial K}{\partial \theta_i}\underline{\phi}^{(r)} + K\frac{\partial \underline{\phi}^{(r)}}{\partial \theta_i} = \frac{\partial \omega_r^2}{\partial \theta_i} M\underline{\phi}^{(r)} + \omega_r^2 \frac{\partial \underline{\phi}^{(r)}}{\partial \theta_i} \tag{B.1}$$

Premultiplying (B.1) with $\underline{\phi}^{(r)}$ and rearranging terms:

$$\frac{\partial \omega_r^2}{\partial \theta_i}\underline{\phi}^{(r)^T} M\underline{\phi}^{(r)} = \underline{\phi}^{(r)^T}\frac{\partial K}{\partial \theta_i}\underline{\phi}^{(r)} + \underline{\phi}^{(r)^T}[K - \omega_r^2 M]\frac{\partial \underline{\phi}^{(r)}}{\partial \theta_i} \tag{B.2}$$

Using the symmetry of K and M, and Equation (2.6.13a), we obtain:

$$\left[\underline{\phi}^{(r)^T}[K - \omega_r^2 M]\frac{\partial \underline{\phi}^{(r)}}{\partial \theta_i}\right]^T = \left(\frac{\partial \underline{\phi}^{(r)}}{\partial \theta_i}\right)^T [K - \omega_r^2 M]\underline{\phi}^{(r)} \tag{B.3}$$
$$= 0$$

Because of (B.3) and (2.6.16), Equation (B.2) implies:

$$\frac{\partial \omega_r^2}{\partial \theta_i} = \underline{\phi}^{(r)^T}\frac{\partial K}{\partial \theta_i}\underline{\phi}^{(r)} \tag{B.4}$$

or using Equation (2.6.10):

$$\frac{\partial \omega_r^2}{\partial \theta_i} = \underline{\phi}^{(r)^T} K_i \underline{\phi}^{(r)} \tag{B.5}$$

Thus, the final expression for $\frac{\partial \omega_r}{\partial \theta_i}$ is obtained:

$$\frac{\partial \omega_r}{\partial \theta_i} = \frac{1}{2\omega_r} \underline{\phi}^{(r)^T} K_i \underline{\phi}^{(r)} \tag{3.9.3}$$

Notice that the evaluation of the partial derivatives of the r^{th} modal frequency with respect to the θ_i's requires calculations involving only the corresponding r^{th} eigenvector $\underline{\phi}^{(r)}$. Also, notice that the eigenvectors in (3.9.3) are assumed to be normalized according to (2.6.16).

Appendix C: An Optimal Choice for the Parameter γ of Section 2.8.

As discussed in Section 2.8, a quadratic polynomial is sought which approximates $f(\underline{\theta})$ well over the entire range of interest of $\underline{\theta}$'s. To measure how well a function $f_1(\underline{\theta})$ approximates another function $f_2(\underline{\theta})$ over the domain of interest of the $\underline{\theta}$'s, the following measure of fit is introduced:

$$J(f_1, f_2) = J(f_2, f_1) = \int_{S(\underline{\theta})} |f_1(\underline{\theta}) - f_2(\underline{\theta})|^2 \pi_{\underline{\theta}}(\underline{\theta}) d\underline{\theta} \qquad (C.1)$$

Note that points with higher prior probability get weighted more heavily. The smaller $J(f_1, f_2)$ is, the better is the fit between $f_1(\underline{\theta})$ and $f_2(\underline{\theta})$ over the domain $S(\underline{\theta})$.

For illustrative purposes, assume the case of a single uncertain parameter θ; in this case, $N_\theta = 1$, $N_l = \frac{N_\theta^2 + 3N_\theta + 2}{2} = 3$. The quadratic approximation for $f(\theta)$ is:

$$f(\theta) \simeq c_0 + c_1\theta + c_2\theta^2 \equiv g(\theta) \qquad (C.2)$$

Equation (C.2) can be rewritten as:

$$f(\theta) \simeq \tilde{c}_0 + \tilde{c}_1(\theta - \bar{\theta}) + \tilde{c}_2(\theta - \bar{\theta})^2 \equiv \tilde{g}(\theta) \qquad (C.3)$$

The coefficients $\underline{c} = [c_0, c_1, c_2]^T$ and $\underline{\tilde{c}} = [\tilde{c}_0, \tilde{c}_1, \tilde{c}_2]^T$ are linearly dependent:

$$\underline{c} = A\underline{\tilde{c}} \qquad (C.4)$$

where

$$A = \begin{bmatrix} 1 & -\bar{\theta} & \bar{\theta}^2 \\ 0 & 1 & -2\bar{\theta} \\ 0 & 0 & 1 \end{bmatrix} \qquad (C.5)$$

The coefficients $\underline{c}$ or $\underline{\tilde{c}}$ are evaluated, according to the discussion in Section 2.8, by fitting $g(\theta)$ or $\tilde{g}(\theta)$ through $N_l = 3$ points $\left(\theta^{(i)}, f(\theta^{(i)})\right)$, $i = 1, 2, 3$. Such points are evalauted to be: $\theta^{(1)} = \bar{\theta}$, $\theta^{(2)} = \bar{\theta} - \gamma\sigma_\theta$ and $\theta^{(3)} = \bar{\theta} + \gamma\sigma_\theta$. The requirement to fit $\tilde{g}(\theta)$ through these three points leads to:

$$\tilde{c}_0 = f(\bar{\theta}) \qquad (C.6a)$$

$$\tilde{c}_0 - \gamma\sigma_\theta\tilde{c}_1 + \gamma^2\sigma_\theta^2\tilde{c}_2 = f(\bar{\theta} - \gamma\sigma_\theta) \qquad (C.6b)$$

$$\tilde{c}_0 + \gamma\sigma_\theta\tilde{c}_1 + \gamma^2\sigma_\theta^2\tilde{c}_2 = f(\bar{\theta} + \gamma\sigma_\theta) \qquad (C.6c)$$

Assume now that the optimal cubic polynomial approximating $f(\theta)$ passing through the points $(\theta^{(i)}, f(\theta^{(i)})), i = 1, 2, 3$ is:

$$f(\theta) \simeq \tilde{d}_0 + \tilde{d}_1(\theta - \bar{\theta}) + \tilde{d}_2(\theta - \bar{\theta})^2 + \tilde{d}_3(\theta - \bar{\theta})^3 \equiv \tilde{h}(\theta) \qquad (C.7)$$

where $\tilde{d}_0, \tilde{d}_1, \tilde{d}_2, \tilde{d}_3$ must satisfy:

$$\tilde{d}_0 = f(\bar{\theta}) \qquad (C.8a)$$

$$\tilde{d}_0 - \gamma\sigma_\theta\tilde{d}_1 + \gamma^2\sigma_\theta^2\tilde{d}_2 - \gamma^3\sigma_\theta^3\tilde{d}_3 = f(\bar{\theta} - \gamma\sigma_\theta) \qquad (C.8b)$$

$$\tilde{d}_0 + \gamma\sigma_\theta\tilde{d}_1 + \gamma^2\sigma_\theta^2\tilde{d}_2 + \gamma^3\sigma_\theta^3\tilde{d}_3 = f(\bar{\theta} + \gamma\sigma_\theta) \qquad (C.8c)$$

By comparing Equations (C.6a,b,c) and (C.8a,b,c), it can be seen that:

$$\tilde{c}_0 = \tilde{d}_0 \qquad (C.9a)$$

$$\tilde{c}_1 = \tilde{d}_1 + \tilde{d}_3\gamma^2\sigma_\theta^2 \qquad (C.9b)$$

$$\tilde{c}_2 = \tilde{d}_2 \qquad (C.9c)$$

By subtracting (C.7) from (C.3), and using (C.9a,b,c), we obtain:

$$\tilde{g}(\theta) - \tilde{h}(\theta) = \tilde{d}_3(\theta - \bar{\theta})\left(\gamma^2\sigma_\theta^2 - (\theta - \bar{\theta})^2\right) \qquad (C.10)$$

The measure of fit between $\tilde{g}(\theta)$ and $\tilde{h}(\theta)$ is found by substituting (C.10) into (C.1):

$$J(\tilde{g}(\theta), \tilde{h}(\theta); \gamma) = \int_0^\infty \tilde{d}_3^2(\theta - \bar{\theta})^2\left(\gamma^2\sigma_\theta^2 - (\theta - \bar{\theta})^2\right)^2 \pi_\theta(\theta)d\theta \qquad (C.11)$$

To obtain the best fit between the quadratic and the cubic approximation of $f(\theta)$, $J(\tilde{g}(\theta), \tilde{h}(\theta); \gamma)$ is minimized with respect to γ:

$$\frac{\partial J(\tilde{g}(\theta), \tilde{h}(\theta); \gamma)}{\partial\gamma} = 4\gamma\sigma_\theta^2\tilde{d}_3^2\int_0^\infty (\theta - \bar{\theta})^2\left(\gamma^2\sigma_\theta^2 - (\theta - \bar{\theta})^2\right)\pi_\theta(\theta)d\theta = 0 \qquad (C.12)$$

or equivalently:

$$\gamma^2\sigma_\theta^2 \int_0^\infty (\theta - \bar{\theta})^2 \pi_\theta(\theta) d\theta = \int_0^\infty (\theta - \bar{\theta})^4 \pi_\theta(\theta) d\theta \qquad (C.13)$$

Solving for γ, we obtain:

$$\gamma = \frac{\left[\int_0^\infty (\theta - \bar{\theta})^4 \pi_\theta(\theta) d\theta\right]^{\frac{1}{2}}}{\sigma_\theta^2} \qquad (C.14)$$

For a Gaussian distribution of θ, (C.14) implies $\gamma = \sqrt{3}$. For a Gamma distribution $\pi(\theta) = g(\theta; \mu_\theta, \nu_\theta)$, [see Equation (2.7.1)], (C.14) implies $\gamma = \sqrt{3 + \frac{6}{\nu_\theta}} = \sqrt{3 + 6\alpha_\theta^2} \simeq \sqrt{3}$ for typical values of coefficients of variations α_θ. The choice $\gamma = \sqrt{3}$ then gives the best quadratic fit to an optimal cubic fit to $f(\theta)$ going through the points $(\theta^{(i)}, f(\theta^{(i)})), i = 1, 2, 3$. The same choice of γ is used in the multivariate case involving $f(\underline{\theta})$.

Appendix D: Pdf of y = ax, where x is Gamma Distributed

Let x be a Gamma distributed uncertain parameter:

$$p(x) = g(x; \mu_x, \nu_x) \tag{D.1}$$

where $g(x; \mu_x, \nu_x)$ is given by (2.7.1). Let $y = ax$ be a transformed uncertain parameter, where $a > 0$ is a deterministic constant. The pdf $p(y)$ must satisfy:

$$p(y) = \frac{p(x)}{|\frac{dy}{dx}|} = \frac{p(x)}{a} \tag{D.2}$$

Substituting (D.1) into (D.2), we obtain:

$$\begin{aligned} p(y) &= \frac{1}{a}\frac{\mu_x^{\nu_x}}{\Gamma(\nu_x)} x^{\nu_x - 1} e^{-\mu_x x} \\ &= \frac{1}{a}\frac{\mu_x^{\nu_x}}{\Gamma(\nu_x)} \left(\frac{y}{a}\right)^{\nu_x - 1} e^{-\mu_x(\frac{y}{a})} \\ &= \frac{1}{\Gamma(\nu_x)} \left(\frac{\mu_x}{a}\right)^{\nu_x} y^{\nu_x - 1} e^{-(\frac{\mu_x}{a})y} \end{aligned} \tag{D.3}$$

Let $\nu_y = \nu_x$, and $\mu_y = \frac{\mu_x}{a}$, then Equation (D.3) can be rewritten:

$$p(y) = \frac{\mu_y^{\nu_y}}{\Gamma(\nu_y)} y^{\nu_y - 1} e^{-\mu_y y} = g(y; \mu_y, \nu_y) \tag{D.4}$$

Thus, $y = ax$ is also Gamma distributed.

Note: It is easy to show that a linear transformation $y = ax + b$, assuming x is Gamma distributed, leads to a Gamma distribution for y, only if $b = 0$ and $a > 0$; this is contrary to the case of a Gaussian distributed parameter where any of its linear transformations are also Gaussian distributed.

Appendix E: An approximation for $p(\underline{\tilde{a}}^o|\mathcal{D}_N, \mathcal{M}_P)$

Based on the supporting notes of J.L. Beck for Beck [1990], an approximation for $p(\underline{\tilde{a}}^o|\mathcal{D}_N, \mathcal{M}_P)$ is derived which is valid for both the globally and locally identifiable cases. This approximation shows that in the neighborhood $\mathcal{H}(\hat{\underline{\tilde{a}}}_k^o)$ of the optimal parameters $\hat{\underline{\tilde{a}}}_k^o = [\hat{\underline{a}}_k^{oT}, \hat{\sigma}^o(\hat{\underline{a}}_k^o)]^T$, $k = 1, \ldots, K$, this distribution coincides with a scaled multi-dimensional Gaussian distribution for $\underline{\tilde{a}}^o = [\underline{a}^{oT}, \sigma^o]^T$ with mean $\hat{\underline{\tilde{a}}}_k^o$ and covariance matrix $A_N^{-1}(\hat{\underline{\tilde{a}}}_k^o)$. In the globally identifiable case, where $K = 1$, the subscript k may be omitted in the following.

First, it will be shown that for a large number of data points N, the optimal parameters $\hat{\underline{\tilde{a}}}_k^o$ correspond to local maxima of $p(\underline{\tilde{a}}^o|\mathcal{D}_N, \mathcal{M}_P)$. By definition, the optimal parameters $\hat{\underline{\tilde{a}}}_k^o$ globally maximize $f_N^o(\hat{X}_{1,N}; \underline{\tilde{a}}^o, \hat{Z}_{1,N})$ and, therefore:

$$\left.\frac{\partial \ln f_N^o(\hat{X}_{1,N}; \underline{\tilde{a}}^o, \hat{Z}_{1,N})}{\partial \underline{\tilde{a}}^o}\right|_{\underline{\tilde{a}}^o = \hat{\underline{\tilde{a}}}_k^o} = \frac{1}{f_N^o(\hat{X}_{1,N}; \hat{\underline{\tilde{a}}}_k^o, \hat{Z}_{1,N})} \left.\frac{\partial f_N^o(\hat{X}_{1,N}; \underline{\tilde{a}}^o, \hat{Z}_{1,N})}{\partial \underline{\tilde{a}}^o}\right|_{\underline{\tilde{a}}^o = \hat{\underline{\tilde{a}}}_k^o} = \underline{0} \tag{E.1}$$

Equation (3.4.6) is rewritten:

$$\ln p(\underline{\tilde{a}}^o|\mathcal{D}_N, \mathcal{M}_P) = \ln k + \ln f_N^o(\hat{X}_{1,N}; \underline{\tilde{a}}^o, \hat{Z}_{1,N}) + \ln \pi_{\underline{\tilde{a}}^o}(\underline{\tilde{a}}^o) \tag{E.2}$$

where $\pi_{\underline{\tilde{a}}^o}(\underline{\tilde{a}}^o) = \pi_{\underline{a}^o, \sigma^o}(\underline{a}^o, \sigma^o)$. Assume that $p(\underline{\tilde{a}}^o|\mathcal{D}_N, \mathcal{M}_P)$ attains a maximum at $\underline{\tilde{a}}_k^{o^*} \in H(\hat{\underline{\tilde{a}}}_k^o)$, then:

$$\begin{aligned} \underline{0} &= \left.\frac{\partial \ln p(\underline{\tilde{a}}^o|\mathcal{D}_N, \mathcal{M}_P)}{\partial \underline{\tilde{a}}^o}\right|_{\underline{\tilde{a}}^o = \underline{\tilde{a}}_k^{o^*}} \\ &= \left.\frac{\partial \ln f_N^o(\hat{X}_{1,N}; \underline{\tilde{a}}^o, \hat{Z}_{1,N})}{\partial \underline{\tilde{a}}^o}\right|_{\underline{\tilde{a}}^o = \underline{\tilde{a}}_k^{o^*}} + \left.\frac{\partial \ln \pi_{\underline{\tilde{a}}^o}(\underline{\tilde{a}}^o)}{\partial \underline{\tilde{a}}^o}\right|_{\underline{\tilde{a}}^o = \underline{\tilde{a}}_k^{o^*}} \end{aligned} \tag{E.3}$$

Expanding $\frac{\partial \ln f_N^o(\hat{X}_{1,N}; \underline{\tilde{a}}^o, \hat{Z}_{1,N})}{\partial \underline{\tilde{a}}^o}$ in a Taylor series about $\underline{\tilde{a}}^o = \hat{\underline{\tilde{a}}}_k^o$ and utilizing (E.1), we obtain:

$$\begin{aligned} \left.\frac{\partial \ln f_N^o(\hat{X}_{1,N}; \underline{\tilde{a}}^o, \hat{Z}_{1,N})}{\partial \underline{\tilde{a}}^o}\right|_{\underline{\tilde{a}}^o = \underline{\tilde{a}}_k^{o^*}} &= \left.\frac{\partial^2 \ln f_N^o(\hat{X}_{1,N}; \underline{\tilde{a}}^o, \hat{Z}_{1,N})}{\partial \underline{\tilde{a}}^o \partial \underline{\tilde{a}}^o}\right|_{\underline{\tilde{a}}^o = \hat{\underline{\tilde{a}}}_k^o} (\underline{\tilde{a}}_k^{o^*} - \hat{\underline{\tilde{a}}}_k^o) \\ &\quad + O(|\underline{\tilde{a}}_k^{o^*} - \hat{\underline{\tilde{a}}}_k^o|^2) \\ &\simeq -B_N(\hat{\underline{\tilde{a}}}_k^o)(\underline{\tilde{a}}_k^{o^*} - \hat{\underline{\tilde{a}}}_k^o) \end{aligned} \tag{E.4}$$

where the $(N_o+1)\times(N_o+1)$ matrix $B_N(\underline{\tilde{a}}^o)$ is defined by:

$$B_N(\underline{\tilde{a}}^o) = -\frac{\partial^2 \ln f_N^o(\hat{X}_{1,N};\underline{\tilde{a}}^o,\hat{Z}_{1,N})}{\partial\underline{\tilde{a}}^o\partial\underline{\tilde{a}}^o} \tag{E.5}$$

The elements of $B_N(\hat{\underline{\tilde{a}}}^o)$ are $O(N)$. Substituting (E.4) into (E.3) and solving for $\underline{\tilde{a}}_k^{o^*}$ results in:

$$\begin{aligned}\underline{\tilde{a}}_k^{o^*} &= \hat{\underline{\tilde{a}}}_k^o + B_N^{-1}(\hat{\underline{\tilde{a}}}_k^o)\frac{\partial \ln \pi_{\underline{\tilde{a}}^o}(\underline{\tilde{a}}^o)}{\partial\underline{\tilde{a}}^o}\Big|_{\underline{\tilde{a}}^o=\underline{\tilde{a}}_k^{o^*}} \\ &= \hat{\underline{\tilde{a}}}_k^o + O(N^{-1})\end{aligned} \tag{E.6}$$

since the elements of $B_N(\hat{\underline{\tilde{a}}}^o)$ are $O(N^{-1})$. Equation (E.6) proves that for a large number of data points N, the optimal parameters $\hat{\underline{\tilde{a}}}_k^o$, $k=1,\ldots,K$ locally maximize the posterior pdf $p(\underline{\tilde{a}}^o|\mathcal{D}_N,\mathcal{M}_P)$. The global maximum of $p(\underline{\tilde{a}}^o|\mathcal{D}_N,\mathcal{M}_P)$ is attained by the solutions $\hat{\underline{\tilde{a}}}_l^o = [\hat{\underline{a}}_l^o,\hat{\sigma}^o]^T$ which satisfy:

$$\pi_{\underline{\tilde{a}}^o,\sigma^o}(\hat{\underline{\tilde{a}}}_l^o) = \max_{k=1,\ldots,K}\pi_{\underline{\tilde{a}}^o}(\hat{\underline{\tilde{a}}}_k^o) \tag{3.4.23}$$

In order to approximate $p(\underline{\tilde{a}}^o|\mathcal{D}_N,\mathcal{M}_P)$ in the neighborhood $\mathcal{H}(\hat{\underline{\tilde{a}}}_k^o)$, expand $\ln p(\underline{\tilde{a}}^o|\mathcal{D}_N,\mathcal{M}_P)$ in a Taylor series about $\underline{\tilde{a}}^o = \hat{\underline{\tilde{a}}}_k^o$, to obtain:

$$\begin{aligned}\ln p(\underline{\tilde{a}}^o|\mathcal{D}_N,\mathcal{M}_P) = \ln p(\hat{\underline{\tilde{a}}}_k^o|\mathcal{D}_N,\mathcal{M}_P) &+ \frac{\partial \ln p(\underline{\tilde{a}}^o|\mathcal{D}_N,\mathcal{M}_P)}{\partial\underline{\tilde{a}}^o}\Big|_{\underline{\tilde{a}}^o=\hat{\underline{\tilde{a}}}_k^o}(\underline{\tilde{a}}^o-\hat{\underline{\tilde{a}}}_k^o) \\ &+ \frac{1}{2}(\underline{\tilde{a}}^o-\hat{\underline{\tilde{a}}}_k^o)^T\frac{\partial^2 \ln p(\underline{\tilde{a}}^o|\mathcal{D}_N,\mathcal{M}_P)}{\partial\underline{\tilde{a}}^o\partial\underline{\tilde{a}}^o}\Big|_{\underline{\tilde{a}}^o=\hat{\underline{\tilde{a}}}_k^o}(\underline{\tilde{a}}^o-\hat{\underline{\tilde{a}}}_k^o) + \text{h.o.t.}\end{aligned} \tag{E.7}$$

where $\underline{\tilde{a}}^o \in \mathcal{H}(\hat{\underline{\tilde{a}}}_k^o)$. Since $p(\underline{\tilde{a}}^o|\mathcal{D}_N,\mathcal{M}_P)$ attains a maximum at $\underline{\tilde{a}}^o = \hat{\underline{\tilde{a}}}_k^o$, it follows that:

$$\underline{0} = \frac{\partial p(\underline{\tilde{a}}^o|\mathcal{D}_N,\mathcal{M}_P)}{\partial\underline{\tilde{a}}^o}\Big|_{\underline{\tilde{a}}^o=\hat{\underline{\tilde{a}}}_k^o} = \frac{1}{p(\underline{\tilde{a}}^o|\mathcal{D}_N,\mathcal{M}_P)}\frac{\partial p(\underline{\tilde{a}}^o|\mathcal{D}_N,\mathcal{M}_P)}{\partial\underline{\tilde{a}}^o}\Big|_{\underline{\tilde{a}}^o=\hat{\underline{\tilde{a}}}_k^o} \tag{E.8}$$

Define the $(N_o+1)\times(N_o+1)$ matrix $A_N(\hat{\underline{\tilde{a}}}_k^o)$ to be:

$$\begin{aligned}A_N(\hat{\underline{\tilde{a}}}_k^o) = &-\frac{\partial^2 \ln p(\underline{\tilde{a}}^o|\mathcal{D}_N,\mathcal{M}_P)}{\partial\underline{\tilde{a}}^o\partial\underline{\tilde{a}}^o}\Big|_{\underline{\tilde{a}}^o=\hat{\underline{\tilde{a}}}_k^o} \\ &- \frac{\partial^2 \ln f_N^o(\hat{X}_{1,N};\underline{\tilde{a}}^o,\hat{Z}_{1,N})}{\partial\underline{\tilde{a}}^o\partial\underline{\tilde{a}}^o}\Big|_{\underline{\tilde{a}}^o=\hat{\underline{\tilde{a}}}_k^o} - \frac{\partial^2 \ln \pi_{\underline{\tilde{a}}^o}(\underline{\tilde{a}}^o)}{\partial\underline{\tilde{a}}^o\partial\underline{\tilde{a}}^o}\Big|_{\underline{\tilde{a}}^o=\hat{\underline{\tilde{a}}}_k^o}\end{aligned} \tag{E.9}$$

For large N, the contribution of the second term is negligible and, therefore:

$$A_N(\hat{\underline{\tilde{a}}}_k^o) \cong B_N(\hat{\underline{\tilde{a}}}_k^o) \tag{E.10}$$

Equation (E.7) may be rewritten, utilizing (E.8) and (E.9), as follows:

$$\ln p(\underline{\tilde{a}}^o|\mathcal{D}_N, \mathcal{M}_P) = \ln p(\hat{\underline{\tilde{a}}}_k^o|\mathcal{D}_N, \mathcal{M}_P) - \frac{1}{2}(\underline{\tilde{a}}^o - \hat{\underline{\tilde{a}}}_k^o)^T A_N(\hat{\underline{\tilde{a}}}_k^o)(\underline{\tilde{a}}^o - \hat{\underline{\tilde{a}}}_k^o) + \text{h.o.t.} \tag{E.11}$$

where $\underline{\tilde{a}}^o \in \mathcal{H}(\hat{\underline{\tilde{a}}}_k^o)$. Thus, the following approximation in the neighborhood of $\hat{\underline{\tilde{a}}}_k^o$ is obtained:

$$p(\underline{\tilde{a}}^o|\mathcal{D}_N, \mathcal{M}_P) \cong p(\hat{\underline{\tilde{a}}}_k^o|\mathcal{D}_N, \mathcal{M}_P)\exp\left(-\frac{1}{2}(\underline{\tilde{a}}^o - \hat{\underline{\tilde{a}}}_k^o)^T A_N(\hat{\underline{\tilde{a}}}_k^o)(\underline{\tilde{a}} - \hat{\underline{\tilde{a}}}_k^o)\right) \tag{E.12}$$

Note that:

$$\begin{aligned} G(\underline{\tilde{a}}^o; \hat{\underline{\tilde{a}}}_k^o, A_N^{-1}(\hat{\underline{\tilde{a}}}_k^o)) = &\frac{1}{(2\pi)^{\frac{N_o+1}{2}}|A_N^{-1}(\hat{\underline{\tilde{a}}}_k^o)|^{\frac{1}{2}}} \\ &\times \exp\left(-\frac{1}{2}(\underline{\tilde{a}}^o - \hat{\underline{\tilde{a}}}_k^o)^T A_N(\hat{\underline{\tilde{a}}}_k^o)(\underline{\tilde{a}}^o - \hat{\underline{\tilde{a}}}_k^o)\right) \end{aligned} \tag{E.13}$$

is a multi-dimensional Gaussian with mean $\hat{\underline{\tilde{a}}}_k^o$ and covariance matrix $A_N^{-1}(\hat{\underline{\tilde{a}}}_k^o)$. Comparing (E.12) with (E.13), it can be concluded that locally, in the neighborhood of $\hat{\underline{\tilde{a}}}_k^o$, the following approximation holds:

$$\begin{aligned} p(\underline{\tilde{a}}^o|\mathcal{D}_N, \mathcal{M}_P) &\cong (2\pi)^{\frac{N_o+1}{2}}|A_N^{-1}(\hat{\underline{\tilde{a}}}_k^o)|^{\frac{1}{2}} p(\hat{\underline{\tilde{a}}}_k^o|\mathcal{D}_N, \mathcal{M}_P) G(\underline{\tilde{a}}^o; \hat{\underline{\tilde{a}}}_k^o, A_N^{-1}(\hat{\underline{\tilde{a}}}_k^o)) \\ &= c|A_N^{-1}(\hat{\underline{\tilde{a}}}_k^o)|^{\frac{1}{2}} \pi_{\underline{\tilde{a}}^o}(\hat{\underline{\tilde{a}}}_k^o) G(\underline{\tilde{a}}^o; \hat{\underline{\tilde{a}}}_k^o, A_N^{-1}(\hat{\underline{\tilde{a}}}_k^o)) \end{aligned} \tag{E.14}$$

where $\underline{\tilde{a}}^o \in \mathcal{H}(\hat{\underline{\tilde{a}}}_k^o)$, and $c = k(2\pi)^{\frac{N_o+1}{2}} f_N^o(\hat{X}_{1,N}; \hat{\underline{\tilde{a}}}_k^o, \hat{Z}_{1,N}) =$ constant, since all $\hat{\underline{\tilde{a}}}_k^o, k = 1, \ldots, K$ globally maximize $f_N^o(\hat{X}_{1,N}; \underline{\tilde{a}}^o, \hat{Z}_{1,N})$.

Note that:

$$
\begin{aligned}
1 &= \int_{S(\underline{\tilde{a}}^o)} p(\underline{\tilde{a}}^o|\mathcal{D}_N, \mathcal{M}_P) d\underline{\tilde{a}}^o \\
&\simeq \sum_{k=1}^{K} \int_{\underline{\tilde{a}}^o \in \mathcal{H}(\hat{\underline{\tilde{a}}}_k^o)} c|A_N^{-1}(\hat{\underline{\tilde{a}}}_k^o)|^{\frac{1}{2}} \pi_{\underline{\tilde{a}}^o}(\hat{\underline{\tilde{a}}}_k^o) G(\underline{\tilde{a}}^o; \hat{\underline{\tilde{a}}}_k^o, A_N^{-1}(\hat{\underline{\tilde{a}}}_k^o)) d\underline{\tilde{a}}^o \\
&= c \sum_{k=1}^{K} |A_N^{-1}(\hat{\underline{\tilde{a}}}_k^o)|^{\frac{1}{2}} \pi_{\underline{\tilde{a}}^o}(\hat{\underline{\tilde{a}}}_k^o) \\
&= c \sum_{k=1}^{K} w_k'
\end{aligned}
\tag{E.15}
$$

where

$$
w_k' = |A_N^{-1}(\hat{\underline{\tilde{a}}}_k^o)|^{\frac{1}{2}} \pi_{\underline{\tilde{a}}^o}(\hat{\underline{\tilde{a}}}_k^o) \tag{3.4.25}
$$

Equations (E.14) and (3.4.25) lead to:

$$
p(\underline{\tilde{a}}^o|\mathcal{D}_N, \mathcal{M}_P) \simeq w_k G(\underline{\tilde{a}}^o; \hat{\underline{\tilde{a}}}_k^o, A_N^{-1}(\hat{\underline{\tilde{a}}}_k^o)) \tag{3.4.27}
$$

where $\underline{\tilde{a}}^o \in \mathcal{H}(\hat{\underline{\tilde{a}}}_k^o)$ and w_k is given by:

$$
w_k = \frac{w_k'}{\sum_{k=1}^{k} w_k'} \tag{3.4.24}
$$

In the globally identifiable case $w_1 = 1$, and, therefore, $p(\underline{\tilde{a}}^o|\mathcal{D}_N, \mathcal{M}_P)$ can be approximated in the neighborhood of its optimal parameters $\hat{\underline{\tilde{a}}}^o = [\underline{\hat{a}}^{o^T}, \hat{\sigma}^o]^T$, with a multi-dimensional Gaussian distribution.